QUANTUM INTERFERENCE AND DECOHERENCE EFFECTS IN NOVEL SYSTEMS

By

SUMANTA DAS

Bachelor of Science in Physics
Presidency College
Calcutta University
Kolkata, West Bengal, India
2001

Master of Science in Physics
Pune University
Pune, Maharastra, India
2003

Submitted to the Faculty of the
Graduate College of
Oklahoma State University
in partial fulfillment of
the requirements for
the Degree of
DOCTOR OF PHILOSOPHY
December, 2009

QUANTUM INTERFERENCE AND DECOHERENCE EFFECTS IN NOVEL SYSTEMS

Dissertation Approved:

Dr. Girish S. Agarwal

Dissertation advisor

Dr. Xincheng Xie

Dr. Albert T. Rosenberger

Dr. Gil Summy

Dr. Daniel Grischkowsky

Dr. A. Gordon Emslie

Dean of the Graduate College

ACKNOWLEDGMENTS

It is a difficult task to write an acknowledgment when over the years many people have influenced your life in different aspects and build you for the sincerity, motivation, tenacity and perseverance one needs for completion of such a hard earned and prestigious degree. Let me start by thanking my high School physics teacher Mr. Asit Das, whose enthusiasm in teaching physics has paved my liking for this subject.

Special thanks and gratitude to my advisor Dr. Girish Agarwal who has motivated me a lot in becoming a sincere and hardworking researcher. His passion and sincerity for science and his eagerness in learning even after being in academics for decades has shown me that the hunt for knowledge is endless. His aggressiveness towards publishing has taught me the importance of communicating your research to your peers. His authority in projecting an idea yet modesty in accepting criticism has taught me how to become a complete and respectable researcher. In addition he is a great teacher and learning from him has been a rewarding experience for me. His vastness in knowledge has provided me with an education not just restricted to quantum optics. I hope all these teachings will help me to foster as a good scientist and researcher in the coming years.

I would also like to acknowledge the contribution of my dissertation committee members, which includes Dr. X. Xie, Dr. A. T. Rosenberger, Dr. D. Grischkowsky and Dr. G. Summy. It has been a wonderful experience interacting with them at different times. Additionally, I want to thank the remaining faculty members of the Physics department for their contributions to my education at OSU.

I would also take this opportunity to thank the department's staff members Susan,

Cindi, Stephanie, Danyelle and Waren for making me feel at home away from home. They had been extremely helpful and had shown extraordinary patience in the face of our never-ending request over the years.

Let me also thank my group mates Amit and Lam for being supportive both personally and professionally during my PhD years. I would do injustice if I dont acknowledge our ex-group members Dr. T. N. Dey, Dr. P. K. Pathak and Dr. A. Kolkiran with whom I have shared several fruitful discussions on various topics over the years.

PhD takes a long time and the dynamics of life during this period is not just restricted to academics. Friends in particular are a key component of this dynamics. Let me take this opportunity to thank several of my friends both at OSU and outside who have made my journey towards this degree a very memorable one. Thanks to Ranjan, Nicklavos, Sandeep and numerous others for many of those cheerful evenings with tea, good food and lots of discussion. Thanks also to Abhisek, Abhirup, Mohit, Parimal, Saiti, Suchetana and Saikat who had helped me in various aspects from time to time. Thanks to Chayan for being extremely supportive throughout many of the ups and downs of my life. My special thanks to Ayon, Sumei and Elijah for helping me with formatting and correcting my dissertation manuscript.

Let me take this opportunity to also thank my family members who had overwhelmingly tolerated both the frustrations and excitements of my PhD life. I thank my father, mother and sister for being supportive and believing in me over the years. Finally this acknowledgment will remain incomplete without appreciating the loyalty, hardship and sacrifice of my wife Farzana. She has shown extreme tolerance and perseverance while I was away from her during all this years of my PhD. I am really very fortunate to have such a nice and loving wife . I am proud to dedicate this thesis to her and my parents.

TABLE OF CONTENTS

LIST OF TABLES

LIST OF FIGURES

CHAPTER 1

INTRODUCTION

Quantum physics and Information theory once thought to be different branches of science have infact been connected since the early days of quantum mechanics. In his paper on black body radiation Planck [1] had already established the relationship between information and entropy through the Boltzmann's constant K_B [1]. This connection would remain hidden until mid 1980's, when it occurred to Richard Feynman who was working on an involved problem in field theory that, if he had a machine that could operate on the principles of quantum mechanics, it would be possible to attain a solution in finite time which otherwise on a classical machine will take a computation time of the order of lifetime of the universe. Following this, Feynman [2] and David Deutsch [3] independently proposed that a quantum mechanical device (a quantum computer as presently known) which could represent the state of quantum systems and could be used to do unitary transformation of that state, would be more efficient in computing the dynamical evolution of the said quantum system.

This idea was not taken seriously until ten years later when Peter Shor [4], discovered an algorithm which when working on a quantum computer would be able to factorize an integer N in polynomial time *i.e.* in $log(N)$ time. This is exponentially faster than the most efficient known classical factoring algorithm. Shor's algorithm generated unprecedented interest as it showed that if one has a quantum computer,

[1]Note that although Boltzmann first linked entropy and probability in 1877, the relation was never expressed with a specific constant until Max Planck first introduced K , in his derivation of the law of black body radiation in $1900 - 1901$. The iconic terse form of the equation $S = K \log W$ on Boltzmann's tombstone is in fact due to Planck, not Boltzmann

it is possible to *break* the widely used public-key cryptography scheme known as RSA with out much difficulty. Note that the strength of RSA lies on the incapability of a classical computer (even the most advanced supercomputer to date working on the principles of classical physics) to factor large numbers in computationally feasible time. The discovery of Shor's algorithm led to an outburst of theoretical and experimental activities in the scientific community and created a whole new field of quantum computation and quantum information [5].

The key aspect of quantum information science that makes it so interesting from the context of both fundamental studies and applications is the existence of a non-local correlation known as entanglement [6]. Entanglement is a phenomenon that exists only between two or more quantum mechanical systems and has no classical analog. Since its discovery entanglement has been at the center of several controversies and has profoundly influenced our understanding of nature. In particular entanglement is quite fascinating as it leads to phenomena like the famous Schrödinger CAT paradox [6] which challenges our perception of the physical reality.

1.1 Quantum Entanglement

With the advent of quantum information sciences, entanglement has evolved during the last decade from being a controversial artifact of the quantum theory to a key resource behind numerous quantum information protocols. Thus, it is important to understand what entanglement is before we can discuss its implications and applications. Suppose we are given a quantum system $\mathcal{S}$ that is composed of two subsystems $\mathcal{S}_1$ and $\mathcal{S}_2$. Then from quantum mechanics we know that the state space of the composite system $\mathcal{S}$ can be written as the tensor product of subsystem spaces, *i.e* the Hilbert space of $\mathcal{S}$ is $H = \otimes_{i=1}^{2} H_i$. Further the superposition principle tells us that

the state of the system $\mathcal{S}$ can then be written as,

$$|\Psi\rangle = \sum_{i_1,i_2} c_{i_1,i_2}|i_1\rangle \otimes |i_2\rangle, \tag{1.1}$$

where $|i_1\rangle$ and $|i_2\rangle$ are the basis vectors spanning the Hilbert space of the subsystems $\mathcal{S}_1$ and $\mathcal{S}_2$ respectively. Now we also know from quantum mechanics that any state vector $|\Psi_1\rangle$ and $|\Psi_2\rangle$ of the subsystems $\mathcal{S}_1$ and $\mathcal{S}_2$, can be expanded in terms of the basis vectors as,

$$|\Psi_1\rangle = \sum_{i_1} c_{i_1}|i_1\rangle; \quad |\Psi_2\rangle = \sum_{i_2} c_{i_2}|i_2\rangle. \tag{1.2}$$

From equations (4.1) and (1.2) we see that if $c_{i_1,i_2} \neq c_{i_1}c_{i_2}$ for any i_1, i_2, then $|\Psi\rangle \neq |\Psi_1\rangle \otimes |\Psi_2\rangle$. The state $|\Psi\rangle$ is then said to be an entangled state and the subsystems $\mathcal{S}_1$ and $\mathcal{S}_2$ entangled. As this entanglement arises between two systems it is also known as bipartite entanglement. If one has n subsystems it is in principle possible to have a n-partite entanglement. Moreover, the entanglement we just defined is for pure states. In practice though, we encounter mixed states more often than pure states. Entanglement of a mixed state is no longer equivalent to being nonproduct states, instead one calls a mixed state of two subsystems $\mathcal{S}_1$ and $\mathcal{S}_2$ entangled if the density matrix of the composite system cannot be written as a sum of the product of the density matrices of the two subsystems, *i.e.*

$$\rho \neq \sum_i p_i \rho_1^i \otimes \rho_2^i, \tag{1.3}$$

ρ_1^i, ρ_2^i being the density matrix of the subsystems 1 and 2 respectively, and p_i their statistical weight in the mixture. A practical and common example of a pure entangled state is the spin singlet state,

$$|\Psi\rangle = \frac{1}{\sqrt{2}}[|\uparrow\rangle_1|\downarrow\rangle_2 - |\downarrow\rangle_1|\uparrow\rangle_2] \tag{1.4}$$

of two spin-$\frac{1}{2}$ particles whose Hilbert space are spanned by the mutually orthogonal basis vectors $|\uparrow\rangle_i$ and $|\downarrow\rangle_i, i = 1, 2$. Now that we have defined what entanglement is let us discuss its physical meaning and implications.

Physically entanglement means that the two subsystems $\mathcal{S}_1$ and $\mathcal{S}_2$ no longer posses any independent physical characteristics and can only be defined by the quantum state $|\Psi\rangle$ of the composite system [2]. It is therefore not possible to have a local measurement or operation on either $\mathcal{S}_1$ or $\mathcal{S}_2$ to determine the complete physical property of the quantum state $|\Psi\rangle$. This is true even after the two subsystems separate physically, as if they have some kind of a memory of their earlier interaction. Thus entanglement creates a nonlocal nonclassical correlation among the systems. This aspect of non-local correlation can be understood well by considering a simple example of two spin-$\frac{1}{2}$ particle.

Suppose a system of spin-$\frac{1}{2}$ particles is described by the spin singlet state (which is an entangle state) of equation (1.4). Then we see that in any measurement on this state, if the first particles is found to be in the "spin up" state, we can immediately infer that the second particle upon similar measurement will always be found in the "spin down" state. Thus due to the non-local correlation, a measurement on the first particle influences the second which then adjusts itself to the "spin down" state to give the desired outcome of measurement on it [3]. Note that there seems to be an apparent violation of special relativity as information about the measurement of the first particle was instantaneous transferred to the second that may be spatially separated by arbitrary distance. In truth though, there is no violation. Even though the measurement on the second particle is instantaneously fixed by the outcome of the first, the complete randomness of the latter outcome means that no useful information

[2] In the classical physics the sub-systems simply add up to make a bigger composite system yet retaining their independent properties

[3] In contrast in classical physics correlations arise often from conservation laws. For example a particle at rest may decay into two identical fragments whose momentum is then correlated following the conservation law. Hence measuring one of the particles momentum tell us the other. But note that the momentums of each particle exists independent of the other and no measurement on one can influence or change the other.

can be transmitted between the partners.

Einstein was quite intrigued by the existence of such nonlocal correlations and termed it "spooky action at a distance". He along with Boris Podolsky and Allen Rosen envisioned a *Gedanken* experiment with two particles and argued in terms of their momentum and position co-ordinates that such nonlocal correlation is an artifact of incompleteness of the quantum theory [7]. This later came to be known as the Einstein-Podolsky-Rosen (EPR) paradox [4]. The EPR paradox led to "hidden variable theories" , where one assumes that the dynamic behavior of a system's properties at a microscopic level appears probabilistic because of some yet unknown parameters so called the *hidden variables*.

1.1.1 The Bell's Inequalities

Until 1964 it was thought that by suitable choice of the hidden variable one can match the predictions of quantum mechanics with hidden variable theories. But then John Bell showed that such hidden variable theories actually predict a *testable inequality relation* among the observables of spin systems that disagrees with the predictions of quantum mechanics [8]. It is worth mentioning that Bell's inequality is a general relation about correlations among systems and is not based on quantum theory.

To understand this inequality let us consider a specific example of a composite system of two spin-$\frac{1}{2}$ particles which are correlated in spin. We then consider three measurement direction of spin of the particles along the unit vectors $\hat{a}, \hat{b}, \hat{c}$ which are in general not mutually orthogonal.

Further suppose that one of the particles belong to some definite type, say $(\hat{a}-, \hat{b}+, \hat{c}+)$, which means that if a projection of spin operator $\vec{S}_i, i = 1, 2$ is taken along the unit vector $\hat{a}$ we will get $(-)$ sign, that along $\hat{b}$, $(+)$ sign and so on. The other particle then should belong to the type $(\hat{a}+, \hat{b}-, \hat{c}-)$ to ensure zero total angular momentum.

[4] A generalization of EPR paradox to composite spin-$\frac{1}{2}$ was later done by D. Bohm

Table 1.1: Spin component matching in correlated measurement

Population	Particle 1	Particle 2
N_1	$(\hat{a}+, \hat{b}+, \hat{c}+)$	$(\hat{a}-, \hat{b}-, \hat{c}-)$
N_2	$(\hat{a}+, \hat{b}+, \hat{c}-)$	$(\hat{a}-, \hat{b}-, \hat{c}+)$
N_3	$(\hat{a}+, \hat{b}-, \hat{c}+)$	$(\hat{a}-, \hat{b}+, \hat{c}-)$
N_4	$(\hat{a}+, \hat{b}-, \hat{c}-)$	$(\hat{a}-, \hat{b}+, \hat{c}+)$
N_5	$(\hat{a}-, \hat{b}+, \hat{c}+)$	$(\hat{a}+, \hat{b}-, \hat{c}-)$
N_6	$(\hat{a}-, \hat{b}+, \hat{c}-)$	$(\hat{a}+, \hat{b}-, \hat{c}+)$
N_7	$(\hat{a}-, \hat{b}-, \hat{c}+)$	$(\hat{a}-, \hat{b}+, \hat{c}-)$
N_8	$(\hat{a}-, \hat{b}-, \hat{c}-)$	$(\hat{a}+, \hat{b}+, \hat{c}+)$

In this way we have a total of eight possibilities which are mutually exclusive and disjoint for the pair of spins. All the eight possibilities are listed in table (1.1).

Let $\mathrm{P}(\hat{a}+, \hat{b}+)$ be the probability that in a random selection, some observer A measures $\vec{S}_1 \cdot \hat{a}$ to be + and observer B measures $\vec{S}_2 \cdot \hat{b}$ to be +, then we should have

$$P(\hat{a}+, \hat{b}+) = \frac{(N_3 + N_4)}{\sum_i^8 N_i}, \tag{1.5}$$

where N_3, N_4 are the number of particle pairs for which this situation is found. In a similar manner we find,

$$P(\hat{a}+, \hat{c}+) = \frac{(N_2 + N_4)}{\sum_i^8 N_i}; \quad P(\hat{c}+, \hat{b}+) = \frac{(N_3 + N_7)}{\sum_i^8 N_i}. \tag{1.6}$$

Now as N_i is positive semidefinite, we can write inequality relations like

$$N_3 + N_4 \leq (N_2 + N_4) + (N_3 + N_7). \tag{1.7}$$

Using equations (1.5, 1.6) in (1.7) we then find,

$$P(\hat{a}+, \hat{b}+) \leq P(\hat{a}+, \hat{c}+) + P(\hat{c}+, \hat{b}+). \tag{1.8}$$

Equation (1.8) is the famous Bell's inequality [8, 9]. Note that this inequality is a mathematical expression of the bound that arises from EPR locality assumption (independence of measurement) which implies that certain combinations of expectation values have definite bound [10]. Now that we know what Bell's inequality is, let us study its implication in respect to the nonlocal quantum correlations - entanglement.

1.1.2 Entanglement and violation of Bell's inequality

Let us now calculate the probabilities for the spin correlated system using quantum mechanics. Our spin-$\frac{1}{2}$ composite system is then characterized by the spin singlet state

$$|\Psi\rangle = \frac{1}{\sqrt{2}}[|\uparrow\rangle_1|\downarrow\rangle_2 - |\downarrow\rangle_1|\uparrow\rangle_2]; \tag{1.9}$$

where we take the quantization axis to be the $z-$ axis. To calculate the probability $P(\hat{a}+, \hat{b}+)$ we need to consider a new quantization axis $\hat{b}$ that makes an angle θ_{ab} with $\hat{a}$ as shown in Fig (1.1).

Following standard spin operator formalism we find the probability that the $\vec{S}_2 \cdot \hat{b}$ measurement yield (+) when particle 2 is in the eigenket of $\vec{S}_2 \cdot \hat{a}$ with negative eigenvalue is given by,

$$\cos^2\left[\frac{(\pi - \theta_{ab})}{2}\right] = \sin^2\left(\frac{\theta_{ab}}{2}\right). \tag{1.10}$$

Hence, we find

$$P(\hat{a}, \hat{b}) = \frac{1}{2}\sin^2\left(\frac{\theta_{ab}}{2}\right). \tag{1.11}$$

Similarly evaluating the other probabilities and substituting them in the inequality (1.8) we get

$$\sin^2\left(\frac{\theta_{ab}}{2}\right) \leq \sin^2\left(\frac{\theta_{ac}}{2}\right) + \sin^2\left(\frac{\theta_{cb}}{2}\right). \tag{1.12}$$

Now for simplicity let us choose $\hat{a}$, $\hat{b}$ and $\hat{c}$ to lie in a plane such that

$$\theta_{ab} = 2\theta; \quad \theta_{ac} = \theta_{cb} = \theta \tag{1.13}$$

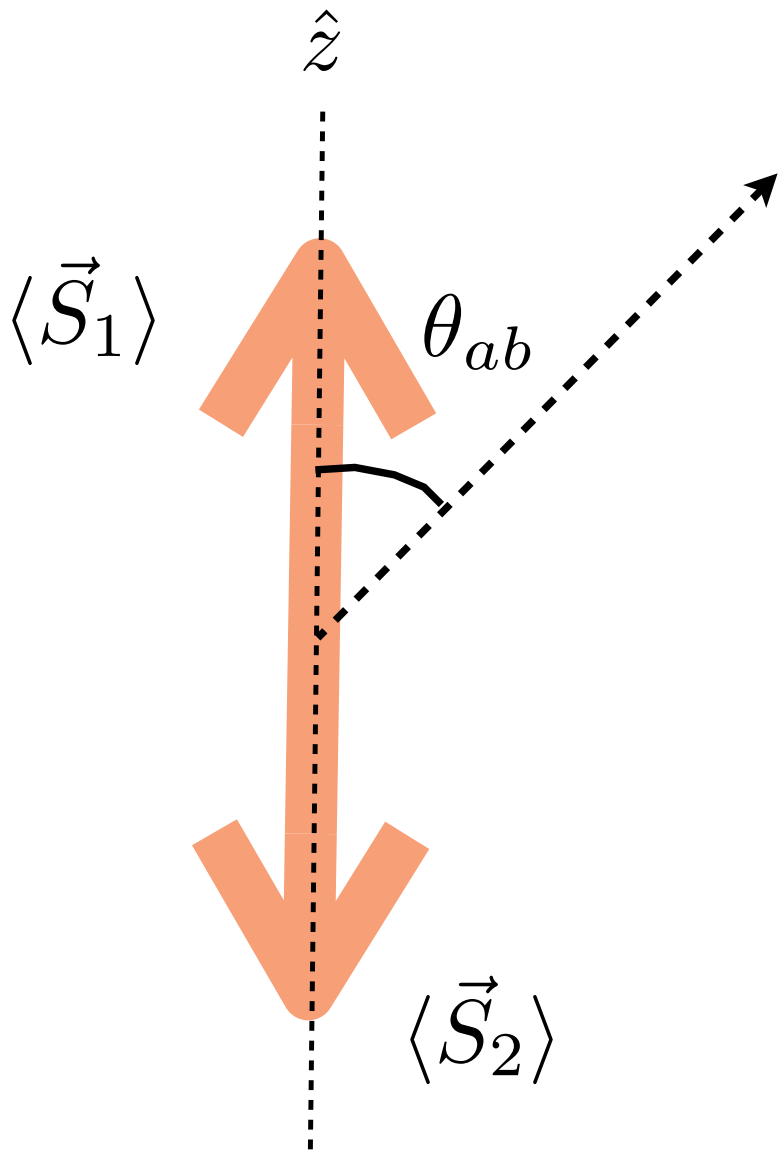

Figure 1.1: Orientation of the spin components in space. $\hat{z}$ being the quantization axis.

then we find that for $0 < \theta < \pi/2$ the inequality is violated [5].

Thus we see that quantum mechanical measurement of the spin correlations can lead to violation of Bell's inequality. Note that in this example we attributed perfect correlations among the two spin-$\frac{1}{2}$particles. In real quantum mechanical systems such correlation are practically impossible and hence experimentally it is difficult to test this inequality. The Bell's inequality was later generalized by Clauser, Horne, Shimony, and Holt [11] with the intent of experimentally testing it. Consider a correlation experiment in which the variables (A_1, A_2) are measured on one subsystem of the whole system and (B_1, B_2) on the other subsystem with both the subsystems spatially separated. Then the hidden variable theory imposes the following constraint on the statistics of the measurements on a large ensemble of such systems,

$$|E(A_1, B_1) + E(A_1, B_2) + E(A_2, B_1) - E(A_2, B_2)| \leq 2, \tag{1.14}$$

where $E(A_i, B_j)$ is the expectation value of the correlation experiment $A_i B_j$ and it is assumed that they are dichotomic *i. e.* have values ± 1 . This is the $CHSH$(Clauser, Horne, Shimony and Holt) inequality which gives experimentally observable bound on any hidden variable theory. Violation of this inequality was found in a series of experiment with linear polarization correlation of two photons during the 70's and 80's thus refuting the existence of hidden variable theory [12, 13, 14]. A schematic diagram showing the basic essence of these experiments is shown in Fig. (1.2). Incidentally this where also the first experiments to demonstrate non-local quantum correlations *i.e.* entanglement among two quantum systems. Moreover, the experimental observations are in accordance with quantum mechanics thus proving its completeness as a theory for studying nature. The maximum violation of Bell's or CHSH inequality

[5]This explanation of violation of Bell's inequality follows closely to that of Modern Quantum Mechanics, J. J. Sakurai, page 228-230

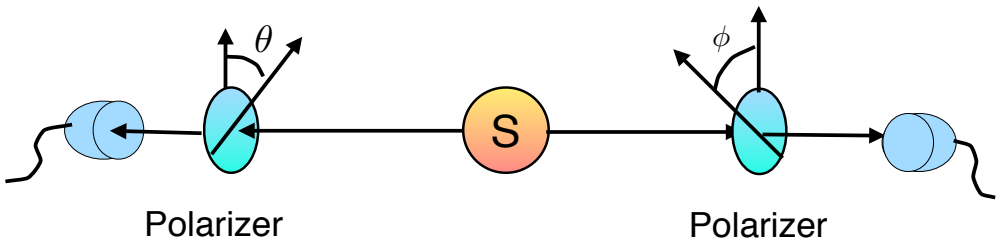

Figure 1.2: Typical experimental arrangement to test Bells inequality. A source emits, say, polarization-entangled pairs of photons. Each photon is sent through a polarizer whose orientation can be varied. Finally behind each polarizer, the transmitted photons are registered. Quantum mechanics predicts a sinusoidal variation of the coincidence count rate as a function of the relative angular orientation of the polarizers. Any such variation violates local realism as expressed by Bells inequality.

is manifested by a set of entangled states known as the Bell's state :

$$\begin{aligned} |\phi^{\pm}\rangle &= \frac{1}{\sqrt{2}}\left[|00\rangle \pm |11\rangle\right] \\ |\Psi^{\pm}\rangle &= \frac{1}{\sqrt{2}}\left[|01\rangle \pm |10\rangle\right], \end{aligned} \tag{1.15}$$

in which case equation (1.14) is $2\sqrt{2}$. Here $|0\rangle, |1\rangle$ can be the spin up, spin down kets for spin-$\frac{1}{2}$ particles or orthogonal polarization H , V for photons. Note that in the case of mixed entangled states their is no particular criteria or inequalities to test the hidden variable theory. However, for bi-partite (two qubit) entanglement, if the mixed state is a Werner state [15] (a mixture of the singlet with white noise) of the form

$$\rho = p|\Psi^{-}\rangle\langle\Psi^{-}| + (1-p)\mathcal{I}/4, \tag{1.16}$$

the $CHSH$ inequality is applicable and can be shown to be violated when $2^{-1/2} < p \leq 1$ [16]. Here ρ is the density matrix of the system, Ψ^{-} are the singlet state (equation 1.15), p the statistical weight of the mixture and $\mathcal{I}$ is the identity operator.

1.2 Producing entanglement

1.2.1 Cascade emission from atoms

The pioneering experiment showing entanglement and the violation of Bell's inequality was performed by Freedman and Clauser in 1972 [12]. They studied the polarization correlation among two photons emitted in the cascade decay of a Ca atom. The schematic diagram of the atomic level structure and the experimental setup are shown in Fig (1.3). The decaying atoms were viewed by two symmetrically placed optical systems, each consisting of two lenses, a wavelength filter, a rotatable and removable polarizer, and a single photon detector. Coincidence rates for two photon detection as a function of the angle ϕ between the planes of the linear polarization defined by the orientation of the inserted polarizers were measure in different configurations : $R(\phi)$, when both polarizers present, R_1, coincidence rate when second

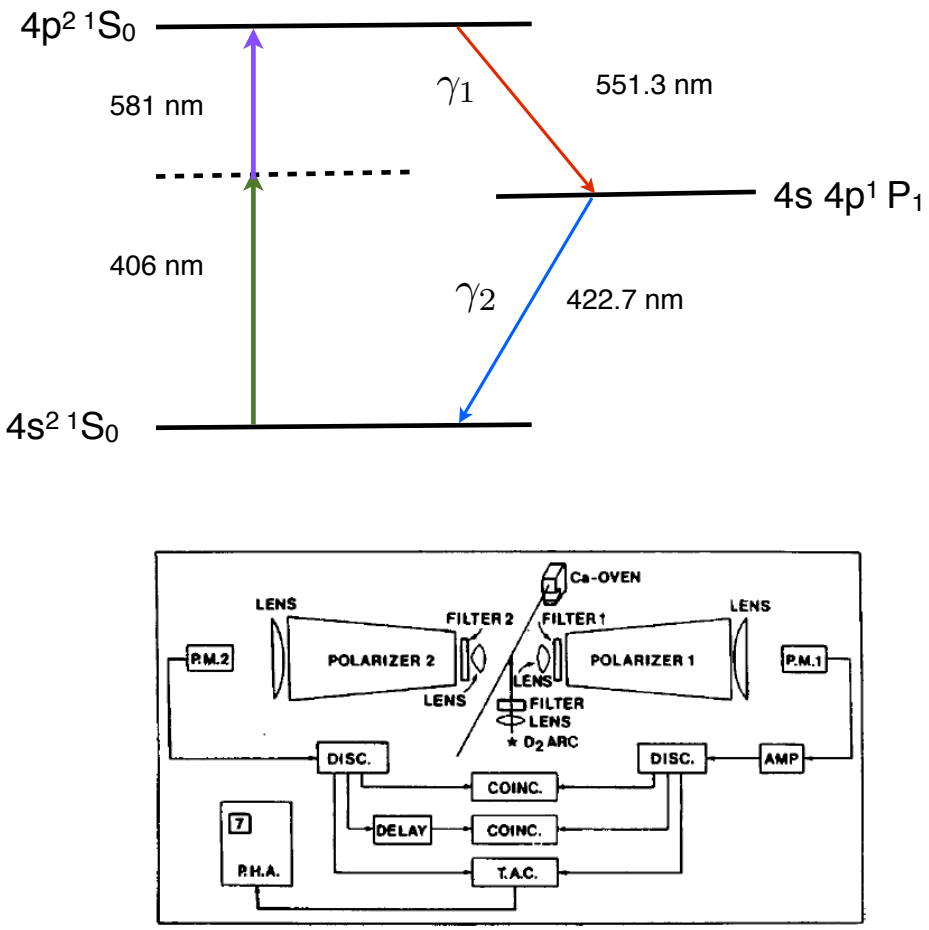

Figure 1.3: Sketch of the atomic level of Ca and experimental setup of the experiment of Freedman and Clauser (1972). The two photons emitted in an atomic cascade in Ca are collected with lenses and, after passage through adjustable polarizers, coincidences are registered using photomultiplier detectors and suitable discriminators and coincidence logic. The observed coincidence counts violate the generalized Bell's inequality (CHSH inequality)

polarizer removed, R_2, when first polarizers removed and R_0 when both polarizers removed. The inequality (1.14) for this set of measurements then takes the form,

$$-1 \leq \Delta(\phi) \leq 0, \tag{1.17}$$

where

$$\Delta(\Phi) = \frac{3R(\phi)}{R_0} - \frac{R(3\phi)}{R_0} - \frac{R_1 + R_2}{R_0}. \tag{1.18}$$

They found that this inequality is not satisfied by quantum mechanical predictions of coincidence rates for a range of values of ϕ. Maximum violation occurs at $\phi = 22.5^0[\Delta(\phi) > 0]$ and $\phi = 67.5^0[\Delta(\phi) < -1]$. These violations proved for the first time that non-local correlations, as predicted by quantum theory, can truly exist in nature (in this case among the photons), thus questioning the EPR notion of physical reality and existence of any hidden variables.

Later Aspect, Grangier and Roger [14] improved upon this result using a high efficiency source of Ca cascade and two channel polarizers (an optical analog of Stern-Gerlach filters). Unlike the earlier experiments [12, 13], by applying the two channel polarizers they were able to measure true dichotomic polarizations of visible photons and thus measure the coincidences required for the $CHSH$ inequalities directly. A schematic diagram of their experimental setup is shown in Fig (1.4). The observed coincidence counts were in agreement with quantum mechanical predictions and violated the $CHSH$ inequality of equation (1.14). Note that the expectation values of the correlation measurement are related to the coincidence counts by the relation

$$E(A_1, B_1) = \frac{1}{N}\left[C_{++}(A_1, B_1) + C_{--}(A_1, B_1) - C_{+-}(A_1, B_1) - C_{-+}(A_1, B_1)\right], \tag{1.19}$$

where it is assumed that each photon is subject to a measurement of linear polarization with a two-channel polarizer whose outputs are + and −. Then, for example $C_{++}(A_1, B_1)$ is the number of coincidences between the + output port of the polarizer measuring photon 1 along A_1 and the + output port of the polarizer measuring

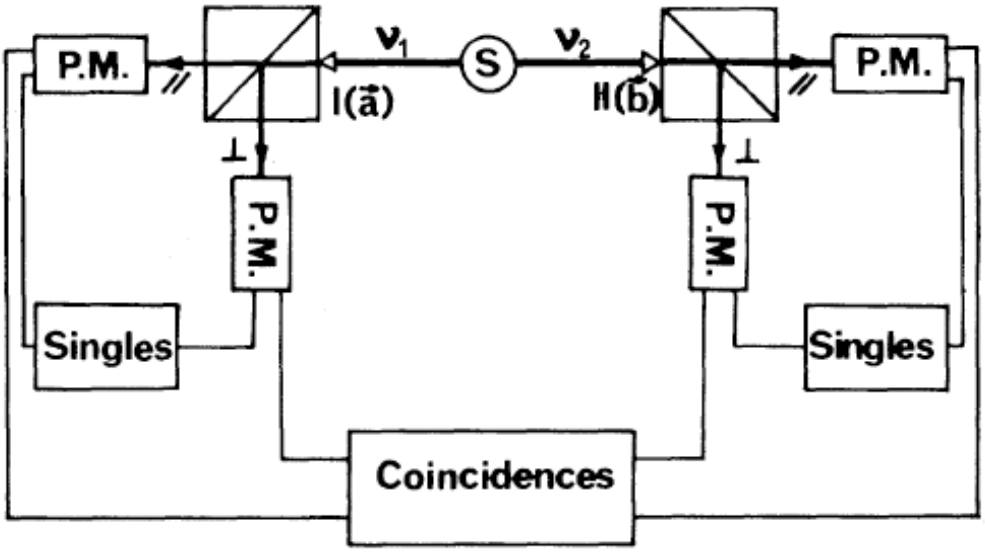

Figure 1.4: Schematic of the experimental set up of Aspect, Grangier and Roger's experiment. Two polarimeters I and II, in orientations $\hat{A}$ and $\hat{B}$, perform the dichotomic measurements of linear polarization of photons. Each polarimeter is rotatable around the axis of the incident beam. The counting electronics monitors the singles and the coincidences. Figure source : PRL **49**, 91 (1982).

photon 2 along B_1. Maximal violation was observed for $A_1 = 50^o, B_1 = 22.5^o, A_2 = 45^o, B_2 = 67.5^o$ where,

$$|E(A_1, B_1) + E(A_1, B_2) + E(A_2, B_1) - E(A_2, B_2)| = 2\sqrt{2}. \tag{1.20}$$

This is to date the maximum known violation of Bell's inequality. In later years several other sources ranging from non-linear crystals to semiconductors have been discovered to produced entanglement. Let us now discuss some of them.

1.2.2 Parametric down conversion

Another method of producing entanglement (in particular bi-partite entanglement) is by spontaneous parametric down conversion (SPDC). This method was first implemented by Alley and Shih [17] for a Bell-inequlity type experiment. In the parametric down conversion process a nonlinear crystal is pumped by a sufficiently strong laser beam. Then, with a certain very small probability, the nonlinear crystal splits incoming photons into pairs of photons of lower energy. The phase-matching conditions which for sufficiently large crystals are practically equivalent to energy and momentum conservation, imply that the momenta and the energies of the two created photons have to sum up to the corresponding value of the original pump photon inside the crystal (see Fig 1.5). Further, the phase matching condition also dictates that the photon pair be entangled in the frequency domain [18]. SPDC is stimulated by random vacuum fluctuations, as such the photon pairs are created at random times. However, if one of the pair (the "signal") is detected at any time then we know its partner (the "idler") is present. In effect, a very rich entangled state results. The two emerging photons are entangled both in energy and in momentum. In type-I down conversion, these two photons have the same polarization while in type-II down conversion, they have different polarization.

Recent experiments using the parametric down conversion process, utilizes type-II down conversion. In this case the two emerging photons having orthogonal polariza-

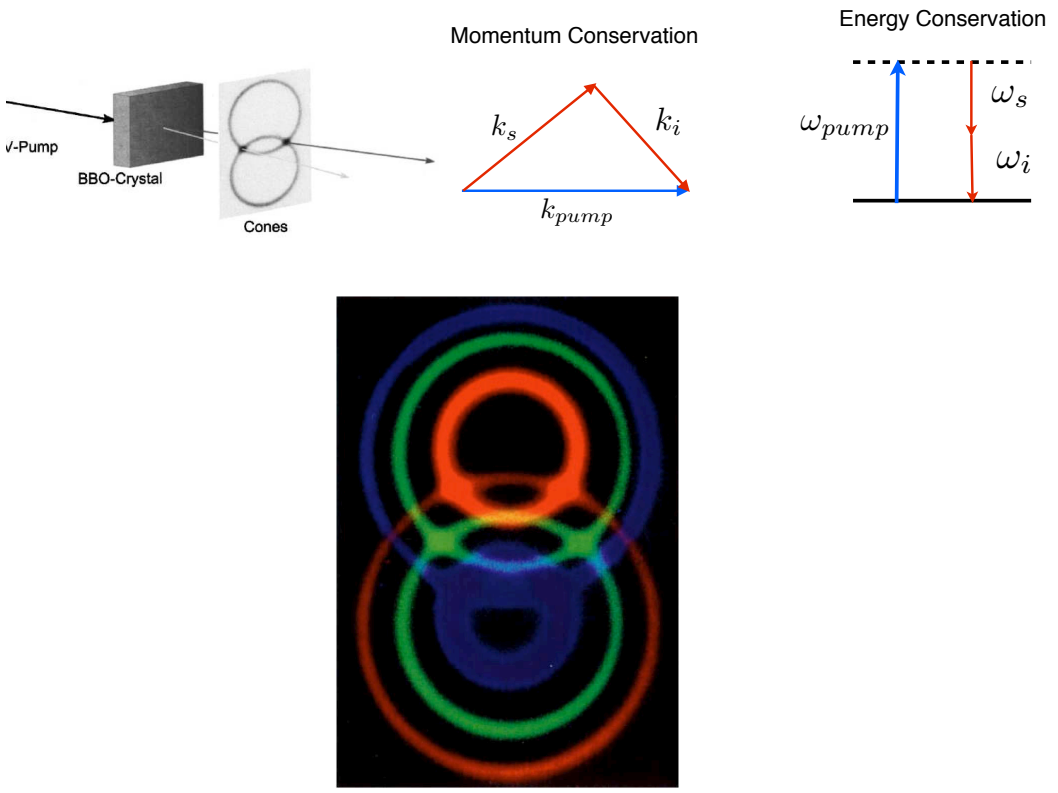

Figure 1.5: Schematic of type-II parametric down conversion to produce directed beams of polarization entangled photons An incident pump photon can spontaneously decay into two photons which are entangled in momentum and energy. Each photon can be emitted along a cone in such a way that two photons of a pair are found opposite to each other on the respective cones. The two photons are orthogonally polarized. Along the directions where the two cones overlap, one obtains polarization-entangled pairs.

tions lead to a polarization-entangled state,

$$|\psi\rangle = \frac{1}{\sqrt{2}} \left[|H\rangle_1 |V\rangle_2 - |V\rangle_1 |H\rangle_2 \right]. \tag{1.21}$$

Here H and V stand for the horizontal and vertical polarization respectively. Note that this being one of the four Bell states, is a maximally entangled state in the polarization basis. Further progress in experiments have demonstrated such polarization entanglement over large distances [19]. SPDC is till now the most widely used method of producing entangled photon states. Several quantum information protocols like teleportation, key distribution, cryptography and communication have been implemented using such polarization entangled photons in recent times [5, 20, 21, 22, 23, 24, 25].

1.2.3 Other methods

The problem with spontaneous down conversion as a source of entanglement is its low efficiency and probabilistic nature. During the last few years several other systems have been investigated for achieving a stable source of entanglement. In particular laser cooled trapped ions [26, 27, 28], cascade emission from semiconductor quantum dots [29, 30, 31, 32] and cold atoms in optical lattices [33, 34, 35, 36] have turned out to be promising alternatives for entanglement generation. Studies invoking coherent interactions (coulomb and dipolar) among ions and trapped atoms have shown the implementation and working of basic quantum logic gates like the C-NOT and phase gates. Systems of a few trapped ions (see Fig. 1.6) have demonstrated quantum-entanglement engineering with high fidelity and are promising candidates for scalable quantum computing. Another approach of using atomic systems for entanglement generation are the cavity-QED techniques This involves quantum optical manipulations and control of coherently exchanging single atoms and excitation between radiation field (see Fig. 1.7). Further control of loss or decoherence rate, including atomic spontaneous emission and photon leakage from the cavity is also under active

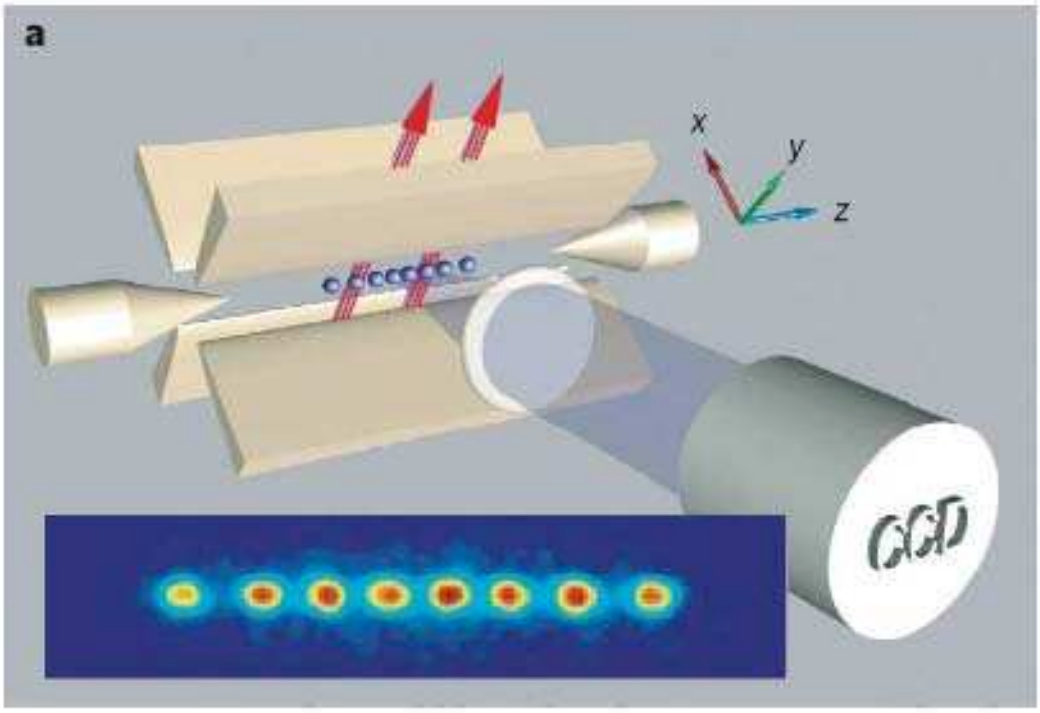

Figure 1.6: A linear quadrupole ion trap containing individually addressed $^{40}Ca^{+}$ ions (blue) is depicted. After cooling by laser beams (red), the trapped ions form a string and are then imaged by using a charge-coupled device (CCD). In the CCD image shown, the spacing of the two centre ions is $\sim 8\mu$m. Figure courtesy: Rainer Blatt and D. J. Wineland, Nature **453**, 1008 (2008)

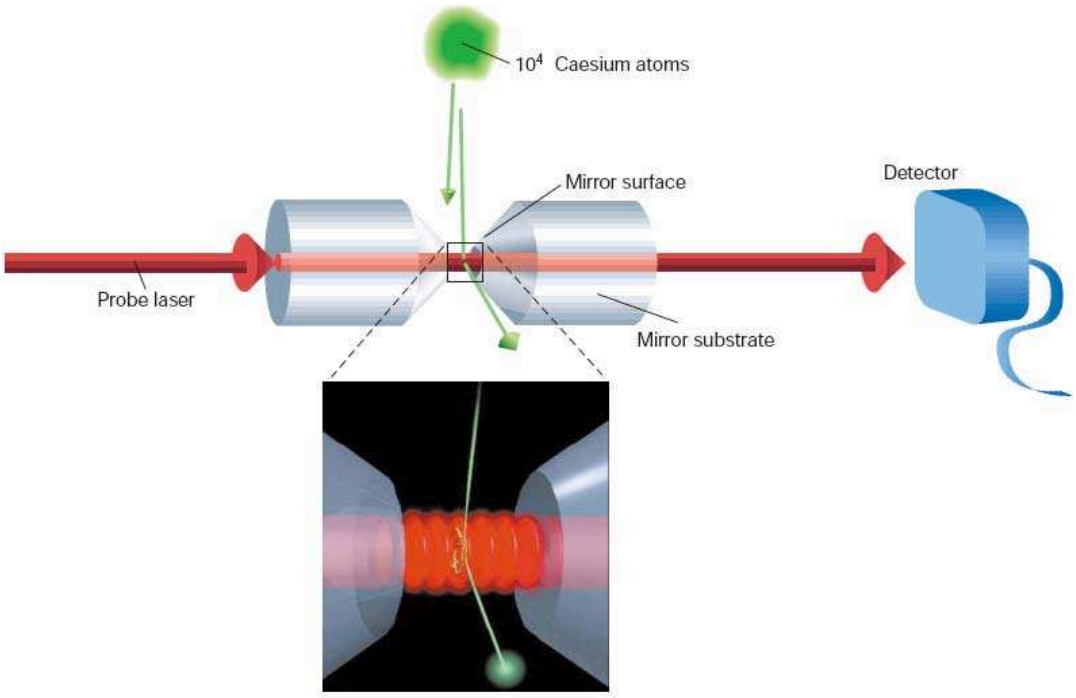

Figure 1.7: Single-atom cavity-QED experiment. Cold caesium atoms are dropped into a high-finesse optical cavity of axial spacing 10 μm. The trajectory of a single atom traversing the cavity is reconstructed (inset) by monitoring the field that leaks out of the cavity. Figure courtesy : C. Monroe, Nature **416**, 238 (2002).

investigations. Several groups across the world are currently working towards this goal [37, 38, 39, 40, 41]. The discovery that optically excited semiconductor quantum dots (QD) can behave as single two level atoms [42, 43, 44, 45, 46, 47, 48, 49, 50] has created the possibility of using the QDs as solid state qubits for quantum computation. Moreover, methods for quantum logic gate implementation with QDs using the coupling or exchange tunneling between two QDs have been proposed [51, 52, 53, 54]. These experiments have created enormous interest in the study of QD system with focus on potential application in quantum information and quantum computation. Recently both charge and spin degrees of freedom in QDs have been studied for the generation of entangled photons (see for example Fig. 1.8) and implementation of quantum logic gates [30, 32, 53, 55, 56].

Further, in last few years studies of nonclassical correlation in evanescently coupled waveguides [57, 58, 59, 60, 61, 62] have shown their utility for entanglement generation [63, 64]. In recent experiments coupled waveguides have been used in realization of a quantum controlled NOT gate [64] and generation of a multimode interferometer on an integrated chip experiment [65, 66]. Further such interferometers can be used to generate arbitrary quantum circuits and entangled states like the NOON states [67].

1.3 Characterization of entanglement

One of the most difficult and less understood aspect of entanglement is its characterization. During the last decade many studies have appeared on this subject (see ref [16] for a detailed account of this). Currently there exists well defined measures of entanglement for bi-partite systems but a definitive multipartite entanglement measure is not yet known. In this section we discuss these bi-partite entanglement measures. In particular we discuss the two qubit concurrence introduced first by Wootters [68] and the Gaussian entanglement measures [70, 71, 72, 73] useful for continuous variable systems. These measures will be later used extensively in chapter (5) and (6) of

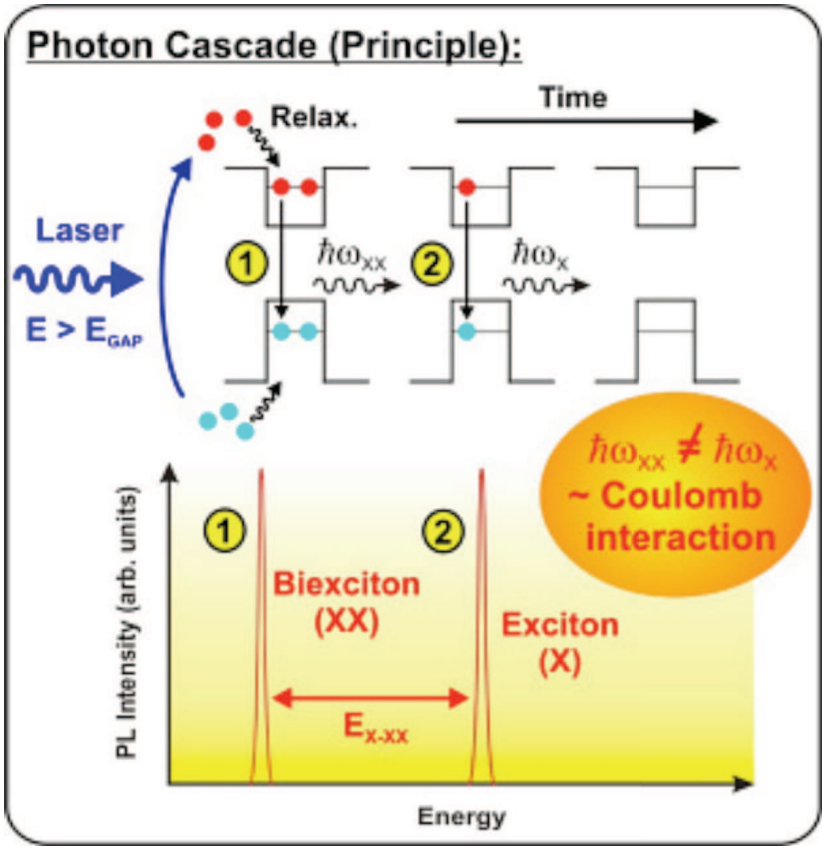

Figure 1.8: Schematic of single and paired photon emission in cascade decay from II-VI and III-V quantum dots. Figure source: www.ihfg.uni-stuttgart.de/.../ullrich/fig2.jpg

the thesis.

1.3.1 Peres separability criterion

A necessary condition for separability of quantum states has been provided by Peres [73], called the positive partial transpose or PPT criterion. It says that if ρ_{AB}, the density matrix of a composite system made of two subsystem A and B, is separable then the new matrix $\rho_{AB}^{T_B}$ with elements defined in some fixed product basis as,

$$\langle m|\langle \mu|\rho_{AB}^{T_B}|n\rangle|\nu\rangle \equiv \langle m|\langle \nu|\rho_{AB}|n\rangle|\mu\rangle, \tag{1.22}$$

will also be a density operator meaning that $\rho_{AB}^{T_B}$ is also a quantum state (it also guarantees the positivity of $\rho_{AB}^{T_A}$ defined in an analogous way). The operation T_B, called a partial transpose, corresponds to transposition of indices corresponding to the second subsystem. Thus when a density operator corresponding to a quantum state fails to satisfy this criterion we can say the quantum state of the bi-partite system is in as entangled state.

1.3.2 Entanglement witness

Entanglement witnesses [16, 74, 75] is another fundamental measure in quantum entanglement theory. These are observables that completely characterize separable states and allow us to detect entanglement physically. According to this measure, the state ρ_{AB} of a bi-partite system belongs to the set of separable states if it has a non-negative mean value,

$$Tr(W\rho_{AB}) \geq 0, \tag{1.23}$$

for all observables W that (a) have at least one negative eigenvalue and (b) have a non-negative mean value on product states or equivalently satisfy the non-negativity condition

$$\langle \psi_A|\langle \phi|W|\psi_A\rangle|\phi_B\rangle \geq 0, \tag{1.24}$$

for all pure product states $|\psi_A\rangle|\phi_B$. The observables W satisfying conditions (a) and (b) above are called the *entanglement witnesses* [75]. Thus, such observables can be said to be entanglement detectors. In particular, one says that entanglement of ρ is detected by witness W if and only if $Tr(W\rho) < 0$ (see the Fig 1.9).

1.3.3 Concurrence

The entanglement for any bipartite qubit system is best identified by examining the concurrence [68, 76, 77], an entanglement measure that relates to the density matrix of the system ρ. Concurrence is a entanglement monotone *i.e.* it cannot be increased by any local operations on the system. The concurrence for a bipartite system is defined as,

$$C(t) = \max\{0, \sqrt{\lambda_1} - \sqrt{\lambda_2} - \sqrt{\lambda_3} - \sqrt{\lambda_4}\}, \tag{1.25}$$

where λ's are the eigenvalues of the non-hermitian matrix $\rho(t)\tilde{\rho}(t)$ arranged in decreasing order of magnitude. The matrix $\rho(t)$ being the density matrix for the bipartite system and the matrix $\tilde{\rho}(t)$ is defined by,

$$\tilde{\rho}(t) = (\sigma_y^{(1)} \otimes \sigma_y^{(2)})\rho^*(t)(\sigma_y^{(1)} \otimes \sigma_y^{(2)}), \tag{1.26}$$

where $\rho^*(t)$ is the complex conjugation of $\rho(t)$ and σ_y is the well known time reversal operator for spin half systems in quantum mechanics,

$$\sigma_y = \begin{pmatrix} 0 & -i \\ i & 0 \end{pmatrix}. \tag{1.27}$$

In the basis defined in equation (1.2) the $\sigma_y^{(1)} \otimes \sigma_y^{(2)}$ operator is given by,

$$\sigma_y^{(1)} \otimes \sigma_y^{(2)} = \begin{pmatrix} 0 & 0 & 0 & -1 \\ 0 & 0 & 1 & 0 \\ 0 & 1 & 0 & 0 \\ -1 & 0 & 0 & 0 \end{pmatrix}. \tag{1.28}$$

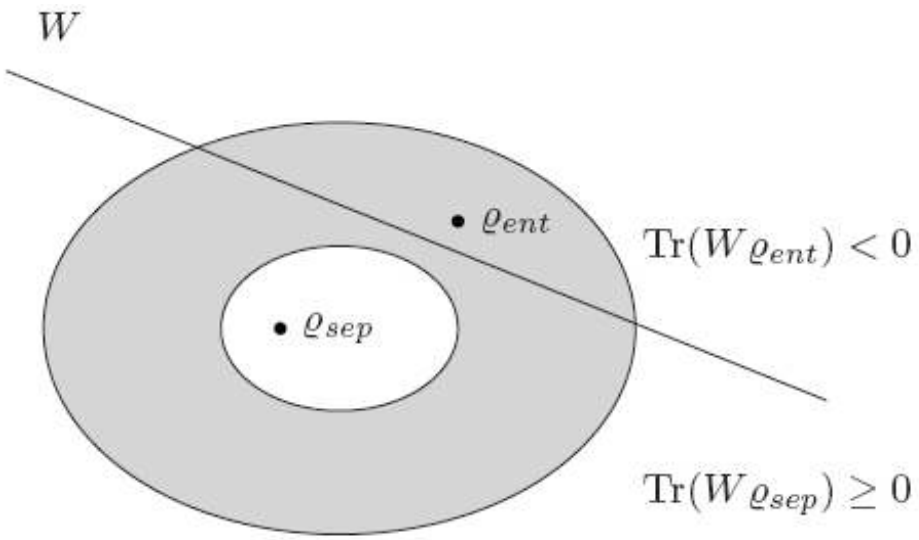

Figure 1.9: The line represents a hyperplane corresponding to the entanglement witness W. All states located to the left of the hyperplane or belonging to it in particular, all separable states provide non-negative mean value of the witness, *i.e.*, $Tr(W\rho_{sep}) \geq 0$ while those located to the right are entangled states detected by the witness.

Note that concurrence varies from $C = 0$ for a separable state to $C = 1$ for a maximally entangled state like the Bell states. The importance of the measure stems from the fact that it allows us to compute the entanglement of formation for two qubits according to [68]

$$E_F = H\left(\frac{1+\sqrt{1-C^2(\rho)}}{2}\right) \tag{1.29}$$

where H is the binary entropy $H(x) = -x\log_2 x - (1-x)\log_2(1-x)$.

1.3.4 Negativity

A simple computable measure of bipartite entanglement termed negativity was introduced first by Zyczkowski *et. al.* [69] and later shown by Vidal and Werner [78] to be a monotone,

$$\mathcal{N} = \sum_{\lambda<0} \lambda, \tag{1.30}$$

where λ are eigenvalues of ρ_{AB}^{PT}. Here PT is a partial transpose with respect to one of the subsystems A or B of the composite system matrix ρ_{AB} . A version of the measure called logarithmic negativity is given by,

$$\begin{aligned} E_{\mathcal{N}}(t) &= \log_2 \parallel \rho^{PT} \parallel, \\ \parallel \rho^{PT} \parallel &= (2\mathcal{N}(\rho)+1) \ , \end{aligned} \tag{1.31}$$

and is the upper bound for distillable entanglement [78]. Here the symbol $\|\,\|$ denotes the trace norm and $\mathcal{N}(\rho)$ is the absolute value of the sum of all the negative eigenvalues of the partial transpose of ρ. The log negativity is a non-negative quantity and a non-zero value of $E_{\mathcal{N}}$ would mean that the state is entangled.

1.3.5 Characterization of continuous variable entanglement

In the famous EPR paper [7] Einstein, Podolsky and Rosen considered a two particle state quantum mechanically correlated with respect to their position and momenta.

They defined a position wavefunction

$$\psi(x_1, x_2) = C\delta(x_1 - x_2 - u), \tag{1.32}$$

with a vanishing normalization constant C. Hence the corresponding quantum state,

$$\int dx_1 dx_2 \psi(x_1, x_2)|x_1, x_2\rangle \propto \int dx|x, x - u\rangle, \tag{1.33}$$

describes perfectly correlated positions ($x_1 - x_2 = u$) and momenta (total momentum zero, $p_1 + p_2 = 0$) [79]. This wavefunction happens to be the first known example of an entangled state. Moreover as the position and momentum variables x_i, p_i can vary continuously in an infinite dimensional space, this wave function is also the first example of continuous variable entanglement. Thus though discrete variable or qubit entanglement came to focus with the advent of quantum information science, entanglement itself came to light in continuous variable setting. The study of continuous variable entanglement has gained much interest in recent times with the observation that many of the quantum communication protocols is achievable in quantum optics utilizing continuous quadrature amplitude of the quantized electromagnetic field (see for example ref. [79] for a comprehensive review on this subject). In this section we focus on how to get a measure of entanglement in case of continuous variables.

Let us consider a continuous variable (CV) system, described by the Hilbert space $\mathcal{H} = \otimes_{i=1}^{n} \mathcal{H}_i$ resulting from the tensor product of the infinite-dimensional Fock spaces $\mathcal{H}_i$'s. Let a_j be the annihilation operator acting on $\mathcal{H}_j$, and $\hat{x}_j = \frac{(a_j + a_j^\dagger)}{\sqrt{2}}$ and $\hat{p}_j = \frac{(a_j - a_j^\dagger)}{\sqrt{2}i}$ be the related quadrature phase operators. The corresponding phase space variables will be denoted by $\hat{x}_i$ and $\hat{p}_i$. Let us then group together the operators $\hat{x}_i$ and $\hat{p}_i$ in a vector of operators $\hat{X} = (\hat{x}_1, \hat{p}_1, ..., \hat{x}_n, \hat{p}_n)$. The canonical commutation relations for the $\hat{X}_i'$s are encoded in the symplectic form $\mathbf{\Omega}$:

$$\begin{aligned} \left[\hat{X}_i, \hat{X}_j\right] &= i\Omega_{ij} \\ \mathbf{\Omega} \equiv \oplus_{i=1}^{n} \omega \qquad & \omega = \begin{pmatrix} 0 & 1 \\ -1 & 0 \end{pmatrix}. \end{aligned} \tag{1.34}$$

There is a class of CV states that are well characterized with respect to separability. This is the class of Gaussian states with Gaussian characteristic functions and quasiprobability distributions. Therefore a Gaussian state ρ is completely characterized by its first and second statistical moments, which form respectively, the vector of first moments $\bar{X} \equiv (\langle \hat{X}_1 \rangle, \langle \hat{X}_1 \rangle, ...\langle \hat{X}_n \rangle, \langle \hat{X}_n \rangle)$ and the covariance matix of elements σ:

$$\sigma_{ij} \equiv \frac{1}{2}\langle \hat{X}_i \hat{X}_j + \hat{X}_j \hat{X}_i \rangle - \langle \hat{X}_i \rangle \langle \hat{X}_j \rangle, \tag{1.35}$$

where for any obervable $\hat{O}$ the expectation value $\langle \hat{O} \rangle = Tr(\rho \hat{O})$. As the first statistical moments can be arbitrarily adjusted by local unitary operations, it does not affect any property related to entanglement or mixedness and thus the behavior of the covariance matrix σ is all important for the study of entanglement.

Let us now consider the hermitian operator $\hat{y} = Y\hat{X}^T$, where $Y \epsilon \mathcal{R}^{2n}$ is an arbitrary real $2n$-dimensional row vector. Positivity of ρ imposes the condition $Tr(\rho \hat{y}^2) \geq 0$ which can be simply recast in terms of second moments as $Y \eta Y^T \geq 0$, with $\eta_{ij} = \langle \hat{X}_i \hat{X}_j \rangle$. This relation along with the canonical commutation relations, can be used in conjunction with equation (1.35) and the arbitrarity nature of Y, to recast the Heisenberg uncertainty principle in the form

$$\sigma + \frac{i}{2}\mathbf{\Omega} \geq 0. \tag{1.36}$$

The *uncertainty principle* (1.36) is the necessary and sufficient constraint σ has to fulfill to be a true covariance matrix [81, 82]. Note that such a constraint implies $\sigma \geq 0$. Based on this uncertainty principle involving the covariance matrix and invoking the Peres [73] separability criterion two different ways of studying Gaussian entanglement has been proposed. One of them is a inequality due to Simon [70] and the other is the logarithmic negativity for Gaussian states [71].

Simon's inequality

Simon recognized that the partial transpose operation on the density matrix ρ defining a bi-partite quantum state acquires, in the continuous variable case, a beautiful geometric interpretation as a mirror reflection in the Wigner phase space. The Wigner distribution of a separable ρ remains a Wigner distribution. This essentially implies that the covariance matrix $\sigma \rightarrow \tilde{\sigma} = \Lambda\sigma\Lambda$, where $\Lambda = \mathsf{diag}(1, 1, 1-1)$. The uncertainty principle then takes the form

$$\tilde{\sigma} + \frac{i}{2}\mathbf{\Omega} \geq 0. \tag{1.37}$$

Thus now for the state to be separable both (1.36) and (1.37) has to be satisfied. Simon used this restriction and the Peres-Horodecki [73, 80] criterion of positivity to derived an inequality

$$\det A \det B + \left(\frac{1}{4} - |\det C|\right)^2 - \mathsf{tr}(A\omega C\omega B\omega C^T\omega) \geq \frac{1}{4}(\det A + \det B), \tag{1.38}$$

where the covariance matrix has a block form

$$\sigma = \begin{pmatrix} A & C \\ C^T & B \end{pmatrix}, \tag{1.39}$$

and A, B, C are 2×2 matrices given by,

$$A = \begin{bmatrix} \langle x_1^2 \rangle & \langle \frac{x_1p_1+p_1x_1}{2} \rangle \\ \\ \langle \frac{x_1p_1+p_1x_1}{2} \rangle & \langle p_1^2 \rangle \end{bmatrix}; \tag{1.40}$$

$$B = \begin{bmatrix} \langle x_2^2 \rangle & \langle \frac{x_2p_2+p_2x_2}{2} \rangle \\ \\ \langle \frac{x_2p_2+p_2x_2}{2} \rangle & \langle p_2^2 \rangle \end{bmatrix}; \tag{1.41}$$

$$C = \begin{bmatrix} \langle \frac{x_1x_2+x_2x_1}{2} \rangle & \langle \frac{x_1p_2+p_2x_1}{2} \rangle \\ \\ \langle \frac{x_2p_1+p_1x_2}{2} \rangle & \langle \frac{p_1p_2+p_2p_1}{2} \rangle \end{bmatrix}. \tag{1.42}$$

This inequality (eqn. 1.38) shows that the Peres-Horodecki criterion is a necessary and sufficient separability condition for all bipartite Gaussian states. Thus any Gaussian state whose covariance matrix violates this inequality can be said to be entangled.

Logarithmic negativity

The measure of entanglement for a Gaussian state can also be characterized by the logarithmic negativity $E_{\mathcal{N}}$, a quantity evaluated in terms of the symplectic eigenvalues of the covariance matrix σ [71]. The elements of the covariance matrix σ are given in terms of the conjugate observables x and p in the form (1.40, 1.41) and (1.42). The condition for entanglement of a Gaussian state is derived from the positive partial transpose (PPT) criterion [73, 70], according to which the smallest symplectic eigenvalue $\tilde{\nu}_<$ of the transpose of matrix σ should satisfy

$$\tilde{\nu}_< < \frac{1}{2}, \tag{1.43}$$

where $\tilde{\nu}_<$ is defined as

$$\tilde{\nu}_< = \mathsf{min}[\tilde{\nu}_+, \tilde{\nu}_- \,] \tag{1.44}$$

and $\tilde{\nu}_\pm$ is given by,

$$\tilde{\nu}_\pm = \sqrt{\frac{\tilde{\Delta}(\sigma) \pm \sqrt{\tilde{\Delta}(\sigma)^2 - 4\mathsf{Det}\sigma}}{2}} \quad , \tag{1.45}$$

where $\tilde{\Delta}(\sigma) = \Delta(\tilde{\sigma}) = \mathsf{Det}(\alpha) + \mathsf{Det}(\beta) - 2\mathsf{Det}(\mu)$. Thus according to the condition (3.5) when $\tilde{\nu}_< \geq 1/2$ a Gaussian state become separable. The corresponding quantification of entanglement given in terms of the logarithmic negativity $E_{\mathcal{N}}$ [71, 78, 69] is then defined as,

$$E_{\mathcal{N}} = \mathsf{max}[0, -\ln\{2\tilde{\nu}_<\}]. \tag{1.46}$$

Thus according to this quantification, for a Gaussian state ρ if $E_{\mathcal{N}} > 0$ the state is entangled and the amount of entanglement is given by the value of $E_{\mathcal{N}}$.

Duan-Giedke-Cirac-Zoller inequality

An inseparability criterion based on the total variance of a pair of Einstein-Podolsky-Rosen (EPR) type operators was proposed for CV systems by Duan, Giedke, Cirac and Zoller [72]. They considered the following EPR like operators,

$$\begin{aligned} \hat{u} &= |a|\hat{x}_1 + \frac{1}{a}\hat{x}_2, \\ \hat{v} &= |a|\hat{p}_1 - \frac{1}{a}\hat{p}_2, \end{aligned} \tag{1.47}$$

where a is an arbitrary non-zero real number. They showed that for any separable quantum state ρ, the total variance of any pair of EPR-like operators in the form (1.47) satisfies a lower bound given by the inequality

$$\langle(\Delta\hat{u})^2\rangle + \langle(\Delta\hat{v})^2\rangle \geq a^2 + \frac{1}{a^2} \quad , \tag{1.48}$$

where $\Delta\hat{\alpha} = \hat{\alpha} - \langle\hat{\alpha}\rangle, \hat{\alpha} = \hat{u}, \hat{v}$. This inequality provides a sufficient condition for entanglement of any bipartite continuous variable states. Furthermore, for all Gaussian states ρ whose covariance matrix satisfy the uncertainty principle (1.36) and the restriction (1.37) , this inequality turns out to be a necessary and sufficient condition for inseparability.

1.4 Decoherence

Now that we have discussed quantum entanglement, a key resource in quantum information and quantum computation, we turn our attention to the subject of *decoherence* - a phenomenon that arises as a result of unavoidable system-environment coupling. The study of decoherence is of fundamental importance being the prime reason of apparent absence of quantum signatures (like the superposition principles) at a macroscopic level [83]. Its consequences have profound implication in different branches of science ranging from quantum information to molecular chemistry. Further, decoherence is a key obstacle in the control and manipulation of quantum features of

microscopic systems and relating them to the system's macroscopic properties. In the context of quantum information sciences decoherence is extremely important as entanglement is known to be susceptible to it [24]. As such a detailed understanding of the interplay between entanglement and decoherence is of utter importance both from the viewpoint of fundamental knowledge and application. Let us now define and understand what decoherence is and why it poses the biggest obstacle in quantum information

The linearity of the Schrödinger equation in quantum mechanics, assures that if at a certain time instant the physical state of a system is known, its state at a later time can be found from the unitary evolution of the system Hamiltonian. An important underlying condition for this to satisfy is that the system remains closed *i.e.* either isolated or weakly interacting with its surrounding (environment) at all time. In practice however, preparing such an isolated system is not possible and any physical system as it evolves dynamically will interact with its environment and thus get influenced by the interaction. This thereby renders the system open and thus its evolution remains no longer unitary. Hence, we have a irreversible loss of information about the system properties due to its interaction with its environment. Consider now a physical system having some initial coherence, then due to its interaction with the environment the environmental degrees of freedom get coupled into this coherence. As these degrees of freedom are typical much larger (infinite) in comparison to that of the system, monitoring the distributed coherence among these degrees are infeasible by any process. Thus one can no longer harness the systems coherence for some useful purpose. This process of irrecoverable loss of quantum coherence of a physical system interacting with its environment is known as *decoherence* [83, 84, 85, 86].

To understand the environment induced decoherence effect better let us next consider a simple system of two level atom with an excited state $|e\rangle$ and ground state $|g\rangle$. The most general density matrix characterising this two level atom can then be

written as,

$$\rho = \rho_{ee}|e\rangle\langle e| + \rho_{gg}|g\rangle\langle g| + \rho_{eg}|e\rangle\langle g| + \rho_{ge}|g\rangle\langle e|. \tag{1.49}$$

Note that the off diagonal terms represent the coherence in the system. Now as the system interacts with the environment during a observation or measurement on a time scale t, the density matrix evolves as

$$\begin{aligned} \rho(t) &= \rho_{ee}|e\rangle\langle e|e^{-t/T_1} + \rho_{gg}|g\rangle\langle g|(1 - e^{t/T_1}) \\ &\quad +[\rho_{eg}|e\rangle\langle g| + \rho_{ge}|g\rangle\langle e|]e^{-t/T_2}. \end{aligned} \tag{1.50}$$

Here T_1 and T_2 correspond to the lifetime of the excited state and the dynamically generated coherences respectively. Now when $t >> T_1, T_2$, we get $\rho_(t \to \infty) = \rho_{gg}|g\rangle\langle g|$, thus the system decays to its ground state. However for $t >> T_2$ but $t < T_1$, which is very common in many microscopic systems we have,

$$\rho(t) = \rho_{ee}|e\rangle\langle e|e^{-t/T_1} + \rho_{gg}|g\rangle\langle g|(1 - e^{-t/T_1}) \tag{1.51}$$

Thus we find that for this time scale the off-diagonal terms have decayed completely thereby causing the system to lose all its coherence. This phenomenon of coherence loss is known as decoherence. Further, it is well known that the rate of decoherence in a system increases exponentially with its size [87]. Thus any non-classical or quantum correlation between two macroscopic system will decay much faster than the response time of the measurement devices. This makes decoherence primarily responsible for the absence of any quantum signatures in our macroscopic world.

How is decoherence an obstacle in the progress of quantum information sciences? To answer this question one has to note that generation of entanglement alone is not sufficient for quantum information and quantum computation. A successful implementation of a quantum computer will require numerous microscopic systems as qubits, and sustained entanglement among the qubits as they evolve dynamically over the period of computation. Thus to use its true potentials one needs to preserve

entanglement over the period of computation. However in any practical realization of quantum information protocols system-environment interaction and hence decoherence would be unavoidable. In addition as decoherence increases rapidly with the size of the system [87] in any realistic computation involving qubits in bulk, entanglement is bound to be severely degraded. In the last few years numerous investigations have shown how decoherence can lead to the decay of entanglement [88, 89, 90, 91] and even to its complete disappearance in a short time [92, 93, 94, 95, 96]. Thus, it is quite clear that one has to control decoherence to be able to harness the power of entanglement for useful application in the field of quantum information sciences.

1.5 Overview

In recent years, much of the scientific research has been motivated towards manipulation of microscopic systems and control of decoherence for useful application in quantum information sciences. Several novel systems like trapped ions, atom in cavities, semiconductor quantum dots (QDs), super-conducting qubits and photonic waveguides have been investigated for the purpose of manipulating the quantum dynamics at a microscopic level. Further, quantum optical studies in atomic and semiconductor systems have led to quantum logic gates implementations using this systems. Semiconductor quantum dots in particular have been found to be promising candidates for basic units in solid state quantum computing. Recently, some success has also been achieved in the manipulation of entanglement in the face of decoherence using coherent light matter interactions [97, 98, 99] and by controlling reservoir properties [100, 101].

We contribute to these endeavors through several interesting and impactful results reported in this thesis. The thesis is primarily focussed on the theoretical study of quantum entanglement and decoherence phenomena in some of the novel microscopic systems which can serve as qubits for quantum computation. We specifically study

trapped ions/neutral atoms, quantum dots and photonic waveguides. We use coherent external electromagnetic fields to manipulate the quantum correlations in these systems and thus achieve external control over the generation and manipulation of entanglement. Moreover, we study the effect of environment induced decoherence on entanglement dynamics in qubits. Our studies are based on the general framework of quantum optics. We use both analytical and numerical techniques. Our predictions are based on realizable experimental parameters and can thus be useful in future experimental implementations.

1.6 Organization

As spontaneous emission is a fundamental limitation on coherence times in atomic systems [102, 103, 104], manipulation and control of the spontaneous emission rate is of great importance in quantum information processing with atoms and ions. Several methods exist to achieve this in atomic systems. One such method is by inducing quantum interference effects known as vacuum induced coherences (VIC)[105]. VIC is a quantum interference effect that arise as a result of interaction between the atomic system and electromagnetic vacuum when certain conditions on the dipole matrix elements between the excited states and the ground state are satisfied. In particular, they have to be non-orthogonal [105, 106]. This in practice is quite hard to realize. It was suggested that the above condition on dipole matrix elements can be bypassed if we consider anisotropic vacuum [107] which for example would be the case while considering emission from excited atoms on nano particles [108]. A recent study by Kiffner et. al.[109] showed that in atomic systems with degenerate transitions j = $1/2 \leftrightarrow$ j = 1/2 VIC effects are prominent. Such degeneracies are commonly found in $^{198}Hg^{+}$ and $^{138}Ba^{+}$ ions in a trap [110, 111]. As these trapped ions can be useful for quantum information processing it is important to study the effect of VIC in these systems.

In chapter 2 we begin our investigation by studying vacuum induced coherence (VIC) effects in trapped ions. We show how the effects of vacuum induced coherence can be realized by studying non-classical photon -photon correlation in the π-polarized fluorescence in j = 1/2 to j = 1/2 transition. The effect of this coherence is reflected in the form of stronger damping and overall larger values of the second order correlation function $G^{(2)}$. These effects should be thus observable in measurements of photon statistics in for example Hg and Ba ion traps.

Chapter 3 describes the generation of a new quantum interference effect in spontaneous emission from a resonantly driven system of two identical two-level atoms due to the spatial variation of the laser phase at the positions of the atoms. This interference affects significantly the spectral features of the emitted radiation and the quantum entanglement in the system. The interference leads to dynamic coupling of the populations and coherences in a basis, determined by the laser phase and represents a kind of vacuum mediated super-exchange between the symmetric and antisymmetric states. This can thus enhance and suppress the spontaneous emission rate in the system.

Chapter 4 presents a theoretical model to study the Intensity-Intensity correlation of polarisation entangled photons emitted in a biexciton-exciton cascade. We calculate the degree of correlation and show how polarisation correlations are affected by the presence of dephasing and energy level splitting of the excitonic states. Our theoretical calculations are in agreement with the recent observation of polarisation dependent Intensity-Intensity correlations from a single semiconductor quantum dot [R. M. Stevenson *et. al. Nature* **439**, 179 (2006)] . Our model can be extended to study polarisation entangled photon emission in coupled quantum dot systems.

Chapter 5 discusses the competition between the dissipative and coherent effects in the entanglement dynamics of two qubits. The coherent interactions are needed for designing logic gate operations with systems like ion traps, semicondutor quantum

dots and atoms. We show that the interactions lead to a phenomenon of periodic disentanglement and entanglement between the qubits. The disentanglement is primarily caused by environmental perturbations. The qubits are seen to remain disentangled for a finite time before getting entangled again. We find that the phenomenon is generic and occurs for wide variety of models of the environment. We present analytical results for the time dependence of concurrence for all the models. The periodic disentanglement and entanglement behavior is seen to be precursor to the sudden death of entanglement (ESD) and can happen, for environments which do not show ESD for noninteracting qubits. Further we also find that this phenomenon can even lead to delayed death of entanglement for correlated environments.

Chapter 6 discusses the viability of coupled waveguides as basic units of quantum circuits. In particular, we study the dynamics of entanglement for the single mode and two mode squeezed vacuum state. We present explicit analytical results for the measure of entanglement in terms of the logarithmic negativity. We also address the effect of loss on entanglement dynamics of waveguide modes. Our results indicate that the waveguide structures are reasonably robust against the effect of loss and thus quite appropriate for quantum architectures.

Finally in chapter 8, we give concluding remarks and indicate the future directions for further work .

CHAPTER 2

PHOTON-PHOTON CORRELATION AS A PROBE OF VACUUM INDUCED COHERENCES IN TRAPPED IONS

2.1 Overview

An early work [105] had predicted an unusual effect of quantum interference in the problem of spontaneous emission. It was shown that in a degenerate V-system one could get population trapping and generation of quantum coherences in the excited states. This comes due to the interference between different channels of spontaneous emission. One of the key conditions for the occurrence was that the dipole matrix elements of the two transitions from the excited states to the common ground state were non-orthogonal. In the meanwhile a very large body of theoretical literature has been devoted to the subject of vacuum induced coherences [112, 113, 114, 115, 116, 117, 118, 119] and a nice review is given in Ref [112]. It was also suggested how the above condition on dipole matrix elements can be bypassed if we consider anisotropic vacuum [107] which for example would be the case while considering emission from excited atoms on nano particles [108]. We thus look for possible realistic systems where vacuum induced coherences (VIC) are observable. Kiffner et. al.[109] showed that an atomic system with degenerate transitions j = 1/2 $\leftrightarrow$ j = 1/2 would be a suitable system where effects of VIC are prominent. They showed how vacuum induced coherences change the spectrum of the emitted radiation. While the results of Kiffner et. al. on the spectrum are quite interesting much of the current experimental effort [110, 120, 121, 122] is focussed on the study of photon-photon correlations [123]. Thus one would like to understand if the vacuum

induced coherences significantly affect the photon-photon correlations. This is the question we examine. The significance of VIC depends on the system under consideration. We deal specifically with the j = 1/2 to j = 1/2 transitions. The details of which are given in the next section where we also explain how VIC are important for such a system. We mention explicitly two systems where we have such transitions and thus these systems would, for example, be candidates for the effect of VIC on photon-photon correlations. These systems are : (A) a single $^{198}Hg^{+}$ ion in a trap [110] and (B) a single $^{138}Ba^{+}$ ion in a trap [120]. In both the cases the ground level is $6s^2S_{1/2}$ and the excited level is $6p^2P_{1/2}$. The measurement of photon-photon correlation for such multilevel systems can be done in the standard way (see [120] and F. Diedrich et. al. [123]).

It may be added that the photon-photon correlations have acquired new significance in the context of quantum information processing and quantum imaging as well as in interferences from independent atoms [121, 122, 124]. Thus it is pertinent to check if VIC effects are to be included in the calculation of photon-photon correlations for a given experimental system.

The organization of this chapter is as follows-in Sec 2 we introduce the model and present the working equations. In Sec 3 we calculate the photon-photon correlations both in presence and in absence of the vacuum induced interference effects. In Sec 4 we present numerical results to highlight the effects of vacuum induced coherences on photon-photon correlations. In Sec 5 we conclude with the outlook and future directions.

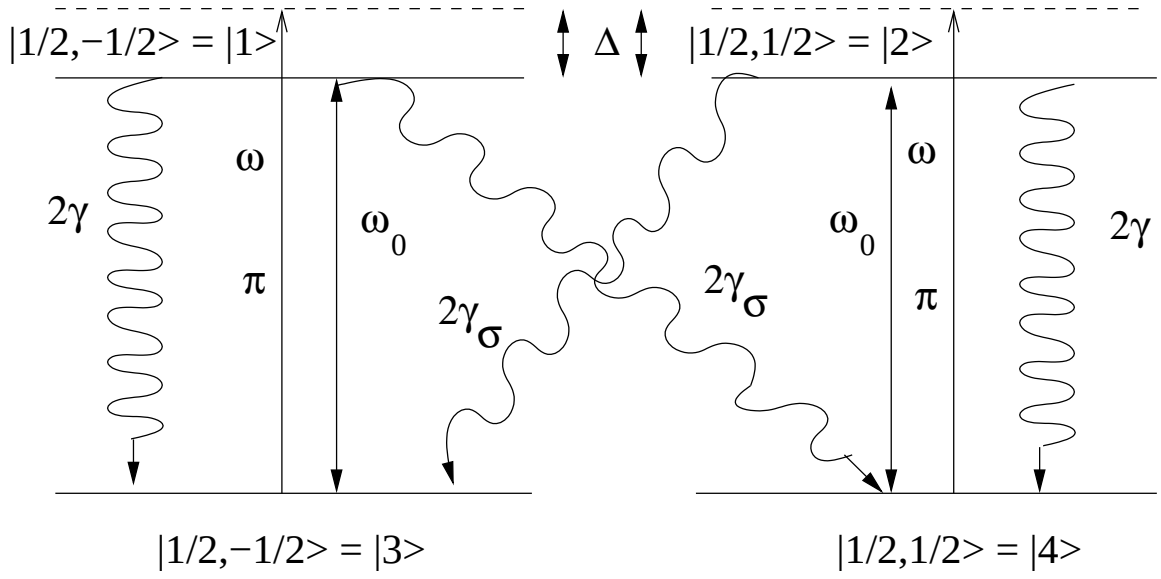

Figure 2.1: Schematic diagram of a four-Level atom modelled by j = 1/2 to j = 1/2 transition

2.2 Model

Fig. (2.1) shows the level scheme of a four-level atom modelled by a j = 1/2 to j = 1/2 transition. This kind of level scheme is realizable for example in $^{198}Hg^{+}$ [110] and $^{138}Ba^{+}$[120] ions. The ground level is $6s^2S_{1/2}$ and the excited level is $6p^2P_{1/2}$. Each of these levels is two fold degenerate. We exhibit the magnetic sub-levels explicitly. The nature of transitions between these levels can be found from various dipole matrix elements. The dipole matrix elements can be obtained from the Wigner-Eckart theorem and the Clebsch-Gordon coefficients. These are found to be

$$\begin{aligned} \vec{d}_{31} = -\vec{d}_{42} = -\frac{1}{\sqrt{6}}\mathcal{D}\hat{e}_z \ , \\ \vec{d}_{41} = \vec{d}^{*}_{32} = \frac{1}{\sqrt{3}}\mathcal{D}\hat{\epsilon}_- \ , \end{aligned} \tag{2.1}$$

with $\hat{\epsilon}_- = (\hat{x} - i\hat{y})/\sqrt{2}$ and $\hat{e}_z$ is the unit vector along the z-direction. In Eq. (2.1) $\mathcal{D}$ denotes the reduced matrix element of the dipole moment operator $\mathbf{d}$. Thus the transitions $|1\rangle \leftrightarrow |4\rangle$ and $|2\rangle \leftrightarrow |3\rangle$ couple to σ^+ and σ^- polarized light respectively. The transitions $|1\rangle \leftrightarrow |3\rangle$ and $|2\rangle \leftrightarrow |4\rangle$ couple to light linearly polarized along the $\hat{e}_z$. The spontaneous decays of the excited state to the two ground states are given by 2γ and $2\gamma_\sigma$ as shown in the figure. The spontaneously emitted photons are π-polarized on the transitions $|1\rangle \leftrightarrow |3\rangle$, $|2\rangle \leftrightarrow |4\rangle$ whereas these are σ-polarized on the transitions $|1\rangle \leftrightarrow |4\rangle$, $|2\rangle \leftrightarrow |3\rangle$. The four-level system is driven by a π polarized monochromatic field of frequency ω ,

$$\mathbf{E}(t) = \mathcal{E}_0 e^{-i\omega t}\mathbf{e}_z + c.c. \ , \tag{2.2}$$

were c.c is the complex conjugate. With this particular choice of polarization, the driving field couples only to the two transitions $|1\rangle \leftrightarrow |3\rangle$ and $|2\rangle \leftrightarrow |4\rangle$. The total Hamiltonian for this atom-field system is given by

$$\mathcal{H} = \mathcal{H}_A + \mathcal{H}_I \ , \tag{2.3}$$

where the unperturbed Hamiltonian for the atom is,

$$\mathcal{H}_A = \hbar \sum_{i=1}^{2} \omega_0 |i\rangle\langle i| \ , \tag{2.4}$$

where energies are measured from the ground level. The interaction Hamiltonian is given by

$$\begin{aligned} \mathcal{H}_I &= -\mathbf{d}.\mathbf{E}(\mathbf{t}) \\ &= \hbar\Omega(|1\rangle\langle 3| - |2\rangle\langle 4|)e^{-i\omega t} + H.c \ , \end{aligned} \tag{2.5}$$

where H.c is the Hermitian conjugate and Ω is the Rabi frequency defined by

$$\Omega = \mathcal{E}_0 \frac{\vec{d}_{42} \cdot \hat{e}_z}{\hbar} \ = \frac{1}{\sqrt{6}} \mathcal{D}\mathcal{E}_0/\hbar; \, , \tag{2.6}$$

The time evolution of this four level system is investigated by studying the density matrix equation. The spontaneous emission is included via the master equation techniques. Following the standard procedure [105] we obtain,

$$\begin{aligned} \dot{\rho} &= -\frac{i}{\hbar}[\mathcal{H}, \rho] + \mathcal{L}\rho \ , \\ \mathcal{L}\rho &= -\gamma_\sigma[|1\rangle\langle 1|\rho + |2\rangle\langle 2|\rho + \rho|1\rangle\langle 1| \\ &+ \rho|2\rangle\langle 2| - 2|3\rangle\langle 3|\rho_{22} - 2|4\rangle\langle 4|\rho_{11}] \\ &- \gamma[|1\rangle\langle 1|\rho + |2\rangle\langle 2|\rho + \rho|1\rangle\langle 1| \\ &+ \rho|2\rangle\langle 2| - 2|3\rangle\langle 3|\rho_{11} - 2|4\rangle\langle 4|\rho_{22}] \\ &+ \gamma[|4\rangle\langle 3|\rho_{21} + |3\rangle\langle 4|\rho_{12}] \ , \end{aligned} \tag{2.7}$$

The last two terms in Eq. (2.7) arise from the vacuum induced interference and it comes as the dipole matrix elements $\vec{d}_{13}$ and $\vec{d}_{24}$ are anti-parallel. In a frame rotating with the frequency of the coherent drive the density matrix equations are,

$$\begin{aligned} \dot{\tilde{\rho}}_{11} &= i\Omega^*\tilde{\rho}_{13} - i\Omega\tilde{\rho}_{31} - 2\Gamma\tilde{\rho}_{11} \ , \\ \dot{\tilde{\rho}}_{22} &= i\Omega\tilde{\rho}_{42} - i\Omega^*\tilde{\rho}_{24} - 2\Gamma\tilde{\rho}_{22} \ , \end{aligned}$$

$$
\begin{aligned}
\dot{\tilde{\rho}}_{33} &= i\Omega\tilde{\rho}_{31} - i\Omega^*\tilde{\rho}_{13} + 2\gamma_\sigma\tilde{\rho}_{22} + 2\gamma\tilde{\rho}_{11} \ , \\
\dot{\tilde{\rho}}_{12} &= -i\Omega\tilde{\rho}_{32} - i\Omega^*\tilde{\rho}_{14} - 2\Gamma\tilde{\rho}_{12} \ , \\
\dot{\tilde{\rho}}_{13} &= -i\Delta\tilde{\rho}_{13} + i\Omega(\tilde{\rho}_{11} - \tilde{\rho}_{33}) - \Gamma\tilde{\rho}_{13} \ , \\
\dot{\tilde{\rho}}_{14} &= -i\Delta\tilde{\rho}_{14} - i\Omega\tilde{\rho}_{12} - i\Omega\tilde{\rho}_{34} - \Gamma\tilde{\rho}_{14} \ , \\
\dot{\tilde{\rho}}_{23} &= -i\Delta\tilde{\rho}_{23} + i\Omega\tilde{\rho}_{21} + i\Omega\tilde{\rho}_{43} - \Gamma\tilde{\rho}_{23} \ , \\
\dot{\tilde{\rho}}_{24} &= -i\Delta\tilde{\rho}_{24} - i\Omega(\tilde{\rho}_{22} - \tilde{\rho}_{44}) - \Gamma\tilde{\rho}_{24} \ , \\
\dot{\tilde{\rho}}_{34} &= -i\Omega\tilde{\rho}_{32} - i\Omega^*\tilde{\rho}_{14} + \gamma\tilde{\rho}_{12} \ ,
\end{aligned}
\tag{2.8}
$$

where

$$
\begin{aligned}
\tilde{\rho}_{ii} = \rho_{ii}; \qquad \tilde{\rho}_{12} = \rho_{12}, \qquad \tilde{\rho}_{34} = \rho_{34}; \\
\tilde{\rho}_{ij} = \rho_{ij}e^{-i\omega t}; \qquad (i = 1,2; j = 3,4) \\
\Gamma = (\gamma_\sigma + \gamma); \qquad \Delta = \omega - \omega_{13} = \omega - \omega_{24} \ ,
\end{aligned}
\tag{2.9}
$$

The remaining equations can be generated by taking complex conjugates and using $\mathrm{Tr}\{\rho\} = 1$. The steady state solution of Eq. (2.8) is found to be

$$
\tilde{\rho}_{12} = \tilde{\rho}_{14} = \tilde{\rho}_{32} = \tilde{\rho}_{34} = 0 \ , \tag{2.10}
$$

$$
\begin{aligned}
\tilde{\rho}_{11} &= \tilde{\rho}_{22} = \frac{1}{2}\frac{|\Omega|^2}{[2|\Omega|^2 + \Gamma^2 + \Delta^2]} \ , \\
\tilde{\rho}_{33} &= \tilde{\rho}_{44} = \frac{1}{2}\frac{|\Omega|^2 + \Gamma^2 + \Delta^2}{[2|\Omega|^2 + \Gamma^2 + \Delta^2]} \ , \\
\tilde{\rho}_{13} &= -\tilde{\rho}_{24} = -\frac{i\Omega}{\Gamma + i\Delta}\{\frac{1}{2}\frac{\Gamma^2 + \Delta^2}{[2|\Omega|^2 + \Gamma^2 + \Delta^2]}\} \ ,
\end{aligned}
\tag{2.11}
$$

As can be seen from Eqs. (2.10) and (2.11) the vacuum induced interference has no effect on the steady state solutions. Thus one should investigate how vacuum induced coherences can show up in dynamical quantities like the correlation functions.

2.3 Photon-Photon Correlations

Since the objective of this chapter is to investigate the observable consequences of the vacuum induced coherence, we focus our attention on the photon statistics of the radiation emitted by our model system. We in particular will calculate photon-photon correlations as currently considerable experimental effort is on such correlations. For this we need to know how to relate the atomic properties with the statistical properties of the spontaneously emitted radiation. The answer to this question already exists in quantum theory. In fact from the existing literature [125], we know that the positive frequency part of the electric-field operator at a point $\vec{r}$ in the far-field zone can be written in terms of the atomic operators as

$$\begin{aligned}
\mathbf{E}^{+}(\vec{r},t) &= \mathbf{E}_0^{+}(\vec{r},t) - k_0^2 \sum_i \{[\hat{R}_i \times (\hat{R}_i \times \vec{d}_{31})|3\rangle\langle 1|_\tau] \\
&+ [\hat{R}_i \times (\hat{R}_i \times \vec{d}_{42})|4\rangle\langle 2|_\tau] + [\hat{R}_i \times (\hat{R}_i \times \vec{d}_{32})|3\rangle\langle 2|_\tau] \\
&+ [\hat{R}_i \times (\hat{R}_i \times \vec{d}_{41})|4\rangle\langle 1|_\tau]\} R_i^{-1} \times e^{-i(k_0 \hat{r}\cdot\vec{r}_i + \omega\tau)} \,, \qquad (2.12)
\end{aligned}$$

where $\vec{R}_i = \vec{r} - \vec{r}_i$, $\vec{r}$ being the distance of the point of observation from the origin and $\vec{r}_i$ being the position of the atom from the origin. Further $\tau = t - \frac{r}{c}$ is the retarded time, $k_o = \frac{\omega_0}{c}$, $\omega_0 = \omega_{13} = \omega_{24}$ and $\vec{d}_{ij}$ is the electric dipole moment operator. The first term on the right of Eq. (2.12) is the free field term and the second term is the retarded dipole field emitted by the atom. The emitted radiation consists of different polarization components- the π and the σ polarized components. In Eq. (2.12) the terms $|3\rangle\langle 1|_\tau$ and $|4\rangle\langle 2|_\tau$ correspond to π polarization whereas the ones $|3\rangle\langle 2|_\tau$ and $|4\rangle\langle 1|_\tau$ correspond to σ polarization. We next calculate the photon-photon correlations and the normalized second order correlations for the emitted radiations from the π transitions of this driven four-level atom. For π polarization the relevant part of the electric field operator is given by,

$$\mathbf{E}^{+}(\vec{r},t) = \mathbf{E}_0^{+}(\vec{r},t) - (\frac{\omega_0}{c})^2 \frac{1}{r}([\hat{n} \times (\hat{n} \times \vec{d}_{31})]|3\rangle\langle 1|_\tau$$

$$+[\hat{n}\times(\hat{n}\times\vec{d}_{42})]|4\rangle\langle 2|_{\tau}) \ , \tag{2.13}$$

where τ as before is the retarded time (t-r/c). In the lowest order correlation the free field term of Eq. (2.13) does not contribute. This can be seen directly from the definition of quantized fields [125], the fact that the field is initially in the vacuum state and the expression for the normally ordered correlation function for the field, $\langle \mathbf{E}^{-}(\vec{r},t)\mathbf{E}^{+}(\vec{r'},t')\rangle$. Hence with no contribution from the free field term the intensity I_{π} of the light emitted on the π transition from the atom is ,

$$\begin{aligned}\langle I_{\pi}\rangle &= \langle \mathbf{E}^{-}_{\pi}(\vec{r},t)\cdot\mathbf{E}^{+}_{\pi}(\vec{r},t)\rangle \\ &= (\frac{\omega_0}{c})^4\frac{1}{r^2}\langle[\hat{n}\times(\hat{n}\times\vec{d}_{31})]^{*}\cdot[\hat{n}\times(\hat{n}\times\vec{d}_{31})]|1\rangle\langle 1|_{\tau} \\ &\quad +[\hat{n}\times(\hat{n}\times\vec{d}_{42})]^{*}\cdot[\hat{n}\times(\hat{n}\times\vec{d}_{42})]|2\rangle\langle 2|_{\tau}\rangle \ ,\end{aligned} \tag{2.14}$$

where we have taken our origin at the location of the atom , $\vec{r}=\hat{n}r$, τ is the retarded time and we used the property $A_{ij}A_{kl} = A_{il}\delta_{kj}$. The negative frequency part of the electric field operator $\mathbf{E}^{-}(\vec{r},t)$ can be found by taking the complex conjugate of the positive frequency part. Now if we assume that the point of observation lies perpendicular to both the polarization and propagation direction we have from Eq. (2.14)

$$\langle I_{\pi}\rangle = (\frac{\omega_0}{c})^4\frac{1}{r^2}(|\vec{d}_{31}|^2\langle|1\rangle\langle 1|\rangle_{\tau} + |\vec{d}_{42}|^2\langle|2\rangle\langle 2|\rangle_{\tau}) \ , \tag{2.15}$$

Eq.(2.15) can be further simplified using Eqs. (2.1) and (2.11), where in using Eq. (2.11) we have assumed that observation is been made at long time limit. The final expression for I_{π} in the long time limit (steady state) is then,

$$\langle I_{\pi}\rangle^{st} = (\frac{\omega_0}{c})^4\frac{|\mathcal{D}|^2}{6r^2}\frac{|\Omega|^2}{[2|\Omega|^2+\Gamma^2+\Delta^2]} \ , \tag{2.16}$$

Eq.(2.16) clearly show that intensity emitted on the π transitions is not altered by vacuum induced coherences and is simply proportional to the steady state population of the excited states.

Let us now investigate what happens incase of two time photon-photon correlations

on the π transitions. The two-time photon-photon correlation for the level scheme in Fig.2.1 can be written as

$$\begin{aligned}
\langle I_\pi(t+\tau)I_\pi(t)\rangle &= \langle \mathbf{E}_\pi^-(\vec{r},t)\mathbf{E}_\pi^-(\vec{r},t+\tau) : \mathbf{E}_\pi^+(\vec{r},t+\tau)\mathbf{E}_\pi^+(\vec{r},t)\rangle \\
&= (\frac{\omega_0}{c})^8 \frac{1}{r^4}\{[\hat{n}\times(\hat{n}\times\vec{d}_{31})]^*\cdot[\hat{n}\times(\hat{n}\times\vec{d}_{31})]\}^2 \\
&\quad \langle(|1\rangle\langle 3| - |2\rangle\langle 4|)_t(|1\rangle\langle 1| + |2\rangle\langle 2|)_{t+\tau} \\
&\quad (|3\rangle\langle 1| - |4\rangle\langle 2|)_t\rangle \ , \qquad (2.17)
\end{aligned}$$

The two-time correlation function which appears in Eq. (2.17) is to be obtained from the solution of the time-dependent density matrix equations (Eq.(2.8)) and the quantum regression theorem [126]. In the rest of the chapter we deal with correlations like (2.17) in steady state where these depend only on time difference τ and thus the retarded time becomes irrelevant. A closer look at Eq. (2.8) show that eight of the fifteen equations form a closed set of linear equations which can be solved to find $|1\rangle\langle 1|_{t+\tau}, |2\rangle\langle 2|_{t+\tau}$ and hence the term $(|1\rangle\langle 1| + |2\rangle\langle 2|)_{t+\tau}$ in Eq. (2.17). Before going further let us list those eight equations,

$$\begin{aligned}
\dot{\tilde{\rho}}_{11} &= i\Omega^*\tilde{\rho}_{13} - i\Omega\tilde{\rho}_{31} - 2\Gamma\tilde{\rho}_{11} \ , \\
\dot{\tilde{\rho}}_{33} &= i\Omega\tilde{\rho}_{31} - i\Omega^*\tilde{\rho}_{13} + 2\gamma_\sigma\tilde{\rho}_{22} + 2\gamma\tilde{\rho}_{11} \ , \\
\dot{\tilde{\rho}}_{13} &= -i\Delta\tilde{\rho}_{13} + i\Omega(\tilde{\rho}_{11} - \tilde{\rho}_{33}) - \Gamma\tilde{\rho}_{13} \ , \\
\dot{\tilde{\rho}}_{31} &= i\Delta\tilde{\rho}_{31} - i\Omega^*(\tilde{\rho}_{11} - \tilde{\rho}_{33}) - \Gamma\tilde{\rho}_{31} \ , \qquad (2.18) \\
\dot{\tilde{\rho}}_{22} &= i\Omega\tilde{\rho}_{42} - i\Omega^*\tilde{\rho}_{24} - 2\Gamma\tilde{\rho}_{22} \ , \\
\dot{\tilde{\rho}}_{44} &= i\Omega^*\tilde{\rho}_{24} - i\Omega\tilde{\rho}_{42} + \gamma_\sigma\tilde{\rho}_{11} + \gamma\tilde{\rho}_{22} \ , \\
\dot{\tilde{\rho}}_{24} &= -i\Delta\tilde{\rho}_{24} - i\Omega(\tilde{\rho}_{22} - \tilde{\rho}_{44}) - \Gamma\tilde{\rho}_{24} \ , \\
\dot{\tilde{\rho}}_{42} &= i\Delta\tilde{\rho}_{42} + i\Omega^*(\tilde{\rho}_{22} - \tilde{\rho}_{44}) - \Gamma\tilde{\rho}_{42} \ ,
\end{aligned}$$

In compact notation this equations can be written as,

$$\dot{\tilde{\rho}} = \mathcal{M}\tilde{\rho} \ , \qquad (2.19)$$

where $\dot{\tilde{\rho}}$, $\tilde{\rho}$ are (8×1) column matrix and $\mathcal{M}$ is a (8×8) square matrix. Now using the method depicted in [127] and using Eq.(2.18) the solution of $\langle|1\rangle\langle 1|_{t+\tau}\rangle$ and $\langle|2\rangle\langle 2|_{t+\tau}\rangle$ can be expressed in the form

$$\begin{aligned}\langle|1\rangle\langle 1|_{t+\tau}\rangle &= f_{11}(\tau)\langle|1\rangle\langle 1|_t\rangle + f_{12}(\tau)\langle|3\rangle\langle|3|_t\rangle \\ &+ f_{13}(\tau)\langle|3\rangle\langle 1|_t\rangle + f_{14}(\tau)\langle|1\rangle\langle 3|_t\rangle \\ &+ f_{15}(\tau)\langle|2\rangle\langle 2|_t\rangle + f_{16}(\tau)\langle|4\rangle\langle 4|_t\rangle \\ &+ f_{17}(\tau)\langle|4\rangle\langle 2|_t\rangle + f_{18}(\tau)\langle|2\rangle\langle 4|_t\rangle \ , \end{aligned} \tag{2.20}$$

$$\begin{aligned}\langle|2\rangle\langle 2|_{t+\tau}\rangle &= f_{51}(\tau)\langle|1\rangle\langle 1|_t\rangle + f_{52}(\tau)\langle|3\rangle\langle|3|_t\rangle \\ &+ f_{53}(\tau)\langle|3\rangle\langle 1|_t\rangle + f_{54}(\tau)\langle|1\rangle\langle 3|_t\rangle \\ &+ f_{55}(\tau)\langle|2\rangle\langle 2|_t\rangle + f_{56}(\tau)\langle|4\rangle\langle 4|_t\rangle \\ &+ f_{57}(\tau)\langle|4\rangle\langle 2|_t\rangle + f_{58}(\tau)\langle|2\rangle\langle 4|_t\rangle \ , \end{aligned} \tag{2.21}$$

where the f's are defined by

$$f_{ik}(\tau) = (e^{\mathcal{M}\tau})_{ik} \ , \tag{2.22}$$

and

$$\begin{aligned}\mathcal{M}_{ik} &= \sum_l P_{il}\Lambda_{ll}P^{-1}_{lk} \\ (e^{\mathcal{M}\tau})_{ik} &= \sum_l P_{il}e^{\Lambda_{ll}\tau}P^{-1}_{lk} \ , \end{aligned} \tag{2.23}$$

Here we have diagonalized the matrix $\mathcal{M}$ with Λ being the eigenvalues and P being the corresponding eigenvectors. We now make use of the quantum regression theorem to obtain the two time correlation function as,

$$\begin{aligned}\langle B^\dagger(t)(|1\rangle\langle 1| + |2\rangle\langle 2|)_{t+\tau}B(t)\rangle &= F_1(\tau)\langle B^\dagger(t)|1\rangle\langle 1|_t B(t)\rangle \\ &+ F_2(\tau)\langle B^\dagger(t)|3\rangle\langle 3|_t B(t)\rangle \\ &+ F_3(\tau)\langle B^\dagger(t)|3\rangle\langle 1|_t B(t)\rangle \end{aligned}$$

$$
\begin{aligned}
&+ \quad F_4(\tau)\langle B^\dagger(t)|1\rangle\langle 3|_t B(t)\rangle \\
&+ \quad F_5(\tau)\langle B^\dagger(t)|2\rangle\langle 2|_t B(t)\rangle \\
&+ \quad F_6(\tau)\langle B^\dagger(t)|4\rangle\langle 4|_t B(t)\rangle \\
&+ \quad F_7(\tau)\langle B^\dagger(t)|4\rangle\langle 2|_t B(t)\rangle \\
&+ \quad F_8(\tau)\langle B^\dagger(t)|2\rangle\langle 4|_t B(t)\rangle \ ,
\end{aligned}
\tag{2.24}
$$

where we define the operator B as, $B^\dagger(t) = (|1\rangle\langle 3| - |2\rangle\langle 4|)_t$; $B(t) = (B^\dagger(t))^\dagger$ and $F_i(\tau) = f_{1i}(\tau) + f_{5i}(\tau)$. Using this new definition of the operator in Eq. (2.17), the expression for the two-time photon-photon correlation becomes,

$$
\begin{aligned}
\langle I_\pi(t+\tau)I_\pi(t)\rangle &= (\frac{\omega_0}{c})^8 \frac{1}{r^4}\{[\hat{n}\times(\hat{n}\times\vec{d}_{31})]^*\cdot[\hat{n}\times(\hat{n}\times\vec{d}_{31})]\}^2 \\
&\times \quad \langle B^\dagger(t)(|1\rangle\langle 1| + |2\rangle\langle 2|)_{t+\tau} B(t)\rangle \ ,
\end{aligned}
\tag{2.25}
$$

which when Eq. (2.24) is used, simplifies to

$$
\begin{aligned}
\langle I_\pi(t+\tau)I_\pi(t)\rangle &= (\frac{\omega_0}{c})^8 \frac{1}{r^4}\{[\hat{n}\times(\hat{n}\times\vec{d}_{31})]^*\cdot[\hat{n}\times(\hat{n}\times\vec{d}_{31})]\}^2 \\
&\times \quad (F_2(\tau)\langle|1\rangle\langle 1|\rangle_t + F_6(\tau)\langle|2\rangle\langle 2|\rangle_t) \ ,
\end{aligned}
\tag{2.26}
$$

In the long time limit $\langle|1\rangle\langle 1|\rangle_t \equiv \tilde{\rho}_{11}(t)$ and $\langle|2\rangle\langle 2|\rangle_t \equiv \tilde{\rho}_{22}(t)$, where $\tilde{\rho}_{11}(t), \tilde{\rho}_{22}(t)$ are the steady state populations of the excited states given by Eq. (2.11). Now following our assumption that the point of observation lies perpendicular to both the polarization and propagation directions and substituting for $\tilde{\rho}_{11}$, $\tilde{\rho}_{22}$ from Eq. (2.11), Eq. (2.26) can be further simplified. The final expression for the two-time photon-photon correlation is then,

$$
\begin{aligned}
G^{(2)}_\pi(\tau) &= \langle I_\pi(t+\tau)I_\pi(t)\rangle \\
&= (\frac{\omega_0}{c})^8 \frac{|\mathcal{D}|^4}{36r^4}(F_2(\tau) + F_6(\tau)) \\
&\times \quad (\frac{1}{2}\frac{|\Omega|^2}{[2|\Omega|^2 + \Gamma^2 + \Delta^2]}) \ ,
\end{aligned}
\tag{2.27}
$$

where we have used Eq. (2.1) for the dipole matrix elements. Note that $F_2(\tau)[F_6(\tau)]$ is the sum of probabilities of finding the atom in the states $|1\rangle$ and $|2\rangle$ given that at $\tau = 0$, the atom was in the state $|3\rangle[|4\rangle]$. In the limit of large τ,

$$G_\pi^{(2)}(\tau) \rightarrow (\frac{\omega_0}{c})^8 \frac{|\mathcal{D}|^4}{36r^4} (\frac{2|\Omega|^2}{[2|\Omega|^2 + \Gamma^2 + \Delta^2]}) \, , \tag{2.28}$$

Next let us derive the expression for two-time photon-photon correlation in absence of interference. In this case the total photon-photon correlation will be a simple addition of photon-photon correlations for radiation emitted on individual π transitions.

$$\begin{aligned}
\mathsf{G}_\pi^{(2)}(\tau) &= \langle I_\pi(t+\tau) I_\pi(t) \rangle \\
&= \langle \mathbf{E}_\pi^-(\vec{r},t) \mathbf{E}_\pi^-(\vec{r},t+\tau) : \mathbf{E}_\pi^+(\vec{r},t+\tau) \mathbf{E}_\pi^+(\vec{r},t) \rangle_{|1\rangle\langle 3|} \\
&+ \langle \mathbf{E}_\pi^-(\vec{r},t) \mathbf{E}_\pi^-(\vec{r},t+\tau) : \mathbf{E}_\pi^+(\vec{r},t+\tau) \mathbf{E}_\pi^+(\vec{r},t) \rangle_{|2\rangle\langle 4|} \, ,
\end{aligned} \tag{2.29}$$

$$\begin{aligned}
&= (\frac{\omega_0}{c})^8 \frac{1}{r^4} \{ [\hat{n} \times (\hat{n} \times \vec{d}_{31})]^* \cdot [\hat{n} \times (\hat{n} \times \vec{d}_{31})] \}^2 \\
&\quad \langle |1\rangle\langle 3|_t (|1\rangle\langle 1|)_{t+\tau} |3\rangle\langle 1|_t \rangle \\
&+ (\frac{\omega_0}{c})^8 \frac{1}{r^4} \{ [\hat{n} \times (\hat{n} \times \vec{d}_{42})]^* \cdot [\hat{n} \times (\hat{n} \times \vec{d}_{42})] \}^2 \\
&\quad \langle |2\rangle\langle 4|_t (|2\rangle\langle 2|)_{t+\tau} |4\rangle\langle 2|_t \rangle \, ,
\end{aligned} \tag{2.30}$$

Finally using Eq. (2.20),(2.21) and (2.11) we get the photon-photon correlation in absence of interference as

$$\begin{aligned}
\mathsf{G}_\pi^{(2)}(\tau) &= (\frac{\omega_0}{c})^8 \frac{|\mathcal{D}|^4}{36r^4} (f_{12}(\tau) + f_{56}(\tau)) \\
&\times (\frac{1}{2} \frac{|\Omega|^2}{[2|\Omega|^2 + \Gamma^2 + \Delta^2]}) \, ,
\end{aligned} \tag{2.31}$$

Here $f_{12}(\tau)[f_{56}(\tau)]$ is the probability of finding the atom in the states $|1\rangle$ $[|2\rangle]$ given that at $\tau = 0$, the atom was in the state $|3\rangle$ $[|4\rangle]$. Eq. (2.31) in the limit of large τ becomes,

$$\mathsf{G}_\pi^{(2)}(\tau) \rightarrow (\frac{\omega_0}{c})^8 \frac{|\mathcal{D}|^4}{36r^4} (\frac{|\Omega|^2}{[2|\Omega|^2 + \Gamma^2 + \Delta^2]}) \, , \tag{2.32}$$

We now further calculate the normalized photon-photon correlation corresponding to Eq. (2.27) and Eq. (2.31). The $g^{(2)}$ function gives the non-classical aspects of photon statistics.

$$g^{(2)}(t+\tau,t) = \frac{\langle I_\pi(t+\tau)I_\pi(t)\rangle}{\langle I_\pi(t+\tau)\rangle\langle I_\pi(t)\rangle} = \frac{(F_2(\tau)+F_6(\tau))\tilde{\rho}_{11}}{4\tilde{\rho}_{11}^2}\ , \tag{2.33}$$

$$\begin{aligned} \mathsf{g}^{(2)}(t+\tau,t) &= \frac{\langle I_\pi(t+\tau)I_\pi(t)\rangle}{(\langle I_\pi(t+\tau)\rangle\langle I_\pi(t)\rangle)_{|1\rangle\langle 3|} + (\langle I_\pi(t+\tau)\rangle\langle I_\pi(t)\rangle)_{|2\rangle\langle 4|}} \\ &= \frac{(f_{12}(\tau)+f_{56}(\tau))\tilde{\rho}_{11}}{2\tilde{\rho}_{11}^2}\ , \end{aligned} \tag{2.34}$$

Here $\tilde{\rho}_{11}$ is the steady state population of the excited state given by Eq. (2.11) and $g^{(2)}$ [$\mathsf{g}^{(2)}$] is the normalized two time photon-photon correlation function corresponding to presence [absence] of vacuum induced interference.

2.4 Numerical Results

In this section we present our numerical results and discuss their consequences. To begin with, we first discuss our method of computation. The decay rates of the excited states to the two ground states, $2\gamma_\sigma$ and 2γ are proportional to $|\vec{d}_{41}|^2$ and $|\vec{d}_{31}|^2$ respectively. From Eq. (2.1) we get, $2\gamma_\sigma \equiv \gamma_0/3$ and $2\gamma \equiv \gamma_0/6$, where γ_0 is proportional to the square of the reduced dipole matrix element. We use these values for the decays in our numerical computation and normalize all the computational parameters with respect to γ_0. Further we use standard subroutines to diagonalize the complex general matrix $\mathcal{M}$ and obtain complex eigenvalues and eigenvectors of the form $(\alpha + i\beta)$.

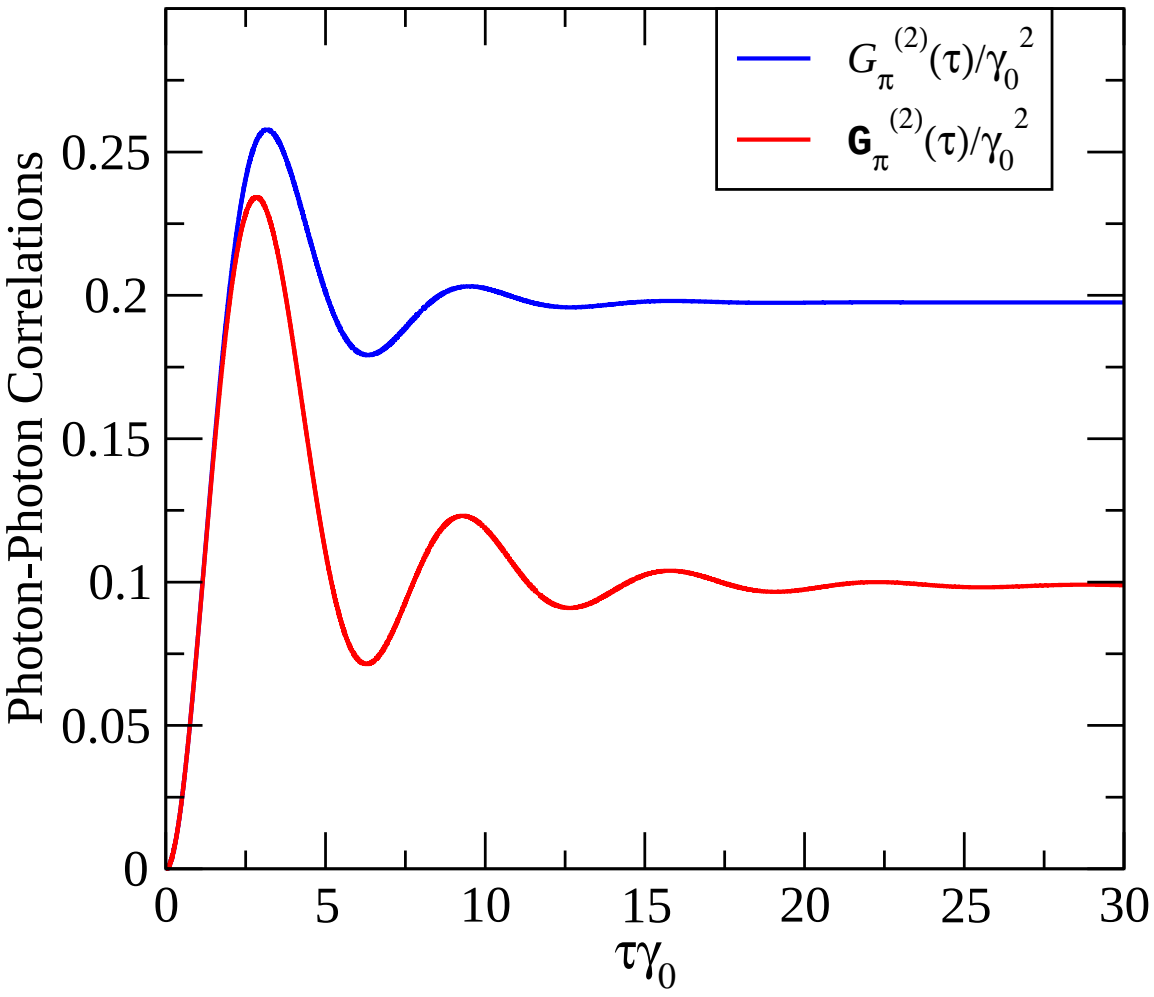

Figure 2.2: Plot of two-time Photon-Photon correlation as a function of time for $\Omega = 0.5\gamma_0, \Delta = 0.0\gamma_0$. where $\gamma_0 = \frac{4|\mathcal{D}|^2\omega_{14}^3}{3c^3}$. All the plotted parameters are normalized with respect to γ_0 rendering them dimensionless. The blue and red lines in this figure and Figs.(2.3,2.4 and 2.6) correspond to photon-photon correlations in presence and absence of VIC respectively.

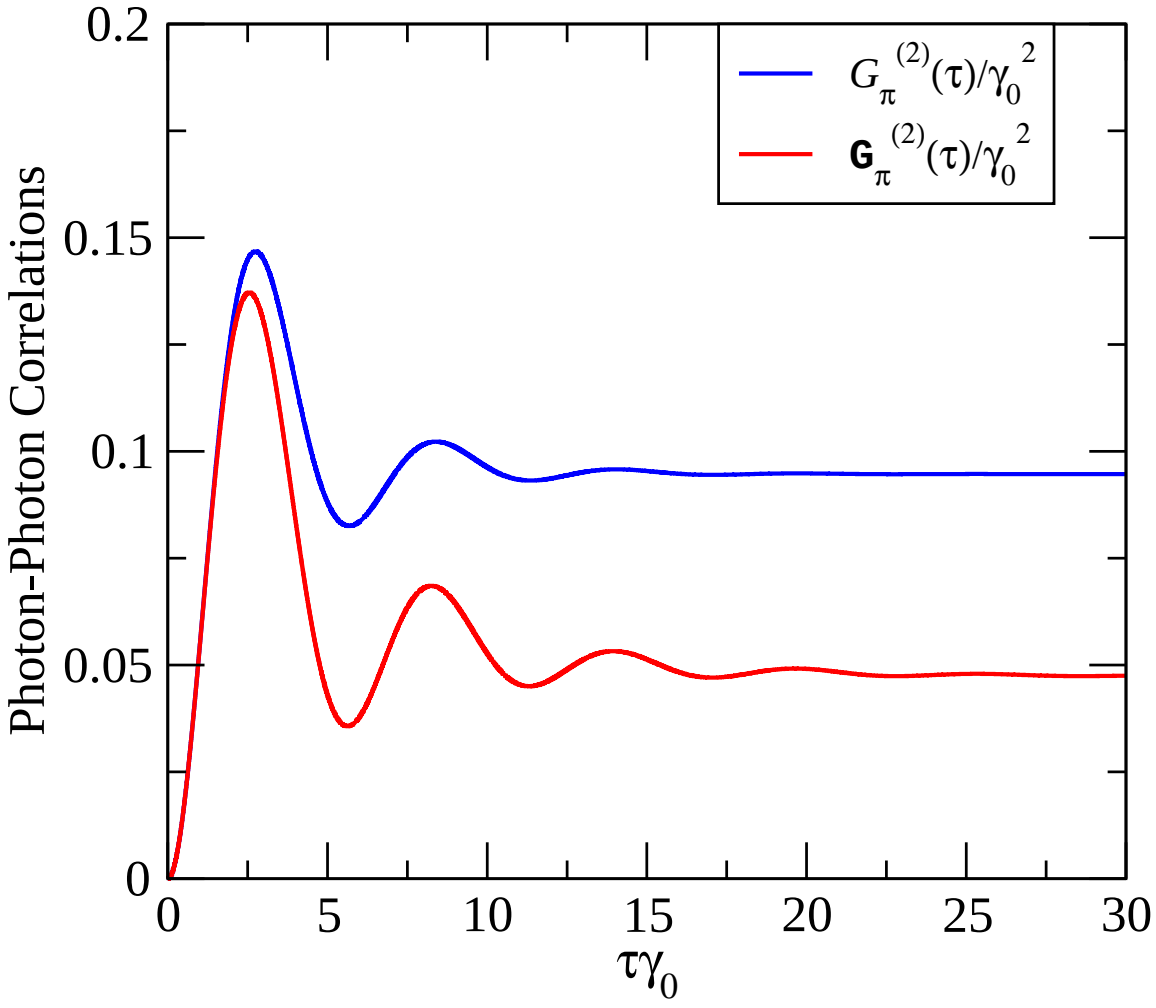

Figure 2.3: Plot of two-time Photon-Photon correlation as a function of time but now for a small detuning $\Delta = 0.5\gamma_0$, other parameters remaining same as in Fig.2.2

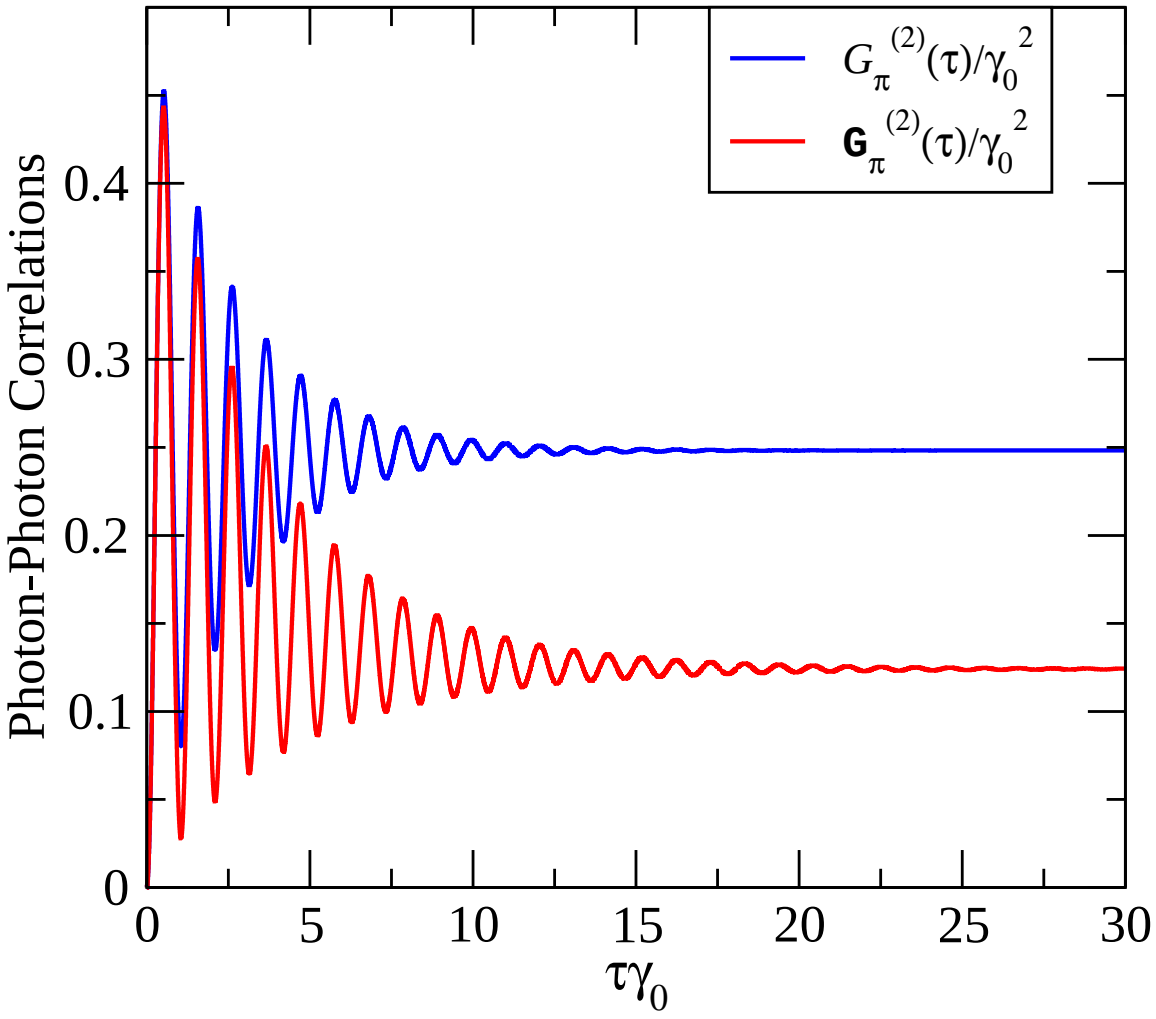

Figure 2.4: Plot of two-time Photon-Photon correlation as a function of time for $\Omega = 3.0\gamma_0, \Delta = 0.0\gamma_0$, where $\gamma_0 = \frac{4|\mathcal{D}|^2\omega_{14}^3}{3c^3}$. All the plotted parameters are dimensionless.

Table 2.1: Eigenvalues(in units of γ_0) for the diagonalized matrix $\mathcal{M}$ corresponding to two different values of the Rabi frequency of the driving field which is on resonance with the atomic transitions.

λ/γ_0	$\Omega = 0.5\gamma_0$	$\Omega = 3.0\gamma_0$
1	(-0.349797,-1.10904)	(-0.375000,5.99870)
2	(-0.349797,1.10904)	(-0.375000,-5.99870)
3	(-0.215794,-1.09726)	(-0.208269,5.99522)
4	(-0.215794,1.09726)	(-0.208269,-5.99522)
5	(-0.300406,0.000000)	(-0.250000,0.000000)
6	(-0.165314,0.000000)	(-0.250000,0.000000)
7	(-0.403098,0.000000)	(-0.333462,0.000000)
8	(0.000000,0.000000)	(0.000000,0.000000)

For all values of detuning and Rabi frequency used in our computation we have two pairs of complex conjugate eigenvalues and four other eigenvalues whose complex part are so small compare to the real part that these complex parts have no significant contributions. Hence these four eigenvalues can be taken to be purely real. Note that this is in contrast to the case of photon-photon correlations for the two level model where the number of eigenvalues is four [128]. The changes in the eigenvalues lead to spectral modification as discussed by Kiffner et. al. [109]. The eigenvalues for $\Omega_c = 0.5\gamma_0$, and $\Omega_c = 3\gamma_0$ and detuning $\Delta = 0$ are listed in the Table (2.1). Note for example that for $\Omega_c = 3\gamma_0$ we have eigenvalues $\pm 5.99870i - 0.375$ and $\pm 5.99522i - 0.208269$. This difference in the real parts can produce a dip in the side bands in the Mollow spectrum [129]. Next we calculate the elements f_{ij} of the 8×8 matrix $[f]$ using Eq. (2.22) and Eq. (2.23). Finally we use the elements f_{ij} corresponding to Eqs. (2.27),(2.31) and Eqs. (2.33),(2.34) to evaluate the two time photon-photon correlations and normalized photon-photon correlations in presence and absence of vacuum induced interference respectively.

The Figs. (2.2-2.4) show photon-photon correlations corresponding to Eqs. (2.27) and (2.31). *The blue and red lines in the figures correspond respectively, to photon-photon correlations in presence and absence of interference.* The correlations calculated in the presence of interference show strong damping of the oscillations and attain an overall higher value as the time separation τ between two counts increases. The differences between $G^{(2)}$ and $\mathsf{G}^{(2)}$ are most noticeable in the limit of large time separation τ. In order to understand this we examine the distinction between $F_2(\tau) = f_{12}(\tau) + f_{52}(\tau)$ and $f_{12}(\tau)$. We recall that $f_{12}[f_{52}]$ was the probability of finding the atom in the state $|1\rangle[|2\rangle]$ given that at $\tau = 0$, it was in the state $|3\rangle$. We exhibit these probabilities in the Fig. (2.5). We observe that the function $f_{52}(\tau)$ starts becoming significant at the time scale of the order of γ_σ^{-1}.

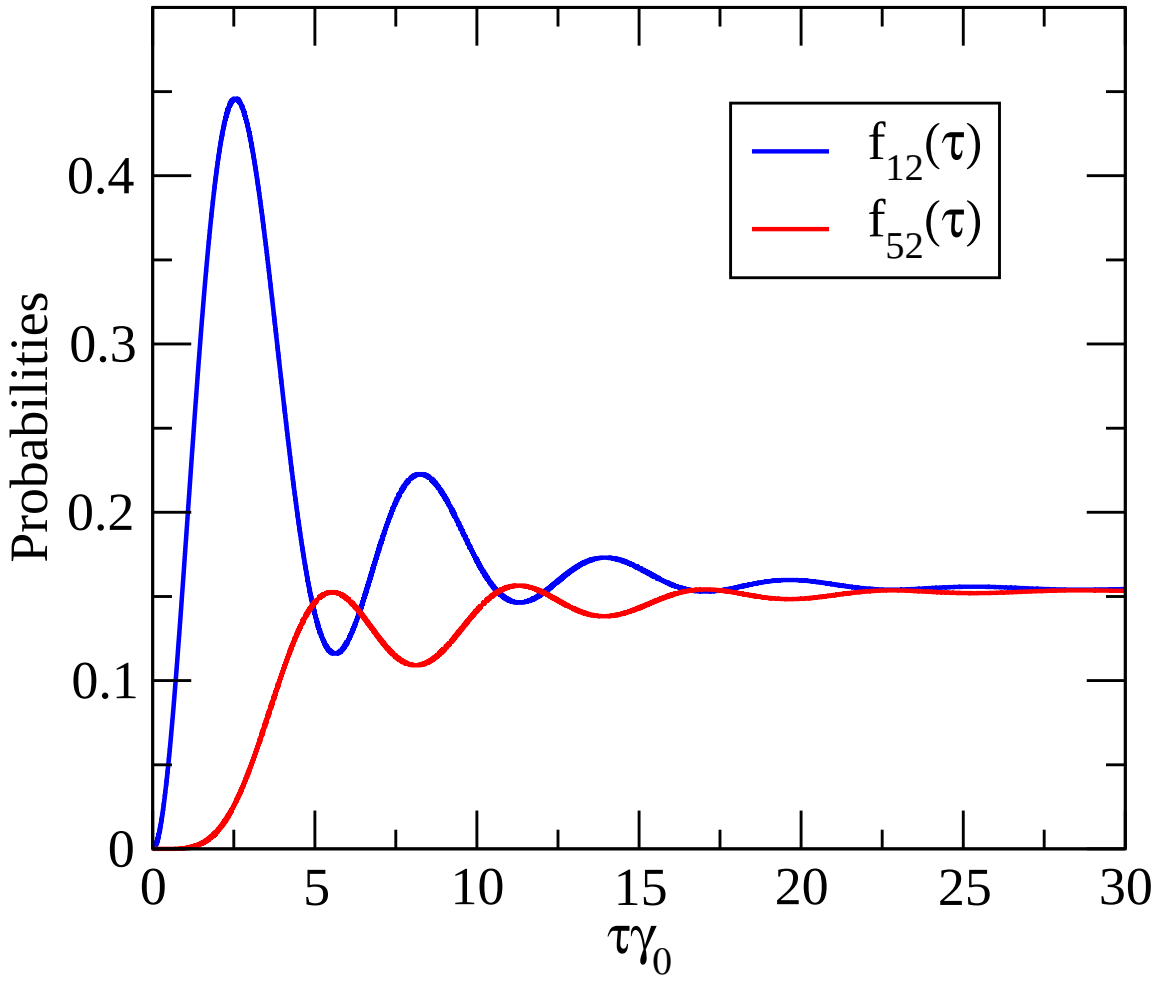

Figure 2.5: Probability for finding the atom in state $|1\rangle$ (f_{12}) and $|2\rangle$ (f_{52}) given that at time $\tau = 0$ the atom was in the state $|3\rangle$ for $\Omega = 0.5\gamma_0, \Delta = 0.5\gamma_0$, where $\gamma_0 = \frac{4|\mathcal{D}|^2\omega_{14}^3}{3c^3}$. All the plotted parameters are dimensionless.

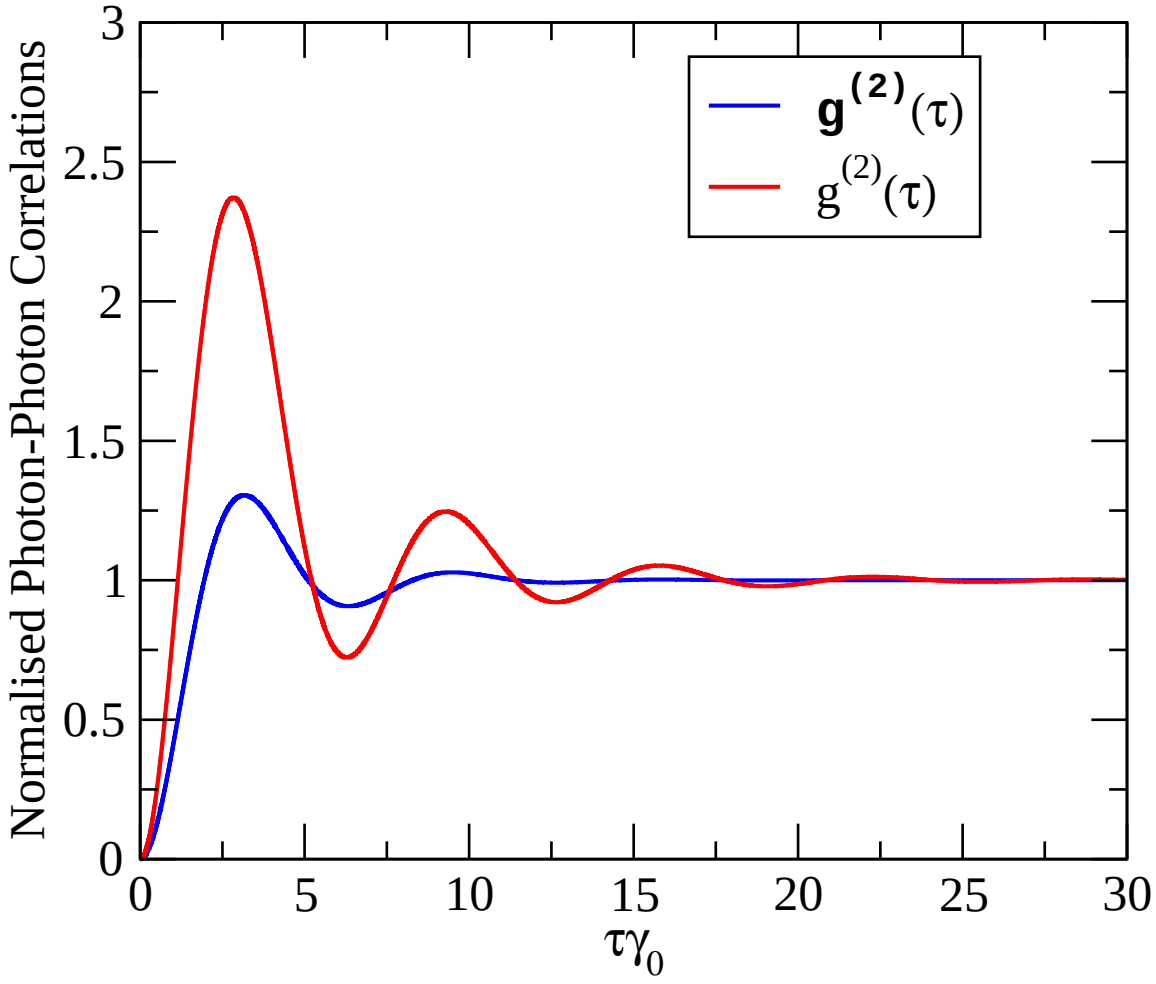

Figure 2.6: Normalized photon-photon correlations plotted as a function of time, for $\Omega = 0.5\gamma_0, \Delta = 0.0\gamma_0$, where $\gamma_0 = \frac{4|\mathcal{D}|^2\omega_{14}^3}{3c^3}$. All the plotted parameters are dimensionless.

Further for large τ, f_{12} and f_{52} become comparable. The physical process that contributes to f_{52} is the following,

$$|3\rangle \xrightarrow[\pi-pol]{laser} |1\rangle \overset{\sigma-photon}{\underset{emission}{\longrightarrow}} |4\rangle \xrightarrow[\pi-pol]{laser} |2\rangle \ . \tag{2.35}$$

Similarly population can start from the state $|4\rangle$ and end up in the state $|1\rangle$ via,

$$|4\rangle \xrightarrow[\pi-pol]{laser} |2\rangle \overset{\sigma-photon}{\underset{emission}{\longrightarrow}} |3\rangle \xrightarrow[\pi-pol]{laser} |1\rangle \ . \tag{2.36}$$

We show normalized photon-photon correlations in a typical case in the Fig. (2.6). In case of interference we observe stronger damping of the oscillations and an overall reduction of the $g^{(2)}$ function at shorter time scales. At long time limits $g^{(2)}(\tau \to \infty)$ is 1. Photon antibunching effect is also visible as $0 \leqslant g^{(2)}(0) < 1$. For shorter time scale we get $g^{(2)}(\tau) \not\leq 1$ a clear signature of the nonclassical nature of the two-time photon-photon correlations.

2.5 Conclusions

In conclusion we have shown that the vacuum induced coherence (VIC) do significantly affect the two-time photon-photon correlations even though they show no effect on the total steady state intensity of the radiation emitted on the π transitions. The effect of this coherence is reflected in form of stronger damping and overall larger values of the correlation function $G^{(2)}$. The level scheme j = 1/2 → j = 1/2 is easily realizable and has already been used, for example in $^{198}Hg^{+}$ [110] in the context of interferences produced by a system of two ions and more recently in $^{138}Ba^{+}$ [120] in the context of emission in presence of a mirror.

The content of this chapter has been published in Phys. Rev. A **77**, 033850 (2008).

CHAPTER 3

QUANTUM INTERFERENCES IN COOPERATIVE DICKE EMISSION FROM SPATIAL VARIATION OF LASER PHASE

3.1 Overview

Spontaneous emission from cooperative systems has been extensively studied since the classic paper of Dicke [105, 131, 132]. The details of the emission depend on the interatomic distances and how the system is initially prepared. The emission can further be influenced if the system is continuously driven by a coherent field. The two atom problem has been especially attractive in this context as many features of cooperative emission can be analyzed in terms of this simple problem. There is renewed interest in these problems for quantum information sciences. Studies have shown that spontaneous emission from cooperative systems leads to quantum entanglement among atoms [132]. Further with the discovery of similarities between semiconductor quantum dots and two level atoms [51, 49, 196], we have a new class of systems where the cooperative effects can be studied in a regime which was difficult to achieve with atoms. In recent times such quantum dot systems are proving especially important in quantum information science [52, 134, 135].

In this chapter we discuss a new quantum interference effect which arises from the spatial variation of the laser phase at the positions of the atoms. We show how this phase variation affects the spectral features of the emitted radiation as well as the quantum entanglement in the system. We further show how populations and coherences, in a basis determined by the laser phase, get coupled dynamically. We demonstrate a kind of super-exchange between the symmetric and anti-symmetric

states and show a strong connection to the well known vacuum induced coherence [107, 118, 136, 137]. Further our results have implications for the decoherence of coupled qubits.

3.2 Model

The dynamical behavior of a system of atoms undergoing cooperative emission can be described by a master equation approach [105]. Let us specifically consider the system of two identical two-level atoms with transition frequency ω. Each atom is described by the spin half angular momentum algebra. The master equation for the dynamical behavior of this kind of a system in the Born, Markov and rotating wave approximation is then given by ref [105] (pg 31-33),

$$\begin{aligned}\frac{\partial\rho}{\partial t} &= -i\omega\sum_j[S_j^z,\rho] - i\sum_{j\neq k}\Omega_{jk}[S_j^+S_k^-,\rho] \\ &- \sum_{jk}\gamma_{jk}(S_j^+S_k^-\rho - 2S_k^-\rho S_j^+ + \rho S_j^+S_k^-),\end{aligned} \tag{3.1}$$

Here (j,k = 1-2) , $\Omega_{jk} = 3/2\gamma\{(1-3\cos^2\theta)[\sin(k_0r_{jk})/(k_0r_{jk})^2+\cos(k_0r_{jk})/(k_0r_{jk})^3]-(1-\cos^2\theta)[\cos(k_0r_{jk})/(k_0r_{jk})]\}$ and $\gamma_{jk} = \gamma\{\sin(k_0r_{jk})/(k_0r_{jk})+1/2(3\cos^2\theta-1)[(3/(k_0r_{jk})^2-1)\sin(k_0r_{jk})/(k_0r_{jk}) - 3\cos(k_0r_{jk})/(k_0r_{jk})^2]\}$ is the spontaneous decay rates for the cooperative system, $2\gamma = 2\gamma_{11} = 2\gamma_{22} = 4|\vec{d}_{eg}|^2\omega^3/3\hbar c^3$ is the Einstein's A coefficient, $k_0 = \omega/c$, $\vec{d}_{eg}$ is the dipole moment and ρ is the density operator for the system. θ is the angle between the direction of the dipole moment and the line joining the jth and the kth atom, whose distance is denoted by $r_{jk} = |\vec{r}_j - \vec{r}_k|$. If we assume this angle to be random, and take an average for all possible orientations, then the coefficients in the master equation simplify considerably and are given by $\Omega_{jk} = -\gamma\cos(k_0r_{jk})/k_0r_{jk}$, $\gamma_{jk} = \gamma\sin(k_0r_{jk})/k_0r_{jk}$. The second term in the master equation (3.1) is the dipole-dipole (d-d) interaction term. It arises from the virtual photon exchange between pairs of atoms. It becomes especially significant at small interatomic distances and has important consequences. For example it can lead to two photon resonance which

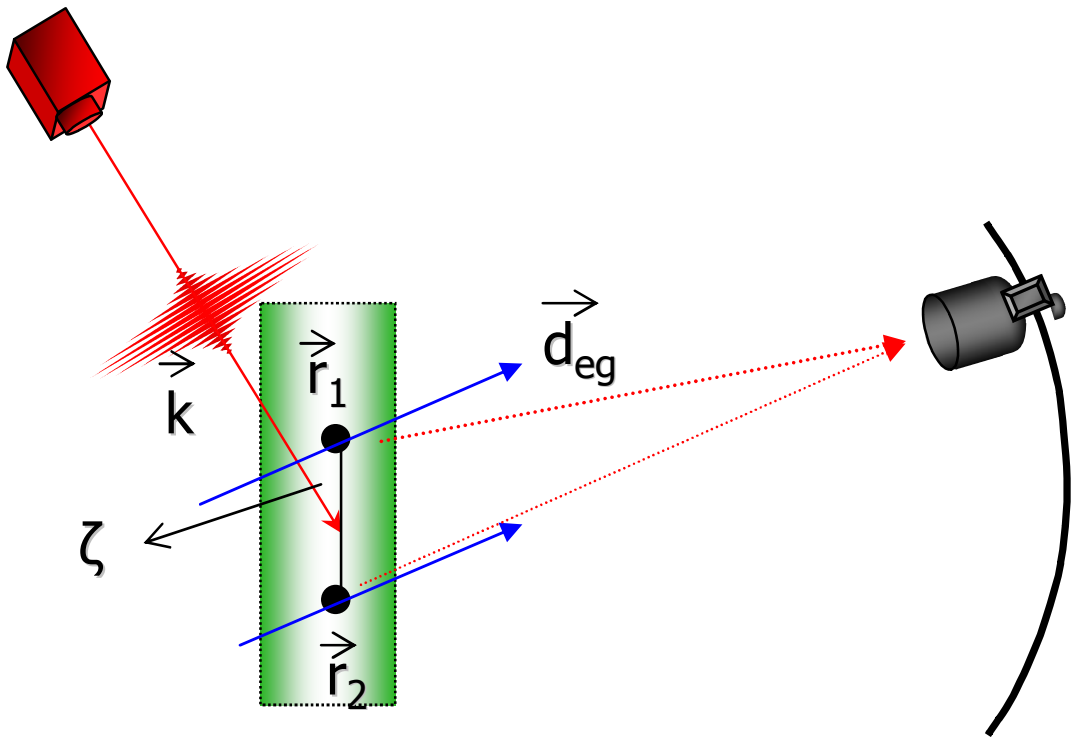

Figure 3.1: Diagrammatic representation of a setup to detect the cooperative emission from a system of two identical two-level atoms. The atoms are driven resonantly by a weak laser of frequency ω and propagation vector $\vec{k}$. ζ is the angle between the laser propagation direction and the orientation of the atoms. $\vec{d}_{eg}$ is the dipole moment of the atoms and $\vec{r}_1, \vec{r}_2$ are the position vectors of the atoms 1 and 2.

was predicted and later observed experimentally [138].

Here we assume that the atoms are continuously driven by a resonant laser propagating in the direction $\vec{k}$ with frequency ω. The driving term is hence given by,

$$\mathcal{H}_c = -\hbar \sum_j (G e^{i\vec{k}\cdot\vec{r}_j - i\omega t} S_j^+ + G e^{-i\vec{k}\cdot\vec{r}_j + i\omega t} S_j^-), \tag{3.2}$$

where (j = 1,2) and $G = \vec{d}_{eg} \cdot \vec{\mathcal{E}}_o/\hbar$ is the Rabi frequency. Note that we have included the spatially varying phase factors in the driving term. This would affect the dynamical evolution of the system.

3.3 Quantum interference induced by laser phase

Our main focus in this chapter is to investigate new effects arising from such a phase variation. We specifically demonstrate how such phase factors can bring out new interference effects which can be experimentally investigated by studying the spectrum of the emitted radiation. While in this chapter we concentrate on spectral features and entanglement, a previous work [118] has examined the effect of laser phase on emission rates. Further we specifically concentrate on the case where the relative inter-atomic distance is smaller than a wavelength when such interferences are even more dramatic. The relative orientation $\phi = \vec{k} \cdot (\vec{r}_j - \vec{r}_k) = 2\frac{\pi}{\lambda}|\vec{r}_j - \vec{r}_k| \cos\zeta$ of the two atoms and the direction of propagation of the laser drive is especially important in this context. Here ζ is the angle between the direction of the laser drive and the line joining the jth and the kth atom (see Fig.3.1). The quantum interference effects discussed in this chapter disappear if the relative orientation is perpendicular to the direction of propagation of the laser field. When the driving laser is weak, it is adequate to consider the generated states in the single photon space and clearly with two atoms starting in the ground state $|g\rangle \equiv |g_1, g_2\rangle$ we would generate the symmetric state $|s\rangle$ which depends on the phase of the laser at the location of two atoms [118],

$$|s\rangle \equiv \frac{1}{\sqrt{2}}(e^{i\vec{k}\cdot\vec{r}_1}|e,g\rangle + e^{i\vec{k}\cdot\vec{r}_2}|g,e\rangle). \tag{3.3}$$

Thus one would expect that once the system is excited to the state $|s\rangle$, it would decay to $|g\rangle$. However we show that due to quantum interferences associated with the spatial phase ϕ, the system could also be found in the antisymmetric state $|a\rangle$ defined as ,

$$|a\rangle \equiv \frac{1}{\sqrt{2}}(e^{i\vec{k}\cdot\vec{r}_1}|e,g\rangle - e^{i\vec{k}\cdot\vec{r}_2}|g,e\rangle). \tag{3.4}$$

Clearly, if we are working with single photon excitation then it should be adequate to deal with the states $|s\rangle, |a\rangle$ and $|g\rangle$. In order to see this we find from the master equation that the population in the symmetric state $|s\rangle$ is governed by,

$$\begin{aligned} \dot{\rho}_{ss} &= -2(\gamma + \gamma_{12}\cos\phi)\rho_{ss} - i\sin\phi(\gamma_{12} + i\Omega_{12})\rho_{as} \\ &\quad + i\sin\phi(\gamma_{12} - i\Omega_{12})\rho_{sa}, \end{aligned} \tag{3.5}$$

We immediately see that the population in the symmetric state decays at the rate $2(\gamma + \gamma_{12}\cos\phi)$, however it is also effected by the presence of atomic coherence terms ρ_{as} and ρ_{sa} which are dynamically generated. This coupling of populations to the coherences is at the heart of the quantum interference phenomenon [139] that we discuss in this chapter. From Eq.(3.5) it is clear that this coupling vanishes when the laser propagates in a direction perpendicular to the location of the two atoms($\phi = 0$). Further from the structure of Eq.(3.5) we can say that such quantum interferences should be especially important for smaller inter-atomic distances as then Ω_{12} is large and the coherence terms strongly influence the population dynamics of the symmetric state. Note further that for small times the effect of the quantum interferences does not show up as the solution of ρ_{ss} is then,

$$\rho_{ss} \cong 1 - 2t(\gamma + \gamma_{12}\cos\phi), \tag{3.6}$$

and hence the effect of interferences should appear in physical parameters which are determined by the long time dynamics. From the master equation we find that if the system starts in the initial state $|s\rangle$, then the population ρ_{aa} of the antisymmetric

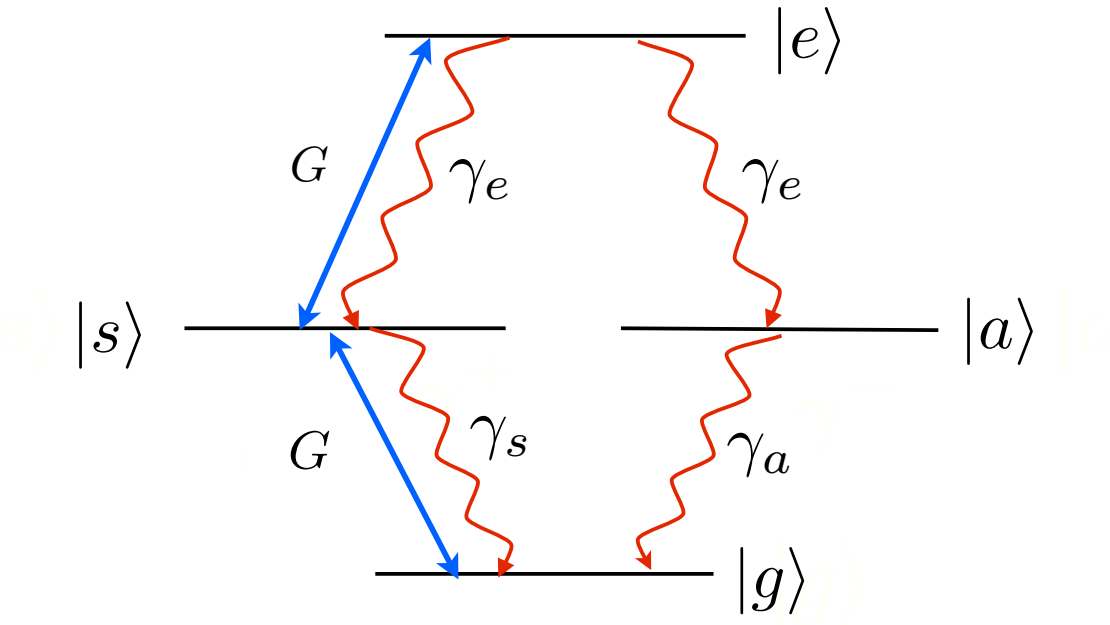

Figure 3.2: The two atom Dicke state configuration

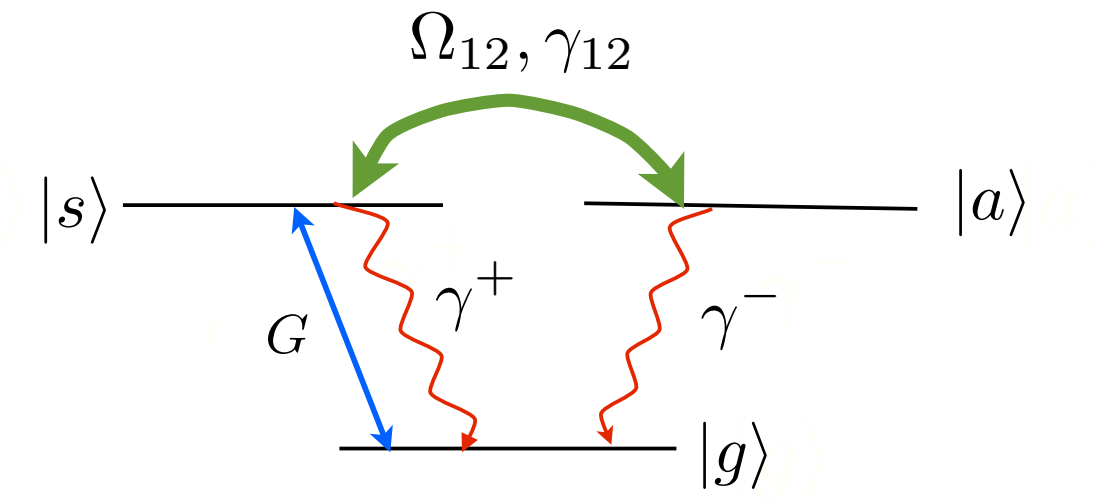

Figure 3.3: Schematic diagram showing population exchange between the symmetric and anti-symmetric state due to non-zero laser phase which generates dynamical coherences in ths system.

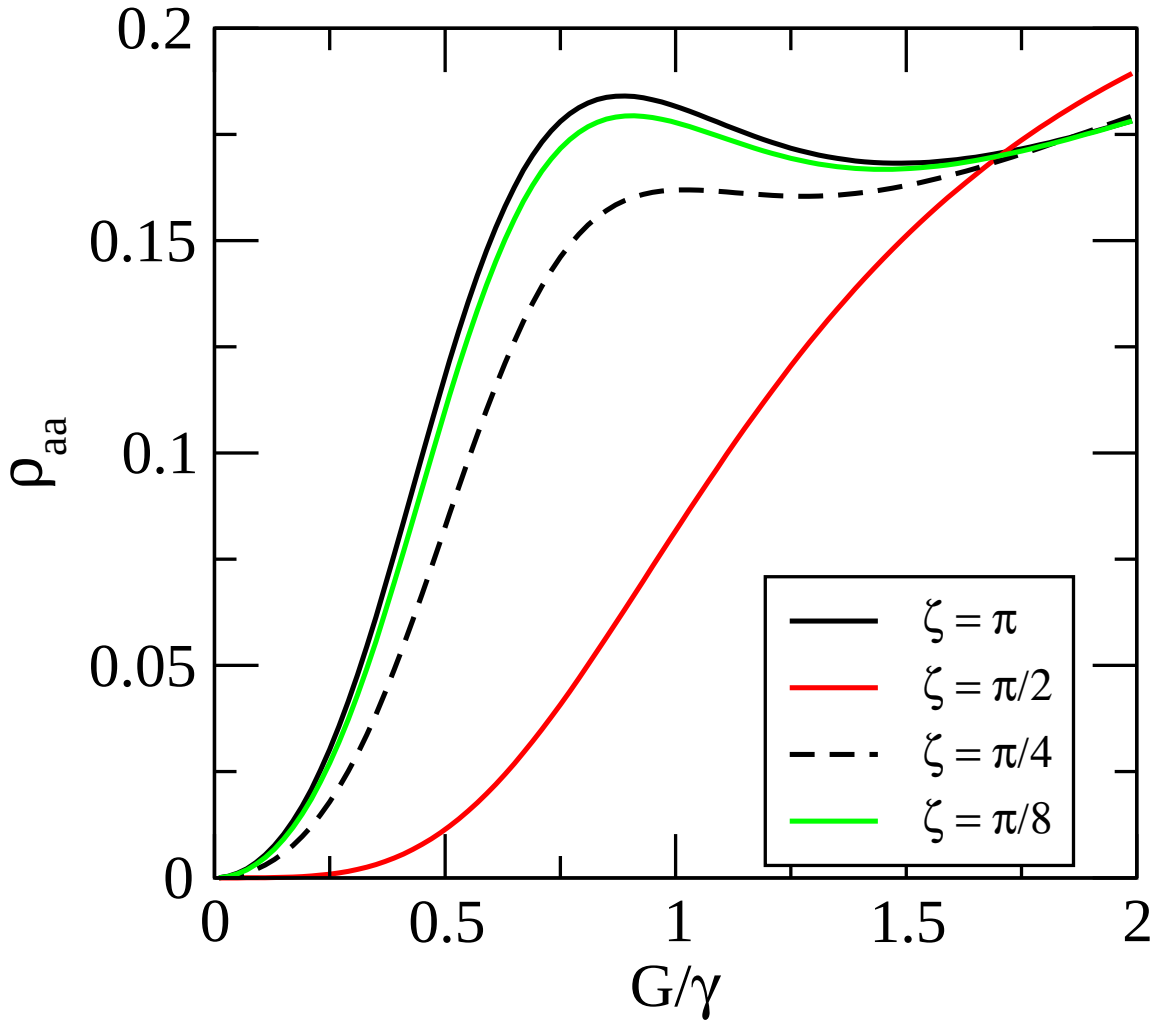

Figure 3.4: Population of the anti-symmetric state as function of the Rabi frequency for an inter-atomic distance of $\lambda/8$ and different orientation of the laser. All plotted parameters are dimensionless.

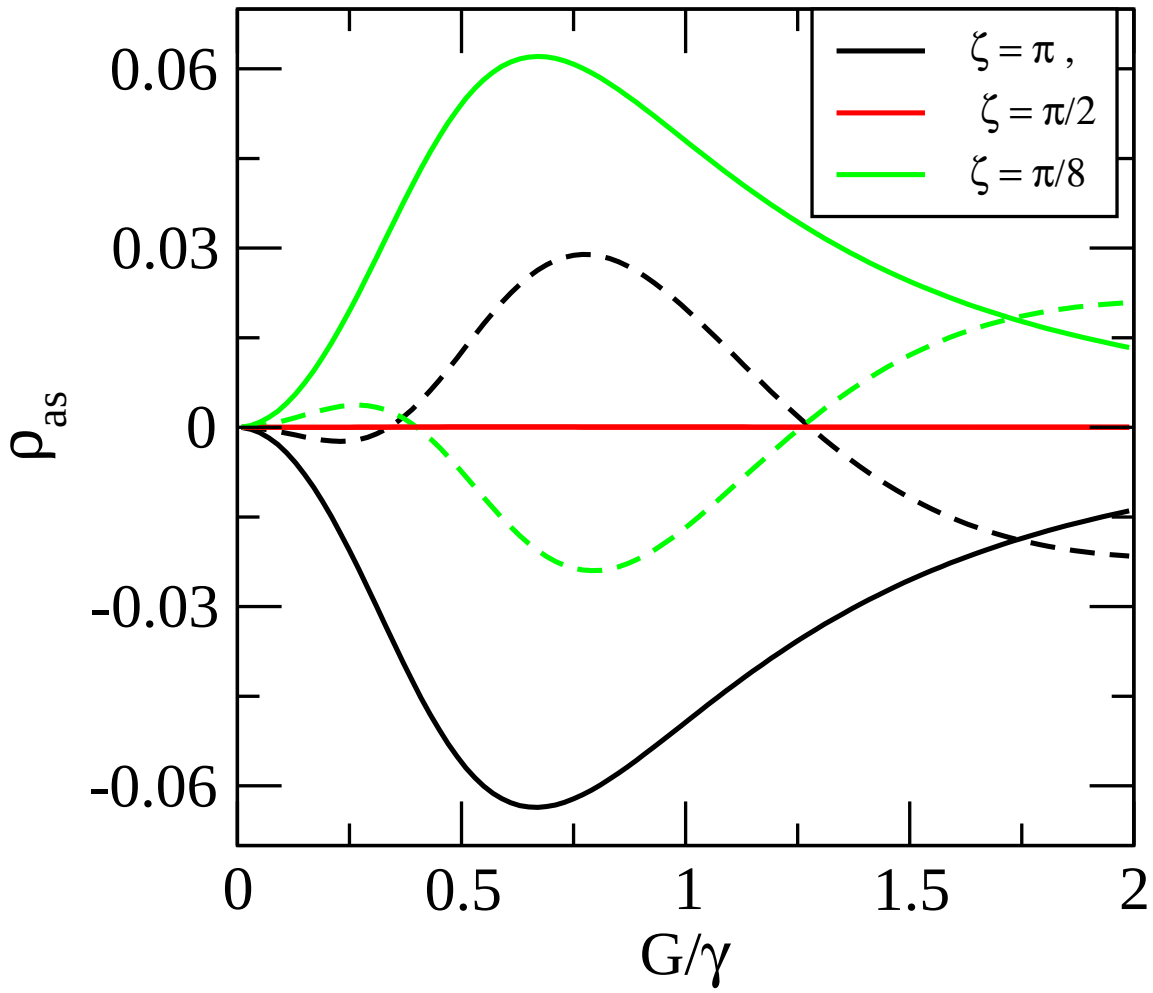

Figure 3.5: Atomic coherence ρ_{as} as a function of the Rabi frequency for an interatomic distance of $\lambda/8$ and for different orientations of the laser. The solid and dashed lines correspond to the real and imaginary parts of ρ_{as}.

state $|a\rangle$ grows as,

$$\rho_{aa} \sim \sin^2\phi(|\gamma_{12} + i\Omega_{12}|^2 t^2), \tag{3.7}$$

Thus the states $|s\rangle$ and $|a\rangle$ get coupled by the vacuum of the electromagnetic field provided that $\phi \neq 0$ (modulo π). This is a process in which the transition $|s\rangle \rightarrow |a\rangle$ is mediated via the state $|g\rangle$. It is to be noticed that the asymmetric state for small values of the driving field remains unpopulated if $\zeta = \pi/2$ ($\phi = 0$)[see Fig. 3.4]. However at larger values of the Rabi frequency the two photon state $|e, e\rangle$ gets populated and this changes the dynamical evolution leading to the population of the state $|a\rangle$. In Fig.(3.5) we show the coherence ρ_{as} which is quite significant for non-zero values of the angle ζ.

3.4 Effect of quantum interference on co-operative emission spectrum

To investigate the effects of this interference we study the steady state spectrum of cooperative emission. The incoherent part of the steady state emission spectrum integrated over all solid angles is given by,

$$\begin{aligned} S(\omega) &= \mathsf{Re}\sum_{ij}\gamma_{ij}\int_0^\infty d\tau e^{-z\tau}\lim_{t\to\infty}[\langle\hat{S}_i^+(t+\tau)\hat{S}_j^-(t)\rangle \\ &\quad -\langle\hat{S}_i^+(t+\tau)\rangle\langle\hat{S}_j^-(t)\rangle]_{z=i(\omega-\omega_0)/\gamma}. \end{aligned} \tag{3.8}$$

A detailed treatment of how to calculate the emission spectrum for such two atom systems undergoing cooperative emission is discussed in appendix A. We have calculated Eq.(3.8) when the system is driven weakly by a coherent field and for small interatomic distances. Under these conditions the quantum interference effects are dominant. The results of our numerical calculations are shown in Figs (3.6-3.7). In the Fig (3.6) we show the incoherent part of the normalized steady state spectrum for a weak coherent drive ($G = 0.1\gamma$) and small inter-atomic separation, $r_{12} = \lambda/8$. We have normalized the incoherent part of the steady state spectrum by dividing it with two times the steady state value of $[\langle S^+S^-\rangle - \langle S^+\rangle\langle S^-\rangle]$ for a single two level atom

[129]. The spectrum exhibits a doublet structure because of the strong dipole-dipole interaction Ω_{12} for small inter-atomic distances. The quantum interferences arising from the spatial phase factor ϕ determine the characteristics of the doublets. For example the peak of the doublet is almost seven times greater, when $\vec{k}$ is parallel or anti-parallel to $\vec{r}_{12}$ in comparison to when $\vec{k} \perp \vec{r}_{12}$. The Fig.(3.7) shows the incoherent steady state spectrum for a moderately strong driving field strength ($G = 1.0\gamma$). The inset in Fig.(3.7) is for still larger field strength. The doublet structure vanishes for moderately strong drive as seen in Fig.(3.7) and we get only the broadened central peak at $\omega = \omega_0$. The quantum interference leads to pronounced asymmetry in the spectrum. For even higher field strength (inset of Fig. 3.7) the cooperative effects are almost insignificant and we get the Mollow spectrum [129] for a two level atom.

3.5 Dynamical coherences induced by vacuum

The coupling of coherences to populations in the Dicke problem of cooperative emission can be understood as vacuum induced coherence effect[105, 132, 118, 137]. This can be appreciated more clearly at the level of Schrödinger equation. The basic Hamiltonian between the vacuum of the electromagnetic field and the atoms in the interaction picture can be written as,

$$\mathcal{H}_I(t) = \sum_{jks} \{ g_{jks} a_{ks} e^{-i\omega_{ks}t} (S_j^+ e^{-i\omega t} + S_j^- e^{i\omega t}) + H.C. \}, \tag{3.9}$$

Here $g_{jks} = -i(2\pi ck/\hbar L^3)^{1/2} (\vec{d} \cdot \hat{\epsilon}_{ks}) e^{i\vec{k}\cdot\vec{r}_j}$ is the vacuum coupling strength and the field annihilation(creation) operator is given by $a_{ks}(a_{ks}^\dagger)$. The subscripts (k, s) denote the kth mode of the field with polarization along $\hat{\epsilon}_{ks}$. The initial state is $|s, \{0_{ks}\}\rangle$, and the final state is $|a, \{0_{ks}\}\rangle$. Iterating the Schrödinger equation to second order in $\mathcal{H}_I(t)$ we find that the lowest order non-vanishing contribution to the transition amplitude is,

$$\frac{d}{dt}\langle a|s(t)\rangle \equiv -\frac{1}{\hbar^2} \lim_{t\to\infty} \int_0^t d\tau \langle a, \{0_{ks}\}|\mathcal{H}_I(t)\mathcal{H}_I(\tau)|s, \{0_{ks}\}\rangle. \tag{3.10}$$

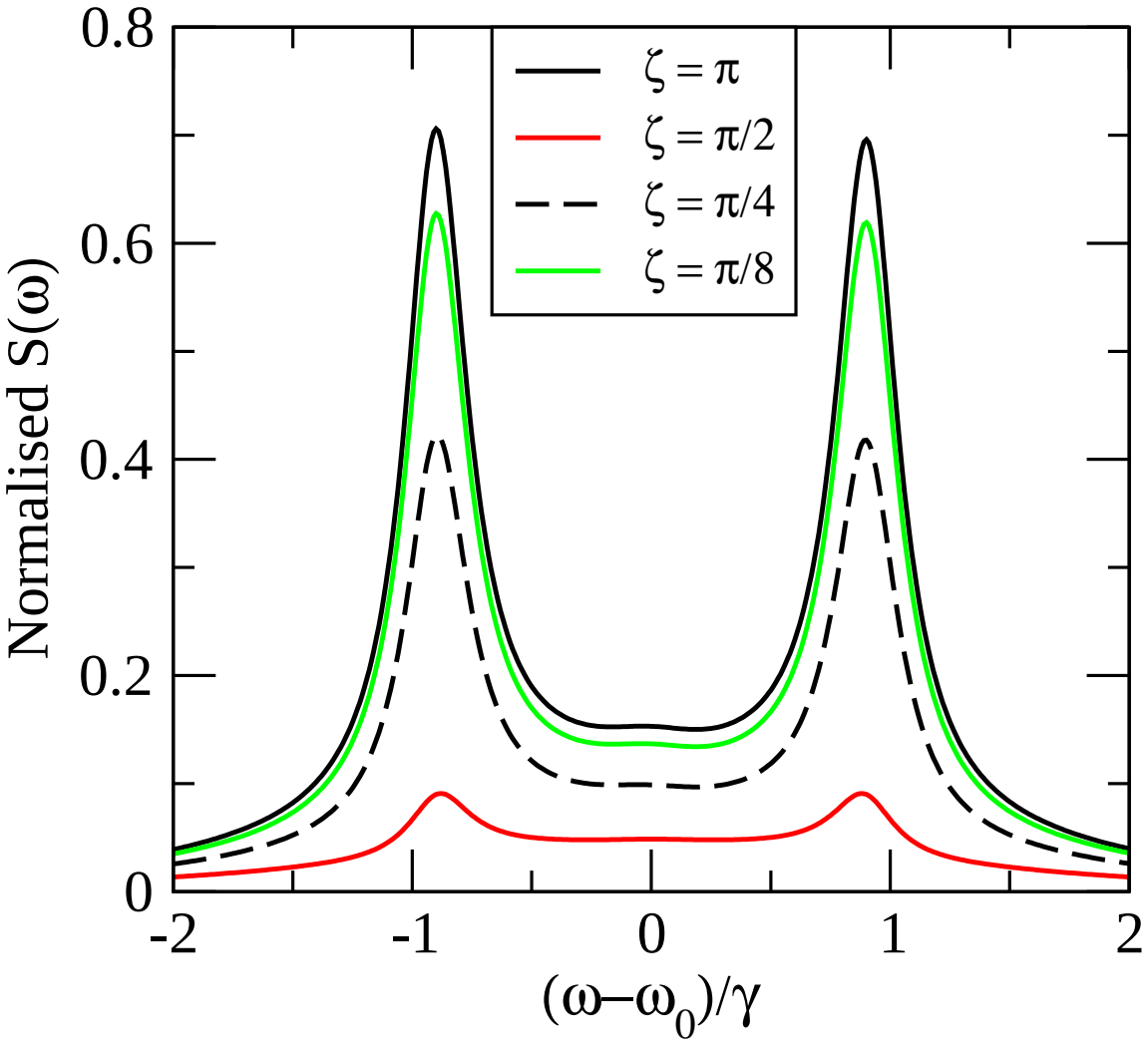

Figure 3.6: Normalized steady state spectrum of incoherent emission from two identical two level atoms for interatomic separation of $\lambda/8$ and Rabi frequency of 0.1γ. The relative orientation is given by $\phi = 2\frac{\pi}{\lambda}|\vec{r}_i - \vec{r}_j|\cos\zeta$.

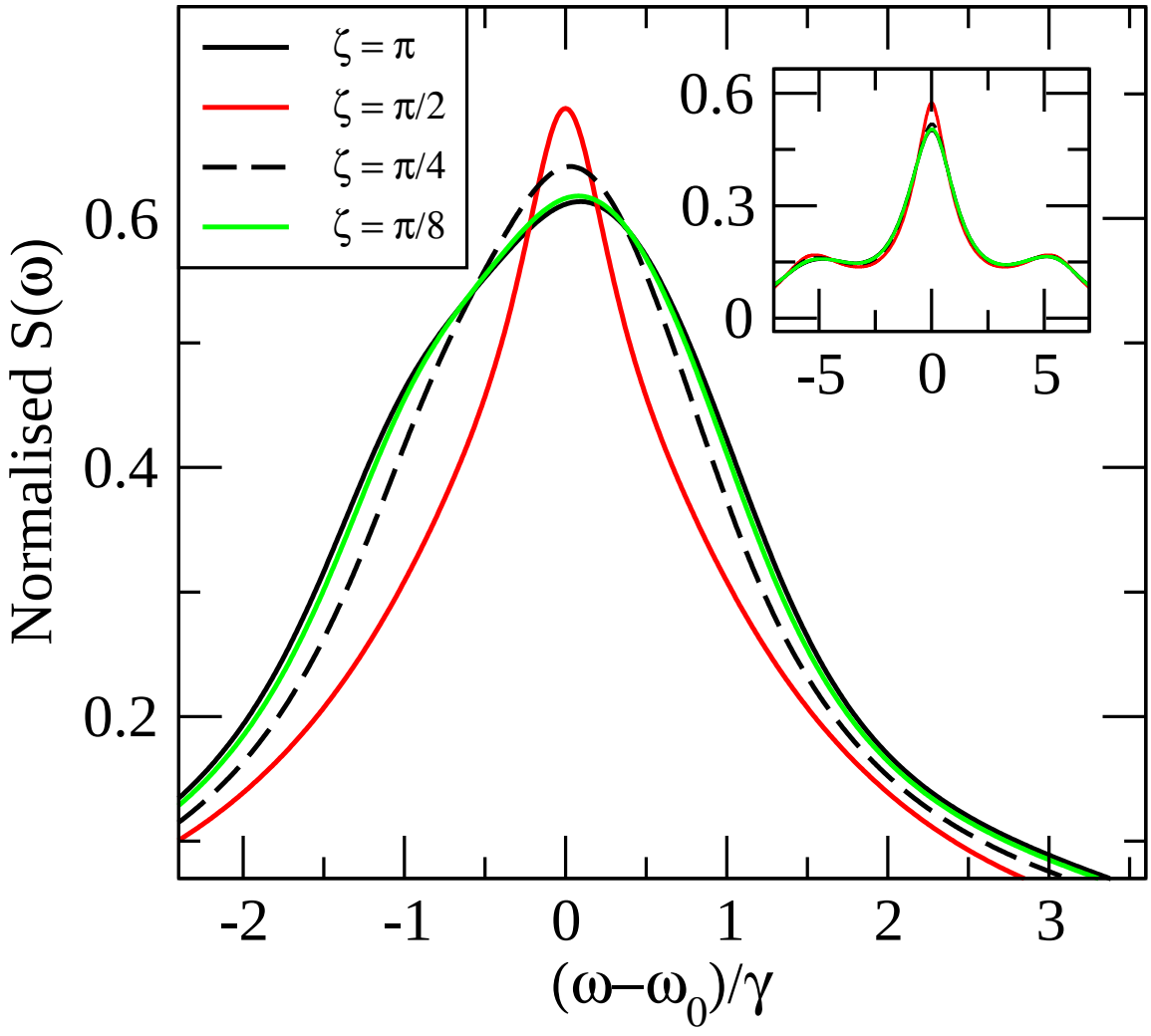

Figure 3.7: Normalized steady state spectrum of incoherent emission for interatomic separation of $\lambda/8$ and Rabi frequency G = 1.0γ. In the inset we show the spectrum for G = 3.0γ.

A long calculation (check appendix B for a rigorous derivation of this result) then leads to,

$$\frac{d}{dt}\langle a|s(t)\rangle \sim i \sin\phi(\gamma_{12} + i\Omega_{12}), \tag{3.11}$$

One can clearly see that this transition amplitude is zero if $\phi = 0$(modulo π). The second order transition amplitude (3.11) from the state $|s\rangle$ to $|a\rangle$ is mediated via the ground state $|g\rangle$. We have thus shown an intriguing connection between the quantum interference effects arising from spatial variations of the laser phase and the vacuum induced coherence effects.

3.6 Quantum correlation

We conclude the chapter with a discussion of how the quantum entanglement between two atoms (qubits) also depends in a significant way on the spatial variation of the phase ϕ. Note that the entanglement in this system arises from the fact that the density operator of the two atoms does not factorize, $\rho \neq \rho^{(i)} \otimes \rho^{(j)}$. This happens due to cooperative emission [132]. The non-factorizability of the density matrix is especially significant due to the Ω_{12} term in the dynamics. We show in the Fig.(3.8), existence of the quantum correlation $\Gamma_{12} = \mathsf{Re}[\langle \hat{S}_1^+ \hat{S}_2^- \rangle / \langle \hat{S}_1^+ \rangle \langle \hat{S}_2^- \rangle] - 1$ for small inter-atomic distance and for different values of the angle between laser propagation direction and the line joining the two atoms. In the absence of any entanglement in the system such correlation would vanish. One can see clearly from the Fig.(3.8) that at small interatomic separation the presence of the laser phase significantly effects the quantum correlation. Around $r_{12} \sim \lambda/6$ the value of the quantum correlation is about 25 times more in presence of the laser phase ($\zeta = \pi, \pi/8$) in comparison to when $\phi = 0 (\zeta = \pi/2)$. Thus the quantum interference can lead to strong entanglement in the system at small interatomic separation. One can further characterize quantitatively such entanglement by calculating its concurrence.

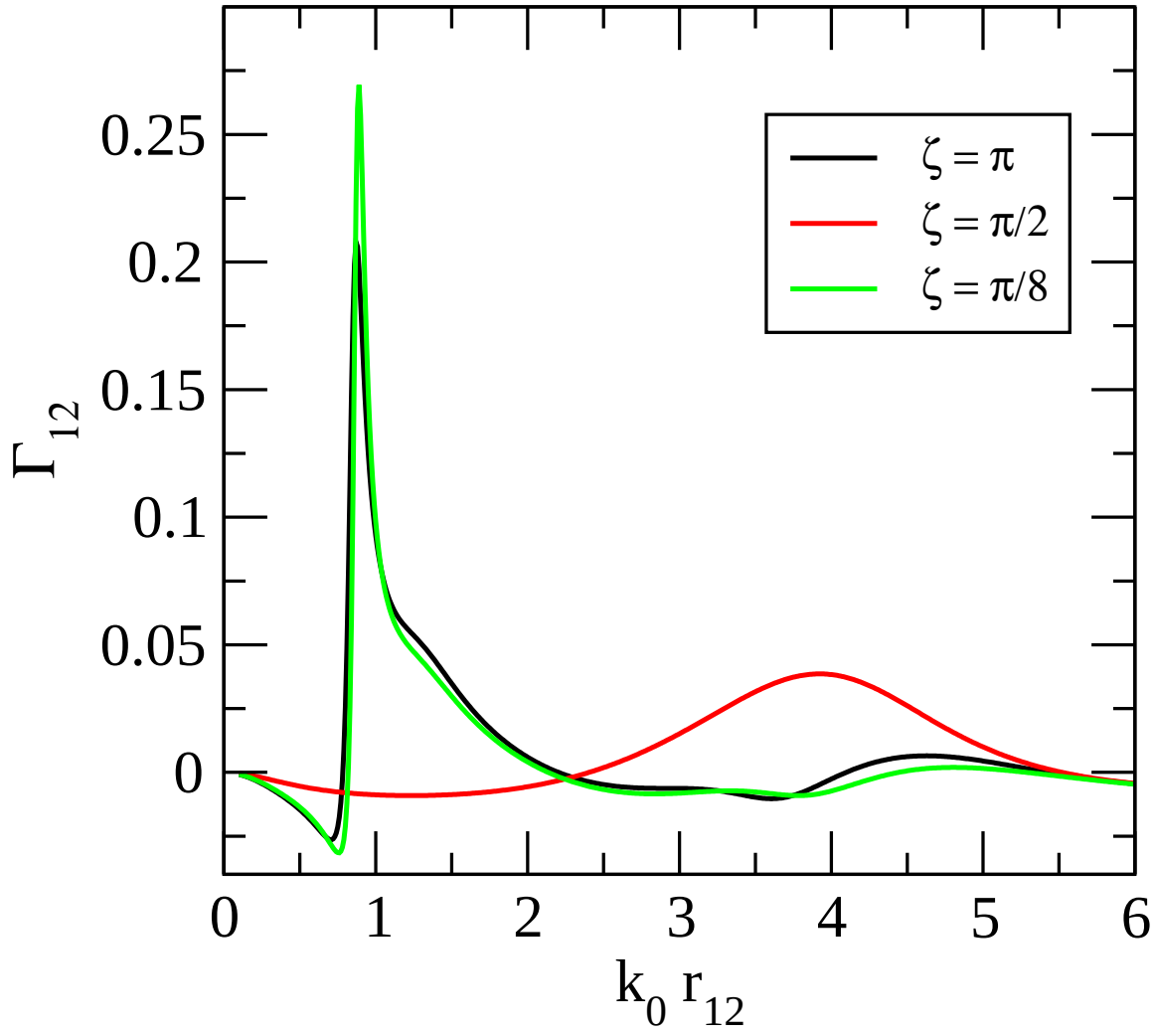

Figure 3.8: The quantum correlation between two atoms $\Gamma_{12} = \mathsf{Re}[\langle \hat{S}_1^+ \hat{S}_2^- \rangle / \langle \hat{S}_1^+ \rangle \langle \hat{S}_2^- \rangle] - 1$ as a function of distance between the atoms for a Rabi frequency of $G = 0.1\gamma$.

3.7 Conclusion

We have shown how the variation of the laser phase at the positions of the atoms can lead to new quantum interference effects. The phase variation is found to affect the spectral features of cooperative emission significantly and generate strong entanglement in the system. We further demonstrate that the coupling between the symmetric and antisymmetric states has strong connections to the vacuum induced coherence in the system. A plausible system for the observation of the interference effects of this chapter would be semiconductor quantum dots. Note that the splitting in photoluminescence spectra from a system of coupled quantum dots was observed [196]. The dots in these experiments satisfy the condition, wavelength $\gg$ interdot distance $\gtrsim$ size of the dot. Thus our theoretical results sould be observable in such systems.

The content of this chapter has been published in Phys. Rev. Lett. **101**, 153601 (2008).

CHAPTER 4

NONCLASSICAL CORRELATION OF POLARIZATION ENTANGLED PHOTONS IN A BIEXCITON-EXCITON CASCADE

4.1 Introduction

Polarization correlations of photons emitted in cascade emission are well known phenomenon and numerous theoretical and experimental studies exist in the literature on this subject since the early days of quantum optics [11, 12, 13, 14, 140, 141, 142]. Some of the earlier studies were motivated in testing generalised Bell's inequalities [11], the existence of hidden variables and whether quantum mechanics was a non-local theory or not [12, 13, 14], following the question raised by Einstein, Podolsky and Rosen [7]. In recent times polarization correlated photon pairs have become important in the field of quantum information science due to their entangled nature. Moreover many applications of quantum information, such as quantum key distribution [20], efficient optical quantum computing [21], long distance quantum communication using quantum repeaters [22] and implementation of quantum telecommunication schemes [23] require single photon pairs per cycle. This requirement of entangled photon pairs per cycle of excitation could be satisfied by cascade emission from a single atom or atom like systems like semiconductor quantum dots, provided one gets over the inherent asymmetries. Recently such cascade emission has been reported for semiconductor quantum dots [29, 30, 31, 32]. It was further seen that polarization entanglement of the emitted photon pairs was degraded by the presence of energy level splitting of the intermediate excitonic states and any incoherent process that leads to a population transfer between the two intermediate excitonic states [31, 32, 143]. Moreover dephas-

ing arising due to interaction of the quantum dot with its solid state environment can also degrade the entanglement [144]. Some recent studies have also shown how the fidelity of entanglement depends on excitonic level splitting [145] and the dynamics of the incoherent dephasing [146]. Different methods have been proposed to reduce and control the incoherent dephasing and energy level splitting of the excitonic states thereby preserving the entanglement in the system [31, 32, 143, 145, 147, 148, 149]. Further, methods to enhance the generated entanglement by coupling the quantum dot to a micro-cavity have also been proposed [55, 150]. As quantum dot systems are of great importance for future applications in quantum information science, a clear yet simple model for understanding the effects of all these different decoherence mechanism on the dynamics of the system is required. Thus we develop, in this chapter, a simple theoretical model to analytically study the influence of different decoherence mechanisms and the intermediate state splitting on the generation of polarization entangled photon pairs in cascade emission.

4.2 Model

We consider a four level system undergoing cascade emission as our model. We show a schematic diagram of such a cascade in Fig (4.1). The excited state $|i\rangle$ and the intermediate states $|\alpha\rangle$, $|\beta\rangle$ would correspond to the biexcitonic and optically active excitonic states respectively in a quantum dot. Further $|j\rangle$ is taken to be the ground state. Here $2\gamma = 2(\gamma_1 + \gamma_3)$ is the total spontaneous emission rate of the state $|i\rangle$, $2\gamma_2$, $2\gamma_4$ are the spontaneous emission rates of the states $|\alpha\rangle$ and $|\beta\rangle$ respectively and $2\gamma_{\beta\alpha}(2\gamma_{\alpha\beta})$ is the incoherent dephasing rate of the state $|\alpha\rangle$ ($|\beta\rangle$). The energy level splitting of the intermediate state is given by Δ. In this type of four-level cascade scheme there are two decay paths for the excited state, $|i\rangle \rightarrow |\alpha\rangle \rightarrow |j\rangle$ and $|i\rangle \rightarrow |\beta\rangle \rightarrow |j\rangle$. The generation of entanglement in these scheme is attributed to the fact that these decay paths can become indistinguishable. The eigenbasis of

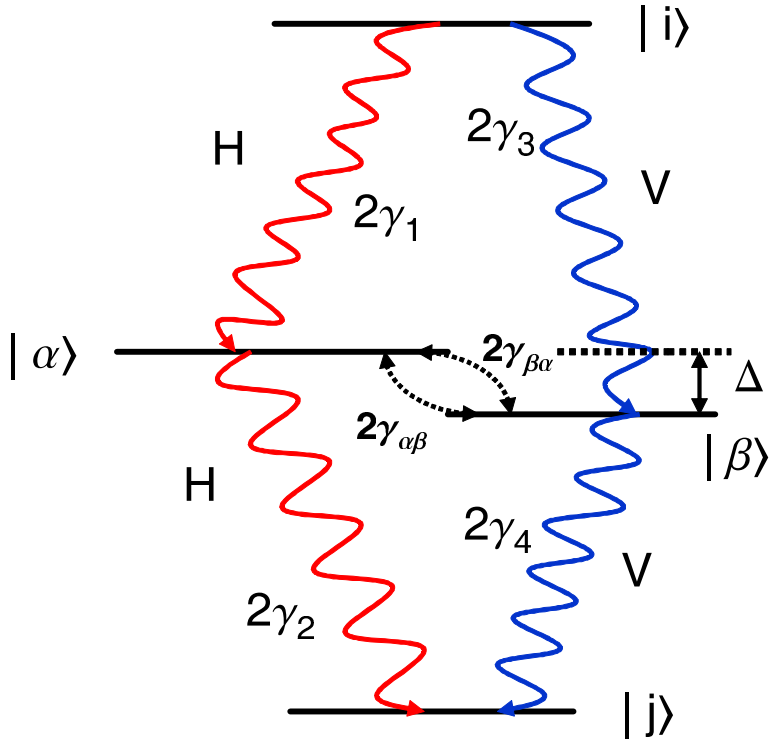

Figure 4.1: Schematic diagram of a four level cascade system. Here H and V refers to horizontally and vertically polarized photon emission. Δ is the energy level separation of the intermediate states and γ's are the spontaneous emission rates given by $\gamma_k = 2\omega_{kl}^3|\vec{d}_{kl}|^2/3\hbar c^3$. The incoherent dephasing rates of the intermediate states are given by $2\gamma_{\alpha\beta}$ and $2\gamma_{\beta\alpha}$ respectively.

this system is formed by the four states $(\{|i\rangle\},\{|\alpha\rangle\},\{|\beta\rangle\},\{|j\rangle\})$. In this basis the radiative transition from the excited state generates two collinearly polarized photons with linear polarizations along two orthogonal directions denoted by H (horizontal) and V (vertical). When the states $|\alpha\rangle$ and $|\beta\rangle$ are degenerate, the decay paths become indistinguishable and we get a maximally entangled two photon state [7, 29]

$$|E\rangle = \frac{1}{\sqrt{2}}(|H_1H_2\rangle + |V_1V_2\rangle). \tag{4.1}$$

In practical systems like atoms and quantum dots these levels are usually non degenerate and hence the entanglement of the emitted photon pairs depend completely on the degree of degeneracy and dynamics of these intermediate states. In our model we have taken them to be non-degenerate and study the effect of such intermediate level splitting on the correlation of the emitted photon pairs. To understand the effect of incoherent dephasing and energy level splitting of the excitonic state on the dynamics of emitted photon pairs from the cascade, we need to study the two time second order correlations. This is given by,

$$\begin{aligned}\langle II\rangle &= \langle \hat{\epsilon}^*_{(\theta_1,\phi_1)}\cdot\vec{E}^-(\vec{r},t)\hat{\epsilon}^*_{(\theta_2,\phi_2)}\cdot\vec{E}^-(\vec{r},t+\tau) \\ &\quad : \hat{\epsilon}_{(\theta_2,\phi_2)}\cdot\vec{E}^+(\vec{r},t+\tau)\hat{\epsilon}_{(\theta_1,\phi_1)}\cdot\vec{E}^+(\vec{r},t)\rangle.\end{aligned} \tag{4.2}$$

where $\langle II\rangle$ stands for the two time polarization angle dependent intensity-intensity correlation $\langle I_{(\theta_2,\phi_2)}(\vec{r},t+\tau)I_{(\theta_1,\phi_1)}(\vec{r},t)\rangle$. Further $E^+(\vec{r},t)(E^-(\vec{r},t))$ is the positive (negative) frequency part of the quantized electric field operator at a point $\vec{r}$ in the far-field zone and $\hat{\epsilon}_{(\theta,\phi)}$ is the polarization unit vector of the measured radiation at the detector along any arbitrary direction given by (θ,ϕ). $\hat{\epsilon}_{(\theta,\phi)}$'s are related to the linear polarization unit vectors $\hat{\epsilon}_H, \hat{\epsilon}_V$ (where H stands for horizontal and V for vertical) by

,

$$\begin{bmatrix} \hat{\epsilon}^{(1)}_{(\theta,\phi)} \\ \hat{\epsilon}^{(2)}_{(\theta,\phi)} \end{bmatrix} = \begin{bmatrix} \cos\theta & e^{-i\phi}\sin\theta \\ -e^{i\phi}\sin\theta & \cos\theta \end{bmatrix} \begin{bmatrix} \hat{\epsilon}_H \\ \hat{\epsilon}_V \end{bmatrix} \tag{4.3}$$

and these satisfy the relation $(\hat{\epsilon}^{(1)}_{(\theta,\phi)} \cdot \hat{\epsilon}^{(2)*}_{(\theta,\phi)}) = 0$. The above relation can be understood as a unitary transformation between a basis defined by the linear polarisation unit vectors and a basis defined by $\hat{\epsilon}^{(1)}$ and $\hat{\epsilon}^{(2)}$. In an experimental setup the angles θ, ϕ would correspond to the orientation of the optic axis of a half/quarter wave plate to the direction of propagation of the emitted radiation. Let us now consider for simplicity that both the levels $|\alpha\rangle$ and $|\beta\rangle$ in Fig (4.1) have the same incoherent dephasing rates i.e. $\gamma_{\alpha\beta} = \gamma_{\beta\alpha}$. Further we assume that the spontaneous decay rates of the intermediate levels are also equal. Such assumptions are well justified as they do not influence the dynamics of the system significantly and yet lead to a simplified form of the second order correlation, thereby providing a better understanding of the problem. Under the above assumptions and for $\phi_1 = \phi_2 = 0$ the form of the two-time polarization angle dependent intensity-intensity correlation is found to be ,

$$\begin{aligned} \langle I(\theta_2, t+\tau) I(\theta_1, t)\rangle &= \left(\frac{\omega_0}{c}\right)^8 \frac{1}{2r^4} \mathcal{D}_1^2 \mathcal{D}_2^2 \langle |i\rangle\langle i|_t\rangle \\ &\times \{e^{-2\gamma_2\tau} + \cos 2\theta_1 \cos 2\theta_2 e^{-2(\gamma_2+2\gamma_{\alpha\beta})\tau} \\ &+ \sin 2\theta_1 \sin 2\theta_2 e^{-2(\gamma_2+\gamma_{\alpha\beta})\tau} \cos(\Delta\tau)\} \end{aligned} \tag{4.4}$$

where $\mathcal{D}_1 = |\vec{d}_{\alpha i}| = |\vec{d}_{\beta i}|$ and $\mathcal{D}_2 = |\vec{d}_{j\alpha}| = |\vec{d}_{j\beta}|$. The above simple form of the second order correlation has been derived to match our theoretical analysis to that of the experiment results [32]. For details of the mathematical analysis leading to the generalised form of the two time intensity-intensity correlation the reader is referred to section 4 of this chapter. One can clearly see from Eq no. (4.4) that the second order correlation is profoundly influenced by both the incoherent dephasing rates as well as the energy level splitting of the intermediate states. Note further, that in the presence of small Δ this becomes equivalent to the second order correlations measured in ref.[12, 13, 14]. Next we define a quantity the degree of correlation c_μ as,

$$c_\mu = \frac{\langle I_\mu I_\mu\rangle - \langle I_\mu I_{\mu'}\rangle}{\langle I_\mu I_\mu\rangle + \langle I_\mu I_{\mu'}\rangle} \tag{4.5}$$

where μ, μ' stands for mutually orthogonal polarization basis. The degree of correlation varies between $+1$ and -1, where $+1$ represents perfect correlation (-1 for anti-correlation) and 0 represent no polarization correlation.

4.3 Results and Discussion

4.3.1 Effect of excitonic level splitting on the correlation

In Fig (4.2) we show how the time averaged degree of correlation varies with the basis angle for different values of splitting Δ, of the excitonic levels. Note that here the excitonic level dephasing $\gamma_{\alpha\beta}$ has been taken to be zero. We see that the degree of correlation is independent of the polarization basis when $\Delta = 0$ and takes a value $c_\mu = 1$. This correspond to perfect polarization correlation among the emitted photons. From the expression of c_μ it is clear that this can happen only when the cross-polarized correlations vanishes and the emitted photons are perfectly co-polarized. One can even see this explicitly from Eq no. (4.4) by putting the values of $\theta_1, \theta_2 = \theta_1 + \pi/2$ for H-V , D-D$'$ and V-H basis. where H, V, D and D$'$ stand for horizontal, vertical, diagonal and orthodiagonal polarization basis respectively. Further as the cross-polarized correlations are absent the pair of photons emitted in one excitation cycle can take either of the two paths $|i\rangle \rightarrow |\alpha\rangle \rightarrow |j\rangle$ or $|i\rangle \rightarrow |\beta\rangle \rightarrow |j\rangle$ thus making these paths indistinguishable. As a consequence we do not get the "Welcher Weg" or which path information thereby making the final state of the emitted photon pair entangled in both the linear and diagonal polarization basis. The generated entangled states can hence be written as $1/\sqrt{2}(|HH\rangle + |VV\rangle)$ and $1/\sqrt{2}(|DD\rangle + |D'D'\rangle)$ for the rectilinear and diagonal basis respectively. Note further that in this case perfect anti-correlation ($c_\mu =$ -1) is expected for measurement in the circularly polarized basis with the entangled state given by $1/\sqrt{2}(|RL\rangle + |LR\rangle)$. Thus one should get perfectly cross-polarized photons as the co-polarized correlations vanish in this basis. This is

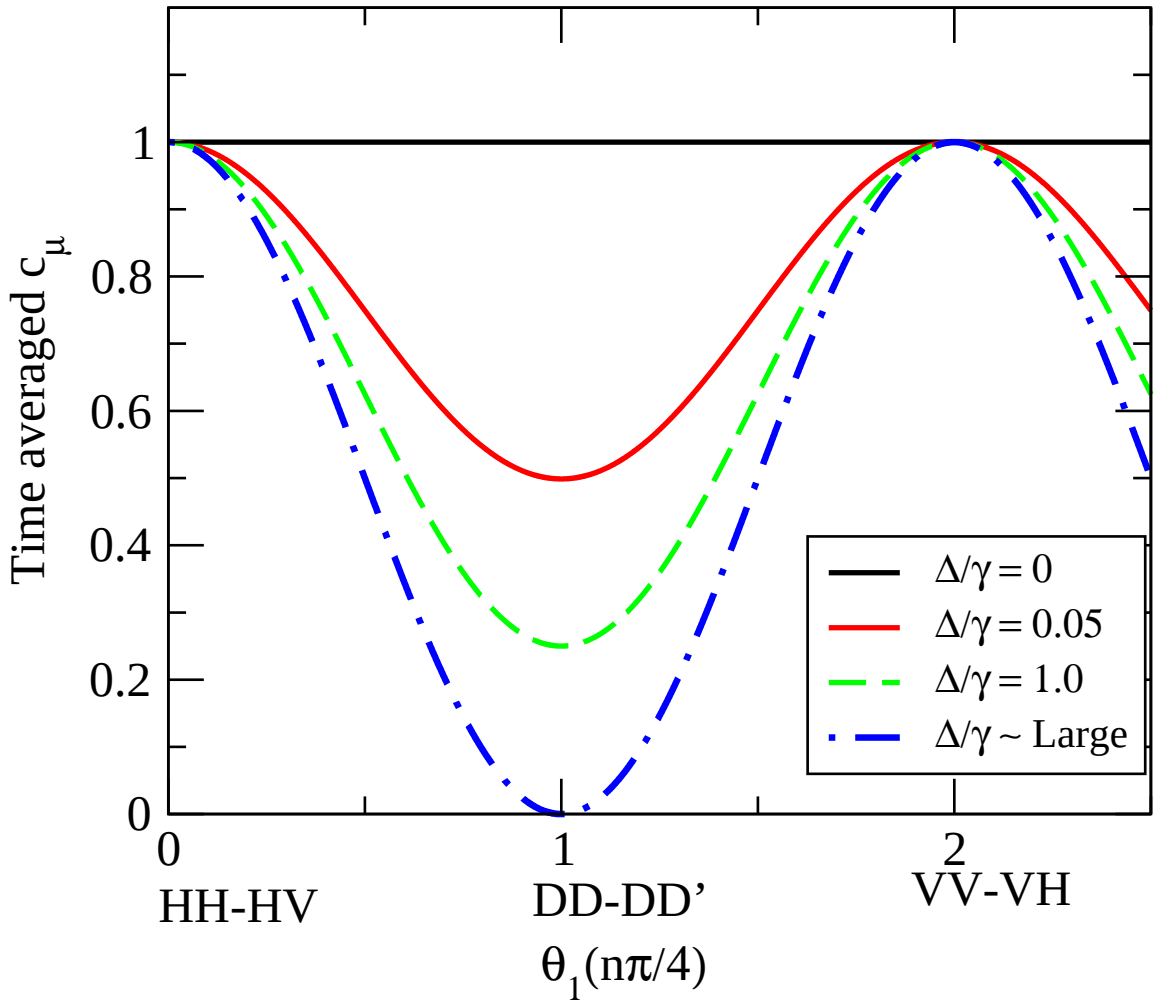

Figure 4.2: Degree of correlation averaged over time as a function of basis angle, for different excitonic level splitting Δ. H , D, D′, V stands for horizontal, diagonal, orthodiagonal and vertical polarization basis respectively. Here we have considered zero dephasing of the excitonic states. All parameters are normalized with respect to γ.

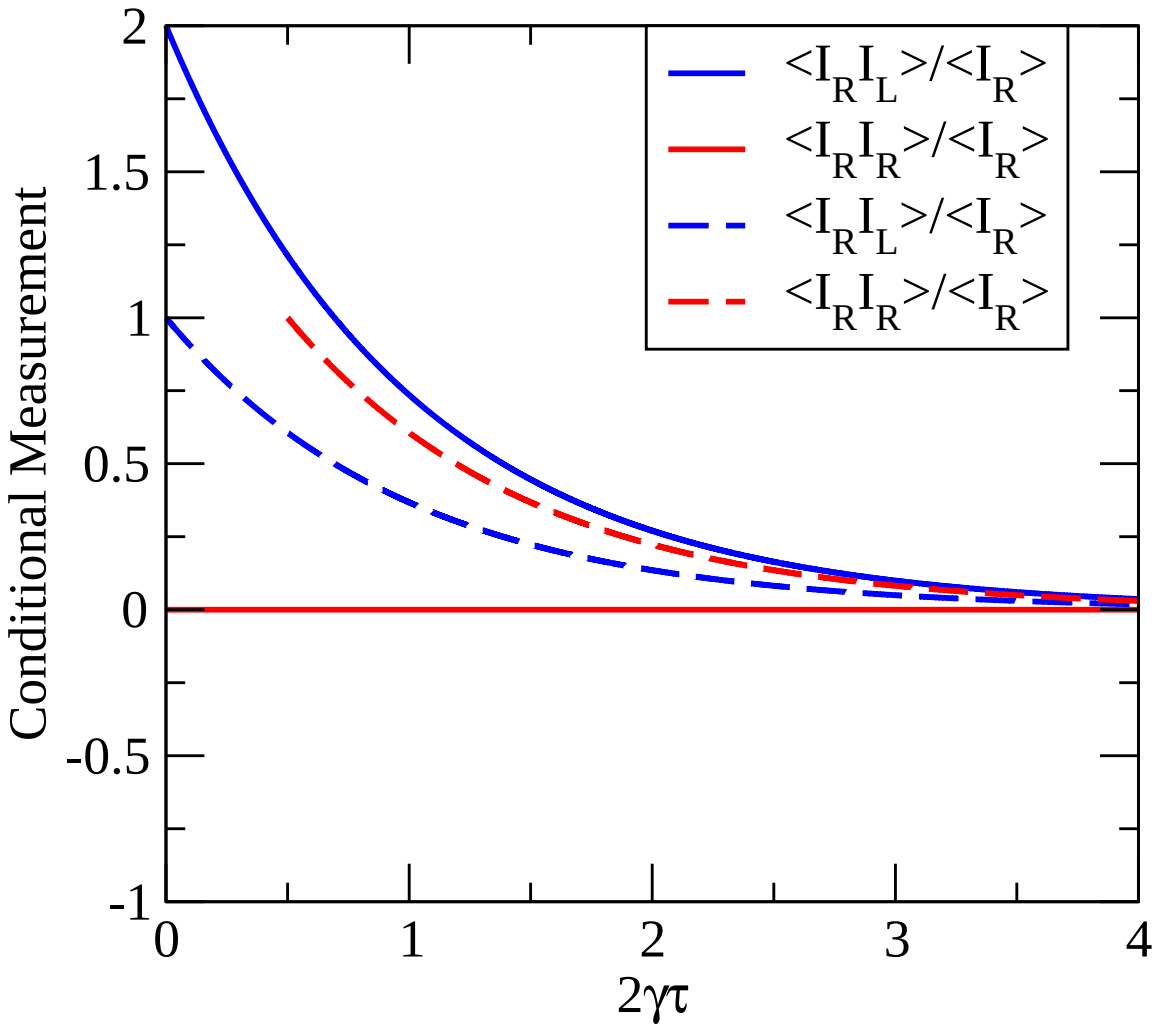

Figure 4.3: Conditional measurement of intensity-intensity correlation in the circular basis. The red curve corresponds to co-polarized ($\theta_1 = \theta_2 = \pi/4, \phi_1 = \phi_2 = -\pi/2$)photons and the blue for cross-polarized ($\theta_1 = \theta_2 = \pi/4, \phi_1 = -\pi/2, \phi_2 = \pi/2$) ones. The solid curve is for $\Delta = 0$ and the broken one for $\Delta \sim$ large. Here R and L stands for right and left circular polarisation. The R-R correlation curve in case of large splitting is time shifted for better comparison to the R-L correlation. All parameters are normalized with respect to γ.

exactly what we get from the general expression of Eq no. (4.4) [see section 4, Eq no. (4.13)] and is shown by the solid curves in Fig (4.3).

Further in Fig (4.2) we see that the degree of correlation is practically independent of the excitonic level splitting Δ in the rectilinear basis. As we change our polarization basis the effect of Δ becomes significant. In the diagonal basis for example with the increase in level splitting the degree of correlation gradually decreases and eventually vanishes. In presence of Δ, the cross-polarization does not vanish and we have a which path information for the emitted photons when we measure the second order correlations, thus destroying any entanglement in the system. The behaviour of the correlations in the circular basis in the presence of large excitonic level splitting is shown by the broken curves in Fig (4.3). One can clearly see that there is no polarization correlation at all for large Δ. The sinusoidal behaviour of c_μ for non zero values of Δ as seen in Fig (4.2) is in agreement with the classical linear polarization correlation behaviour. Note that our theoretical results are in agreement to experimentally observed data [32].

It should be noted that in our analysis we have concentrated on the calculation of the quantum correlation c_μ. This was also measured in the experiment of Stevenson *et. al.* We have not examined measures of entanglement like concurrence. This is because if Δ -the intermediate state exciton splitting is nonzero, then horizontal and vertical photons have different frequencies. This amounts to saying that we have for nonzero Δ quantum states which are characterized by two different parameters and measures of entanglement in such situations do not exist.

4.3.2 Effect of decoherence on the correlation

In figures (4.4) and (4.5) we show how the incoherent dephasing of the intermediate excitonic states affect the time averaged degree of correlations c_μ when excitonic states are non-degenerate ($\Delta \neq 0$) and degenerate ($\Delta = 0$) respectively. Note that here we

have assumed that both the intermediate states have same dephasing rates. One can clearly see that the effect is different for different measurement bases. The degree of polarization correlation for example in the rectilinear basis decreases with increasing dephasing irrespective of whether the excitonic states are non-degenerate or degenerate. For large dephasing rates the emitted photon pairs become almost un-correlated in their polarisation. This is attributed to the presence of significant cross-polarized correlation for large dephasing rates of the intermediate states. The incoherent dephasing of the intermediate levels causes an incoherent population transfer among the states $|\alpha\rangle$ and $|\beta\rangle$ thereby allowing the second photon to be emitted with orthogonal polarization to the first one. In the diagonal basis on the other hand the dephasing does not affect the correlation at all for large Δ but significantly decreases the correlation when $\Delta = 0$ for large dephasing rates. So we see that in diagonal basis even when the intermediate levels are degenerate we can still have significant cross-correlation if there is some incoherent relaxation process by which they can get coupled. This in turn spoils the quantum correlation in the system as can be seen clearly from Fig (4.5). In Fig (4.6) we show how the correlations behave in the circular basis in presence of large dephasing rate ($\gamma_{\alpha\beta}/\gamma = 10$) for both non-degenerate and degenerate intermediate states. We find that in the circular basis decoherence arising due to the incoherent dephasing does not affect the degree of correlation of the emitted photons when Δ is large. Further we find that for degenerate intermediate levels, even though the degree of correlation $c_\mu = -1$ for zero time delay, it vanishes at all later time in presence of the large dephasing. Thus the decoherence makes the perfectly anti-correlated photons completely uncorrelated. The incoherent relaxation process discussed by us here are practically present in the biexcitonic-excitonic cascade in quantum dots [144, 146]. Thus we have shown by a simple model how the decoherence arising due to such incoherent processes would strongly affect the quantum correlations.

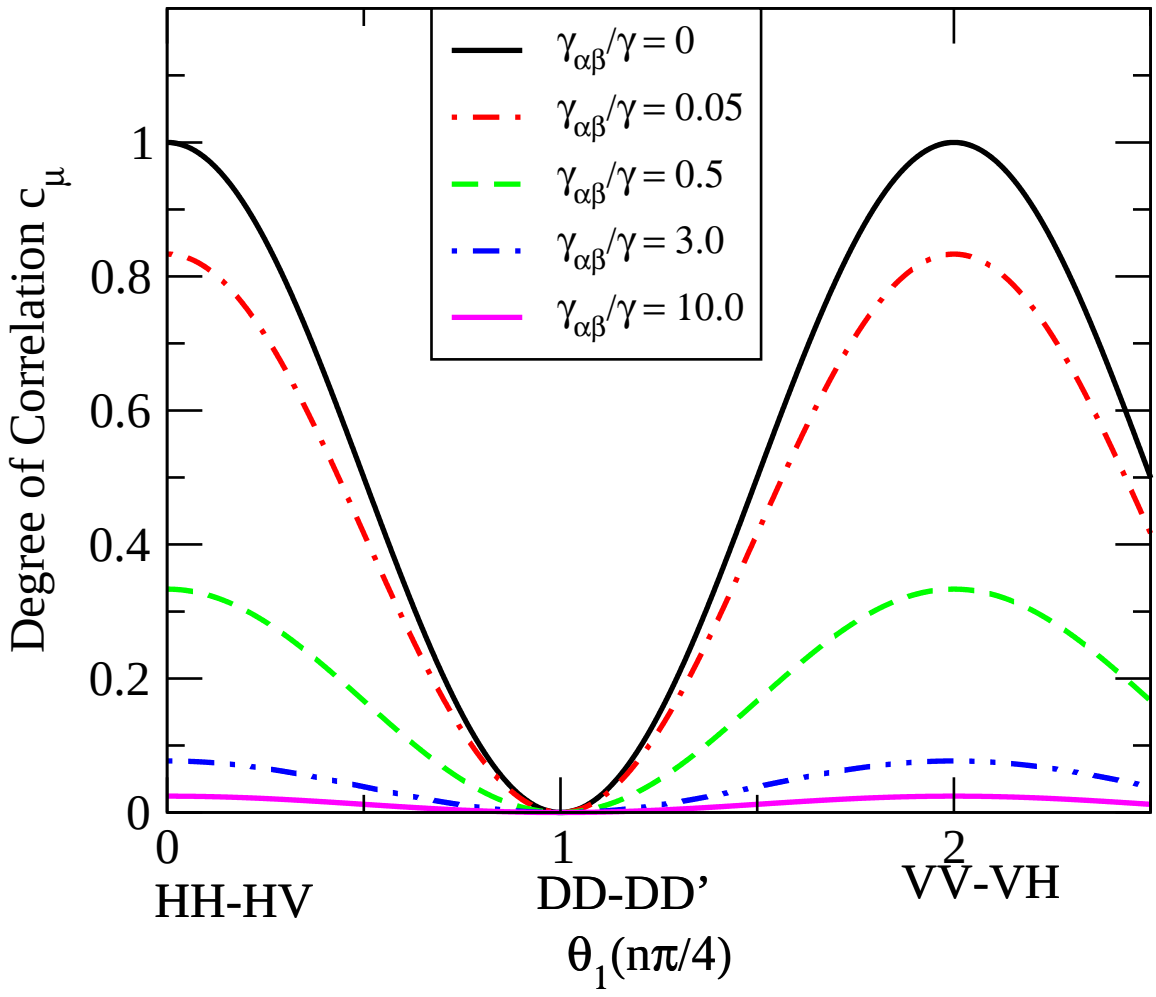

Figure 4.4: Degree of correlation averaged over time as a function of basis angle, for large Δ and different incoherent dephasing rates $\gamma_{\alpha\beta}$ of the intermediate level. Here we have assumed that both the intermediate states dephase at same rate i.e $\gamma_{\alpha\beta} = \gamma_{\beta\alpha}$. H , D, D′, V stands for horizontal, diagonal, orthodiagonal and vertical basis respectively.

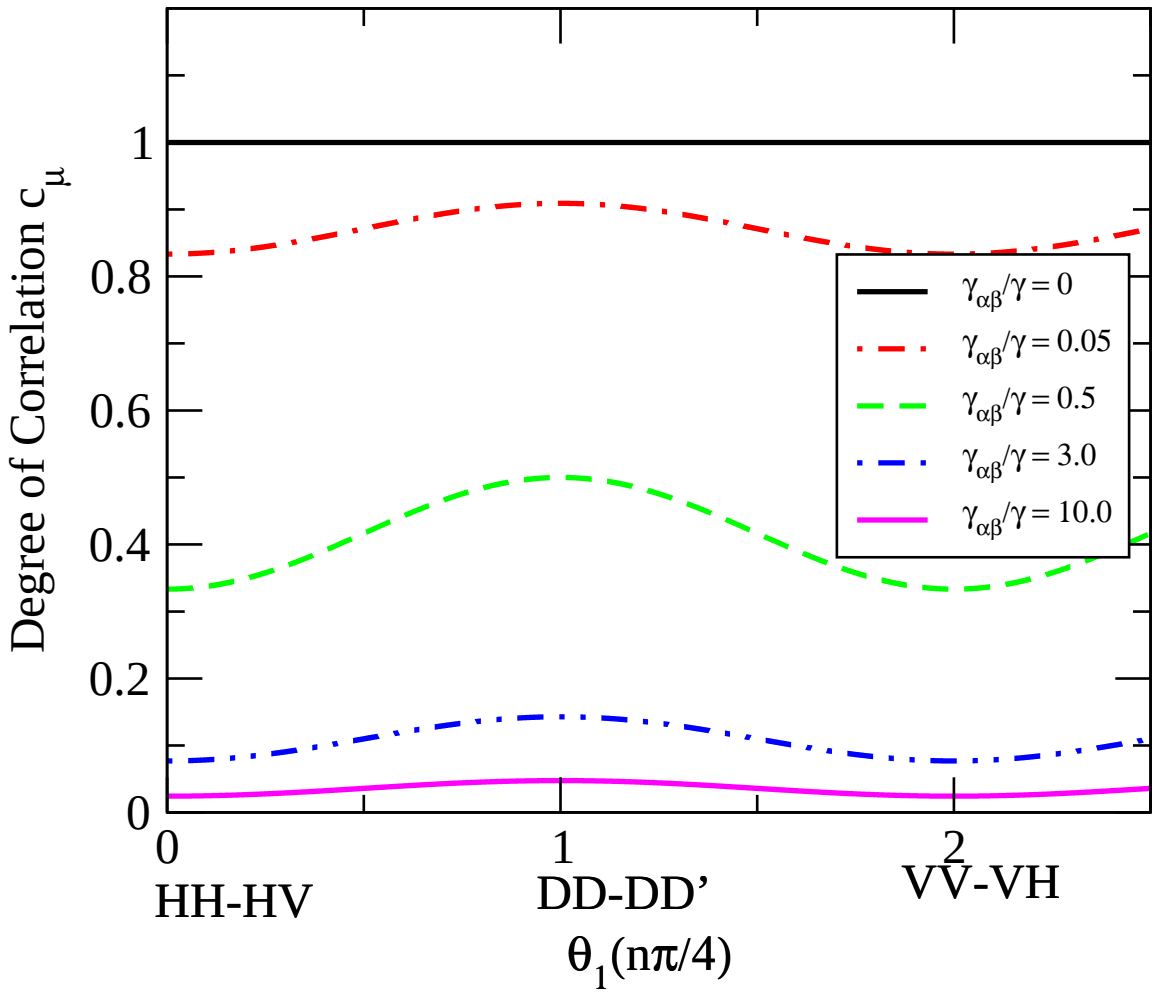

Figure 4.5: Degree of correlation averaged over time as a function of basis angle, for $\Delta = 0$ and different incoherent dephasing rates $\gamma_{\alpha\beta}$ of the intermediate level. Here we have assumed that both the intermediate states dephase at same rate i.e $\gamma_{\alpha\beta} = \gamma_{\beta\alpha}$. H , D, D′, V stands for horizontal, diagonal, orthodiagonal and vertical basis respectively.

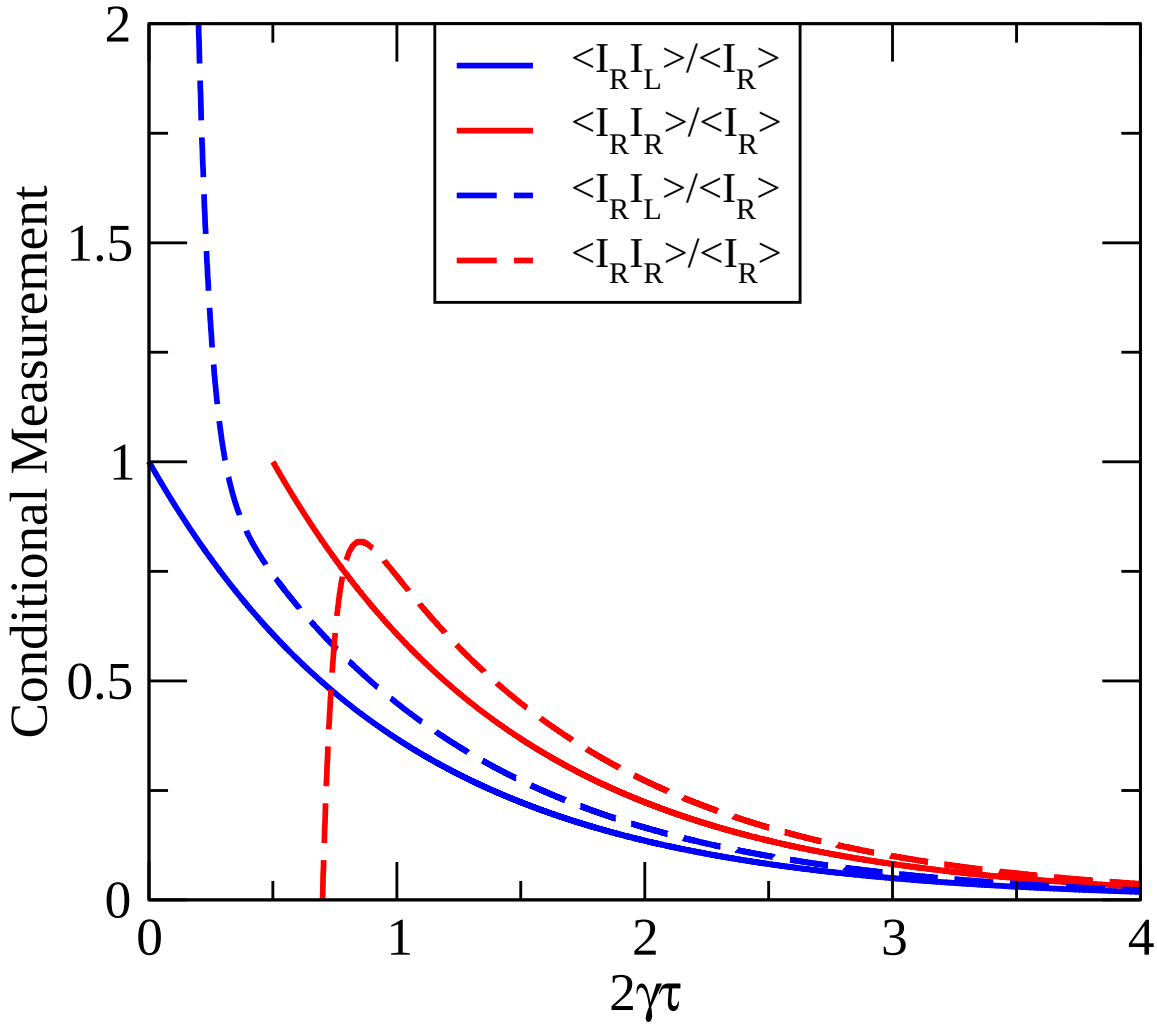

Figure 4.6: Conditional measurement of intensity-intensity correlation in the circular basis for incoherent dephasing $\gamma_{\alpha\beta}/\gamma = 10$. The red curve corresponds to co-polarized ($\theta_1 = \theta_2 = \pi/4, \phi_1 = \phi_2 = -\pi/2$)photons and the blue for cross-polarized ($\theta_1 = \theta_2 = \pi/4, \phi_1 = -\pi/2, \phi_2 = \pi/2$) ones. The solid curve is for $\Delta \sim$ large and broken one for $\Delta = 0$. Here R and L stands for right and left circular polarisation. The R-R correlation curve are time shifted for better comparison to the R-L correlation.

4.4 Intensity-Intensity correlation of emitted photons

Our model consists of a biexcitonic state and two excitonic states labelled as $|i\rangle$ and $|\alpha\rangle, |\beta\rangle$ respectively. The equilibrium state is labelled as $|j\rangle$. The biexcitonic state decays by emission of either a horizontally (H) polarized photon ($|i\rangle \rightarrow |\alpha\rangle$) or a vertically(V) polarized photon ($|i\rangle \rightarrow |\beta\rangle$)[29, 30]. The excitonic state $|\alpha\rangle(|\beta\rangle)$ decays to the equilibrium state $|j\rangle$ by emission of a H(V)- polarized photon. The two excitonic states have a energy difference of $\hbar\Delta$. Note that the splitting of the excitonic state in quantum dots arises due to anisotropic electron-hole exchange interactions [152, 153]. Figure (4.1) show a schematic diagram of our model. The eigenbasis of this system is formed by the four states $(\{|i\rangle\}, \{|\alpha\rangle\}, \{|\beta\rangle\}, \{|j\rangle\})$. In this basis the unperturbed Hamiltonian $\mathcal{H}$ is given by,

$$\mathcal{H} = \sum_k \hbar\omega_k |k\rangle\langle k|, \tag{4.6}$$

where $\hbar\omega_k$ is the energy of the four levels $(k = i, \alpha, \beta, j)$. Note that this kind of energy level scheme has been extensively used to study the cascade emission in quantum dots [31, 143, 144, 145, 146]. The spontaneous emission and dephasing effects in the system are incorporated via a master Eq no. technique [105] under the Born, Markov and rotating wave approximations and is given by,

$$\begin{aligned}
\mathcal{L}\rho &= -\gamma\{S_{ii}, \rho\} - \gamma_2\{S_{\alpha\alpha}, \rho\} - \gamma_4\{S_{\beta\beta}, \rho\} - \gamma_{\beta\alpha}\{S_{\alpha\alpha}, \rho\} \\
&- \gamma_{\alpha\beta}\{S_{\beta\beta}, \rho\} + 2(\gamma_1\rho_{ii}S_{\alpha\alpha} + \gamma_3\rho_{ii}S_{\beta\beta} + \gamma_2\rho_{\alpha\alpha}S_{jj} \\
&+ \gamma_4\rho_{\beta\beta}S_{jj}) + 2\left(\gamma_{\beta\alpha}\rho_{\alpha\alpha}S_{\beta\beta} + \gamma_{\alpha\beta}\rho_{\beta\beta}S_{\alpha\alpha}\right).
\end{aligned} \tag{4.7}$$

Here $2\gamma = 2(\gamma_1 + \gamma_3)$ is the total spontaneous emission rate of the biexcitonic state $|i\rangle$, $2\gamma_2(\ 2\gamma_4)$ and $2\gamma_{\beta\alpha}(2\gamma_{\alpha\beta})$ are the spontaneous emission rate and incoherent dephasing rate of the excitonic state $|\alpha\rangle(|\beta\rangle)$ (see Fig. 4.1). Such incoherent dephasing arises in quantum dots due to it's interaction with the solid-state environment (in form of spin flip processes or phonon scattering) [144]. The curly bracket $\{.., ..\}$ stands for the anti-

commutator and $S_{kl} = |k\rangle\langle l|(S^{\dagger}_{kl} = |l\rangle\langle k|$) is the atomic lowering (raising) operator which follow the simple angular momentum commutation relations. To study the dynamical evolution of this four-level cascade system we solve for the time evolution of the density operator which is given by,

$$\frac{\partial \rho}{\partial t} = -\frac{i}{\hbar}[\mathcal{H}, \rho] + \mathcal{L}\rho, \tag{4.8}$$

We will set the energy of the state $|j\rangle$ equal to zero henceforth. On substituting Eq nos. (4.6) and (4.7) in (4.8) and solving for the population terms we get,

$$\begin{aligned}
p_i(t) &= e^{-2\gamma t} p_i(0); \qquad p_i = \rho_{ii} - R/2\gamma \\
\rho_{\alpha\beta}(t) &= e^{-(a_0 - i\Delta)t}\rho_{\alpha\beta}(0); \\
\rho_{\alpha\alpha}(t) &= e^{-a_0 t}\left(\cosh(At) + \frac{\Gamma_a}{A}\sinh(At)\right)\rho_{\alpha\alpha}(0) \\
&\quad + 2e^{-a_0 t}\frac{\gamma_{\alpha\beta}}{A}\sinh(At)\rho_{\beta\beta}(0) \\
&\quad + \frac{R}{2\gamma}C(t) + p_i(0)e^{-2\gamma t}D(t); \\
\rho_{\beta\beta}(t) &= e^{-a_0 t}\left(\cosh(At) - \frac{\Gamma_a}{A}\sinh(At)\right)\rho_{\beta\beta}(0) \\
&\quad + 2e^{-a_0 t}\frac{\gamma_{\beta\alpha}}{A}\sinh(At)\rho_{\alpha\alpha}(0) \\
&\quad + \frac{R}{2\gamma}F(t) + p_i(0)e^{-2\gamma t}K(t).
\end{aligned} \tag{4.9}$$

Here R signifies a constant feeding of population into the state $|i\rangle$ from some arbitrary state $|n\rangle$. Note that in our model we are only concerned with the dynamics of the cascade decay once the upper level is populated, and thereby do not consider explicitly the pumping of the biexciton state $|i\rangle$. Further the excitonic level splitting $\Delta = \omega_\alpha - \omega_\beta$, $a_0 = (\gamma_2 + \gamma_4 + \gamma_{\alpha\beta} + \gamma_{\beta\alpha})$, $\Gamma_a = (\gamma_4 - \gamma_2 + \gamma_{\alpha\beta} - \gamma_{\beta\alpha})$ and $A = \sqrt{\Gamma_a^2 + 4\gamma_{\alpha\beta}\gamma_{\beta\alpha}}$. The time dependent coefficients C, D, F and K are given by,

$$\begin{aligned}
C(t) &= \left(2\gamma_1\left(1 + \frac{\Gamma_a}{A}\right) + 4\frac{\gamma_3\gamma_{\alpha\beta}}{A}\right)\frac{1 - e^{-(a_0 - A)t}}{2(a_0 - A)} \\
&\quad + (A \to -A)\,,
\end{aligned} \tag{4.10}$$

$$
\begin{aligned}
D(t) &= \left(2\gamma_1\left(1+\frac{\Gamma_a}{A}\right)+4\frac{\gamma_3\gamma_{\alpha\beta}}{A}\right)\frac{1-e^{-(a_0-A-2\gamma)t}}{2(a_0-A-2\gamma)} \\
&\quad +(A\rightarrow -A)\,, \\
F(t) &= \left(2\gamma_3\left(1-\frac{\Gamma_a}{A}\right)+4\frac{\gamma_1\gamma_{\beta\alpha}}{A}\right)\frac{1-e^{-(a_0-A)t}}{2(a_0-A)} \\
&\quad +(A\rightarrow -A)\,, \\
K(t) &= \left(2\gamma_3\left(1-\frac{\Gamma_a}{A}\right)+4\frac{\gamma_1\gamma_{\beta\alpha}}{A}\right)\frac{1-e^{-(a_0-A-2\gamma)t}}{2(a_0-A-2\gamma)} \\
&\quad +(A\rightarrow -A)\,.
\end{aligned}
$$

The effect of non-degenaracy of the excitonic states and their incoherent dephasing on the dynamical evolution of the system shows up if one studies the two-time non-classical second order correlation defined in Eq no. (4.2). For our four level system the explicit form of the positive frequency part of the electric field operator is given by [105],

$$
\begin{aligned}
\vec{E}^{(+)}(\vec{r},t) &= \vec{E}_0^{(+)}(\vec{r},t)-\left(\frac{\omega_0}{c}\right)\frac{1}{r}(\left[\hat{n}\times(\hat{n}\times\vec{d}_{\alpha i})\right]|\alpha\rangle\langle i|_t \\
&+ \left[\hat{n}\times(\hat{n}\times\vec{d}_{\beta i})\right]|\beta\rangle\langle i|_t \\
&+ \left[\hat{n}\times(\hat{n}\times\vec{d}_{j\alpha})\right]|j\rangle\langle\alpha|_t \\
&+ \left[\hat{n}\times(\hat{n}\times\vec{d}_{j\beta})\right]|j\rangle\langle\beta|_t). \qquad (4.11)
\end{aligned}
$$

Finally using Eq no. (4.11) in (4.2) we get the general form of the two time intensity-intensity correlation

$$
\begin{aligned}
\langle II\rangle &= \left(\frac{\omega_0}{c}\right)^8\frac{1}{r^4}\{\langle[(\hat{\epsilon}_H\cdot\vec{d}_{\alpha i})^*\cos\theta_1|i\rangle\langle\alpha|_t \\
&+ (\hat{\epsilon}_V\cdot\vec{d}_{\beta i})^* e^{i\phi_1}\sin\theta_1|i\rangle\langle\beta|_t] \\
&\times (|\hat{\epsilon}_H\cdot\vec{d}_{j\alpha}|^2\cos^2\theta_2|\alpha\rangle\langle\alpha|_{t+\tau}+|\hat{\epsilon}_V\cdot\vec{d}_{j\beta}|^2\sin^2\theta_2|\beta\rangle\langle\beta|_{t+\tau} \\
&+ e^{-i\phi_2}(\hat{\epsilon}_H\cdot\vec{d}_{j\alpha})^*(\hat{\epsilon}_V\cdot\vec{d}_{j\beta})\cos\theta_2\sin\theta_2|\alpha\rangle\langle\beta|_{t+\tau} \\
&+ e^{i\phi_2}(\hat{\epsilon}_H\cdot\vec{d}_{j\alpha})(\hat{\epsilon}_V\cdot\vec{d}_{j\beta})^*\cos\theta_2\sin\theta_2|\beta\rangle\langle\alpha|_{t+\tau}) \\
&\times \left[(\hat{\epsilon}_H\cdot\vec{d}_{\alpha i})\cos\theta_1|\alpha\rangle\langle i|_t+(\hat{\epsilon}_V\cdot\vec{d}_{\beta i})e^{-i\phi_1}\sin\theta_1|\beta\rangle\langle i|_t\right]\rangle\}.
\end{aligned}
\qquad (4.12)
$$

The two time correlation function that appears in Eq no. (4.12) is evaluated by invoking the quantum regression theorem [126] and Eq no. (4.9). Finally we get,

$$\begin{aligned}
\langle II\rangle &= \left(\frac{\omega_0}{c}\right)^8 \frac{1}{4r^4}\mathcal{D}_1^2\mathcal{D}_2^2\langle|i\rangle\langle i|_t\rangle \\
&\times \{f_1(\tau)+w_1(\tau)+f_2(\tau)+w_2(\tau) \\
&+ (\cos 2\theta_1+\cos 2\theta_2)(f_1(\tau)-w_2(\tau)) \\
&+ (\cos 2\theta_1-\cos 2\theta_2)(w_1(\tau)-f_2(\tau)) \\
&+ \cos 2\theta_1\cos 2\theta_2(f_1(\tau)+w_2(\tau)-f_2(\tau)-w_1(\tau)) \\
&+ \sin 2\theta_1\sin 2\theta_2(e^{-i(\phi_1+\phi_2)}u(\tau)+e^{i(\phi_1+\phi_2)}u^*(\tau))\}.
\end{aligned} \tag{4.13}$$

Here $\mathcal{D}_1 = |\vec{d}_{\alpha j}| = |\vec{d}_{\beta j}|$ and $\mathcal{D}_2 = |\vec{d}_{j\alpha}| = |\vec{d}_{j\beta}|$. The f's, w's and u are found from the solutions of the density matrix Eq no.s (4.9) and are given by,

$$\begin{aligned}
f_1(\tau) &= e^{-a_0\tau}\left(\cosh(A\tau)+\frac{\Gamma_a}{A}\sinh(A\tau)\right), \\
f_2(\tau) &= 2e^{-a_0\tau}\frac{\gamma_{\alpha\beta}}{A}\sinh(A\tau), \\
w_1(\tau) &= 2e^{-a_0\tau}\frac{\gamma_{\beta\alpha}}{A}\sinh(A\tau), \\
w_2(\tau) &= e^{-a_0\tau}\left(\cosh(A\tau)-\frac{\Gamma_a}{A}\sinh(A\tau)\right), \\
u(\tau) &= e^{-(a_0-i\Delta)\tau}.
\end{aligned} \tag{4.14}$$

The Eq no. (4.13) gives the most general form of the two time intensity-intensity correlations for arbitrary polarization directions and for any system undergoing a cascade emission. In the special case of $\phi_1 = \phi_2 = 0$, $\gamma_{\alpha\beta} = \gamma_{\beta\alpha}$ and $\gamma_2 = \gamma_4$ this reduces to the simplified result (4.4) of section (2).

4.5 Conclusions

In conclusion we have developed a simple theory to understand how the dephasing and energy level splitting of the excitonic states can affect polarization entanglement

of photons emitted in a biexciton-exciton cascade. We have also shown how these effects are important in determining whether the emitted photon pairs are classically correlated or entangled in different polarization basis. Further we have shown that our theoretical calculation is in agreement with the experimental results found in context to such cascade emissions in quantum dots.

The content of this chapter has been published in J. Phys. B. **41**, 225502 (2008).

CHAPTER 5

COMPETING EFFECTS OF COHERENT INTERACTION AND ENVIRONMENTAL DECOHERENCE IN QUBITS

5.1 Overview

It is now well understood that entanglement is the key resource for implementation of many quantum information protocols like teleportation, cryptography, logic operations and quantum communications [3, 4, 5, 24, 134]. Bi-partite entanglement i.e entanglement among two quantum mechanical systems each envisaged as a quantum bit (a quantum mechanical two level system analogous to a classical bit), has been found to be particularly important in this context. Numerous methods of producing qubit-qubit entanglement have been investigated during the past decade. A method, which is of particular interest in the context of quantum logic gate operations with systems like ion-traps and semiconductor nanostructures, relies on the coherent interactions among the qubits [26, 27, 51, 52, 53, 134, 135, 155, 156, 157]. An earlier proposal by Barenco *et. al.* [51] has shown how one can implement a fundamental quantum gate like the C-NOT gate using dipole-dipole interaction among two quantum dots modeled as two qubits. This was followed by another proposal from DiVincenzo and Loss [52] in which they showed how the Heisenberg exchange interaction between two quantum dots can be used to implement universal one and two-qubit quantum gates. In their model the qubit is realized as the spin of the excess electron on a single-electron quantum dot. They proposed the electrical gating of the tunneling barrier between neighbouring quantum dots to creat a Heisenberg coupling between the dots. Finally they showed explicitly how by controlling the exchange

coupling one can implement a quantum swap gate and XOR operation. Moreover they also showed the implementation of single qubit rotation using a pulsed magnetic field. Further in a later work Cirac and Zoller [26] discovered that by using the coulombic interaction among two ions one can implement a two-qubit quantum logic gate operation. Clearly many proposals require interacting qubits for two qubit quantum gates.

However for a computation to progress efficiently one needs sustained entanglement among the qubits as they dynamically evolve in time. This can be achieved effectively if the quantum mechanical system under evolution is weakly interacting with its surrounding. In practice though as the system evolves the system - environment interaction becomes stronger thereby inhibiting loses in its initial coherence. This loss of quantum coherence is known as decoherence [87] and leads to degradation of entanglement. Thus the study of dynamical evolution of two entangled qubits coupled to environmental degrees of freedom is of fundamental importance in quantum information sciences [88, 89, 90, 91, 92, 93, 158]. One study in particular predicted a remarkable new behavior in the entanglement dynamics of a bi-partite system. It reported that a mixed state of an initially entangled two qubit system, under the influence of a pure dissipative environment becomes completely disentangled in a finite time [92]. This was termed as *Entanglement Sudden Death* (ESD) [94] and was recently observed in two elegantly designed experiments with photonic qubits [95] and an atomic ensemble [96]. Note that an earlier proposal have discussed a pausible experiment to observe ESD in cavity QED and trapped ion systems [159]. The phenomenon of ESD has motivated numerous theoretical investigation in other bipartite systems involving pairs of atomic, photonic, and spin qubits [160, 161, 162, 163], multiple qubits [164] and spin chains [165, 166, 167]. Further ESD has also been studied for different environments including collective vacuum noise [169], classical noise [170] and thermal noise [171, 172, 173]. Moreover random matrix environments have been

studied [174, 175]. These authors [175], also point out the differences in the time evolution of concurrence arising from the internal dynamics of two entangled qubits due to the level splitting of each qubit.

ESD in continuous variable systems has also been extensively studied. In particular the problem of oscillators interacting with different environments has attracted lots of interest [91, 176, 177, 178, 179, 180]. Note that the conditions leading to ESD and probable ways of suppressing it are currently being actively investigated [159, 181]. In particular it has been shown how ESD can be avoided by using external modulation with an electromagnetic field [97, 98, 182] and can even lead to sudden birth for some cases [99]. Moreover sudden birth of entanglement has also been predicted for structured heat baths [100, 101] and certain choice of initial conditions of the entangled qubits [183]. In another recent work it has been shown that under a pure dephasing environment for a general two mode N-photon state ESD does not occur [184]. This result was explicitly proven for a general 3-photon state of the form $|\Psi\rangle = a|30\rangle + b|21\rangle + c|12\rangle + d|03\rangle$.

Even though numerous investigations on ESD in a variety of systems have been done so far, the question of ESD in interacting qubits remains open. In this chapter we investigate this question for a system of interacting qubits in contact with various models of the environment. We show that due to coherent qubit-qubit interactions two initially entangled qubits, get repeatedly disentangled and entangled as they dynamically evolve leading to dark and bright periods in entanglement [185]. Moreover we find that the amplitude of bright periods reduce with time and eventually at some finite time vanishes completely, thereby causing death of entanglement. Our investigations also reveal that the length of the dark periods depends on the initial condition of the entangled qubits and also on the interaction strength. Further we find dark and bright periods in entanglement in the presence of interactions among the qubits, for initial states which do not exhibit sudden death but simple asymptotic decay of

entanglement in absence of the interaction. We find *the existence of dark and bright periods to be generic for interacting qubits and occurs for a wide variety of models for the environment*. We show this explicitly by considering various models of the environment which induce correlated decays, pure and correlated dephasing of the qubits. All of these models exhibit the phenomenon of dark and bright periods even though some of them do not show ESD.

The organization of this chapter is as follows. In Sec 2 we discuss the model for two interacting qubits in contact with a simple dissipative environment and formulate their dynamical evolution by solving the quantum-Louiville equation of motion. In Sec 3 we develop the theory to study the dynamics of entanglement of the two interacting qubits and calculate the time evolution of the concurrence under the influence of environmental perturbations. In Sec 4 we study the entanglement dynamics of two interacting qubits under the influence of pure dephasing environment. We find that coherent qubit-qubit interaction not only leads to dark and bright periods in entanglement it also delays the onset of ESD. Further in Sec 5 we do a detailed study of the dynamics of qubit-qubit entanglement for both non-interacting and interacting qubits for two different correlated models of the environment. In Sec 5.5.1 we focus on dissipative environments inducing correlated decay of the qubits. Here we find that for non-interacting qubits there is no ESD and even though entanglement vanishes for certain initial conditions at some instant, it gets partially regenerated quickly and then decays very slowly. When we include the interaction among the qubits we find that entanglement exhibits the phenomenon of dark and bright periods. We further study the behavior of two qubit entanglement for a pure correlated dephasing environment in Sec 5.5.2. We find that the correlated dephasing leads to delay of ESD in absence of qubit-qubit interactions. We see that the degree of delay depends on the strength of the correlation. Here again when we include the qubit-qubit interaction we observe dark and bright periods in entanglement with a much later onset of ESD.

In each section we mention the earlier works. Finally in Sec 6 we summarize our findings.

5.2 Qubit-Qubit Interaction

The model that we consider for our study consist of two initially entangled interacting qubits, labeled A and B. Each qubit can be characterized by a two-level system with an excited state $|e\rangle$ and a ground state $|g\rangle$. Further we assume that the qubits interact independently with their respective environments. This leads to both local decoherence as well as loss of entanglement of the qubits. The decoherence, for instance can arise due to spontaneous emission from the excited states. Figure (5.1). show a schematic diagram of our model. The Hamiltonian for our model is then given by,

$$\mathcal{H} = \hbar\omega_0(S_A^z + S_B^z) + \hbar v(S_A^+ S_B^- + S_B^+ S_A^-), \tag{5.1}$$

where v is the interaction between the two qubits, S_i^z, S_i^+, S_i^- (i =A,B) are the atomic energy, raising and lowering operators defined as $S_i^z = 1/2(|e_i\rangle\langle e_i| - |g_i\rangle\langle g_i|), S_i^+ = |e_i\rangle\langle g_i| = (S_i^-)^\dagger$ respectively and obey angular momentum commutation algebra. We would use the two qubit product basis given by,

$$\begin{aligned} |1\rangle &= |e\rangle_A \otimes |e\rangle_B \qquad & |2\rangle &= |e\rangle_A \otimes |g\rangle_B \\ |3\rangle &= |g\rangle_A \otimes |e\rangle_B \qquad & |4\rangle &= |g\rangle_A \otimes |g\rangle_B \end{aligned} \tag{5.2}$$

Now as each qubit independently interacts with its respective environment, the dynamics of this interaction can be treated in the general framework of master equations. The time evolution of the density operator ρ which gives us information about the dynamics of the system can then be evaluated from the quantum-Liouville equation of motion,

$$\dot{\rho} = -\frac{i}{\hbar}[\mathcal{H}, \rho] + \mathcal{L}\rho, \tag{5.3}$$

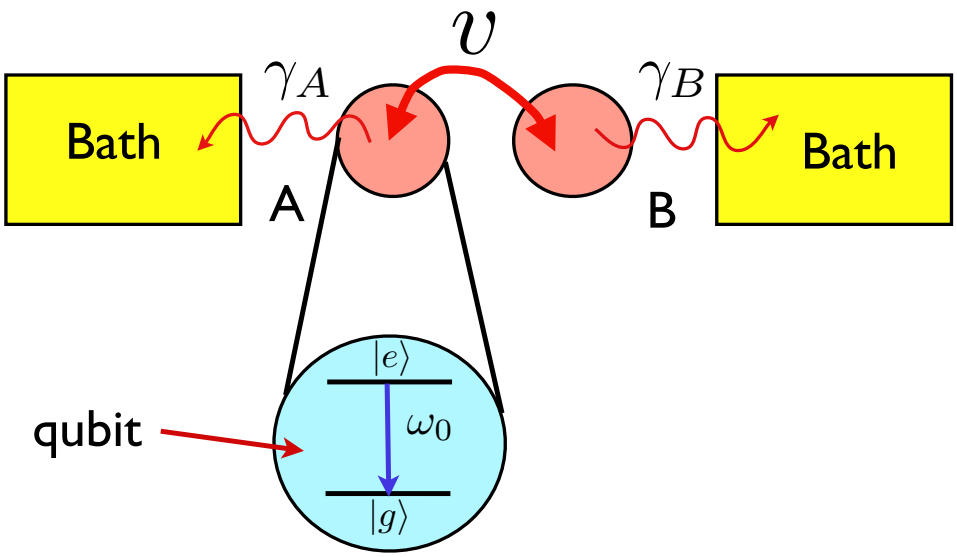

Figure 5.1: Schematic diagram of two qubits modelled as two two-level atom coupled to each other by an interaction parameter v. Here $|e\rangle, |g\rangle$ signifies the excited and ground states and ω_0 their corresponding transition frequency. The qubits A and B independently interact with their respective environments (baths) which lead to local decoherence as well as loss in entanglement.

where $\mathcal{L}\rho$ includes the effect of the interaction of the environment with the qubits. Note that in its simplest form this can be considered to be a spontaneous emission process induced by the vacuum fluctuation of the radiation field. For the case of a simple dissipative environment with which the qubits are interacting independently, the effect will be decay of the excited state and any initial coherences of the qubit. As an example say for qubit A this can be written as,

$$\begin{aligned} \dot{\rho}_{ee} &= -2\gamma_A \rho_{ee} \\ \dot{\rho}_{eg} &= -\gamma_A \rho_{eg}. \end{aligned} \tag{5.4}$$

The above equation together with the normalization $Tr[\rho] = 1$ and symmetry of the density matrix, define completely the dynamical system. The effect of the environment as elucidated in Eq no. (5.4) can be written in a compact form in terms of the atomic operators S^+, S^- as,

$$\mathcal{L}\rho = -\sum_{j=A,B} \frac{\gamma_j}{2}(S_j^+ S_j^- \rho - 2S_j^- \rho S_j^+ + \rho S_j^+ S_j^-), \tag{5.5}$$

where the terms $\gamma_A(\gamma_B)$ gives the decay rate of qubit A (B) to the environment. We give the complete analytical solution of Eq no. (5.3) in the basis defined by Eq no. (5.2) for coupling to a dissipative environment Eq no. (5.5) in appendix C

5.3 Concurrence Dynamics

To investigate the effect of interaction among the two qubits on decoherence we need to study the dynamics of two qubit entanglement. The entanglement for any bipartite system is best identified by examining the concurrence [68, 77], an entanglement measure that relates to the density matrix of the system ρ. The concurrence for two qubits is defined as,

$$C(t) = \max\{0, \sqrt{\lambda_1} - \sqrt{\lambda_2} - \sqrt{\lambda_3} - \sqrt{\lambda_4}\}, \tag{5.6}$$

where the λ's are the eigenvalues of the non-hermitian matrix $\rho(t)\tilde{\rho}(t)$ arranged in non-increasing order of magnitude. The matrix $\rho(t)$ being the density matrix for the two qubits and the matrix $\tilde{\rho}(t)$ is defined by,

$$\tilde{\rho}(t) = (\sigma_y^{(1)} \otimes \sigma_y^{(2)})\rho^*(t)(\sigma_y^{(1)} \otimes \sigma_y^{(2)}), \tag{5.7}$$

where $\rho^*(t)$ is the complex conjugate of $\rho(t)$ and σ_y is the well known time reversal operator for spin half systems in quantum mechanics. Note that concurrence varies from $C = 0$ for a separable state to $C = 1$ for a maximally entangled state. Though in general the two qubit density matrix ρ will have all sixteen elements, here we consider the initially entangled qubits to be in a mixed state [92] given by the density matrix,

$$\begin{aligned} \rho &\equiv 1/3(a|1\rangle\langle 1| + d|4\rangle\langle 4| + (b+c)|\psi\rangle\langle\psi|); \\ |\psi\rangle &= \frac{1}{\sqrt{b+c}}(\sqrt{b}|2\rangle + e^{i\chi}\sqrt{c}|3\rangle); \\ & \frac{a+b+c+d}{3} = 1; \end{aligned} \tag{5.8}$$

where a, b, c are independent parameters governing the nature of the initial state of the two entangled qubits. Note that the entanglement part of the state depends on the initial phase χ. Following Eq no.(5.8) one can see that the initial two qubit density matrix has only six-elements. In the matrix form ρ is then given by,

$$\rho(0) = \frac{1}{3}\begin{pmatrix} a & 0 & 0 & 0 \\ 0 & b & z & 0 \\ 0 & z^* & c & 0 \\ 0 & 0 & 0 & d \end{pmatrix}. \tag{5.9}$$

Here $z = e^{i\chi}\sqrt{bc}$ are the single photon coherences. Using the solution of the quantum-Liouville equation from appendix (C) it can be shown that the *initial density matrix* (5.9) *preserves its form for all t*. Finally we calculate the concurrence defined by (5.6) and (5.7) for the two qubits as,

$$C(t) = \mathsf{Max}\{0, \tilde{C}(t)\}, \tag{5.10}$$

where $\tilde{C}(t)$ is given by,

$$\tilde{C}(t) = 2\left\{|\rho_{23}(t)| - \sqrt{\rho_{11}(t)\rho_{44}(t)}\right\} \tag{5.11}$$

Let us now consider a particular class of mixed states with a single parameter a satisfying intially $a \geq 0$, $b = c = |z| = 1$ and $d = 1 - a$ [92]. Note that then (5.8), has the structure similar to a Werner state [15]. On using the dynamical evolution of the density matrix elements from appendix (C) and this set of initial conditions in (5.11), we obtain,

$$\begin{aligned} \tilde{C}(t) &= \frac{2}{3}e^{-\gamma t}[(\cos^2\chi + \sin^2\chi\cos^2(2vt))^{1/2} \\ &- \sqrt{a(1-a+2w^2+w^4a)}], \end{aligned} \tag{5.12}$$

where $w = \sqrt{1-e^{-\gamma t}}$. One can clearly see the dependence of $\tilde{C}(t)$ on the interaction v among the qubits and the initial phase χ. We see from (5.12) that in absence of the interaction v, concurrence becomes independent of the initial phase and yields the well established result of Yu and Eberly [92].

Note that $\tilde{C}(t)$ can become negative if,

$$a(1-a+2w^2+w^4a) > (1-\sin^2\chi\sin^2(2vt)), \tag{5.13}$$

in which case concurrence is zero and the qubits get disentangled. To understand how the interaction would effect entanglement we study the analytical result of Eq no. (5.12) for different values of the parameter a and χ. In Fig (5.2) we show the time dependence of the entanglement for $v = 5\gamma$ and for different values of the initial phase χ. The inset of Fig (5.2) shows the long time behavior of entanglement for this case. In Fig (5.2) we show that for $a = 0.4$, the non-interacting qubits ($v = 0$) exhibit sudden death of entanglement (ESD) [visible more clearly in the inset] whereas when they interact ($v \neq 0$) the concurrence oscillates between zero and non-zero values with diminishing magnitudes and eventually shows ESD. Thus the initially entangled qubits in presence of interaction v gets repeatedly disentangled and entangled before

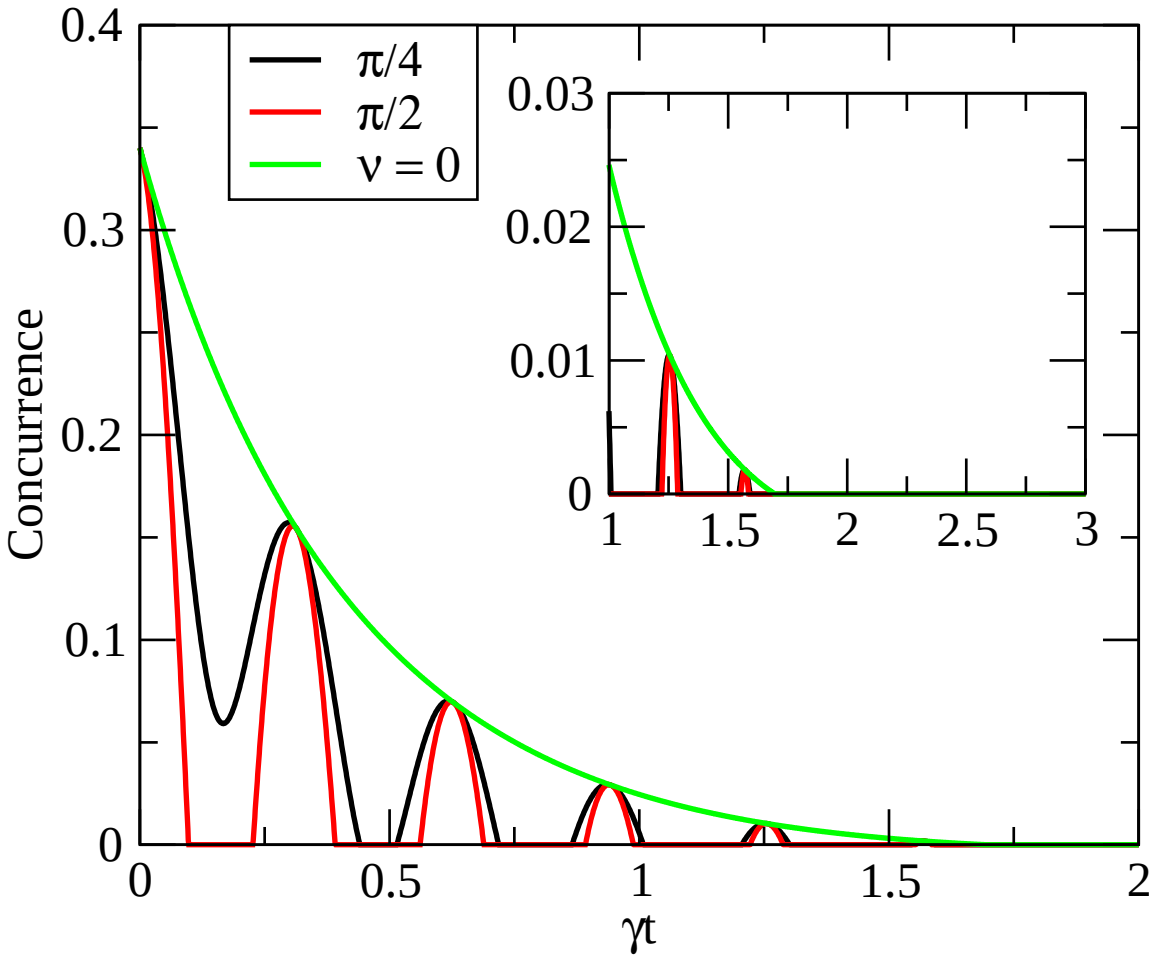

Figure 5.2: Concurrence as a function of time for two initially entangled, interacting qubits with initial conditions $a = 0.4, b = c = |z| = 1.0$ and two different initial phases $\chi = \pi/4$ (black curve) and $\chi = \pi/2$ (red curve). The inset shows the long time behavior of concurrence. Here interaction strength is taken to be $v = 5\gamma$.

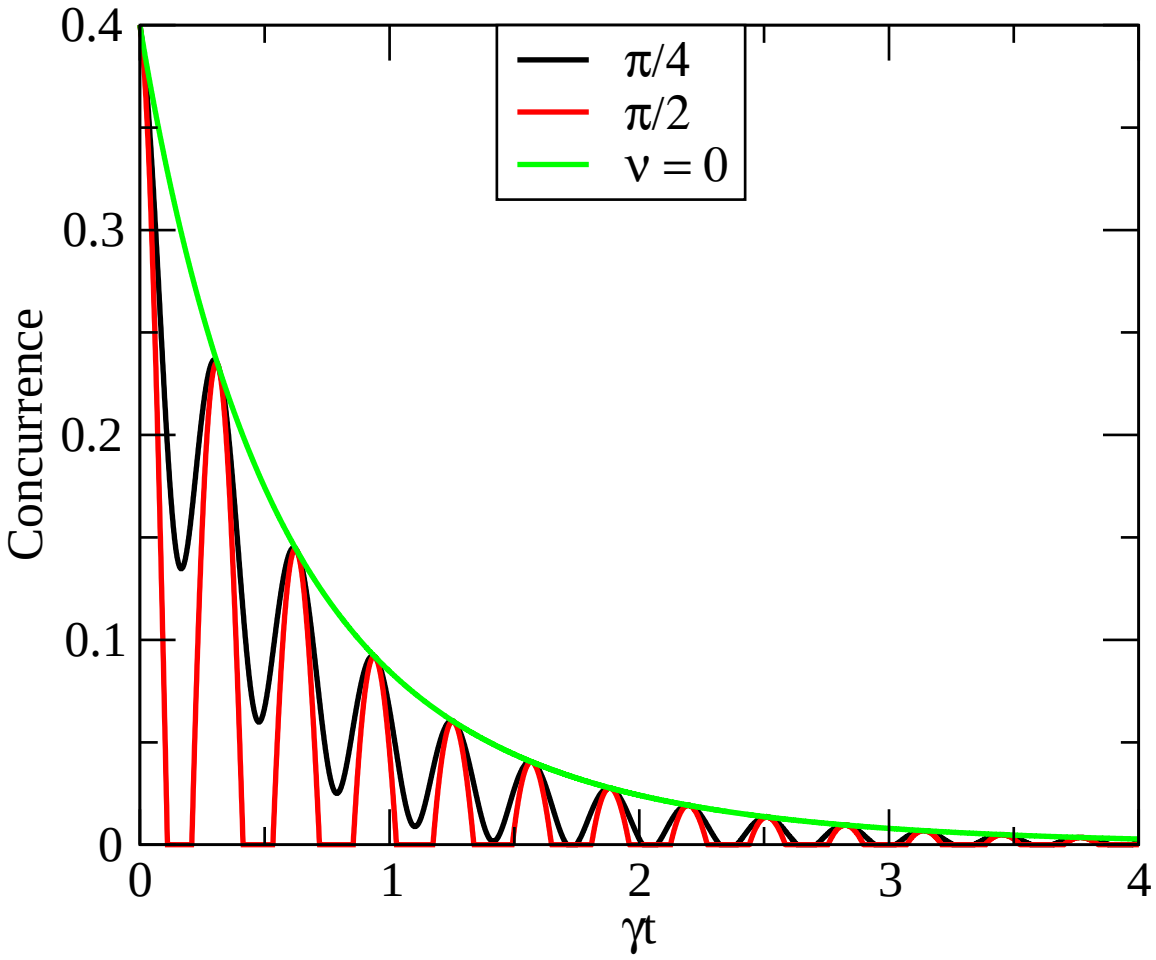

Figure 5.3: Concurrence as a function of time for two initially entangled, interacting qubits with initial conditions $a = 0.2, b = c = |z| = 1.0$ and two different initial phases $\chi = \pi/4$ (black curve) and $\chi = \pi/2$ (red curve). Here interaction strength is taken to be $v = 5\gamma$.

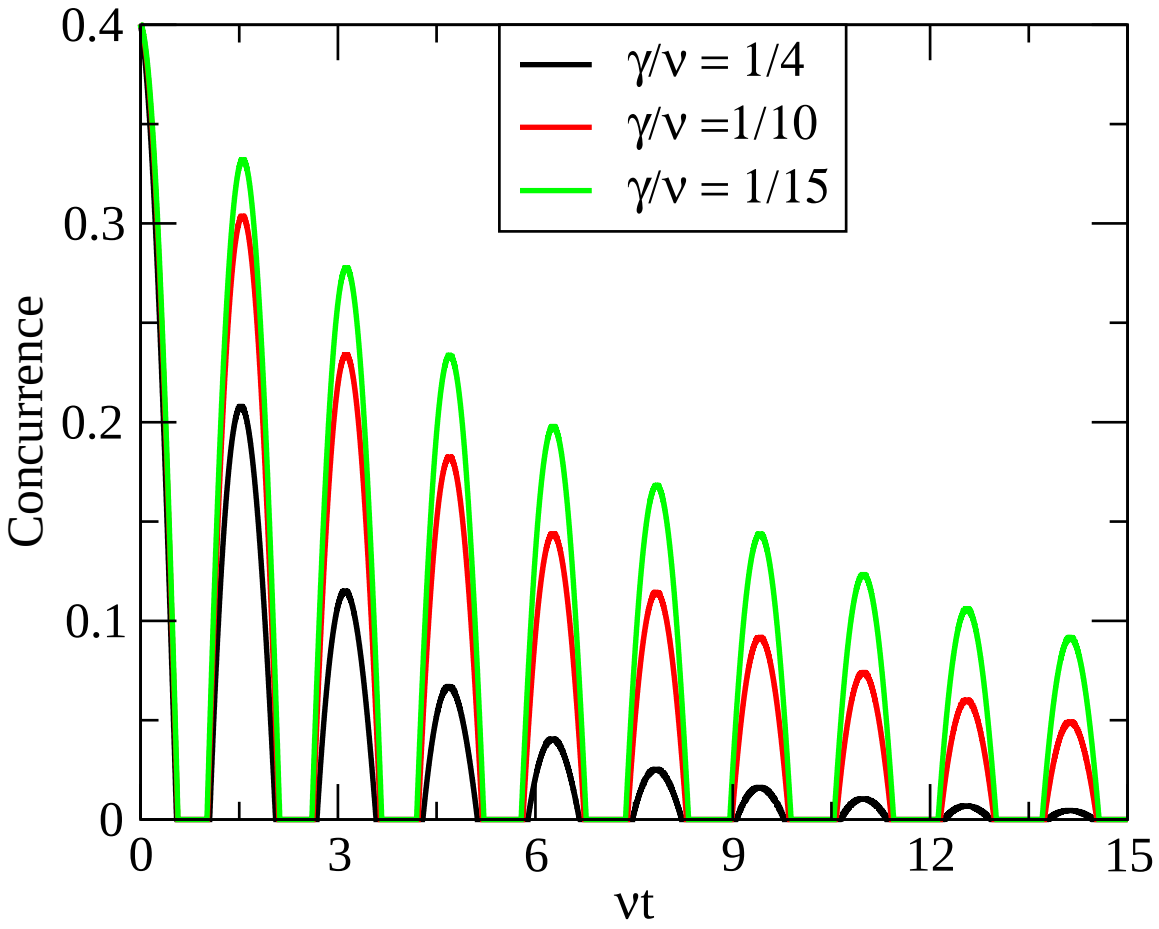

Figure 5.4: Concurrence as a function of time for different decay rates of two initially entangled qubits with initial conditions $a = 0.2, b = c = |z| = 1, \chi = \pi/2$.

finally becoming completely disentangled. Hence as a result of interaction between the qubits, the concurrence exhibits *bright and dark periods* in the entanglement. The magnitude of the bright periods diminishes with time and eventually at longer time this behavior vanishes completely leading to death of entanglement (ESD). Further we observe that when concurrence becomes zero, it remains zero for a time range before reviving. The length of a dark period is determined by the condition (5.13). It is worth mentioning here that such bright and dark periodic behavior in entanglement has been predicted for qubits undergoing unitary evolution in a lossless cavity [188]. In Fig (5.3) we plot the concurrence for $a = 0.2$. Note that for $a = 0.2$, no ESD is observed when the qubits are non-interacting and the concurrence monotonically goes to zero as $t \longrightarrow \infty$. For $v \neq 0$, we observe the bright and dark periods in entanglement with diminishing magnitudes and $C(t) \longrightarrow 0$ as $\longrightarrow \infty$. The Fig (5.4) shows the bright and dark periods in two qubit entanglement for three different spontaneous decay rates and $a = 0.2$. The initial phase χ is chosen to be $\pi/2$. For this value of a we observe no ESD but only collapse and revival as expected. In Fig (5.5) and (5.6) we plot the dyamical evolution of entanglement when $(\gamma = 0)$, i.e in absence of any environmental perturbation. This is an ideal case of close quantum systems whose dynamics is only influenced by the initial condition of the entangled qubits and the inter-qubit interactions. In this case we get,

$$\tilde{C}(t) = \frac{2}{3}[\sqrt{\cos^2\chi + \sin^2\chi\cos(2vt)} - \sqrt{a(1-a)}] \tag{5.14}$$

For both the case of $a = 0.2$ and $a = 0.4$ with an initial phase of $\chi/4$, we observe sinusoidal behavior of entanglement. We find that there is no ESD in the absence of the environment effects in this case. For another value of the initial phase $\chi/2$ we observe dark and bright periods of entanglement. The periods of disentanglement (dark periods) are governed by the condition $\sqrt{a(1-a)} > |\cos(2vt)|$. It is clearly visible from the plots that in absence of any environment the amplitude of the bright periods does not diminish at all and thus the qubits gets back their initial entanglement com-

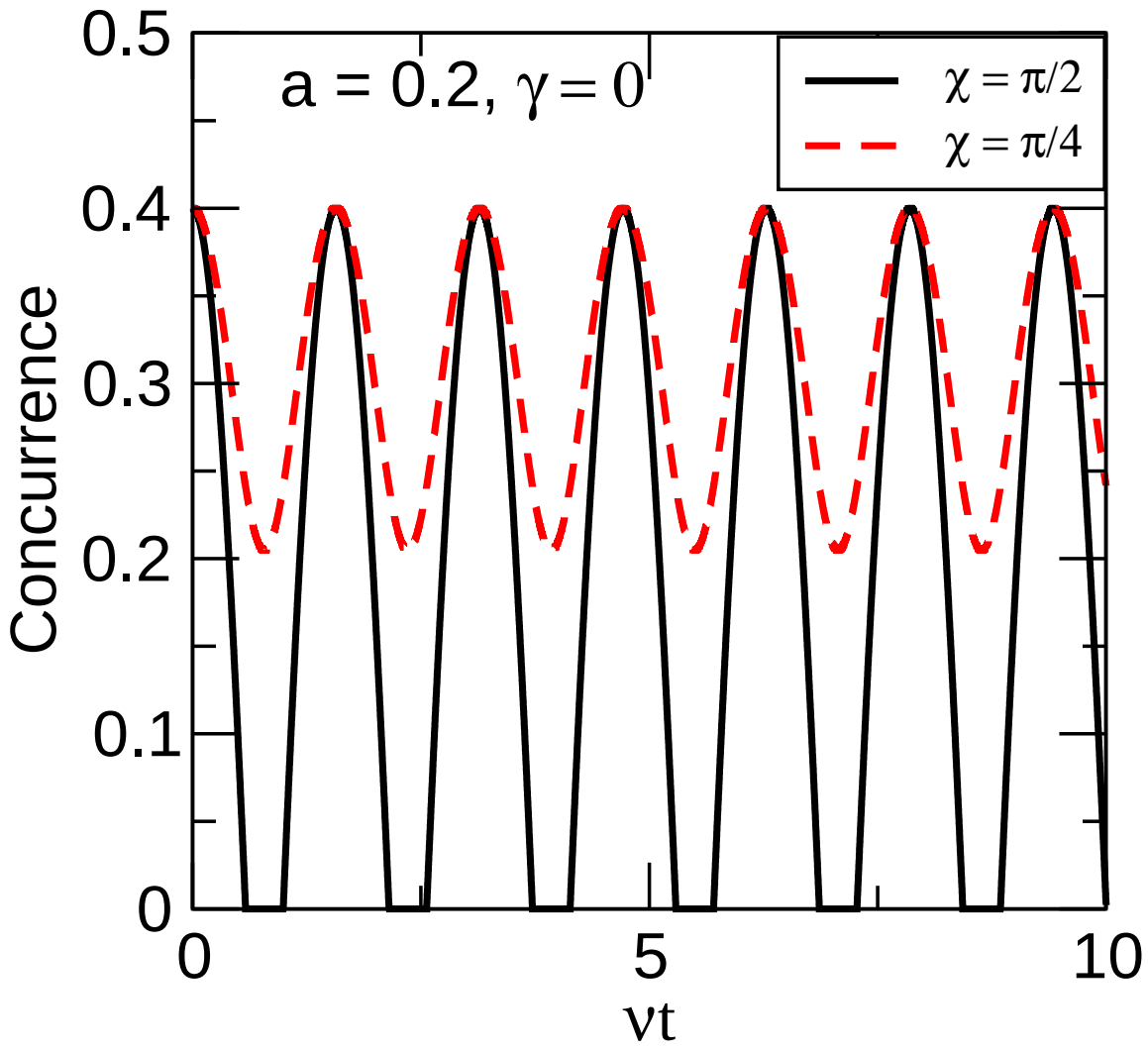

Figure 5.5: Evolution of Concurrence for two initially entangled, interacting qubits with initial conditions $a = 0.4, b = c = |z| = 1.0$ and different initial phases χ. Here $\gamma = 0$. The magnitude of bright periods in absence of environment does not diminish in magnitude.

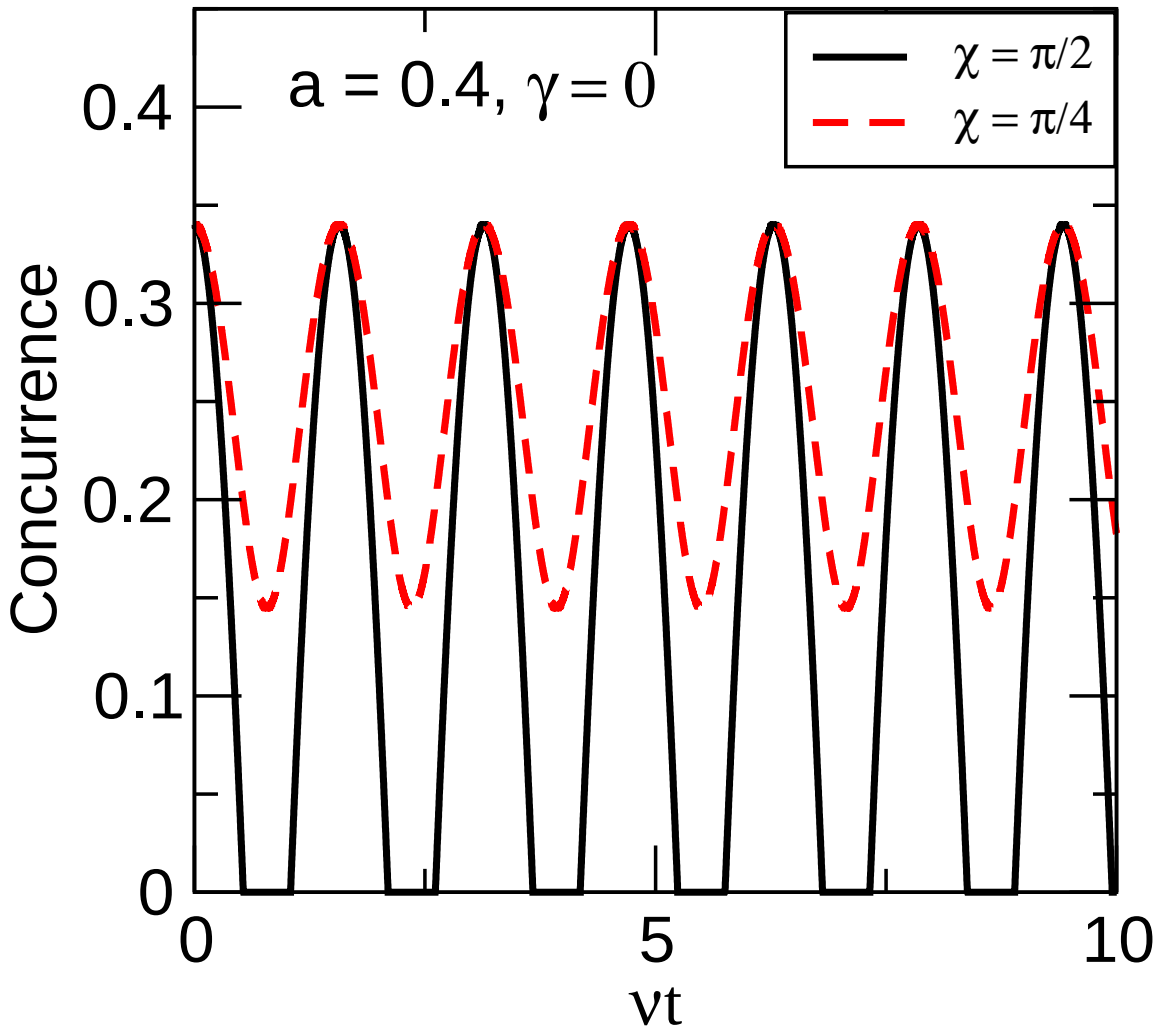

Figure 5.6: Evolution of Concurrence for two initially entangled, interacting qubits with initial conditions $a = 0.4, b = c = |z| = 1.0$ and different initial phases χ. Here $\gamma = 0$. The magnitude of bright periods in absence of environment does not diminish in magnitude.

pletely. This regeneration of entanglement is due to the inter-qubit interactions. Note that similar behavior in concurrence dynamics (collapse and revival of entanglement) has been predicted in earlier studies of non-interacting qubits in atom cavity systems. For example it was shown that for the double Jaynes-Cumming (JC) [186] model, with completely undamped non-interacting cavities entanglement shows a periodic death and re-birth feature [187]. This was attributed to exchange of information between the finite number of cavity modes and the atoms - a new kind of temporary decoherence mechanism. In another work, pairwise concurrence was calculated among four qubits, where the qubits were formed by the cavity modes and atoms [189]. Here again JC like interactions between the atom and cavity gives rise to dark and bright period in the entanglement dynamics of the qubits. It was shown that during the period when the concurrence between the cavities vanish, the concurrence between the atoms reaches its peak and vice-versa. This only happens as the cavities where assumed to be lossless with finite number of mode and thus without environmental decoherence. Further it was shown that for qubits remotely located and in contact with their respective environment when driven independently by single mode quantized field, one gets dark and bright periods of entanglement instead of ESD, a feature similar to single atom behavior in cavity quantum electrodynamics [188, 190]. *These works* [186, 187, 188, 189, 190] *differ from our's as we focus on the effect of interaction among the qubits in presence of a decohering environment.* Note that in a more recent work it was shown how oscillators interacting with a correlated finite temperature Markovian bath can lead to dark and bright periods in entanglement for certain initial conditions [180].

5.4 Pure Dephasing of the Qubits

In order to demonstrate the generic nature of our results, we consider other models of the environment. A model which has been successfully used in experiments [191]

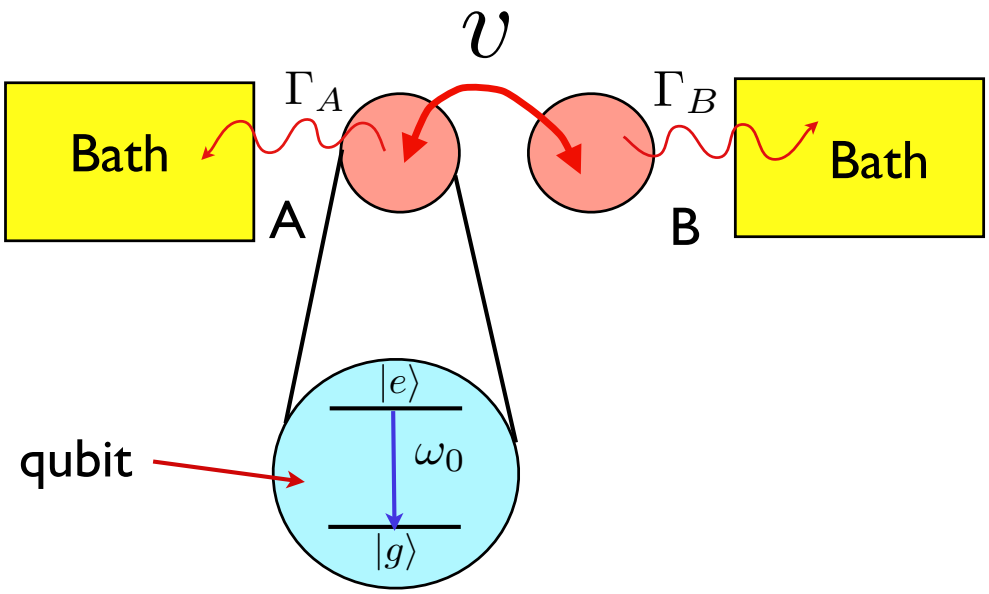

Figure 5.7: Schematic diagram of two qubits modelled as two two-level atom coupled to each other by an interaction parameter v. Here $|e\rangle, |g\rangle$ signifies the excited and ground states and ω_0 their corresponding transition frequency. The qubits A and B independently dephase to their respective environments (baths) which leads to decoherence and thus loss in entanglement. The corresponding dephasing rates are given by Γ_A and Γ_B respectively.

involves pure dephasing. The mathematical formulation for this kind of an environmental model can be done via a master equation technique and is given by,

$$\mathcal{L}\rho = -\sum_{i=A,B} \Gamma_i (S_i^z S_i^z \rho - 2S_i^z \rho S_i^z + \rho S_i^z S_i^z) \tag{5.15}$$

where $\Gamma_A(\Gamma_B)$ is the dephasing rate of qubit A (B). Substituting (5.15) in (5.3) we get the equation for dynamical evolution of the qubits under the influence of this kind of an environment. Note that in this model the populations do not decay as a result of the interaction with the environment whereas the coherences like $\rho_{23}(t)$ decay as $\rho_{23}(0)e^{-(\Gamma_A+\Gamma_B)t}$. Let us now study the the effect of interaction v between the qubits on the dynamics of entanglement. We assume the same initial density matrix of Eq no. (5.9) with the initial conditions $d = 1-a, b = c = |z| = 1$ and $a \geq 0$ to calculate the concurrence. One can clearly see from the solution of quantum-Louiville equation given in appendix (D) that under pure dephasing, the *form of matrix in* (5.9) *is preserved for all time*. Using the solutions of the master Eq no. (5.3) derived in appendix (D) for the environment effects given by (5.15) and substituting in equations (5.10), (5.11) we get the time dependent concurrence for this model to be,

$$\begin{aligned} \tilde{C}_D(t) &= \frac{2}{3}[e^{-\tau}\{e^{-2\tau}\cos^2\chi + \sin^2\chi\{\cos(\Omega_1\tau) \\ &\quad -\frac{1}{\Omega_1}\sin(\Omega_1\tau)\}^2\}^{1/2} - \sqrt{a(1-a)}], \end{aligned} \tag{5.16}$$

where the suffix D signifies that the concurrence is calculated for a dephasing environment and we assume $\Gamma_A = \Gamma_B = \Gamma$. Here $\tau = \Gamma t$ and $\Omega_1 = \sqrt{(2v/\Gamma)^2 - 1}$. For $v = 0$ we get $\tilde{C}_D(t) = 2/3[e^{-2\tau} - \sqrt{a(1-a)}]$, which is independent of the initial phase χ. We find *death of entanglement* for $\tau > -1/2 \ln \sqrt{a(1-a)}$. Note that Yu and Eberly [94] have considered this case earlier but for $a = 1$ only in which case there is no ESD. In Fig (5.8) and (5.9) we show the time dependence of entanglement for a purely dephasing model, for different values of a and initial coherences governed by the phase χ. From the figures it is seen that for $v \neq 0$, the two qubit entanglement exhibits

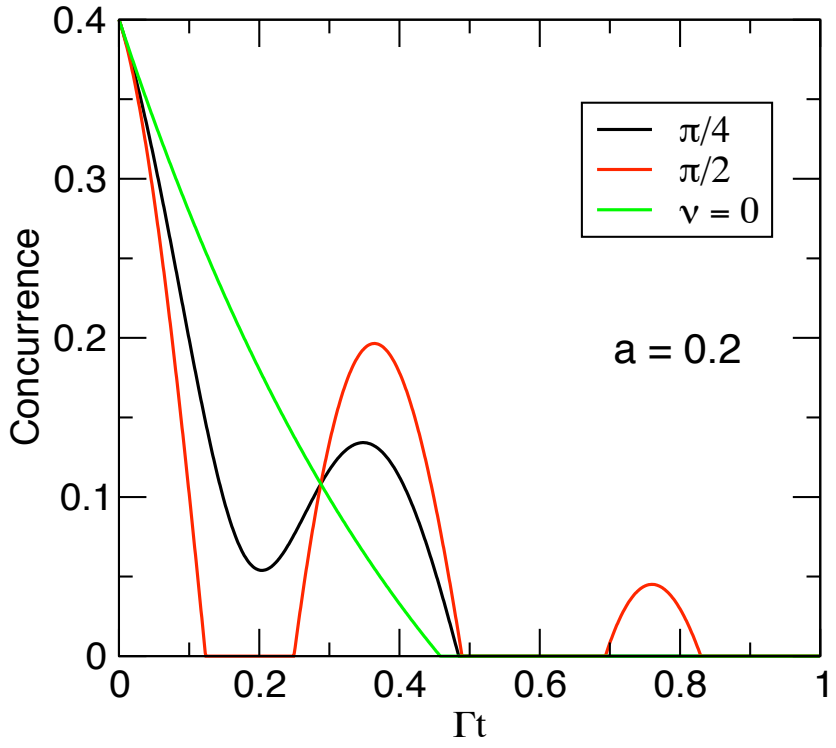

Figure 5.8: Concurrence as a function of time with initial conditions $b = c = |z| = 1$ and two different values of the initial phase χ for the dephasing model. The red and black curve in figure is for $\chi = \pi/4$ and $\pi/2$ respectively. Here the interaction parameter is taken to be $v/\Gamma = 4$.

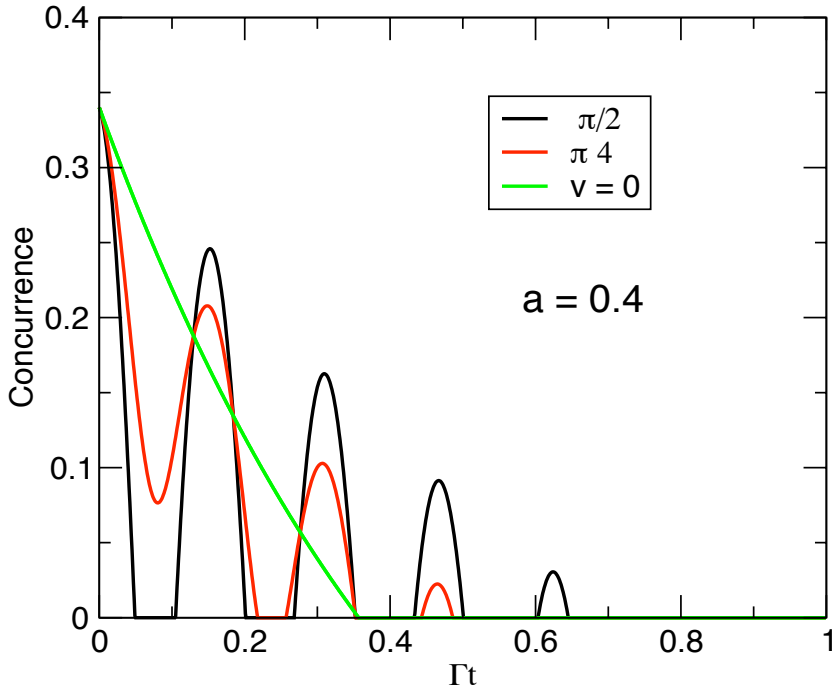

Figure 5.9: Concurrence as a function of time with initial conditions $b = c = |z| = 1$ and two different values of the initial phase χ for the dephasing model. The red and black curve in figure is for $\chi = \pi/4$ and $\pi/2$ respectively. Here the interaction parameter is taken to be $v/\Gamma = 4$.

the bright and dark periods. Further we also see that for $v \neq 0$, entanglement exhibits this feature even beyond the time when ESD occurs for noninteracting qubits. Moreover Fig (5.9) shows that the frequency of this periodic feature increases with increase in strength of the interaction v. The dark period between two consecutive bright periods arises as a result of $\tilde{C}_D(t) < 0$, for some time range. This physically means that the two-qubits remain disentangled during this time range.

5.5 Concurrence Dynamics in Correlated Environmental Models

5.5.1 Effect of Correlated Dissipative Environment

We next consider an environment involving correlated decay and show how coupling to such environment can lead to new effects in the entanglement dynamics for two qubit systems. We will consider the case of both non-interacting as well as interacting qubits for this model of the environment. To keep the analysis simple and get a better physical insight on the decoherence effect of this environment we will first study the case of non-interacting qubits. We assume as before that the qubits interacts independently with their respective environments with decay rates γ_A and γ_B. Further we assume that the qubits are close enough ($r << \lambda$, r being the inter-qubit distance and λ the wavelength of emitted radiation in process of a decay) such that they can undergo a correlated decay with decay rates $\Gamma_{AB}(\Gamma_{BA})$ for qubits $A(B)$. Whether this would lead to further decoherence is a question we want to investigate. Note that the entanglement dynamics of two non-interacting two level atoms in presence of dissipation caused by spontaneous emission was studied earlier in details by Jakóbczyk and Jamróz [168]. They even considered correlated model of dissipative environment and showed possible destruction of initial entanglement and possible creation of a transient entanglement between the atoms. Further they also discussed the question of non-locality and how it is influenced by the spontaneous emission by explicitly showing the violation of Bell-CSHS inequality. One of the chief difference between this

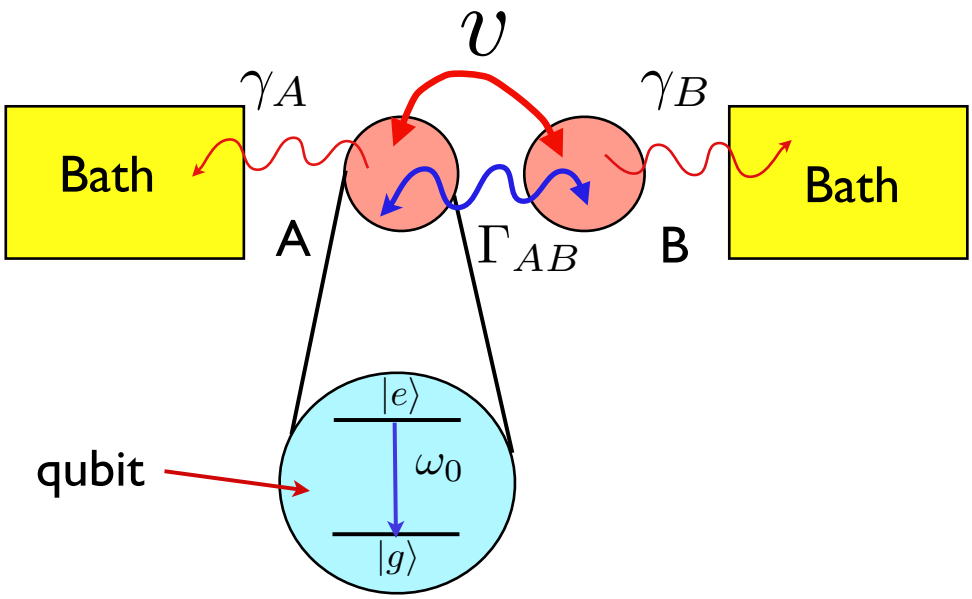

Figure 5.10: Schematic diagram of two qubits modelled as two two-level atom coupled to each other by an interaction parameter v. Here $|e\rangle, |g\rangle$ signifies the excited and ground states and ω_0 their corresponding transition frequency.The qubits A and B independently interact with their respective environments (baths) which lead to local decoherence as well as loss in entanglement.

work and ours is the initial density matrix ρ considered and the interaction introduced between the qubits . While we consider the possibility of both the qubits (atoms) to be initially excited and show its important consequences on the decay dynamics, they have neglected this effect by putting $\rho_{11}(0) = 0$. We would show later in this chapter (as can also be seen from their results) that the dissipative environment preserve the form of the initial ρ. Hence $\rho_{11}(t) = 0$ for all time in their case. Moreover, in a recent work the entanglement dynamics of two initially entangled qubits for collective decay model was studied in context to ESD, by Ficek and Tanas [132]. They considered an initial density matrix of the from,

$$\begin{aligned} \rho &= |\Psi_0\rangle\langle\Psi_0|; \\ |\Psi_0\rangle &= \sqrt{p}|e_1, e_2\rangle + \sqrt{(1-p)}|g_1, g_2\rangle \end{aligned} \tag{5.17}$$

It can be clearly seen that in this case the two-qubits are initially prepared in an entangled state by the two-photon coherences. They further show that for this initial condition the single photon coherences are never generated. Moreover the dipole-dipole interaction that they consider for the two qubit system have no influence for this initial condition. Ficek and Tanas predicted dark periods and revival in the two qubit entanglement in their work due to the correlated nature of the bath, we on the other hand consider the initial density matrix of the form (5.9) with single photon coherences and show that any coherent interaction among the qubits does influence the entanglement dynamics at all later time.

We now include the effect of a dissipative environment with both independent and correlated decay of the qubits via a master equation technique given by,

$$\begin{aligned} \mathcal{L}\rho &= -\sum_{j,k=A,B} \frac{\Gamma_{ij}}{2}(S_j^+ S_k^- \rho - 2S_k^- \rho S_j^+ + \rho S_j^+ S_k^-), \\ \Gamma_{jj} &= \gamma_j \end{aligned} \tag{5.18}$$

The time evolution of the density operator ρ which gives us information about the dynamics of the system can then be evaluated by solving the quantum-Liouville Eq

no. (5.3) with the environmental effect included by Eq no. (5.18) and taking $v = 0$. Next as before we consider the qubits to be intially entangled with their initial state to be a mixed state defined by the density matrix (5.9). We then solve the quantum-Louiville equation to study the dynamical evolution of the system. We give an for explicit solution of the time dependent density matrix elements for the qubits in appendix (E). One can clearly see from appendix (E) that for this kind of model of the environment, as before *the initial density matrix preserves its form for all time t*. Now using appendix (E) in equations (5.10) and (5.11) and the initial conditions $a \geq 0, d = 1 - a$, $b = c = |z| = 1$, we obtain the concurrence dynamics of two initially entangled non-interacting qubits for this model of the environment as,

$$\begin{aligned} \tilde{C}(t) &= \frac{2}{3}e^{-\gamma t}\{[\{\cos\chi\cosh(\Gamma t) - \sinh(\Gamma t) + a\zeta(t)\}^2 \\ &\quad + \sin^2\chi]^{1/2} - \sqrt{3a[1-\kappa(t)]}\}, \end{aligned} \tag{5.19}$$

where $\zeta(t)$ and $\kappa(t)$ are given by ,

$$\begin{aligned} \zeta(t) &= e^{-\gamma t}\{\left(\frac{1+\Gamma/\gamma}{1-\Gamma/\gamma}\right)(e^{(1-\Gamma/\gamma)\gamma t} - 1) \\ &\quad - \left(\frac{1-\Gamma/\gamma}{1+\Gamma/\gamma}\right)(e^{(1+\Gamma/\gamma)\gamma t} - 1)\}, \end{aligned} \tag{5.20}$$

$$\begin{aligned} \kappa(t) &= \frac{1}{3}ae^{-2\gamma t}\{1 + \left(\frac{1+\Gamma/\gamma}{1-\Gamma/\gamma}\right)(e^{(1-\Gamma/\gamma)\gamma t} - 1) \\ &+ \left(\frac{1-\Gamma/\gamma}{1+\Gamma/\gamma}\right)(e^{(1+\Gamma/\gamma)\gamma t} - 1)\} + \frac{2}{3}e^{-\gamma t}\{\cosh(\Gamma t) \\ &\quad - \cos\chi\sinh(\Gamma t)\}, \end{aligned} \tag{5.21}$$

For simplicity we have assumed equal decay rates of both the qubits, $\gamma_A = \gamma_B = \gamma$ and $\Gamma_{AB} = \Gamma_{BA} = \Gamma$. One can clearly see the dependence of $\tilde{C}(t)$ on the correlated environmental effect given by Γ and the initial phase χ in Eq no. (5.19). We see from (5.19), (5.20) and (5.21) that for $\Gamma = 0$, concurrence becomes independent of the

initial phase and yields the result of Yu and Eberly [92]. Note that $\tilde{C}(t)$ can become negative if,

$$\begin{aligned} 3a[1-\kappa(t)] \;\; > \;\; & [\{\cos\chi\cosh(\Gamma t)-\sinh(\Gamma t)+a\zeta(t)\}^2 \\ & +\sin^2\chi] \end{aligned} \tag{5.22}$$

in which case concurrence is zero and the qubits get disentangled. To understand how correlated decay of the qubits might effect their entanglement we study the analytical result of Eq no. (5.19) for different values of the parameter a and χ. In Fig (5.11) we show the time dependence of entanglement for $a = 0.2$ and two different values of initial phase χ and correlated decay rate of $\Gamma = 0.8\gamma$. Note that for $\Gamma = 0$, there is no ESD in this case [92] and concurrence monotonically goes to zero as $t \longrightarrow \infty$. For $\Gamma \neq 0$ we observe new behavior in the entanglement of the qubits. Concurrence is seen to have a much slower decay in comparison to when $\Gamma = 0$. For a initial phase of $\chi = \pi/4$ we observe that the condition in Eq no. (5.22) is satisfied and entanglement vanishes temporarily *i.e* the qubits get disentangled. The entanglement gets regenerated at some later time and finally goes to zero very slowly as $t \longrightarrow \infty$. Note that this disentanglement and re-entanglement phenomenon is non periodic and is very sensitive to initial coherence among the qubits, for example it do not occur when the initial coherence is governed by the phase $\chi = \pi/2$. In Fig (5.12) we plot concurrence for $a = 0.4$. For this value of a ESD is observed for $\Gamma = 0$ but not for $\Gamma \neq 0$. Instead we observe disentanglement and regeneration of entanglement among the qubits for $\chi = \pi/4$. Here again we find that no dark and bright periods nor any ESD for initial phase of $\chi = \pi/2$. Further, note that for initial phase $\chi = \pi/4$ we have a longer time interval during which the qubits remain disentangled before getting entangled again, in comparison to the case for $a = 0.2$. Thus we find that the time interval between disentanglement and regeneration of entanglement as well as the magnitude of regeneration strongly depends on the initial coherences of the

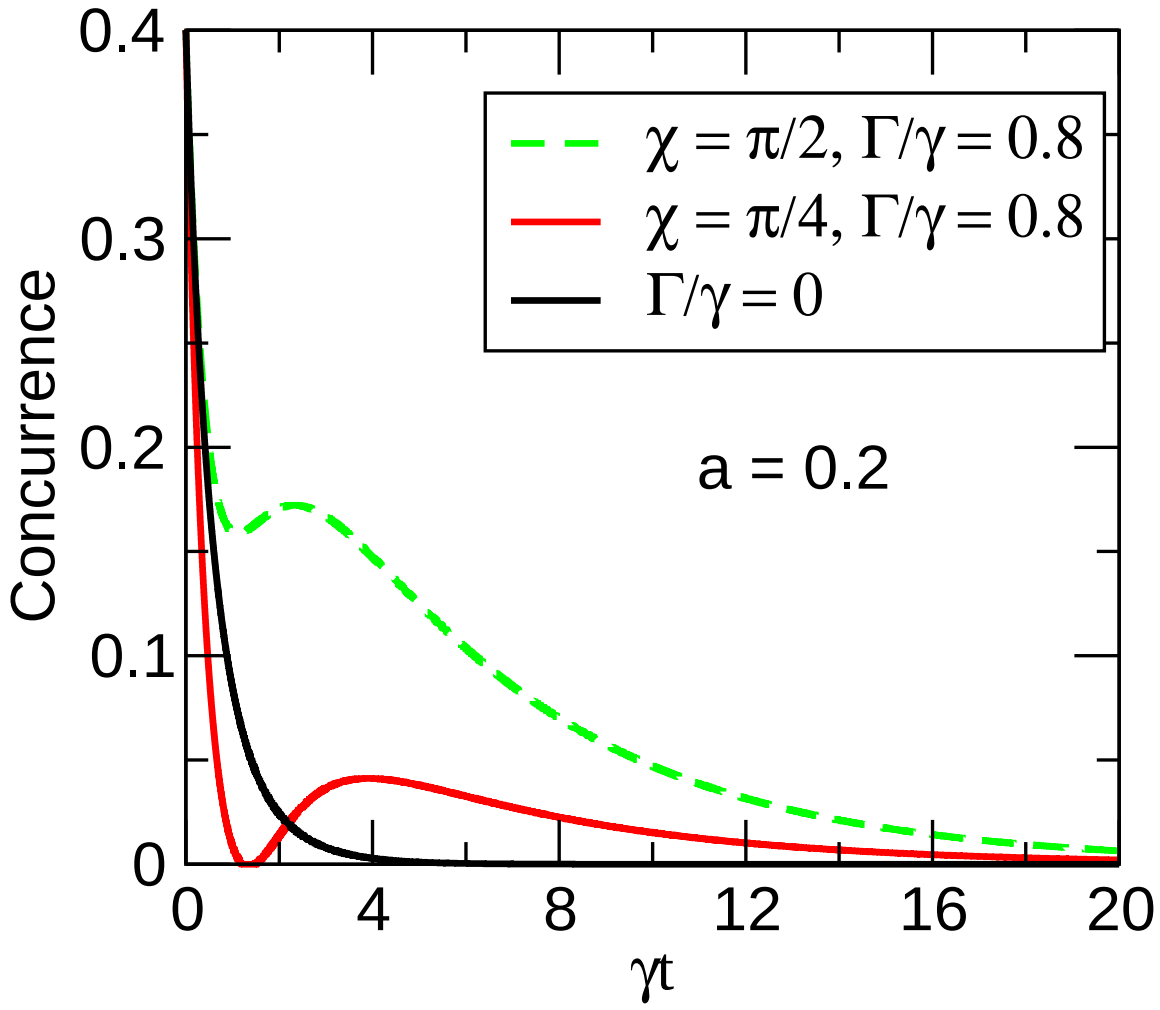

Figure 5.11: Time evolution of concurrence for $a = 0.2, b = c = |z| = 1$ and two different initial phases χ for two non-interacting qubits in contact with a correlated dissipative environment. Here $\Gamma/\gamma = 0$ signifies absence of common bath for the qubits.

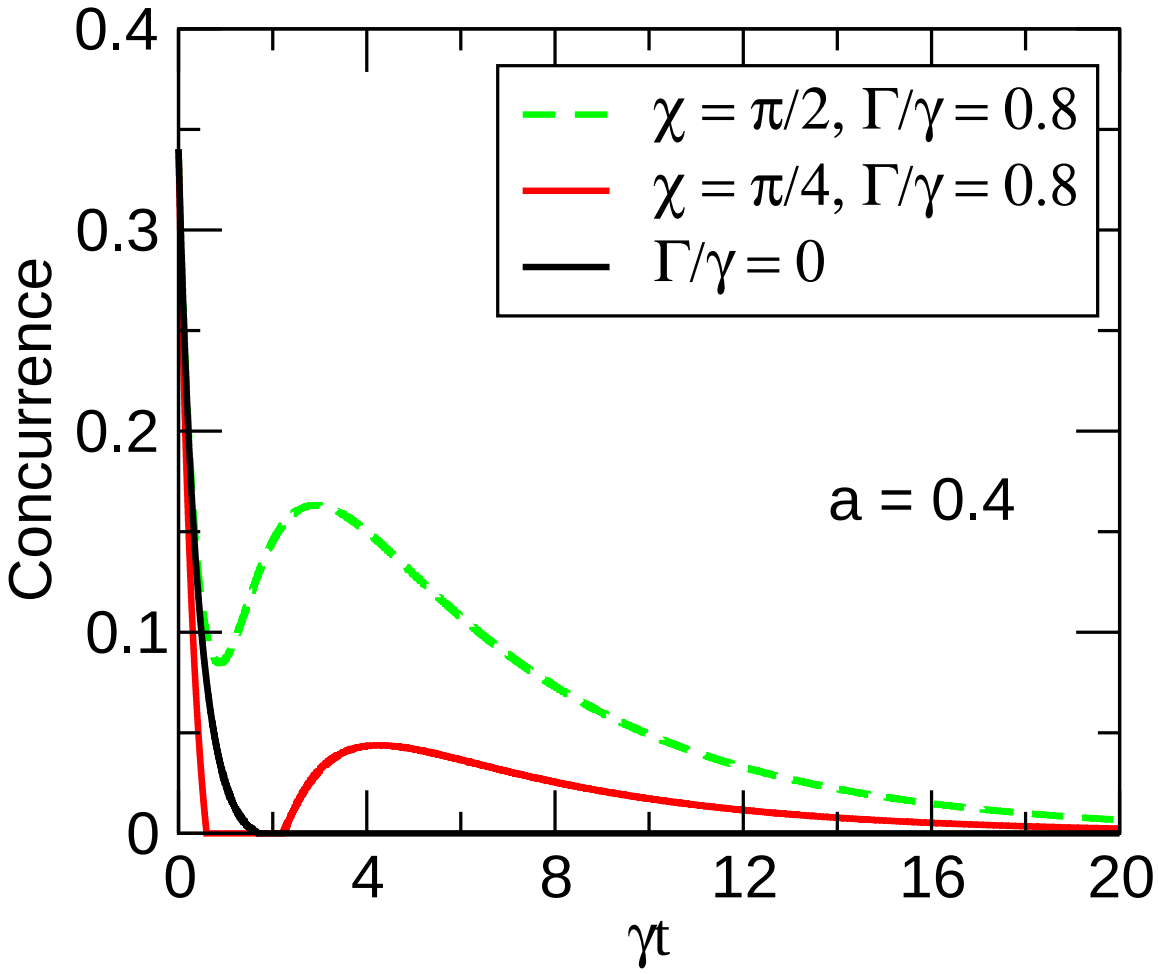

Figure 5.12: Time evolution of concurrence govern by the initial condition $a = 0.4$ for two non-interacting qubits in contact with a correlated dissipative environment. Here all other initial parameters remains the same as fig (5.10). $\Gamma/\gamma = 0$ signifies absence of any common bath in which case entanglement sudden death (ESD) is observed.

initially entangled qubits. Hence we can conclude that for non-interacting qubits in contact with a dissipative correlated environment no ESD occurs.

Let us now consider the case of two initially entangled interacting qubits in contact with the correlated environment. The dynamical evolution of the system in presence of interaction v for correlated model of environment is evaluate in details in appendix (F). We use the solutions of appendix (F) in (5.10) to calculate the concurrence for this environment. Note that the solutions are essentially valid under the assumption that our initial two qubit density matrix ρ is given by Eq no. (5.9). Further we consider as before that the two entangled qubit's evolution is governed by the initial conditions $a \geq 0, d = 1 - a$, $b = c = |z| = 1$. Hence the time dependent concurrence for two initially entangled interacting qubits becomes,

$$\begin{aligned} \tilde{C}(t) &= \frac{2}{3}e^{-\gamma t}\{[\{\cos\chi\cosh(\Gamma t) - \sinh(\Gamma t) + a\zeta(t)\}^2 \\ &\quad + \cos^2(2vt)\sin^2\chi]^{1/2} - \sqrt{3a[1-\kappa(t)]}\}, \end{aligned} \tag{5.23}$$

$$C(t) = \mathsf{Max}\{0, \tilde{C}(t)\} \quad ; \tag{5.24}$$

where $\zeta(t)$ and $\kappa(t)$ are given by equations (5.20) and (5.21) respectively. The dependence of concurrence for $\tilde{C}(t) > 0$ on the interaction strength v between the qubits is clearly visible in Eq no. (5.23). Further now we can see that the condition of complete disentanglement of the qubits is given by,

$$\begin{aligned} 3a[1-\kappa(t)] &> [\{\cos\chi\cosh(\Gamma t) - \sinh(\Gamma t) + a\zeta(t)\}^2 \\ &\quad + \cos^2(2vt)\sin^2\chi] \end{aligned} \tag{5.25}$$

When condition (5.25) is satisfied, $\tilde{C}(t) < 0$ and hence $C(t) = 0$. Next to study the effect of qubit-qubit interaction on the entanglement dynamics we plot the time dependent concurrence for different value of a, initial phase χ and correlated decay rates of $\Gamma = 0.8\gamma$ in figures (5.13) and (5.14). We observe in the figures that for an

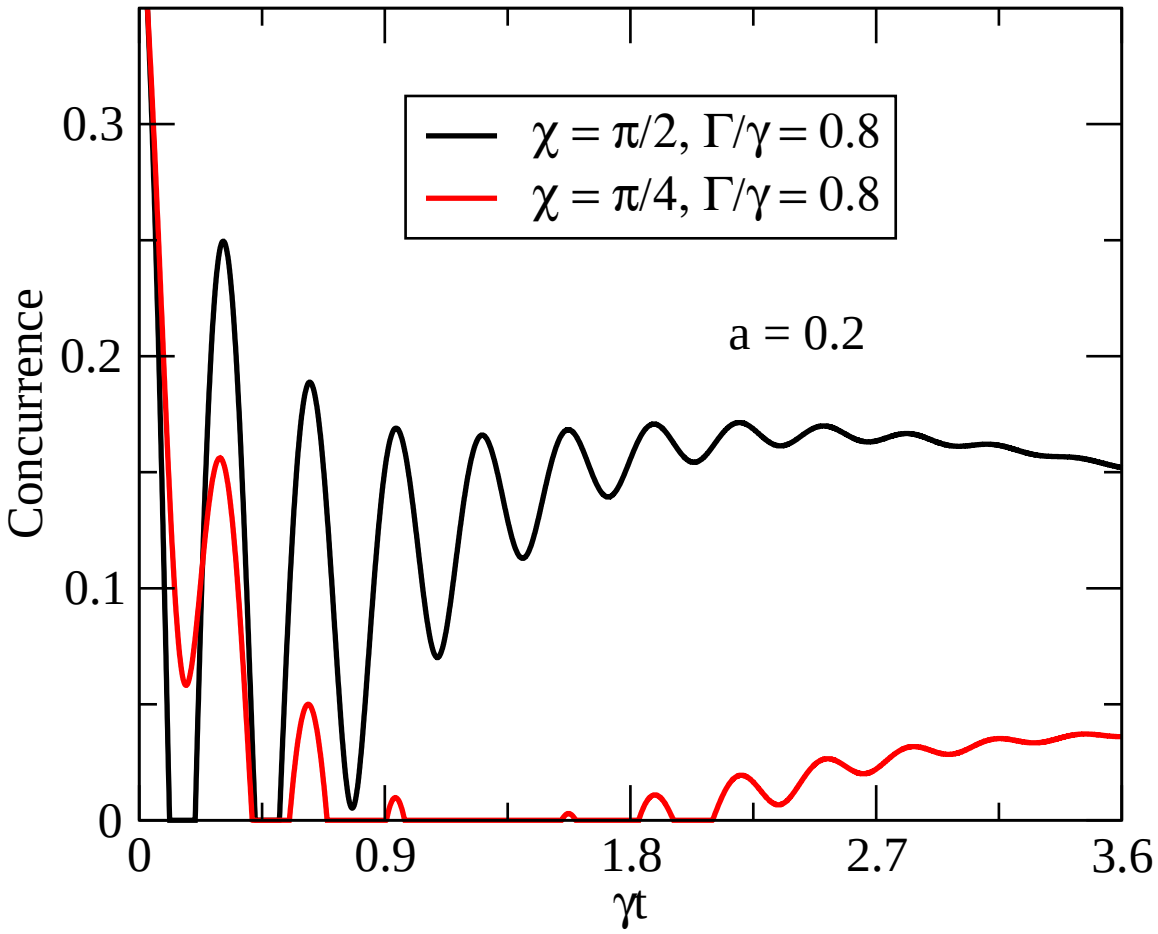

Figure 5.13: Time evolution of concurrence for interacting qubits in contact with a correlated dissipative environment with correlated decay rate of $\Gamma/\gamma = 0.8$. Here $b = c = |z| = 1$. A long period of disentanglement is observed for initial phase $\chi = \pi/4$. Here the interaction strength among the qubits is taken to be $v/\gamma = 5.0$

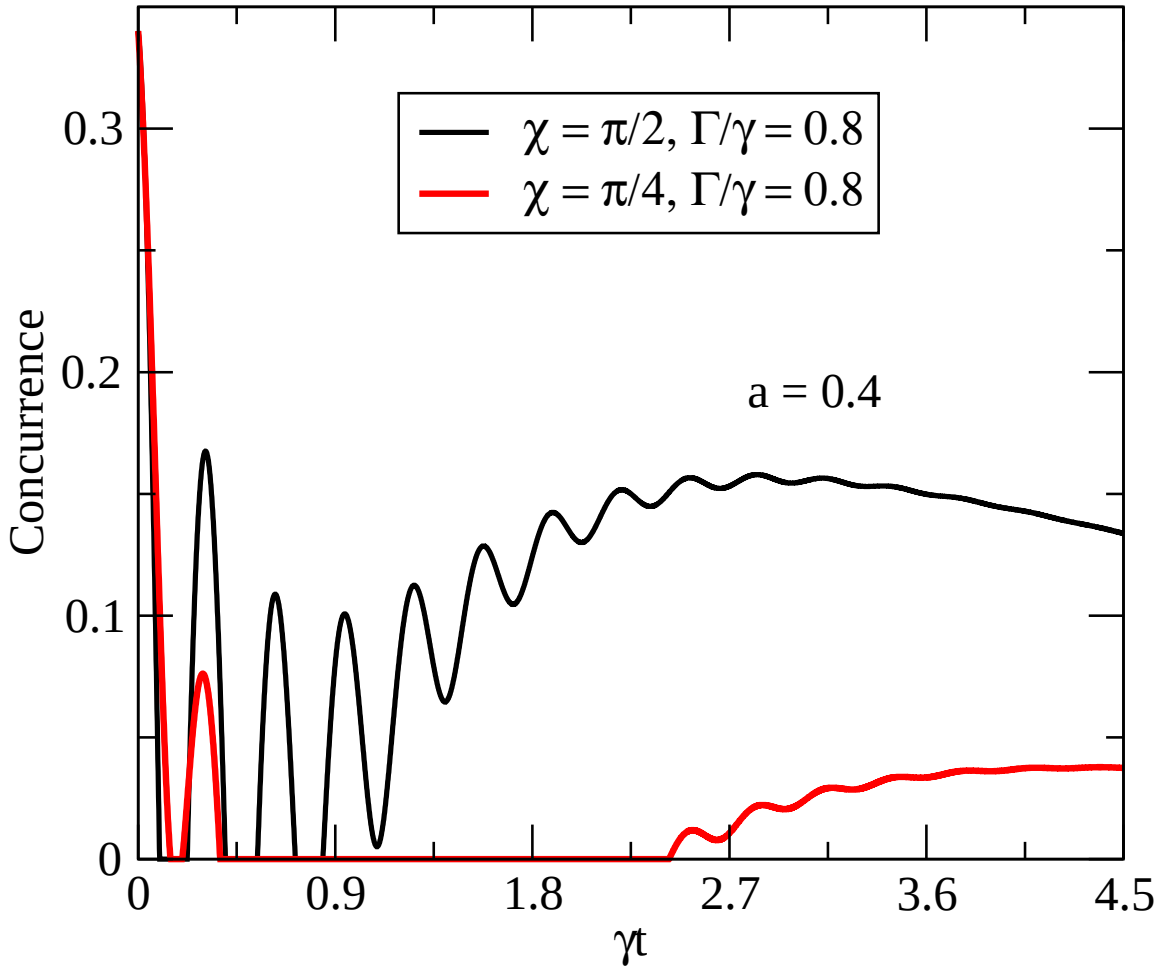

Figure 5.14: Time evolution of concurrence for interacting qubits in contact with a correlated dissipative environment for same parameters as Fig (9) and $a = 0.4$. The dark and bright periodic features sustain for a longer time for initial phase of $\chi = \pi/2$. Much longer period of disentanglement now observed for $\chi = \pi/4$.

initial phase of $\chi = \pi/2$ concurrence exhibits dark and bright periods at initial time for both $a = 0.2$ and $a = 0.4$. For longer time the concurrence shows a damped oscillatory behavior. We attribute this effect to the competition between the fast inter-qubit interactions v and the environmental decays. For longer time the correlated decay becomes dominant and leads to a slow damped oscillatory decay of the entanglement. For $\chi = \pi/4$ the dark and bright periods are not very pronounced and is over shadowed very quickly by the correlated decay. Note that for this value of initial phase we find that there exist a long period of time during which the qubits remain disentangled. At a much later time entanglement gets regenerated and increases initially and then starts decaying very slowly after. This behavior is quite different from the dark and bright periods seen for other models of the environment. Thus we see that for interacting qubits there is no ESD for this model of the environment. Instead we find dark and bright periods with long period of disentanglement whose occurrence depends on the initial coherence.

5.5.2 Delay of ESD by Correlated Dephasing Environment

Finally we consider a purely correlated dephasing model of the environment and study the effect of such an environment on the entanglement dynamics of two qubits. Note that this kind of model is popular among solid state systems like semiconductor quantum dots. We will study the behavior of entanglement for both non-interacting and interacting qubits. As before to keep our analysis simple and to get a better physical insight to the question of decoherence for this kind of environment we will first study the case of non-interacting qubits. We will then generalize our results by introducing the interaction among the qubits. For non-interacting qubits the Hamiltonian for our model is given by (5.1) with $v = 0$. The effect of the dephasing environment on the qubits is included via a master equation technique and is given

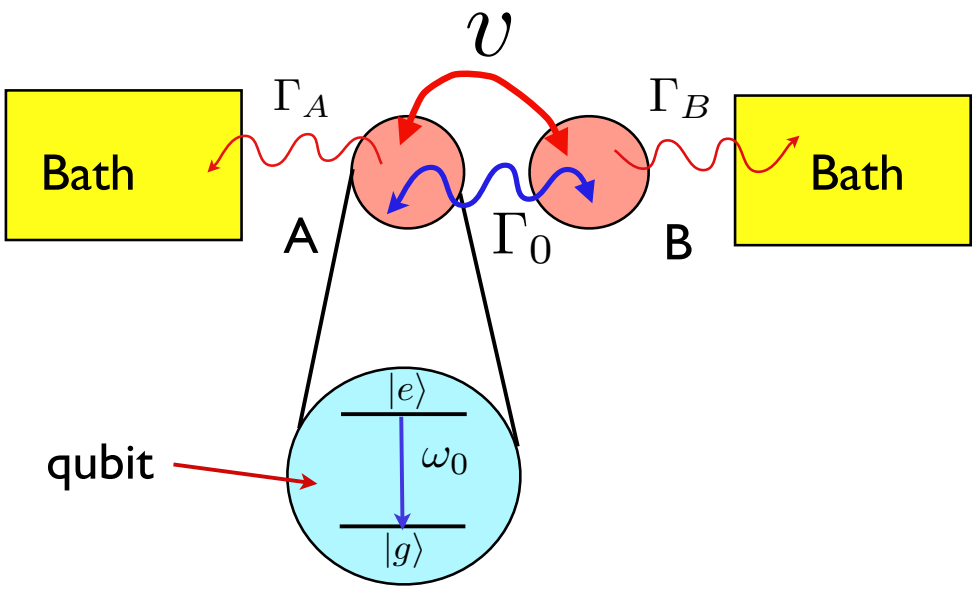

Figure 5.15: Schematic diagram of two qubits modelled as two two-level atoms. Here ω_0 is the transition frequency of the excited state $|e\rangle$ to the ground state $|g\rangle$. The qubits A and B independently dephase to their environments (baths) with a dephasing rate of Γ_A, Γ_B respectively. The qubits can also interact with the environment collectively when they are at proximity giving rise to correlated dephasing represented by the decay rate Γ_0.

by,

$$\begin{aligned}\mathcal{L}\rho &= -\sum_{i=A,B}\Gamma_i(S_i^zS_i^z\rho - 2S_i^z\rho S_i^z + \rho S_i^zS_i^z) \\ &\quad -2\Gamma_0(S_A^zS_B^z\rho - S_B^z\rho S_A^z + \rho S_A^zS_B^z - S_A^z\rho S_B^z),\end{aligned} \tag{5.26}$$

where $\Gamma_A(\Gamma_B)$ and $2\Gamma_0$ are respectively the independent and correlated dephasing rate of qubit A (B) . The dynamical evolution of this system can then be studied by solving the quantum-Louiville Eq no. (5.3) for $v = 0$ and including the effect of environment by using (5.26). We now consider as earlier that the initial state of the two qubits is defined by the density matrix ρ (5.9). Then the solution of the quantum-Louiville equation for this model of the environment is given by,

$$\rho_{11}(t) = \frac{1}{3}a, \quad \rho_{22}(t) = \frac{1}{3}b, \quad \rho_{33}(t) = \frac{1}{3}c, \tag{5.27}$$

$$\rho_{23}(t) = \frac{1}{3}|z|e^{-(\Gamma_A+\Gamma_B-2\Gamma_0)t}e^{i\chi} \tag{5.28}$$

$$\rho_{32}(t) = \rho_{23}^*(t), \quad \rho_{44}(t) = 1 - \rho_{11}(t) - \rho_{22}(t) - \rho_{33}(t) \tag{5.29}$$

All other matrix elements of the two qubit density matrix ρ are zero. Now using the solutions of (5.29) it is straight forward to show that, for pure dephasing of the qubits, the *form of matrix in* (5.9) *is preserved for all time*. Note that in such a model the populations do not decay as a result of the interaction with the environment whereas the coherences like $\rho_{23}(t)$ decay as $\sim \rho_{23}(0)e^{-(\Gamma_A+\Gamma_B-2\Gamma_0)t}$ for $\chi = 0$ or mod π. Let us now study the effect of correlated dephasing of the qubits on the dynamics of entanglement. For the initial conditions $d = 1-a, b = c = |z| = 1$ and $a \geq 0$ on using (5.27) in (5.10) we get the expression for time dependent concurrence as,

$$\tilde{C}_D(t) = \frac{2}{3}\left\{e^{-2(\Gamma-\Gamma_0)t} - \sqrt{a(1-a)}\right\} \tag{5.30}$$

where we have assumed $\Gamma_A = \Gamma_B = \Gamma$ for simplicity. From Eq no. (5.30) it is clearly seen that in a purely dephasing environment entanglement among the qubits

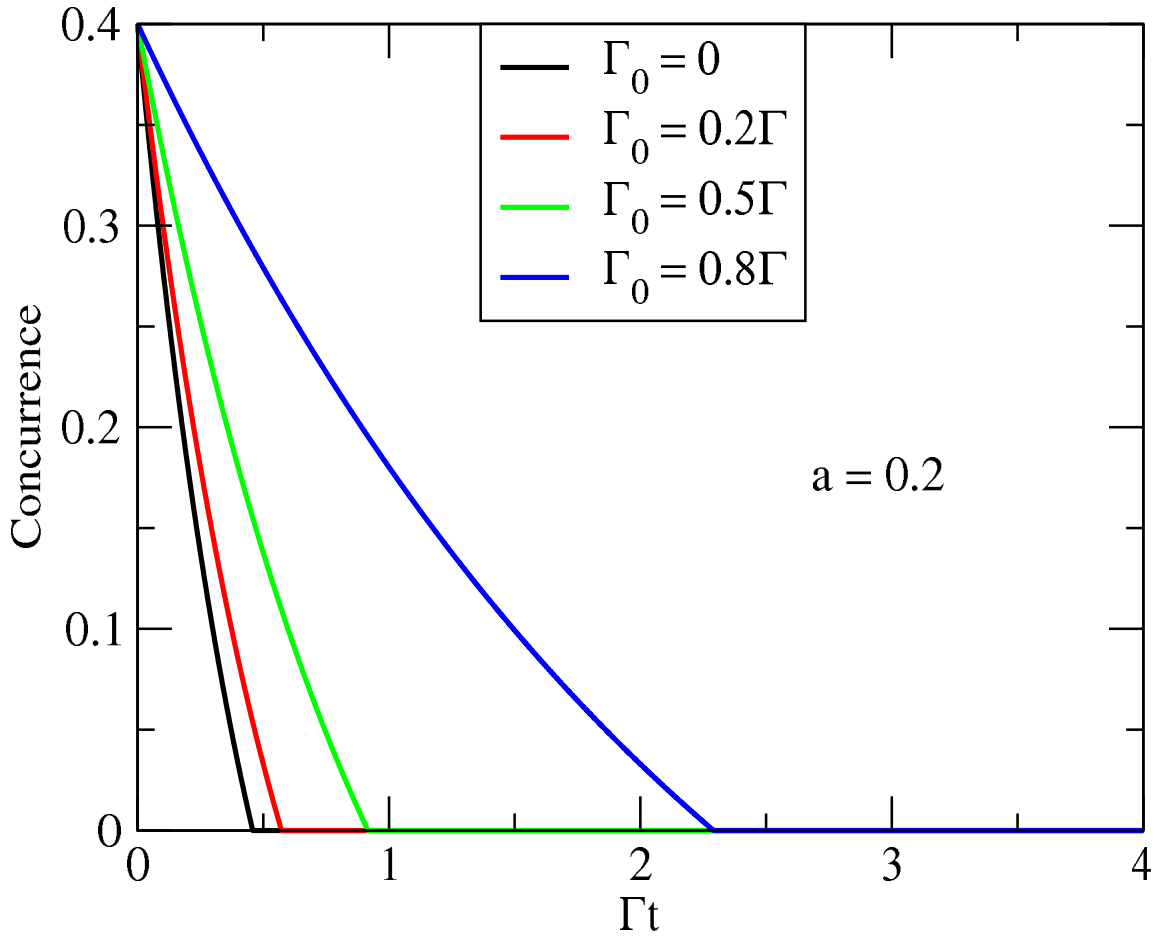

Figure 5.16: Time evolution of concurrence for two non-interacting qubits in contact with a purely dephasing environment for initial condition given by $a = 0.2$ and $b = c = |z| = 1$. The effect of correlated dephasing shows up as delay in the onset of ESD.

is independent of the initial coherence given by χ and depends only on a and Γ_0. In Fig (5.16) we plot the time dependence of concurrence for $a = 0.2$. We find that the effect of correlated dephasing is manifested in the delay of the onset of ESD. The time for the onset of ESD is given by $t \geq 1/2(\Gamma - \Gamma_0)\{1/\ln\sqrt{a(1-a)}\}$. From the figure its is clealy visible that with increase in correlated decay Γ_0, the onset of ESD gets delayed further until $\Gamma_0 = \Gamma$, when concurrence bceomes independent of the dephasing rates and is given by $C = 2/3[1 - \sqrt{a(1-a)}]$. This situation represents a decoherence free subspace where concurrence becomes solely dependent on the value of a *i.e* population of the excited state of the two qubits. Note that this kind of situation has already been tailored to study entanglement in decoherence free subspace [18].

Let us now include the interaction among the qubits and study how this interaction might influence the entanglement dynamics for this model of the environment. The Hamiltonian of the two qubit system and its coupling to the environment is then given by equations (5.1) and (5.26) respectively. To study the dynamics of entanglement we follow a similar process as described earlier. We use the solution of quantum-Louiville equation derived explicitly in appendix (G) and substitute them in Eq no. (5.10) to calculate the time dependence of concurrence C. With the initial conditions $a = 1 - d, b = c = |z| = 1$, then we get,

$$\begin{aligned}
\tilde{C}_D(t) &= \frac{2}{3}[e^{-(\Gamma-\Gamma_0)t}\{e^{-2(\Gamma-\Gamma_0)t}\cos^2\chi \\
&+ \sin^2\chi(\cos(\Omega' t) - \frac{(\Gamma-\Gamma_0)}{\Omega'}\sin(\Omega' t))^2\}^{1/2} \\
&- \sqrt{a(1-a)}]; \qquad (5.31) \\
C(t) &= \mathsf{Max}\{0, \tilde{C}_D(t)\} \qquad (5.32)
\end{aligned}$$

where $\Omega' = \sqrt{4v^2 - (\Gamma - \Gamma_0)}$ and we have assumed $\Gamma_A = \Gamma_B$. One can clearly see the dependence of concurrence on the interaction v among the qubits for $\tilde{C}_D > 0$. Note that due to the interaction among the qubits now concurrence becomes dependent of the initial phase χ. To understand the behavior of entanglement in presence of

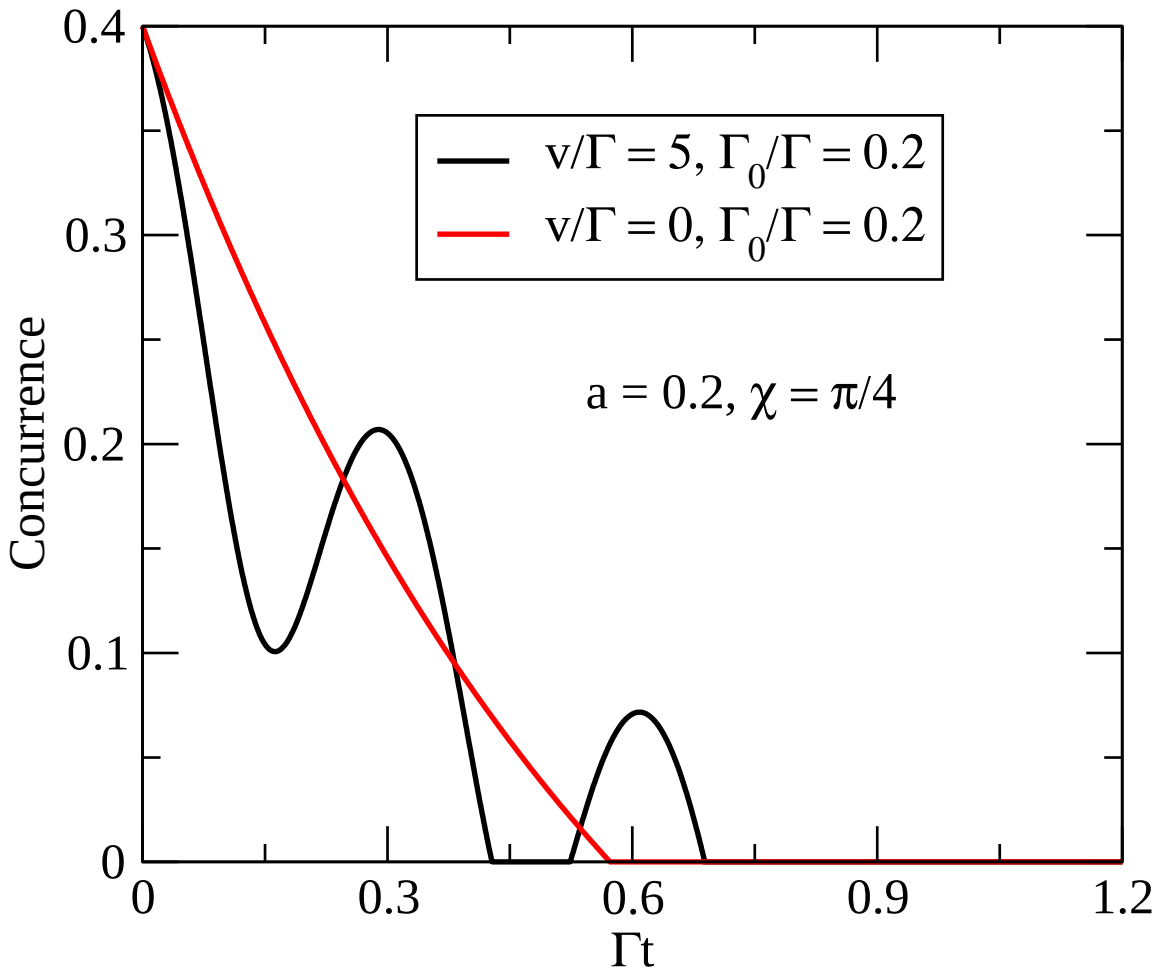

Figure 5.17: Time evolution of concurrence for two interacting qubits with interaction strength $v/\Gamma = 5.0$ in contact with a purely correlated dephasing environment and initial condition $a = 0.2., \chi = \pi/4, b = c = |z| = 1$. The red curve correspond to concurrence of non-interacting qubits. Concurrence is seen to exhibit initial oscillations followed by dark and bright periods with eventual death of entanglement in presence of interaction. The interaction also leads to delayed death of entanglement. Here Γ_0 is the correlated dephasing rate.

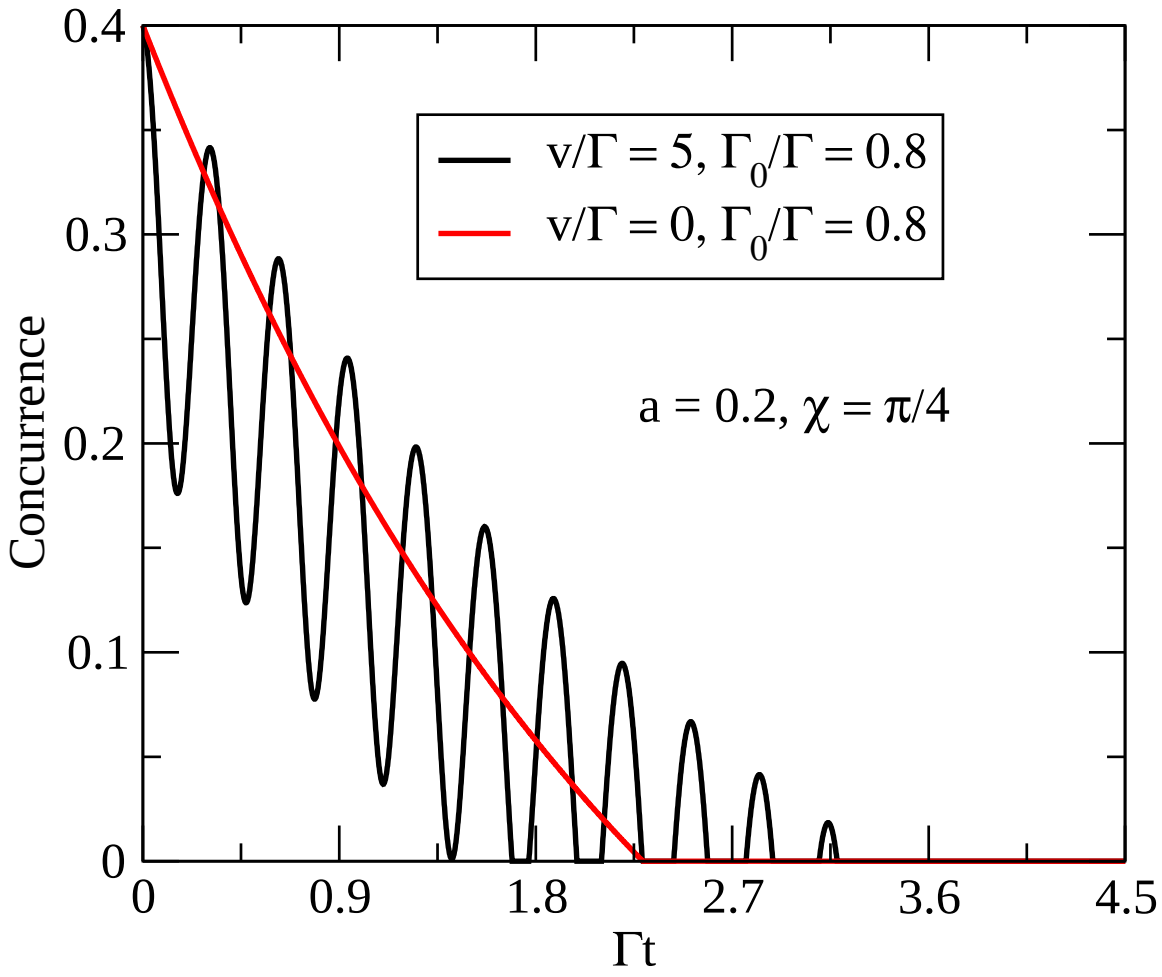

Figure 5.18: Time evolution of concurrence for two interacting qubits in contact with a correlated dephasing environment with same parameters as for Fig (5.17) but higher correlated dephasing rates. The effect of higher correlated dephasing manifests itself by increasing the periodicity of dark and bright features in concurrence . Here again we find that dark and bright periods is followed by death of entanglement.

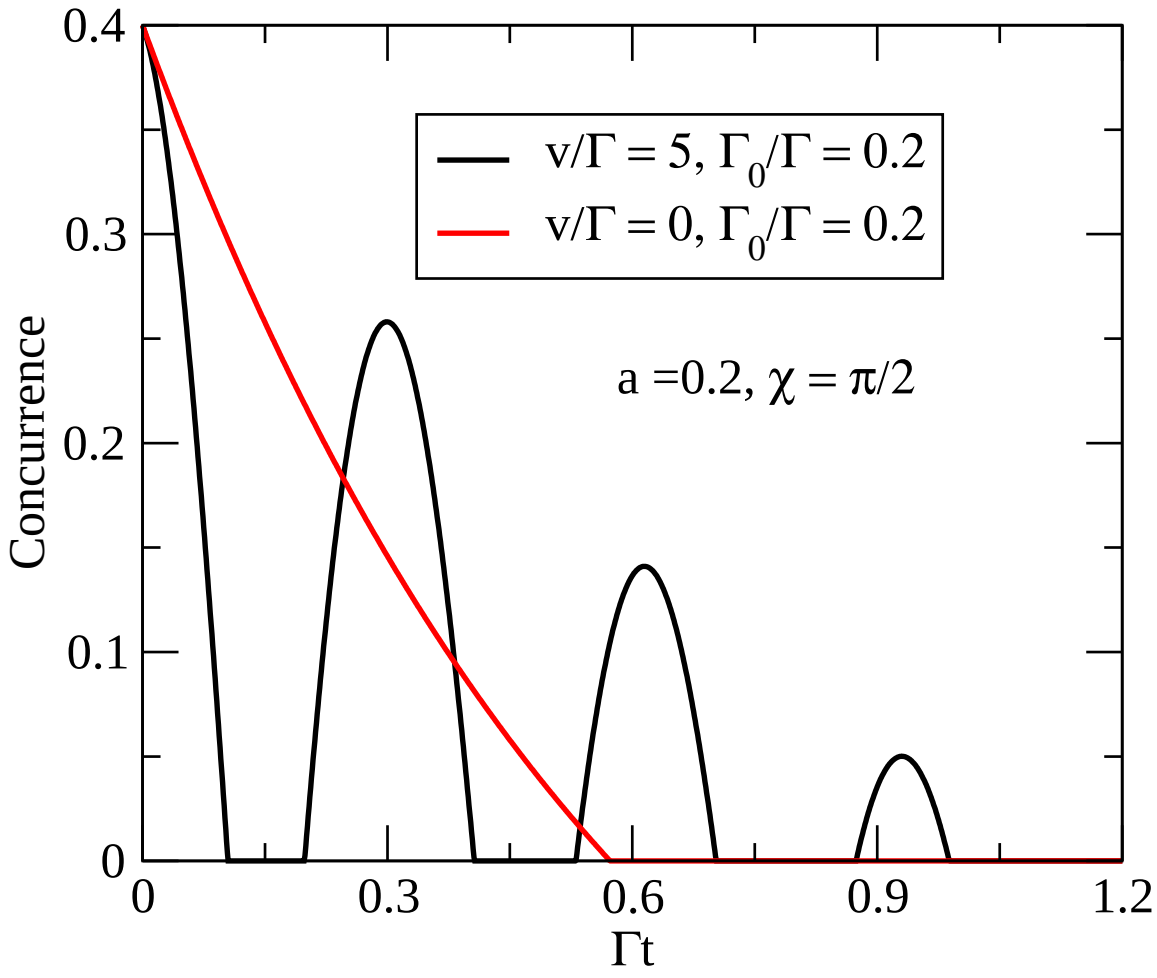

Figure 5.19: Time evolution of concurrence for two interacting qubits in contact with a correlated dephasing environment with initial condition $a = 0.2., \chi = \pi/2, b = c = |z| = 1$. Concurrence is seen to be sensitive to initial coherence among the two qubits. It does not exhibit initial oscillations for this value of χ but dark and bright periods with eventual death of entanglement in presence of interaction. Here the interaction strength is taken to be $v/\Gamma = 5.0$

interaction ($v/\gamma = 5.0$) among the qubits we plot the time dependence of concurrence for different initial phase χ and correlated dephasing rates Γ_0 in figures (5.17-5.19). We consider the case, $a = 0.2$ only to do a comparative study on the behavior of concurrence in presence and absence of inter-qubit interactions. Note that we have already discussed the effect of correlated dephasing on the two qubit entanglement for this value of a. Let us now focus on any new feature that arises due to the qubit-qubit interactions. We can see clearly from Fig (5.17) that for $v \neq 0, \chi = \pi/4$ the two qubit concurrence shows a damped oscillatory behavior which leads to dark and bright periods at longer time before eventual death of entanglement. The generation of dark and bright periods is seen to delay the death of entanglement even further in comparison to that induced by correlated dephasing in absence of qubit-qubit interactions. Moreover in Fig (5.18) we see that both the oscillatory behavior as well as dark and bright periods is enhanced with an increase in correlated dephasing rate. When we change the initial phase to $\pi/2$ for $\Gamma_0 = 0.2\Gamma$ we find (figure 5.19) no oscillatory behavior in entanglement rather a completely dark and bright periodic feature with eventual delayed death. Thus we see that the onset of dark and bright periods for this kind of environment model is profoundly influenced by the initial coherence of the two qubit system.

The phenomenon of dark and bright periods in entanglement should have direct consequences for systems like ion traps , quantum dots, the later being currently the forerunner in implementation of quantum logic gates. The interaction between qubits considered in this chapter are inherently present in these systems. In quantum dots for example, $\gamma^{-1} \sim$ few ns and one can get a very large range of the parameter Γ^{-1} (1-100's of ps) [192]. Further the interaction strength v can have a range between 1μev - 1 mev depending on gate biasing [53, 193, 194, 195]. An earlier study [196] reports $\gamma \sim 40 - 100\mu$ev and coupling strength of $\sim 100 - 400\mu$ev, thereby making $v/\gamma \sim 1 - 10$ for quantum dot molecules. Thus experimental parameters are in the

range we used for our numerical calculation.

5.6 Summary

In summary we have done a detailed study of decoherence effect for non-interacting and interacting initially entangled qubits in contact with different environments at zero temperature. We have shown how the interaction between qubits generates the phenomenon of dark and bright periods in the entanglement dynamics of an intially entangled two qubit system in contact with different environments. We found this feature of dark and bright periods to be generic and to occur for various models of the environment. As an example, in a correlated dissipative environment, we found the phenomenon of dark and bright periods in entanglement dynamics even though there is no sudden death of entanglement. Moreover, for purely dephasing models of the environment, we found that the dark and bright periods delay the ESD. We found that there is no sudden death of entanglement for a correlated dissipative environment, but rather, depending on the initial coherences in the system entanglement can show a substantially slower decay and the phenomenon of dark and bright periods for interacting qubits. For a simple pure dephasing environment as well as for correlated dephasing environment we have shown the existence of sudden death of entanglement. Due to correlated dephasing we found delayed death of entanglement. Further, in the correlated dephasing model, we found that the onset of dark and bright periods is sensitive to the initial coherence in the system. The frequency of dark and bright periods was found to depend on the strength of the interaction between the qubits as well as on the correlated decay and dephasing rates.

The content of this chapter has been published in two papers in J. Phys. B. **42**, 141003 (2009), **42**, 205502 (2009).

CHAPTER 6

STUDY OF CONTINUOUS VARIABLE ENTANGLEMENT AND DECOHERENCE IN PHOTONIC QUANTUM CIRCUITS

6.1 Overview

Waveguides coupled through evanescent waves are known to be extremely efficient in manipulating the flow of light and have been investigated extensively in the last two decades [57, 198, 199, 200]. Many key quantum effects like quantum interference, entanglement and quantum random walk have been investigated in these systems [201, 202, 203, 204, 205]. Fig. (6.1) shows a schematic diagram of an array of channel waveguides used in many of the experiments. Quantum correlations have also been investigated in waveguide arrays [204] using two-photon input states both in terms of separable and entangled two-photon state. These studies have shown various features associated with quantum interference. Moreover, coupled waveguides arrays have been used to study the discrete analogue of the Talbot effect [58]. In addition recent works with coupled waveguides have shown realization of different condensed matter effects like Bloch oscillations and Anderson localization [59, 61].

Entanglement between the waveguide modes and behavior of nonclassical light in coupled waveguides have also attracted a great deal of interest [62, 63, 206]. Moreover in recent years coupled waveguides have been used in realization of quantum circuits for quantum information purposes [64] and the generation of a multimode interferometer on an integrated chip experiment [65, 66]. These interferometers can be used to generate arbitrary quantum circuits and entangled states similar to NOON states [67]. Entanglement between waveguide modes is at the heart of many of these

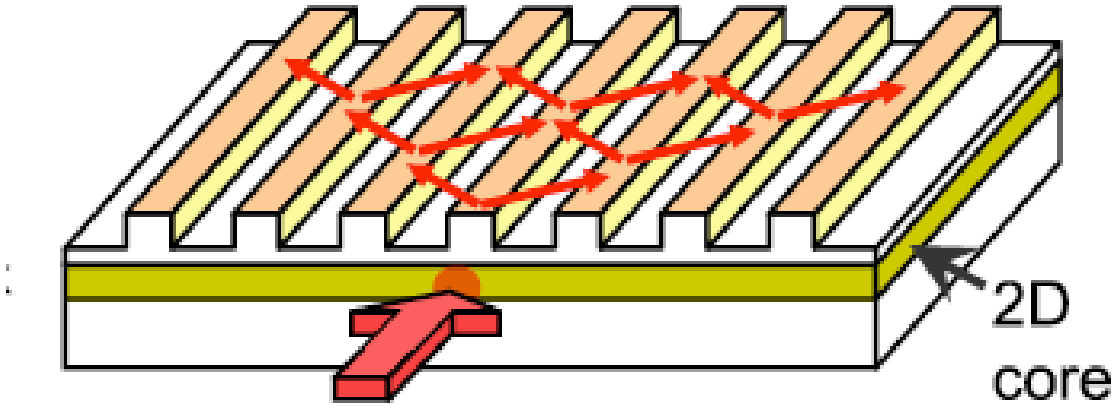

Figure 6.1: Schematic diagram of an array of evanescent coupled channel waveguides built on a substrate. One of the waveguides is excited. Numerous different quantum effects can be studied in such systems.

experiments. In particular, for effective use of these waveguide circuits in quantum computation and communication tasks sustainability of generated entanglement in the presence of decoherence is very important [5, 24]. light of this, it is imperative to study measures of entanglement in waveguides including loss.

In this chapter we investigate the question of entanglement and its behavior in the presence of loss, in a simple system of two single mode waveguides, which are coupled through the overlap of evanescent fields. This simple system serves as a unit or the basic element for constructing a quantum circuit [207]. The input light to the coupled waveguide system is usually produced by a parametric down-conversion (PDC) process, at high gain which produces important nonclassical states of light like the squeezed states. We thus consider single mode and two mode squeezed states as the input to our waveguides and study their respective entanglement dynamics. We present explicit analytical results for the evolution of entanglement in terms of logarithmic negativity. We further investigate the question of possible effects of loss on the entanglement dynamics in waveguides by considering lossy waveguide modes. We find that in this coupled waveguides, entanglement shows considerable robustness against loss.

The organization of the chapter is as follows: In Sec 2, we describe the model and derive analytical result for the field modes of the coupled waveguide system. In Sec 3 , we then study the time evolution of entanglement by evaluating the logarithmic negativity for two classes of squeezed input states : (6.3.1) separable two mode squeezed state and (6.3.2) entangled two mode squeezed state. The effect of loss in waveguides on the entanglement dynamics is then discussed in Sec 4. Finally we summarize our results in Sec 5.

6.2 The Model

We consider a system with two single mode waveguides, coupled through nearest-neighbor interaction as shown in Fig. (6.4). Let a and b be the field operators for the modes in each waveguide. These obey bosonic commutation relations $[a, a^\dagger] = 1$; $(a \to b)$. The Hamiltonian describing the evanescent coupling between the waveguide mode in such a system of two coupled waveguides can be derived using the coupled mode theory [208, 209]. The coupling among the waveguides is incorporated in this framework by treating it as a perturbation to the mode amplitudes. It is assumed that the presence of the second waveguide perturbs the medium outside the first waveguide. This creates a source of polarization outside the first waveguide, which thereby leads to modification of the amplitude of the mode in it. Further, the amplitude of the modes in each waveguide is assumed to be a slowly varying function of the propagation distance. Moreover, in this perturbative approach the coupling does not effect the propagation constant or transverse spatial distribution of the waveguide modes. The field of the first waveguide has a similar effect on the second waveguide. Under these assumptions, the field mode of the composite structure are governed by the Helmholtz equation which gives two coupled first order differential equations which can be solved to obtain the time evolution of field modes in the coupled waveguide structure. The corresponding description for the nonclassical light can be studied by quantizing the field amplitudes as has been done in the work of Lai et. al. [210]. Following an approach similar to that developed by Lai et. al., we can write the corresponding quantum mechanical Hamiltonian for the coupled waveguide as

$$H = \hbar\omega(a^\dagger a + b^\dagger b) + \hbar J(a^\dagger b + b^\dagger a) \ , \tag{6.1}$$

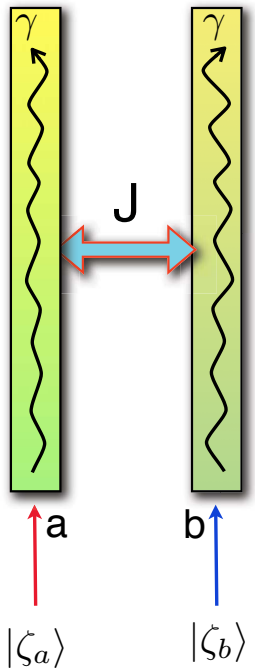

Figure 6.2: Schematic diagram of a coupled waveguide system. The parameter J gives the coupling between the waveguide modes and γ is the decay rate. The inputs to the waveguides can be single mode $|\zeta_a\rangle = \exp(\frac{r}{2}\{a^{\dagger 2} - a^2\})|0\rangle$; $(a \rightarrow b)$ or two mode $|\xi\rangle = \mathsf{exp}[r(a^\dagger b^\dagger - ab)]|00\rangle$ squeezed states.

where the first two terms correspond to the free energy of the waveguide modes and the last two terms account for the evanescent coupling between the waveguide modes with J as the coupling strength. The coupling J depend on the distance between the waveguides. The input to the coupled waveguide system can be in a separable or an entangled state. Let γ be the loss rates of the modes a and b. The loss γ arises from the loss in the material of the waveguide. Table I below gives the experimental values of coupling parameter J and loss γ for different waveguide systems.

Table 6.1: Approximate values of some of the parameters used in waveguide structures [211, 212, 213]. The loss, usually quoted in dB/cm, for different waveguides is converted to frequency units used in this chapter by using the formula, $10\ Log(\frac{P_{out}}{P_{in}}) \equiv 10\ Log(e^{-2\gamma/c})$, where P_{in} is the input power, P_{out} is the power after traveling unit length.

Waveguide Type	Coupling parameter J (sec^{-1})	Loss γ (sec^{-1})	γ/J
Lithium Niobate ($LiNbO_3$)	1.83×10^{10} - 4.92×10^{10}	3×10^9	1/7-1/20
AlGaAs	2.46×10^{11}	2.7×10^{10}	1/10
Silica	1.53×10^{11}	3×10^9	1/50

As known the silica waveguides have very little intrinsic loss and should be preferable in many applications. Nevertheless the loss is to be included as this could be detrimental in long propagation for example in the study of quantum random walks. Since the two waveguides are identical, we have taken the loss rate of both the modes to be the same. We can model the loss in waveguides in the framework of system-reservoir interaction well known in quantum optics and is given by,

$$\begin{aligned} \mathcal{L}\rho &= -\frac{\gamma}{2}(\hat{a}^\dagger\hat{a}\rho - 2\hat{a}\rho\hat{a}^\dagger + \rho\hat{a}^\dagger\hat{a}) \\ &\quad -\frac{\gamma}{2}(\hat{b}^\dagger\hat{b}\rho - 2\hat{b}\rho\hat{b}^\dagger + \rho\hat{b}^\dagger\hat{b})\ , \end{aligned} \tag{6.2}$$

where ρ is the density operator corresponding to the system consisting of fields in the modes a and b. The dynamical evolution of any measurable $\langle O \rangle$ in the coupled waveguide system is then governed by the quantum-Louiville equation of motion given by,

$$\dot{\rho} = -\frac{i}{\hbar}[H, \rho] + \mathcal{L}\rho, \tag{6.3}$$

where $\langle \dot{O} \rangle = \mathrm{Tr}\{O\dot{\rho}\}$, the commutator gives the unitary time evolution of the system under the influence of coupling and the last term account for the loss. Note that in absence of loss (lossless waveguides) the time evolution of the field operators can be evaluated using the Heisenberg equation of motion and is given by

$$\begin{aligned} a(t) &= a(0)\cos(Jt) - ib(0)\sin(Jt), \\ b(t) &= b(0)\cos(Jt) - ia(0)\sin(Jt). \end{aligned} \tag{6.4}$$

Next we will study the entanglement characteristics of photon number and squeezed input states as they propagate through the waveguides. To keep the analysis simple, in the next few sections we consider the case of lossless waveguide modes ($\gamma = 0$). We defer the discussion of loss on entanglement to Sec. IV.

6.3 Evolution of entanglement for Gaussian input states

6.3.1 Separable two mode squeezed state as an input

We next study the generation and evolution of entanglement for the case of squeezed input states. For this purpose we first consider a separable squeezed input state coupled to the modes a and b of the waveguide given by

$$|\zeta\rangle = |\zeta_a\rangle \otimes |\zeta_b\rangle; \tag{6.5}$$

where $|\zeta_a\rangle(|\zeta_b\rangle)$ are single mode squeezed states defined as

$$|\zeta_a\rangle = \exp(\frac{r}{2}\{a^{\dagger 2} - a^2\})|0\rangle; \quad (a \to b). \tag{6.6}$$

where r is taken to be real. The squeezed vacuum state falls under the class of Gaussian states and thus one needs to consider continuous variable entanglement in this case. We take an approach suitable for continuous variables and discussed previously in section (1.3.5) of the introduction to calculate the measure of entanglement in our coupled waveguides. It is to be noted that evolution of Gaussian states has been studied for many different model Hamiltonians [214, 215, 216, 217]. We focus on the practical case of propagation of light produced by a down converter in coupled waveguides which currently are used in quantum architectures and quantum random walks.

It is well known that a two mode squeezed state like $|\zeta\rangle$ can be completely characterized by its first and second statistical moments given by the first moment: $(\langle x_1\rangle, \langle p_1\rangle, \langle x_2\rangle, \langle p_2\rangle)$ and the covariance matrix σ. Note that since the first statistical moments can be arbitrarily adjusted by local unitary operations, it does not affect any property related to entanglement or mixedness and thus the behavior of the covariance matrix σ is all important for the study of entanglement. The measure of entanglement is then characterized by the logarithmic negativity $E_{\mathcal{N}}$, a quantity evaluated in terms of the symplectic eigenvalues of the covariance matrix σ [70, 72]. The elements of the covariance matrix σ are given in terms of conjugate observables, x and p in the form

$$\sigma = \begin{bmatrix} \alpha & \mu \\ \\ \mu^T & \beta \end{bmatrix}; \tag{6.7}$$

where α, β and μ are 2×2 matrices given by,

$$\alpha = \begin{bmatrix} \langle x_1^2\rangle & \langle \frac{x_1p_1+p_1x_1}{2}\rangle \\ \\ \langle \frac{x_1p_1+p_1x_1}{2}\rangle & \langle p_1^2\rangle \end{bmatrix}; \tag{6.8}$$

$$\beta = \begin{bmatrix} \langle x_2^2 \rangle & \langle \frac{x_2 p_2 + p_2 x_2}{2} \rangle \\ \\ \langle \frac{x_2 p_2 + p_2 x_2}{2} \rangle & \langle p_2^2 \rangle \end{bmatrix}; \tag{6.9}$$

$$\mu = \begin{bmatrix} \langle \frac{x_1 x_2 + x_2 x_1}{2} \rangle & \langle \frac{x_1 p_2 + p_2 x_1}{2} \rangle \\ \\ \langle \frac{x_2 p_1 + p_1 x_2}{2} \rangle & \langle \frac{p_1 p_2 + p_2 p_1}{2} \rangle \end{bmatrix}. \tag{6.10}$$

Here x_1, x_2 and p_1, p_2 are given in terms of the normalized bosonic annihilation (creation) operators $a(a^\dagger)$, $b(b^\dagger)$ associated with the modes a and b respectively,

$$\begin{aligned} x_1 &= \frac{(a + a^\dagger)}{\sqrt{2}}, \quad x_2 = \frac{(b + b^\dagger)}{\sqrt{2}}; \\ p_1 &= \frac{(a - a^\dagger)}{\sqrt{2}i}, \quad p_2 = \frac{(b - b^\dagger)}{\sqrt{2}i}. \end{aligned} \tag{6.11}$$

The observables x_j, p_j satisfy the cannonical commutation relation $[x_k, p_j] = i\delta_{kj}$. The condition for entanglement of a Gaussian state like $|\zeta\rangle$ is derived from the PPT criterion [70, 73], according to which the smallest symplectic eigenvalue $\tilde{\nu}_<$ of the transpose of matrix σ should satisfy

$$\tilde{\nu}_< < \frac{1}{2}. \tag{6.12}$$

where $\tilde{\nu}_<$ is defined as

$$\tilde{\nu}_< = \mathsf{min}[\tilde{\nu}_+, \tilde{\nu}_- \,]; \tag{6.13}$$

and $\tilde{\nu}_\pm$ is given by,

$$\tilde{\nu}_\pm = \sqrt{\frac{\tilde{\Delta}(\sigma) \pm \sqrt{\tilde{\Delta}(\sigma)^2 - 4\mathsf{Det}\sigma}}{2}} \quad ; \tag{6.14}$$

where $\tilde{\Delta}(\sigma) = \Delta(\tilde{\sigma}) = \mathsf{Det}(\alpha) + \mathsf{Det}(\beta) - 2\mathsf{Det}(\mu)$. Thus according to the condition (6.12) when $\tilde{\nu}_< \geq 1/2$ a Gaussian state become separable. The corresponding

quantification of entanglement is given by the logarithmic negativity $E_{\mathcal{N}}$ [69, 71, 78] defined as,

$$E_{\mathcal{N}}(t) = \mathsf{max}[0, -\ln\{2\tilde{\nu}_{<}(t)\}]; \tag{6.15}$$

which constitute an upper bound to the *distillable entanglement* of any Gaussian state [71]. On evaluating the covariance matrix σ for the state (6.5) for $\gamma = 0$ (no loss), using equation (6.3), (6.4) and (6.11), we find

$$\alpha = \beta = \begin{bmatrix} c & 0 \\ 0 & d \end{bmatrix}; \qquad \mu = \begin{bmatrix} 0 & e \\ e & 0 \end{bmatrix}; \tag{6.16}$$

where d, e, c are given by

$$\begin{aligned} c &= \frac{1}{2}\{\cosh(2r) + \sinh(2r)\cos(2Jt)\}; \\ d &= \frac{1}{2}\{\cosh(2r) - \sinh(2r)\cos(2Jt)\}; \\ e &= -\frac{1}{2}\sinh(2r)\sin(2Jt). \end{aligned} \tag{6.17}$$

The corresponding symplectic eigenvalues $\tilde{\nu}_{\pm}$ are then given by

$$\tilde{\nu}_{\pm} = \sqrt{cd} \pm e. \tag{6.18}$$

One can clearly see from equations (6.15), (6.17) and (6.18) the dependence of logarithmic negativity $E_{\mathcal{N}}$ on coupling strength J between the waveguides and the squeezing parameter r. In Fig (6.5), we plot the logarithmic negativity as a function of scaled time, $\theta = Jt$ for the state $|\zeta\rangle$. Here t is related to the length l of the waveguide and its refractive index n by $t = nl/v$, v being the velocity of light. We see from Fig (6.5) that as $|\zeta\rangle$ is separable at $t = 0$, $E_{\mathcal{N}} = 0$ initially, but as Jt increases, it oscillates periodically between a non-zero and zero value. Thus the initially separable state $|\zeta\rangle$ becomes periodically entangled and disentangled as its propagates through the waveguide. We attribute this periodic generation of entanglement to the coupling J among the waveguides. We further find that $\tilde{\nu}_{<} = 1/2$ at certain points along the waveguide given by $2\theta = (k+1)\pi, k = 0, 1, 2, 3, ...$ Note that at this points $E_{\mathcal{N}}$

vanishes and $|\zeta\rangle$ becomes separable. At all other points the state $|\zeta\rangle \neq |\zeta_a\rangle \otimes |\zeta_b\rangle$. We see that $E_{\mathcal{N}}$ is maximum and has a value equal to the amount of squeezing $2r$ at the points given by $2\theta = (k+1)\pi/2$. Hence at this points the initial seperable state $|\zeta\rangle$ becomes maximally entangled and is given by,

$$|\zeta\rangle \equiv \mathsf{exp}\{e^{i\pi} r(a^\dagger b^\dagger + ab)\}|00\rangle \tag{6.19}$$

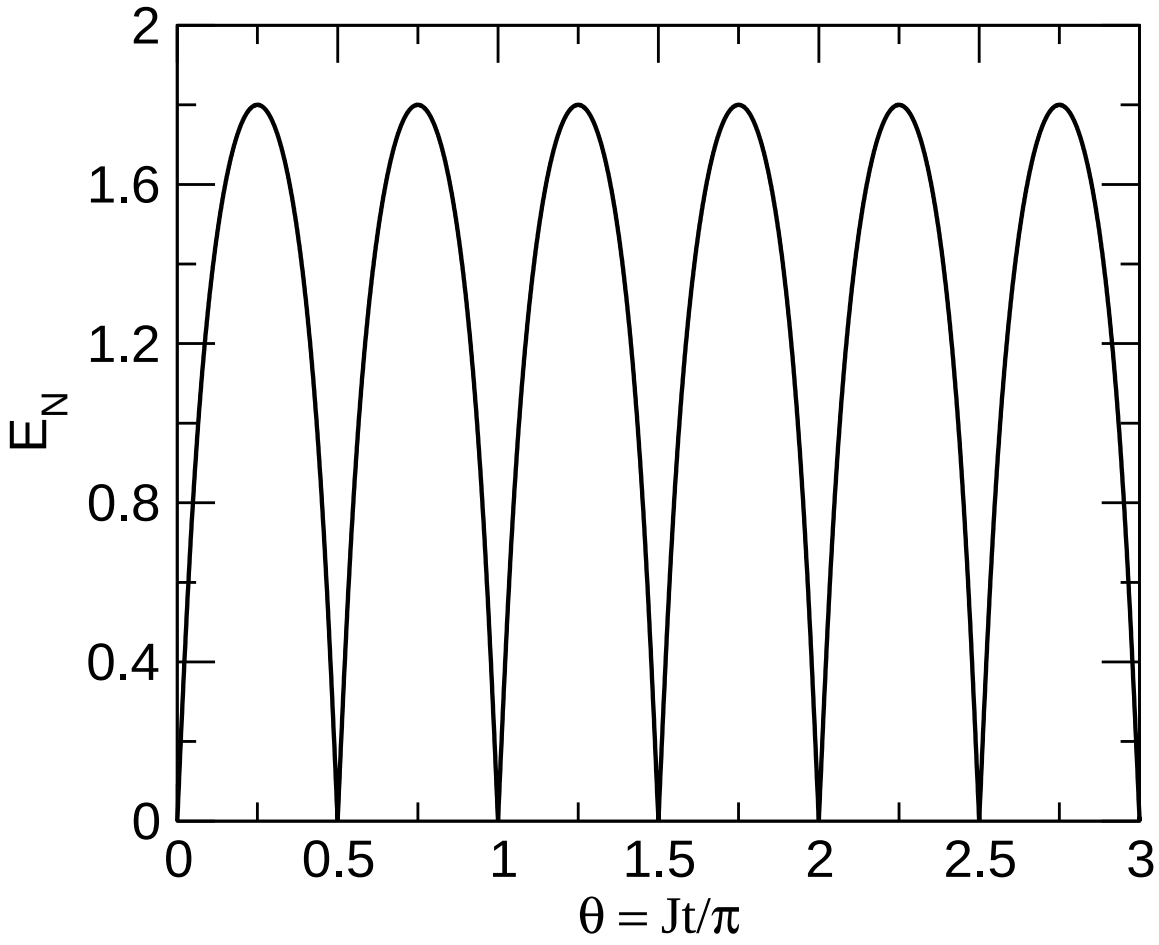

Figure 6.3: Plot of the time dependent logarithmic negativity $E_{\mathcal{N}}$ for the state $|\zeta\rangle$. Here amount of squeezing is taken to be $r = 0.9$.

6.3.2 Entangled two mode squeezed state as an input

Let us now study the dynamical evolution of a two mode squeezed state $|\xi\rangle$ as an input to the waveguide,

$$|\xi\rangle = \mathsf{exp}[r(a^\dagger b^\dagger - ab)]|00\rangle. \tag{6.20}$$

As before we consider r to be real. To quantify the entanglement of the state $|\xi\rangle$ we need to evaluate the logarithmic negativity $E_{\mathcal{N}}$. Thus we first evaluate the covariance matrix σ for the state $|\xi\rangle$ using equations (6.3) with $\gamma = 0$, (6.4) and (6.11). We find σ to be

$$\sigma = \begin{bmatrix} f & g & h & 0 \\ g & f & 0 & -h \\ h & 0 & f & g \\ 0 & -h & g & f \end{bmatrix}, \tag{6.21}$$

where f, g and h are given by,

$$\begin{aligned} f &= \frac{1}{2}\cosh(2r), \\ g &= -\frac{1}{2}\sinh(2r)\sin(2Jt), \\ h &= \frac{1}{2}\sinh(2r)\cos(2Jt). \end{aligned} \tag{6.22}$$

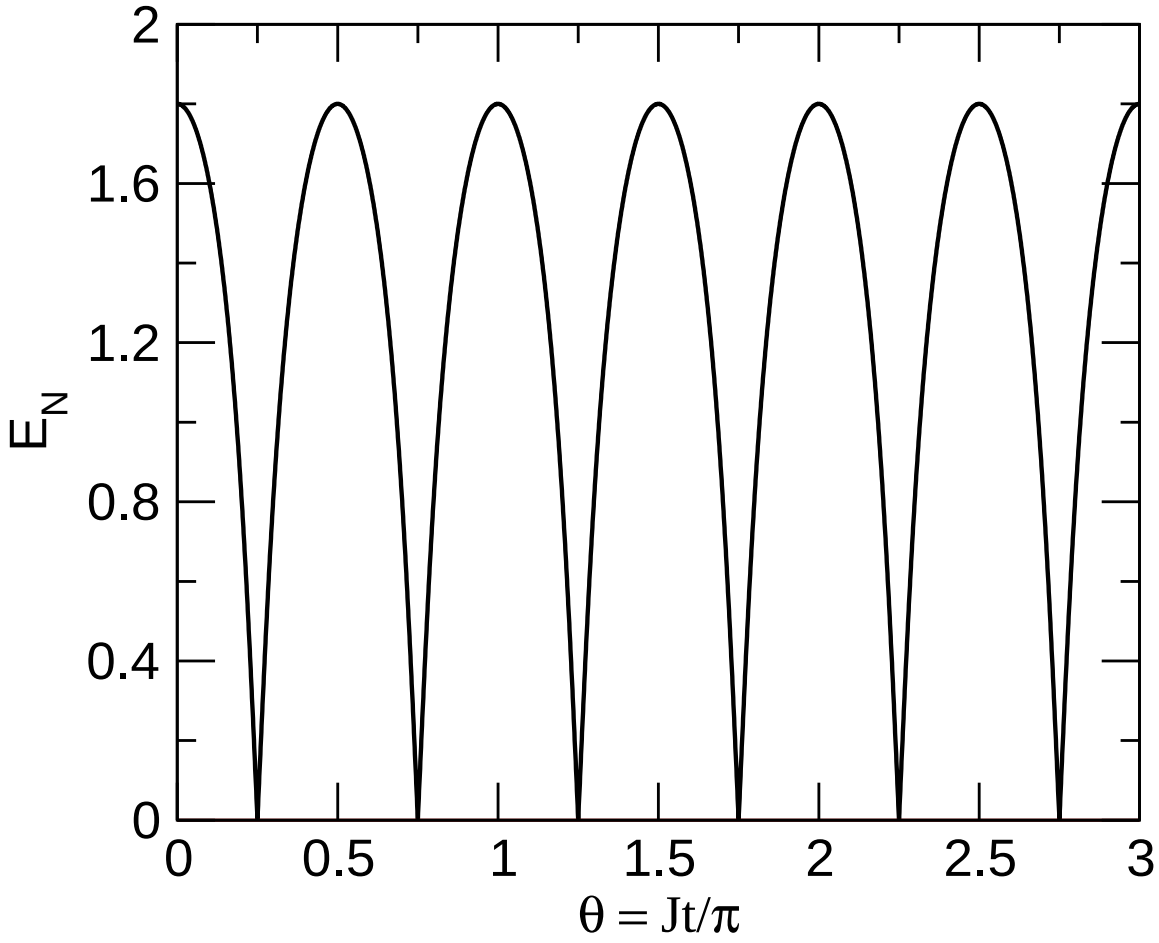

Figure 6.4: Time evolution of logarithmic negativity $E_{\mathcal{N}}$ for the initial entangled state $|\xi\rangle$. Here the squeezing is taken to be $r = 0.9$.

The corresponding symplectic eigenvalues $\tilde{\nu}_{\pm}$ is then given by,

$$\tilde{\nu}_{\pm} \;=\; \sqrt{(f+g)(f-g)} \pm h. \tag{6.23}$$

The logarithmic negativity $E_{\mathcal{N}}$ can then be evaluated using equations (6.15), (6.22) and (6.23). From equations (6.22) and (6.23) the dependence of $E_{\mathcal{N}}$ on the squeezing r and the coupling J between the waveguides is clearly visible. From equation (6.23) we find that $E_{\mathcal{N}} = 0$ *i.e.* entanglement become zero when, $2\theta = (k+1)\pi/2$ as then $\tilde{\nu}_{<} = 1/2$ and thus the initially entangled state $|\xi\rangle$ becomes separable, i.e $|\xi\rangle = \mathsf{exp}\{\frac{r}{2}e^{i\pi}(a^{\dagger 2}+a^2)\}|0\rangle \otimes \mathsf{exp}\{\frac{r}{2}e^{i\pi}(b^{\dagger 2}+b^2)\}|0\rangle$. In Fig (6.6) we plot the time evolution of $E_{\mathcal{N}}$ for $r = 0.9$. We see that entanglement oscillates periodically between zero and non-zero values. We further find that in this case the oscillations in $E_{\mathcal{N}}$ is $\pi/4$ out of phase to that for the initial separable state $|\zeta\rangle$. This oscillatory behavior of entanglement is as discussed before, due to the coupling J among the waveguides. Each time the states get separable, the presence of coupling leads to interaction among the modes of the waveguides and creats back the entanglement. We see from the figure that logarithmic negativity $E_{\mathcal{N}}$ reaches maximum at later times at the points $2\theta = (k+1)\pi$ and is equal to $2r$. Thus at these points the state $|\xi\rangle$ regains its initial form given by equation (6.20).

6.4 Lossy Waveguides

In this section we study the entanglement dynamics of lossy waveguides ($\gamma \neq 0$). The loss γ arises from the loss in the material of the waveguide. In this case the dynamical evolution of the waveguide modes is governed by the full quantum-Louiville equation (6.3). We next consider the cases of both photon number state and squeezed states at the input of the waveguide and discuss the influence of the loss on their respective entanglement evolution.

6.4.1 Effect of Leakage on Gaussian Entanglement

For the input squeezed state $|\zeta\rangle$ of equation (6.5) we find that elements of the covariance matrix σ in presence of loss become dependent on the decay rate γ and is given by,

$$\sigma = \begin{bmatrix} c' & 0 & 0 & e' \\ 0 & d' & e' & 0 \\ 0 & e' & c' & 0 \\ e' & 0 & 0 & d' \end{bmatrix}; \tag{6.24}$$

where c', d', e' are given by

$$\begin{aligned} c' &= \frac{1}{2}\{1 + e^{-2\gamma t}\sinh^2(r) + e^{-2\gamma t}\sinh(2r)\cos(2Jt)\}; \\ d' &= \frac{1}{2}\{1 + e^{-2\gamma t}\sinh^2(r) - e^{-2\gamma t}\sinh(2r)\cos(2Jt)\}; \\ e' &= -\frac{1}{2}e^{-2\gamma t}\sinh(2r)\sin(2Jt). \end{aligned} \tag{6.25}$$

The corresponding symplectic eigenvalue $\tilde{\nu}$ of the covariance matrix is then found to be

$$\tilde{\nu}_{\pm} = \sqrt{c'd'} \pm e'. \tag{6.26}$$

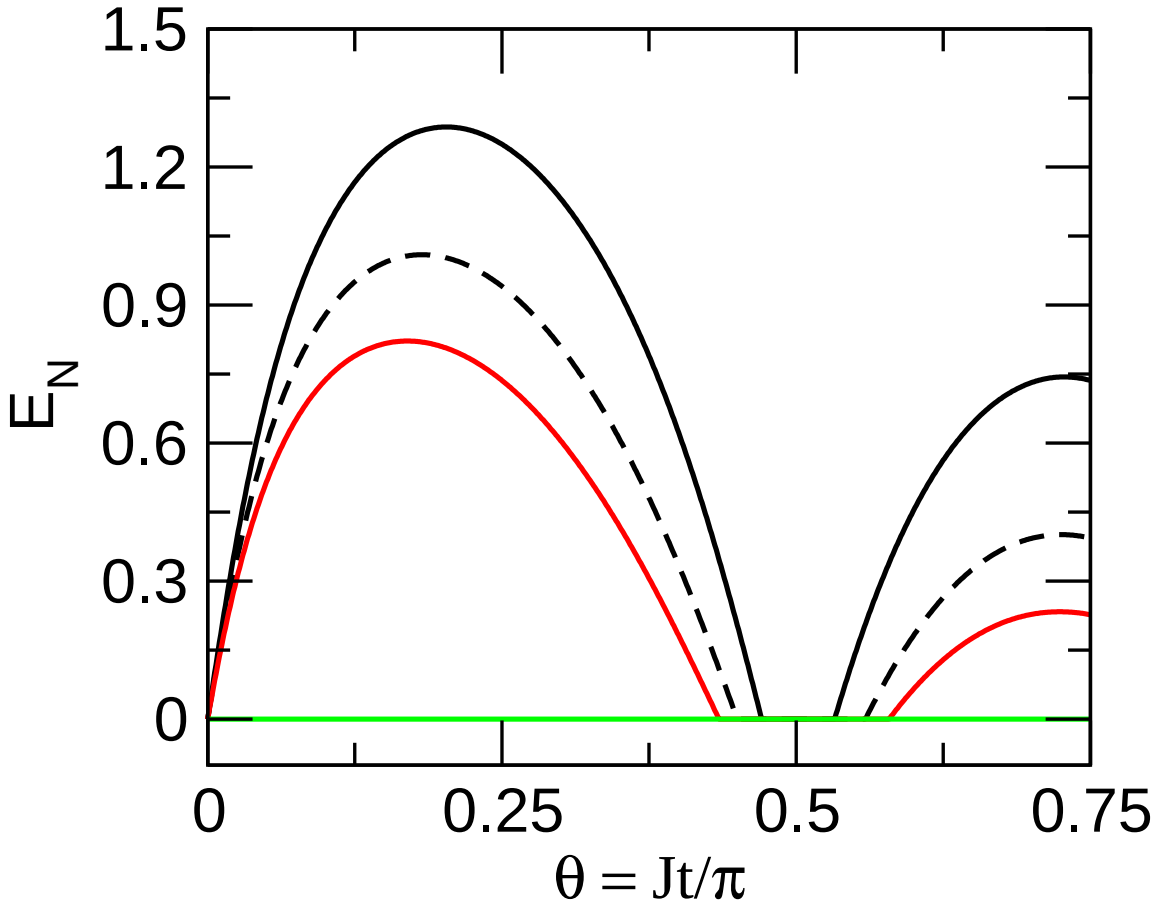

Figure 6.5: Time evolution of the logarithmic negativity $E_{\mathcal{N}}$ in presence of leakage of the waveguide modes for the input state $|\zeta\rangle$. The decay rates of the modes are given by $\gamma/J = 0.1$ (solid black), $\gamma/J = 0.2$ (broken black) and $\gamma/J = 0.3$ (red). Here the squeezing is taken to be $r = 0.9$. The leakage leads to new behavior in the entanglement.

On substituting equation (6.26) in (6.15) and using (6.25) we get the logarithmic negativity for lossy waveguides. To study the dependence of entanglement on loss of the waveguide modes we plot the logarithmic negativity $E_{\mathcal{N}}$ for different decay rates γ/J in Fig (6.7). As for the case of single photon states we focus on the range of θ important from the experiment point of view. We see new features in the entanglement dynamics as an effect of the loss. We see from figure (6.7) that in presence of loss the maximum value of entanglement for the state $|\zeta\rangle$ reduces in comparison to the case of lossless waveguides. However it is important to note that this decrease is not substantial. We further find that with increase in decay rate, the entanglement maximum shifts but does not show considerable reduction (the maximum changes by only 0.4 as the decay rate becomes three times). Thus we see that entanglement is quite robust against decoherence in this coupled waveguide systems. The robustness of entanglement dynamics is an artifact of coherent coupling among the waveguide modes. This findings hence suggest that coupled waveguide can be used as an effective quantum circuit for use in quantum information computations. Further we see another new feature in entanglement in Fig (6.7). We find that there exist an interval of θ during which the state $|\zeta\rangle$ remains separable. Note that in absence of loss the state $|\zeta\rangle$ becomes separable momentarily and entanglement starts to build up instantaneously once it becomes zero (see figure 6.5.) Thus this feature that entanglement remains zero for certain interval of time arises solely due to loss.

In Fig (6.8) we plot the long time behavior for entanglement of the state $|\zeta\rangle$ with very small decay rate of $\gamma/J = 0.1$ and squeezing parameter $r = 0.9$. We see that entanglement decays slowly with increasing θ as the magnitude of $E_{\mathcal{N}}$ diminish successively with every oscillations. In addition periods of disentanglement arises repeatedly in its oscillations. We find that the length of this periods increases with increasing θ. It is worth mentioning here that this kind of behavior has been predicted earlier for two

qubit entanglement [185, 219]. Next we study the effect of the decay of waveguide mode on the entanglement dynamics of the initial entangled Gaussian state $|\xi\rangle$ given in equation (6.20). We find in this case the covariance matrix to be

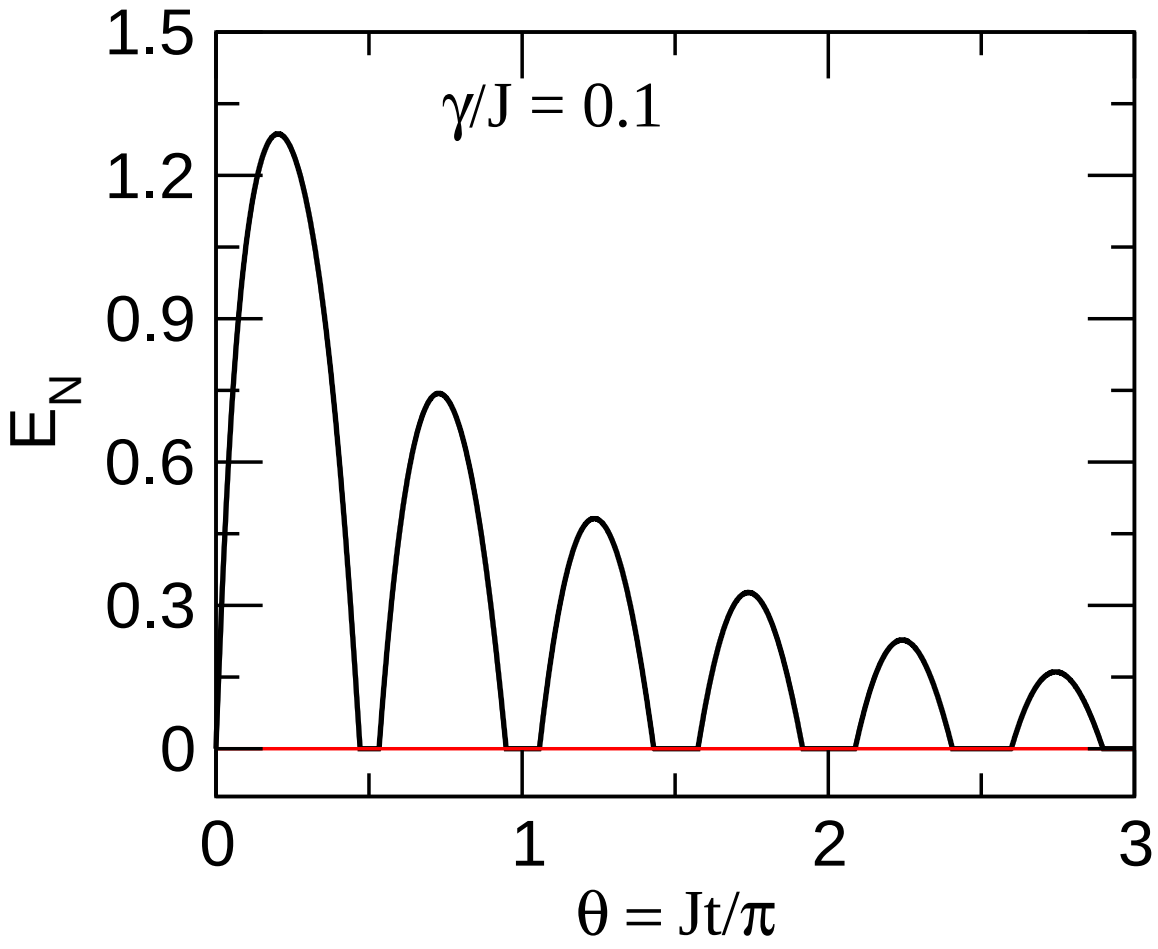

Figure 6.6: Long time behavior of the logarithmic negativity $E_{\mathcal{N}}$ in presence of leakage of the waveguide modes for the initial separable input state $|\zeta\rangle$.

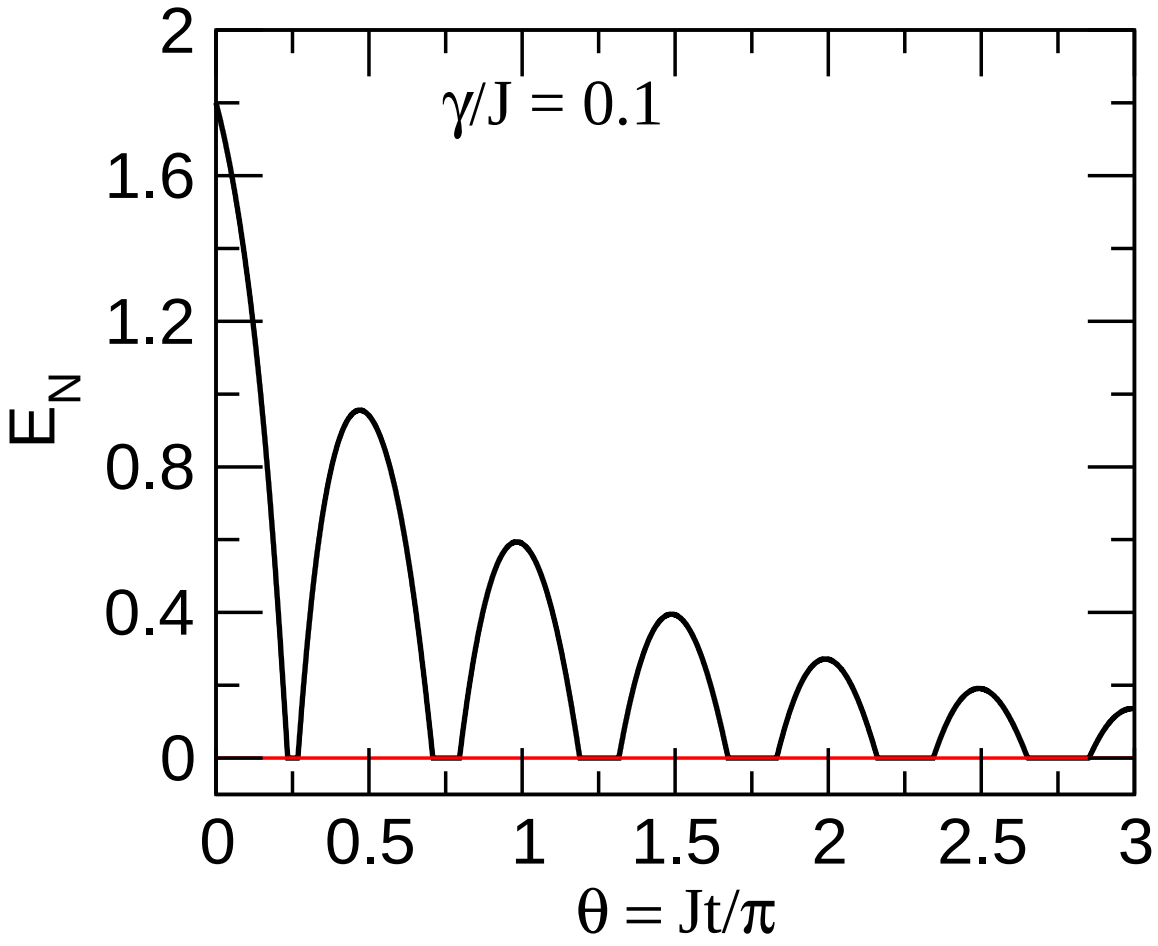

Figure 6.7: Time evolution of the logarithmic negativity $E_{\mathcal{N}}$ in presence of leakage of the waveguide modes for the initial entangled input state $|\xi\rangle$. Here γ is the decay rate of the modes and squeezing is taken to be $r = 0.9$.

$$\sigma = \begin{bmatrix} f' & g' & h' & 0 \\ g' & f' & 0 & -h' \\ h' & 0 & f' & g' \\ 0 & -h' & g' & f' \end{bmatrix}; \tag{6.27}$$

where f', g', h' are given by

$$\begin{aligned} f' &= \frac{1}{2} + e^{-2\gamma t}\sinh^2(r), \\ g' &= -\frac{1}{2}e^{-2\gamma t}\sinh(2r)\sin(2Jt), \\ h' &= \frac{1}{2}e^{-2\gamma t}\sinh(2r)\cos(2Jt). \end{aligned} \tag{6.28}$$

In this case we find that the symplectic eigenvalues $\tilde{\nu}_\pm$ are dependent on the decay rate of the waveguide modes and is given by

$$\tilde{\nu}_\pm = \sqrt{m_+ m_-} \pm h', \tag{6.29}$$

where $m_\pm(t) = 1 - e^{-2\gamma t}[1 - \{\cosh(2r) \pm \sinh(2r)\sin(2Jt)\}]$. The corresponding measure of entanglement given by the logarithmic negativity $E_\mathcal{N}$ can then be calculated by using equations (6.15), (6.28) and (6.29). In Fig (6.9) we plot the logarithmic negativity $E_\mathcal{N}$ for the state $|\xi\rangle$ as a function of θ in presence of loss. We find similar behavior in the entanglement dynamics as seen earlier for the separable state $|\zeta\rangle$. We find in Fig (6.9) that entanglement of the state $|\xi\rangle$ decreases slowly with increasing θ for non-zero γ/J. Thus as for the separable states, in case of initial entangled input states entanglement is found to be quite robust in the face of loss. In addition to this we also see in Fig (6.9) periods of disentanglement appearing successively as θ increases.

The loss in waveguides that we discussed in this section arises due to material properties like change in refractive index and absorption. On the other hand there

can be decay of the waveguide modes in the form of leakage to its surrounding also. It should be noted that leakage is inherently different from the evanescent coupling as the former can arise due to scattering and refraction due to refractive index difference at the waveguide boundaries. Thus the analysis of this section is also valid when the leakage is important as for example is the case when one couples channel waveguides to slab waveguides [201, 220].

6.5 Conclusion

To conclude, we investigated the time evolution of entanglement in a coupled waveguide system. We quantified the degree of entanglement between the waveguide modes in terms of logarithmic negativity. We have given explicit analytical results for logarithmic negativity in the case of initially separable single photon states and for separable as well as entangled squeezed states. We have also addressed the question of decoherence in coupled waveguide systems by considering loss of waveguide modes. For the lossy waveguides we found that the entanglement shows considerable robustness even for substantial loss. Note that our results are based on experimental parameters and thus should be relevant for applications of waveguides in quantum information sciences. Our results serve as guide for experiments dealing with entanglement in waveguide structures. For efficient use of these waveguides, one should choose the waveguide parameter like $\theta = Jt$ so that one is away from values where the entanglement is a minimum.

CHAPTER 7

SUMMARY AND FUTURE PROSPECTS

7.1 Summary of our findings

To summarize, we studied quantum interferences in novel microscopic systems like atoms, ions, quantum dots and photonic waveguides for potential application in quantum information sciences. We specifically focused on the nonlocal quantum correlations *i.e* entanglement that can be generated as a result of such quantum interferences. Further we also did a detailed study of decoherence effects of the environment on the time evolution of entanglement in such systems. We found that degenerate atomic transitions in trapped $^{138}Ba^{+}$ and $^{198}Hg^{+}$ ions can provide us with an alternative to observe the effect of vacuum induced coherences (VIC)- a quantum interference effect that arises as a result of interaction of a quantum system with the electromagnetic vacuum fluctuations (chapter 2). We found that VIC leads to stronger quantum correlations among the emitted photons.

In a subsequent work (chapter 3) we found new quantum interference effects in a two level atomic system comprising of two atoms or quantum dots. This quantum interference was induced by manipulating the spatial phase of the incident coherent field and led to substantial modification of the Dicke incoherent emission spectrum. Further the population dynamics of the Dicke states in this system was found to be governed by a vacuum induced super-exchange. We also found signatures of laser phase induced creation of entanglement in these systems by studying the quantum correlations among the dipole moment operators. Next we studied quantum correlations of biexciton cascade emission in quantum dots (chapter 4). We proposed a

realistic theoretical model for the bi-exciton cascade in quantum dots incorporating both structural asymmetries and decoherence effects due to the interaction of the dot with its solid-state environment. We showed that the predictions of our model were in agreement with the experimental results existing in literature. Thus we were successful in providing a simple understanding of the underlying physical processes in these microscopic systems.

In the later part of our investigation we studied the problem of two interacting entangled qubits (which can be atoms, ions or quantum dots) in contact with the environment (chapter 5). This is an interesting problem in the context of decoherence effects on the functionality of quantum logic gates implemented using entangled quantum dots or ions. We studied several different model of qubit-environment interaction applicable in a wide range of systems and showed the effect of decoherence. We found that the competitions of environmental decoherence and qubit-qubit interactions lead to the generation of bright (entanglement) and dark (disentanglement) periods in the time evolution of entanglement. This was found to be a generic behavior and occurs for all the models that we considered. Moreover we discovered that the length and frequency of the periods depend on the initial coherences among the two qubits and the strength of interaction respectively. Further we found that depending on the initial excitation of the qubits, entanglement can be destroyed completely in short time due to decoherence.

Finally we studied the system of evanescent coupled photonic waveguides that are currently of interest due to their scalability and robustness for constructing quantum information circuits (chapter 6). In line with current experiments we considered a system of two evanescent coupled waveguides and studied continuous variable entanglement and effect of decoherence on it. We found that when the output light fields from a parametric down converter (which are squeezed states at high gain of the amplifier) are the inputs to the waveguides, entanglement is dynamically generated

among the field modes. This occurs as a result of the evanescent coupling. Further we also found that as light propagates through the waveguides entanglement oscillates between zero and non-zero values. Moreover we studied decoherence effects in this systems in form of propagation loss in the waveguide or leakage to its surrounding substrate. We found that this systems are quite robust to decoherence and thus suitable for quantum circuit engineering.

7.2 Future prospects

There are many open questions that stem from the work in this thesis which warrant future considerations. We discuss a few of these questions that are particularly important in respect to quantum information sciences.

The effects of spatial variation of laser phase on the incoherent Dicke co-operative emission spectrum as discussed in chap. 3 can change for finite spatial extensions of the quantum dots. This can be an important issue in the practical utilization of such two dot systems. Moreover we found a strong quantum correlation for certain distance of separation among the dots, which can be a signature of stronger entanglement in these systems under certain configuration. Thus our findings open up questions like size dependence of dots on their fluorescence spectrum, entanglement. Moreover it is known that for dots in a micro-cavity the spontaneous emission and dephasing can be manipulated due to cavity-dot coupling. Thus multiple dots in a micro-cavity environment would be worth investigating. Further our studies showed that even small excitonic level splitting does not allow efficient generation of entanglement in this system. This hence raises the question of how to get control over manipulating this level splitting for utilization of these systems as true sources of entanglement. A probable way to achieve such control might be by using laser induced AC-stark shifts of one of the excitonic levels. The findings of chap. 6 for evanescent coupled waveguides opens up the question of entanglement dynamics and decoherence effects

for a broader class of non-classical input states of light, like the CAT states and photon added coherent states. Moreover, our study of loss in this system shows that for truthful implementation of these systems in quantum circuitry the behavior of single qubit and two qubit gate operations using waveguides should include losses and their effects on gate fidelities. We showed in chap. 5 the importance of qubit-qubit interaction in the entanglement dynamics of qubits. Such investigation needs to be extended for multi-qubit systems. It would be specially interesting to extend the work of chap. 5 to the GHZ and W states. Further, study of decoherence effects of finite temperature environments in such interacting qubits should also be interesting from a quantum computation perspective.

Further to save entanglement over long periods, a way would be by coupling the qubits to environments with memory. Quantum dots and photonic band gap materials are excellent examples of realistic systems where one can find such long time memory of the environments. In particular earlier studies in photonic band gap materials have shown [221, 222] that near the band edge the nature of spontaneous emission from an atom is very different. In particular some population remains trapped in the excited state. Thus photonic band gap materials are expected to be promising systems for preserving entanglement in the long time limit if the qubits are encoded in such materials. A comprehensive study of entanglement and decoherence phenomenon in photonic band gap material should open up new directions in the field of quantum information and computation.

BIBLIOGRAPHY

[1] M. Planck, *Ann Phys* **4**, 553 (1901)

[2] R. P. Feynman, *Int. J. Theoret. Phys.* **21**, 467 (1982)

[3] D. Deutsch, *Proc. R. Soc. Lond. A.* **400**, 97 (1985)

[4] P. W. Shor, *Proc. Annu. Symp. Found. Comput. Sci.*, 124 (1994)

[5] M. A. Nielsen, and I. L. Chuang, *Quantum Computation and Quantum Information* (Cambridge Univ. Press, Cambridge, UK, 2000)

[6] E. Schrödinger, *Naturwissenschaften* **23**, 807 (1935).

[7] A. Einstein, B. Podolsky, and N. Rosen, Phys. Rev. **47**, 777 (1935).

[8] J. S. Bell, Physics (Long Island City, New York) **1**, 195 (1964); J. S. Bell, 1987, Speakable and Unspeakable in Quantum Mechanics (Cambridge University, Cambridge).

[9] J. J. Sakurai, *Modern Quantum Mechanics*, (Addison-Wesley, New York, 2000).

[10] Anton Zeilinger, Rev. Mod. Phys **71**, S288 (1999).

[11] J. F. Clauser, M. A. Horne , A. Shimony and R. A. Holt, Phys. Rev. Lett **23**, 880 (1969).

[12] S. J. Freedman and J. F. Clauser, Phys. Rev. Lett. **28**, 938 (1972).

[13] A. Aspect, P. Grangier and G. Roger, Phys. Rev. Lett. **47**, 460 (1981).

[14] A. Aspect, P. Grangier and G. Roger, Phys. Rev. Lett. **49**, 91 (1982).

[15] R. F. Werner, Phys. Rev. A **40**, 4277 (1989).

[16] R. Horodecki, *et. al.* Rev. Mod. Phys. **81**, 865 (2009).

[17] C. O. Alley, and Y. H. Shih, 1986, in *Proceedings of the Second International Symposium on Foundations of Quantum Mechanics in the Light of New Technology*, (Tokyo, 1986), edited by M. Namiki et al. (Physical Society of Japan), p. 47.

[18] P. Kwiat, H. Weinfurter, T. Herzog, and A. Zeilinger, Phys. Rev. Lett. **74**, 4763 (1995).

[19] W. Tittel, J. Brendel, B. Gisin, T. Herzog, H. Zbinden, and N. Gisin, Phys. Rev. A **57**, 3229 (1998).

[20] A. K. Ekert Phys. Rev. Lett. **67**, 661 (1991).

[21] E. Knill, R. Laflamme, and G. J. Milburn Nature **409**, 46 (1996).

[22] H-J . Briegel, W. Dur, J. I. Cirac and P. Zoller Phys. Rev. Lett. **81**, 5932 (1998).

[23] T. Chaneliere *et. al.* Phys. Rev. Lett. **96**, 093604 (2006).

[24] C. H. Bennet and G. Brassard, Proceedings of the IEEE International Conference on Computers, Systems, and Signal Processing, Bangalore, p. 175 (1984); C. H. Bennett, *et. al.* Phys. Rev. Lett. **70**, 1895 (1993); C. H. Bennett, and D. P. DiVincenzo, *Nature* **404**, 247 (2000).

[25] D. Boumeester, A. Zeilinger and A. K. Ekert, *The Physics of Quantum Information : Quantum Cryptography, Quantum Teleportation, Quantum Computation* (Springer Verlag, New York 2000).

[26] J. I. Cirac, and P. Zoller, *Nature* **404**, 579 (2000); J. I. Cirac, and P. Zoller, Phys. Rev. Lett. **74**, 4091 (1995).

[27] Rainer Blatt, and D. J. Wineland, *Nature* **453** 1008 (2008); D. J. Wineland, *et. al.*, *Phil. Trans. R. Soc. Lond.* A. **361**, 1349 (2003).

[28] B. B. Blinov, *et. al.*, *Nature* **428**, 153 (2004); D. Kielpinski, C. Monroe, and D. J. Wineland *Nature* **417**, 709 (2002).

[29] O. Benson *et. al.*, Phys. Rev. Lett. **84**, 2513 (2000).

[30] C. Santori *et. al.*, Phys. Rev. Lett. **86**,1502 (2001).

[31] N. Akopian, *et. al.* Phys. Rev. Lett. 96, 130501 (2006).

[32] R. M. Stevenson *et. al.*, *Nature* **439**, 179 (2006).

[33] R. Hanson and D. Awschalom, *Nature* **453**, 1043 (2008). and references therein.

[34] M. Lewenstein, *et. al.*, Adv. Phys. **56**, 243 (2007).

[35] D. Jaksch, and P. Zoller, Ann. Phys. (NY) **315**, 52 (2005).

[36] I. Bloch, J. Dalibard, and W. Zwerger, Many-body physics with ultracold gases. Preprint at http://arxiv.org/abs/0704.3011 (2007); I. Bloch *Nature Phys* **1**, 23 (2005).

[37] Barak Dayan *et. al.*, *Science* **319**, 1062 (2008); A. D. Boozer, *et. al.*, Phys. Rev. Lett. **98**, 193601 (2007); R. Miller *et. al.* J. Phys. B **38**, S551 (2005); J. Ye, D. W. Vernooy, H. J. Kimble, Phys. Rev. Lett. **83**, 4987 (1999).

[38] K. S. Choi, *et. al.*, *Nature* **452**, 67 (2008); H. J. Kimble, *Nature* **453**, 1023 (2008); J. Laurat, *et. al.*, Phys. Rev. Lett. **99**, 180504 (2007).

[39] H. de Riedmatten, *et. al.*, Phys. Rev. Lett. **97**, 113603 (2006); D. Felinto, *et. al.*, Phys. Rev. A **72**, 053809 (2005).

[40] P. Maunz *et. al.*, *Nature* **428**, 50 (2004); P.W.H. Pinkse *et. al.*, *Nature* **404**, 365 (2000); G. Rempe Applied Physics B **60**, 233 (1995).

[41] T. Meunier *et. al.*, Phys. Rev. Lett. **94**, 010401 (2005) J. M. Raimond, M. Brune, and S. Haroche, Rev. Mod. Phys. **73**, 565 (2001); P. Goy *et. al.*, Phys. Rev. Lett. **50**, 1903 (1983).

[42] J. H. Davies, *The Physics of Low-dimensional Semiconductors: An Introduction* (Cambridge University Press, Cambridge, U.K. ; NY, USA 1998).

[43] L. Kouwenhoven and C. Marcus, Quantum Dots, Physics World, June 1998.

[44] R. J. Warburton *et. al. Nature* **405**, 926 (2000); M. Bayer *et. al. Nature* **405**, 923 (2000).

[45] P. Michler, *Single Quantum Dots: fundamentals, applications and new concepts, Topics in Applied Phyics* (Springer-Verlag, Berlin Germany, 2003).

[46] P. Michler *et. al. Nature* **406**, 968 (2000); D. Regelman *et. al.* Phys. Rev. Lett. **87**, 257401 (2001).

[47] P. Michler *et. al. Science* **290**, 2282 (2000).

[48] H. Kamada *et. al.* Phys. Rev. Lett. **87**, 246401 (2001); T. H. Stievater, *et. al.* Phys. Rev. Lett. **87**, 133603 (2001); H. Htoon, *et. al.* Phys. Rev. Lett. **88**, 087401 (2002).

[49] Xiaodong Xu, *et. al. Science* **317**, 929 (2007).

[50] Michael Scheibner *et. al.*, *Nature Physics* **3**, 106 (2007).

[51] A. Barenco *et. al.*, Phys. Rev. Lett. **74**, 4083 (1995).

[52] D. Loss, and D. P. DiVincenzo , Phys. Rev. A **57**, 120 (1998).

[53] A. Imamoḡlu *et. al.* Phys. Rev. Lett. **83**, 4204 (1999).

[54] J. R. Petta, *et. al. Science* **309**, 2180 (2005); R. Hanson, and G. Burkard, Phys. Rev. Lett. **98**, 050502 (2007); L. Robledo *et. al. Science* **320**, 772 (2008).

[55] R. Johne *et. al.*, Phys. Rev. Lett. **100**, 240404 (2008).

[56] J. M. Elzerman *et. al.*, *Nature* **430**, 431 (2004); R. Hanson *et. al.*, Phys. Rev. Lett. **94**, 196802 (2005); S. Amasha *et. al.*, Phys. Rev. Lett. **100**, 046803 (2008).

[57] D. N. Christodoulides, F. Lederer and Y. Silberberg, Nature (London) **424**, 817 (2003).

[58] R. Iwanow, D. A. May-Arrioja, D. N. Christodoulides, G. I. Stegeman, Y. Min, and W. Sohler, Phys. Rev. Lett. **95**, 053902 (2005).

[59] Yoav Lahini *et. al.*, Phys. Rev. Lett. **100**, 013906 (2008).

[60] Y. Bromberg, Y. Lahini, R. Morandotti, and Y. Silberberg, Phys. Rev. Lett. **102**, 253904 (2009).

[61] S. Longhi, Phys. Rev. Lett. **101**, 193902 (2008).

[62] S. Longhi, Phys. Rev. Lett. **101**, 193902 (2008).

[63] A. Rai and G. S. Agarwal, Phys. Rev. A **79**, 053849 (2009).

[64] A. Politi, M. J. Cryan, J. G. Rarity, S. Yu, J. L. O'Brien, Science **320**, 646 (2008).

[65] J. C. F. Matthews, A. Politi, A. Stefanov, and J. L. O'Brien, Nature Photonics **3**, 346 (2009).

[66] D. W. Berry and H. M. Wiseman, Nature Photonics **3**, 317 (2009).

[67] A. N. Boto et. al, Phys. Rev. Lett. **85**, 2733 (2000); P. Kok, H. Lee, and J. P. Dowling, Phys. Rev. A **65**, 052104 (2002).

[68] W. K. Wootters, Phys. Rev. Lett. **80**, 2245 (1998).

[69] K. Życzkowski, P. Horodecki, A. Sanpera, and M. Lewenstein, Phys. Rev. A **58**, 883 (1998).

[70] R. Simon, Phys. Rev. Lett. **84**, 2726 (2000).

[71] G. Adesso, A. Serafini, and F. Illuminati, Phys. Rev. A **72**, 032334 (2005).

[72] L. -M. Duan, G. Giedke, J. I. Cirac, and P. Zoller, Phys. Rev. Lett. **84**, 2722 (2000).

[73] A. Peres, Phys. Rev. A **54**, 2685 (1996). A. Peres, Phys. Rev. Lett. **77**, 1413 (1996).

[74] M. Horodecki, P. Horodecki, and R. Horodecki, Phys. Lett. A **223**, 1 (1996).

[75] B. M. Terhal, Phys. Lett. A **271**, 319 (2000).

[76] S. Hill and W. K. Wootters, Phys. Rev. Lett. **78**, 5022 (1997).

[77] S. P. Walborn *et. al.*, *Nature* **440**, 1022 (2006).

[78] G. Vidal and R. F. Werner, Phys. Rev. A **65**, 032314 (2002).

[79] S. L. Braunstein and P. van Loock, Rev. Mod. Phys. **77**, 513 (2005).

[80] P. Horodecki, Phys. Lett. A **232**, 333 (1997).

[81] R. Simon, E. C. G. Sudarshan, and N. Mukunda, Phys. Rev. A **36**, 3868 (1987).

[82] R. Simon, N. Mukunda, and B. Dutta, Phys. Rev. A **49**, 1567 (1994).

[83] W. H. Zurek, Phys. Rev. D **26**, 1862 (1982).

[84] H. D. Zeh, Found. Phys. **1**, 69 (1970).

[85] E. Joos and H. D. Zeh, Z. Phys. B **59**, 223 (1985).

[86] E. Joos, H. D. Zeh, C. Kiefer, D. Giulini, J. Kupsch, I.-O. Stamatescu, *Decoherence and the Appearance of a Classical World in Quantum Theory* (Springer, Berlin, 2003).

[87] W. H. Zurek, Physics Today, 36 Oct. (1991); W. H. Zurek, Rev. Mod. Phys. **75**, 715 (2003).

[88] A. K. Rajagopal, and R. W. Rendell, Phys. Rev. A **63**, 022116 (2001).

[89] L. Diosi, in *Irreversible Quantum Dynamics*, F. Benatti, R. Floreanini, Eds , Springer, New York, (2003).

[90] S. Daffer, K. Wodkiewicz, and J. K. Mclver, Phys. Rev. A **67**, 062312 (2003).

[91] P. J. Dodd, and J. J. Halliwell, Phys. Rev. A **69**, 052105 (2004).

[92] T. Yu, and J. H. Eberly, Phys. Rev. Lett. **93**, 140404 (2004);

[93] F. Mintert, A. R. R. Carvalho, M. Kus, and A. Buchleitner, Phys. Rep. **415**, 207 (2005).

[94] T. Yu, and J. H. Eberly, Phys. Rev. Lett. **97**, 140403 (2006); J. H. Eberly, and T. Yu, *Science* **316**, 579 (2007); T. Yu, and J. H. Eberly *Science* **323**, 598 (2009).

[95] M. P. Almeida *et. al.*, *Science* **316**, 579 (2007).

[96] J. Laurat, *et. al.* Phys. Rev. Lett. **99**, 180504 (2007).

[97] G. Gordon, and G. Kurizki, Phys. Rev. Lett. **97**, 110503 (2006); G. Gordon, Euro. Phys. Lett. **83**, 30009 (2008).

[98] R. Tahira *et. al.*, J. Phys. B **41**, 205501 (2008).

[99] Mahmoud Abdel-Aty, and T. Yu, J. Phys. B. **41**, 235503 (2009).

[100] L. Mazzola *et. al.*, Phys. Rev. A **79**, 042302 (2009).

[101] Thomas Zell *et. al.* Phys. Rev. Lett. **102**, 160501 (2009).

[102] R. Loudon, *Quantum Theory of Light*, 2nd Ed. (Oxford University Press, Oxford 1983).

[103] M. O. Scully and M. S. Zubairy, *Quantum Optics* (Cambridge, New York 1997).

[104] D. F. Walls and G. J. Milburn, *Quantum Optics* 2nd Ed. (Springer New York 2008)

[105] G. S. Agarwal, *Quantum Statistical Theories of Spontaneous Emission and their Relation to other Approaches*, Springer Tracts in Modern Physics, **70** (Springer, New York 1974).

[106] Z. Ficek and S. Swain, *Quantum Interference and Coherence* (Springer New York 2005).

[107] G. S. Agarwal , Phys. Rev. Lett. **84**, 5500 (2000).

[108] A. Rahmani, Patrick C. Chaumet, and Frédérique de Fornel , Phys. Rev. A **63**, 023819 (2001).

[109] M. Kiffner, J. Evers, and C. H. Keitel , Phys. Rev. Lett. **96**, 100403 (2006); M. Kiffner, J. Evers, and C. H. Keitel , Phys. Rev. A **73**, 063814 (2006).

[110] U. Eichmann, J. C. Bergquist, J. J. Bollinger, J. M. Gilligan, W. M. Itano, D. J. Wineland, and M. G. Raizen, Phys. Rev. Lett. **70**, 2359 (1993).

[111] U. Dorner and P. Zoller, Phy. Rev. A **66**, 023816 (2002); Franois Dubin, Daniel Rotter, Manas Mukherjee, Carlos Russo, J*ü*rgen Eschner, and Rainer Blatt, Phys. Rev. Lett. **98**, 183003 (2007).

[112] Z. Ficek and S. Swain , J. Mod. Opt **49**, 3 (2002)

[113] M. Macovei and C. H. Keitel , Phys. Rev. Lett. **91**, 123601 (2003); J*ö*rg Evers and Christoph H. Keitel , Phys. Rev. Lett. **89**, 163601 (2002); C. H. Keitel , Phys. Rev. Lett. **83**, 1307 (1999).

[114] E. Paspalakis and P. L. Knight , Phys. Rev. A **63**, 065802 (2001); E. Paspalakis, N. J. Kylstra, and P. L. Knight , Phys. Rev. Lett. **82**, 2079 (1999).

[115] Z. Ficek and S. Swain , Phys. Rev. A **69**, 023401 (2004); P. Zhou and S. Swain , Phys. Rev. Lett. **77**, 3995 (1996).

[116] G. S. Agarwal and Anil. K. Patnaik , Phys. Rev. A **63**, 043805 (2001); S. Menon and G. S. Agarwal , Phys. Rev. A **57**, 4014 (1998).

[117] K. T. Kapale, M. O. Scully, S. Zhu, and M. S. Zubairy, Phys. Rev. A **67**, 023804 (2003); O. Kocharovskaya, A. B. Matsko, and Y.Rostovtsev, Phys. Rev. A **65**, 013803 (2002); J. Javanainen, Europhys. Lett. **17**, 407 (1992).

[118] Recent works : Marlan O. Scully *et. al* Phys. Rev. Lett. **96**, 010501 (2006); M. O. Scully, Laser Physics **17** 635 (2007); A. Svidzinsky, *et. al* Phys. Rev. Lett. **100**, 160504 (2008); examine the role of VIC in the context of the Dicke problem.

[119] It may be noticed that other terms like spontaneously generated coherence, vacuum induced quantum interferences have been used in the literature.

[120] U. Dorner and P. Zoller, Phy. Rev. A **66**, 023816 (2002); Franois Dubin, Daniel Rotter, Manas Mukherjee, Carlos Russo, J*ü*rgen Eschner, and Rainer Blatt,

Phys. Rev. Lett. **98**, 183003 (2007). Following the earlier theoretical work of Dorner and Zoller this experiment examine photon correlation effects in presence of a mirror whereas we are specifically studying the effects of VIC in the emission in free space.

[121] T. Chanelire, D. N. Matsukevich, S. D. Jenkins, S.-Y. Lan, R. Zhao, T. A. Kennedy, and A. Kuzmich, Phys. Rev. Lett. **98**, 113602 (2007).

[122] P. Maunz, D. L. Moehring, S. Olmschenk, K. C. Younge, D. N. Matsukevich, C. Monroe, *Nature Physics* **3**, 538-541 (2007).

[123] H. J. Kimble , M. Dagenais , L. Mandel , Phys. Rev. Lett. **39**, 691 (1977); F. Diedrich and H. Walther, Phys. Rev. Lett. **58**, 203 (1987).

[124] C. Thiel, T. Bastin, J. Martin, E. Solano, J. von Zanthier, and G. S. Agarwal , Phys. Rev. Lett. **99**, 133603 (2007)

[125] Ref [106], pg. 39-40.

[126] M. Lax , Phys. Rev. **172**, 350 (1968).

[127] G. S. Agarwal, Phys. Rev. A **15**, 814 (1977).

[128] H. J. Carmichael and D. F. Walls, J. Phys B. **9**, L43 (1976).

[129] B. R. Mollow, Phys. Rev. A **188**, 1969 (1969)

[130] S. Menon and G. S. Agarwal , (LASER PHYSICS **9** (4), 813-818 (1999)) show how a nondegenerate four level system can produce modulated response due to VIC.

[131] R. H. Dicke , Phys. Rev. **93**, 99 (1954); J. H. Eberly and N. E. Rehler , Phys. Rev. A **2**, 1607 (1970); R. H. Lehmberg , Phys. Rev. A **2**, 889 (1970); M. Macovei *et. al.* Phys. Rev. Lett. **91**, 233601 (2003); ibid **98**, 043602 (2003).

[132] R. Tanas and Z. Ficek , J. Opt. B **6**, S90 (2004); Z. Ficek and S. Swain , J. Mod. Opt **49**, 3 (2002); J. von. Zanthier *et. al.* Phys. Rev. A **74**, 061802(R) (2006).

[133] Gert Schedelbeck, *et. al. Science* **278**, 1792 (1997); M. Bayer *et. al. Science* **291**, 451 (2001); H. J. Krenner, *et. al.* Phys. Rev. Lett. **94**, 057402 (2005).

[134] David P. DiVincenzo , *Science* **270**, 255 (1995); Xiaoqin Li, *et. al. Science* **301**, 809 (2003).

[135] J. R. Petta, *et. al. Science* **309**, 2180 (2005).

[136] M. Kiffner *et. al.* Phys. Rev. Lett. **96**, 100403 (2006); Yaping Yang *et. al.* Phys. Rev. Lett. **100**, 043601 (2008).

[137] Z. Ficek and B. C. Sanders, Phys. Rev. A **41**, 359 (1990); T. G. Rudolp, Z. Ficek and B. J. Dalton, Phys. Rev. A **52**, 636 (1995).

[138] G. V. Varada and G. S. Agarwal , Phys. Rev. A **45**, 6721 (1992); J. R. R. Leite and C. B. de Araujo, Chem. Phys. Lett. **73**, 71 (1980); C. Hettich *et. al. Science* **298**, 385 (2002); M. Orrit, *Science* **298**, 369 (2002)

[139] S. E. Harris , Phys. Rev. Lett. **62**, 1033 (1989).

[140] C. A. Kocher and E. D. Commins, Phys. Rev. Lett **18**, 575 (1967).

[141] H. Huang and J. H. Eberly, J. Mod. Opt **40**, 915 (1993).

[142] A. Muthukrishnan, G. S. Agarwal, and M. O. Scully, Phys. Rev. Lett. **93**, 093002 (2004).

[143] R. J. Young, *et. al.* N. Journal. Phys **8**, 29 (2006).

[144] U. Hohenester, G. Pfanner, and M. Seliger, Phys. Rev. Lett. **99**, 047402 (2007).

[145] A. J. Hudson, *et.al.* Phys. Rev. Lett. **99**, 266802 (2007).

[146] M. Larque, I. Robert-Philip, and A. Beveratos, Phys. Rev. A **77**, 042118 (2008).

[147] B. D. Gerardot, *et. al.* Appl. Phys. Lett. **90**, 041101(2007).

[148] A. Seguin, *et. al.* Phys. Rev. Lett. **95**, 257402 (2005).

[149] J. E. Avron, *et. al.* Phys. Rev. Lett. **100**, 120501 (2008).

[150] F. Troiani, J. I. Perea, and C. Tejedor, Phys. Rev. B **74**, 235310 (2006).

[151] R. Johne, *et.al.* Phys. Rev. Lett. **100**, 240404 (2008).

[152] D. Gammon, *et. al.* Phys. Rev. Lett **76**, 3005 (1996).

[153] V. D. Kulakovskii, *et. al.* Phys. Rev. lett. **82**, 1780 (1999).

[154] D. Bouwmeester, *et. al. Nature* **390**, 575 (1997); M. Riebe, *et. al. Nature* **429**, 734 (2004); M. D. Barrett, *et. al. Nature* **429**, 737 (2004); S. Olmschenk, *et. al. Science* **323**, 486 (2009).

[155] T. Calarco *et. al.*, Phys. Rev. A **68**, 012310 (2003).

[156] R. Hanson, and G. Burkard, Phys. Rev. Lett. **98**, 050502 (2007).

[157] L. Robledo *et. al. Science* **320**, 772 (2008).

[158] K. Zyczkowski, P. Horodecki, M. Horodecki, and R. Horodecki, Phys. Rev. A **65**, 012101 (2001).

[159] M. F. Santos *et. al.* Phys. Rev. A **73**, 040305(R) (2006).

[160] P. Marek, J. Lee, and M. S. Kim, Phys. Rev. A **77**, 032302 (2008).

[161] Y.-X. Gong et al, Phys. Rev. A **78**, 042103 (2008) .

[162] D. Tolkunov, V. Privman, and P. K. Aravind, Phys. Rev. A **71**, 060308(R) (2005).

[163] C.-S. Chou, T. Yu, and B. L. Hu, Phys. Rev. E **77**, 011112 (2008).

[164] C. E. Lopez, G. Romero, F. Lastra, E. Solano, and J. C. Retamal, Phys. Rev. Lett. **101**, 080503 (2008).

[165] C. Cormick, and J. P. Paz, Phys. Rev. A **78**, 012357 (2008).

[166] C.-Y. Lai, J.-T. Hung, C.-Y. Mou, and P. Chen, Phys. Rev. B **77**, 205419 (2008).

[167] A. Abliz, H. J. Gao, X. C. Xie, Y. S. Wu, and W. M. Liu, Phys. Rev. A **74**, 052105 (2006).

[168] L. Jakóbczyk and A. Jamróz, Phys. Lett. A **318**, 318 (2003).

[169] Z. Ficek, and R. Tanas, Phys. Rev. A **74**, 024304 (2006).

[170] T. Yu, and J. H. Eberly, Opt. Commun. **264**, 393 (2006).

[171] M. Ikram, F.-L. Li, and M. S. Zubairy, Phys. Rev. A **75**, 062336 (2007).

[172] K.-L. Liu, H.-S. Goan, Phys. Rev. A **76**, 022312 (2007).

[173] A. Al-Qasimi, D. F. V. James, Phys. Rev. A **78**, 012117 (2008).

[174] T. Gorin, C. Pineda, and T. H. Seligman, Phys. Rev. Lett. **99**, 240405 (2007).

[175] C. Pineda, T. Gorin, and T. H. Seligman, New J. Phys. **9**, 106 (2007).

[176] A. Serafini *et. al.*, Phys. Rev. A **69**, 022318 (2004).

[177] S. Maniscalco, S. Olivares, and M. G. A. Paris, Phys. Rev. A **75**, 062119 (2007).

[178] J. S. Prauzner-Bechcicki, J. Phys. A **37**, L173 (2004).

[179] F. Benatti, and R. Floreanini, J. Phys. A **39**, 2689 (2006).

[180] J. P. Paz, and A. J. Roncaglia, Phys. Rev. Lett. **100**, 220401 (2008).

[181] S. Bandyopadhyay, and D. A. Lidar, Phys. Rev. A **70**, 010301 (2004).

[182] J. Li, and G. S. Paraoanu, arxiv : 0903.3464 (2009); J. Li, and G. S. Paraoanu, arxiv : 0906.0704 (2009).

[183] Z. Ficek, and R. Tanas, Phys. Rev. A **77**, 054301 (2008).

[184] Asma Al-Qasimi *et. al.*, Opt. Lett. **34**, 268 (2009).

[185] Sumanta Das, and G. S. Agarwal, J. Phys. B. FTC **42**, 141003 (2009).

[186] E. T. Jaynes, and F. W. Cummings, PROC. IEEE **51**, 89 (1963).

[187] M. Yönac, T. Yu, and J. H. Eberly, J. Phys. B. **39**, S621 (2006).

[188] M. Yönac, and J. H. Eberly, Opt. Lett **33**, 270 (2008). This paper reports such bright and dark periods in entanglement for *noninteracting* qubits driven by single mode quantized fields, which is in a way reminiscent of Jaynes-Cummings dynamics.

[189] M. Yönac, T. Yu, and J. H. Eberly, J. Phys. B. **40**, S45 (2007).

[190] Luis Roa, R. Pozo-Gonzalez, M. Schaefer, and P. Utreras-SM, Phys. Rev. A **75**, 063316 (2007).

[191] P. G. Kwait *et. al.*, *Science* **290**, 498 (2000).

[192] P. Bori *et. al.*, Phys. Rev. Lett. **87**, 157401 (2001).

[193] H. J. Krenner *et. al.*, Phys. Rev. Lett. **94**, 057402 (2005).

[194] G. J. Beirne *et. al.*, Phys. Rev. Lett. **96**, 137401 (2006).

[195] J. M. Taylor *et. al.*, Phys. Rev. B **76**, 035315 (2007).

[196] G. Schedelbeck *et. al.*, *Science* **278**, 1792 (1997).

[197] H. J. Briegel, and R. Raussendorf, Phys. Rev. Lett. **86**, 910 (2001).

[198] U. Peschel, T. Pertsch, and F. Lederer, Opt. Lett. **23**, 1701 (1998).

[199] T. Pertsch, P. Dannberg, W. Elflein, A. Brauer, and F. Lederer, Phys. Rev. Lett. **83**, 4752 (1999).

[200] R. Morandotti, U. Peschel, J. S. Aitchison, H. S. Eisenberg, and Y. Silberberg, Phys. Rev. Lett. **83**, 4756 (1999).

[201] S. Longhi, Phys. Rev. A **79**, 023811 (2009).

[202] S. Longhi, Laser Photonics Rev. **3**, 243 (2009).

[203] H. B. Perets, Y. Lahini, F. Pozzi, M. Sorel, R. Morandotti, and Y. Silberberg, Phys. Rev. Lett. **100**, 170506 (2008).

[204] Y. Bromberg, Y. Lahini, R. Morandotti, and Y. Silberberg, Phys. Rev. Lett. **102**, 253904 (2009).

[205] A. Rai, G. S. Agarwal, and J. H. H. Perk, Phys. Rev. A **78**, 042304 (2008).

[206] S. Longhi, Phys. Rev. B **79**, 245108 (2009).

[207] A. Politi, J. C. F. Matthews, and J. L. O'Brien, Science **325**, 1221 (2009).

[208] B. E. A. Saleh, and M. C. Teich, *Fundamentals of Photonics, 2nd Edition* (Wiley, New York 2007), p. 319.

[209] D. Marcuse, Bell System Tech. J. **50**, 1791 (1971); 1817 (1971).

[210] W. K. Lai, V. Bužek, and P. L. Knight, Phys. Rev. A **43**, 6323 (1991).

[211] R. Iwanow, R. Schiek, G. I. Stegeman, T. Pertsch, F. Lederer, Y. Min, and W. Sohler, Phys. Rev. Lett. **93**, 113902 (2004).

[212] U. Peschel et. al, J. Opt. Soc. Am. B **19**, 2637 (2002).

[213] K. B. Mogensen, F. Eriksson, O. Gustafsson, R. P. H. Nikolajsen, and J. P. Kutter, Electrophoresis **25**, 3788 (2004).

[214] P. J. Dodd and J. J. Halliwell, Phys. Rev. A **69**, 052105 (2004).

[215] D. Vitali et. al, Phys. Rev. Lett. **98**, 030405 (2007).

[216] M. B. Plenio, J. Hartley, and J. Eisert, New Journal of Physics **6**, 36 (2004).

[217] G. S. Agarwal, Phys. Rev. A **3**, 828 (1971).

[218] S.M. Barnett and P. Radmore, Methods in Theoretical Quantum Optics (Oxford University Press, 2002) p.168.

[219] Sumanta Das, and G. S. Agarwal, J. Phys. B. **42**, 205502 (2009).

[220] S. Longhi, Phys. Rev. A **78**, 013815 (2008).

[221] S. John, and T. Quang, Phys. Rev. A **50**, 1764 (1994).

[222] T. Quang, S. John, and G. S. Agarwal, Phys. Rev. Lett. **79**, 5238 (1997).

APPENDIX A

EVALUATION OF THE DICKE EMISSION SPECTRUM

The density matrix equations for the two atom system in the bare state basis :

$$
\begin{aligned}
\dot{\rho}_{11} &= -4\gamma\rho_{11} - ig_1\rho_{31} + ig_1^*\rho_{13} - ig_2\rho_{21} + ig_2^*\rho_{12} \\
\dot{\rho}_{22} &= -2\gamma(\rho_{22} - \rho_{11}) - ig_1\rho_{42} + ig_1^*\rho_{24} + ig_2\rho_{21} - ig_2^*\rho_{12} \\
&\quad -(\gamma_{12} + i\Omega_{12})\rho_{32} - (\gamma_{12} - i\Omega_{12})\rho_{23} \\
\dot{\rho}_{33} &= -2\gamma(\rho_{33} - \rho_{11} + -ig_1\rho_{31} - ig_1^*\rho_{13} - ig_2\rho_{43} + ig_2^*\rho_{34} \\
&\quad -(\gamma_{12} + i\Omega_{12})\rho_{23} - (\gamma_{12} - i\Omega_{12})\rho_{32} \\
\dot{\rho}_{12} &= -3\gamma\rho_{12} - ig_1\rho_{32} + ig_1^*\rho_{14} + ig_2(\rho_{11} - \rho_{22}) - (\gamma_{12} - i\Omega_{12})\rho_{13} \\
\dot{\rho}_{13} &= -3\gamma\rho_{13} - ig_2\rho_{23} + ig_2^*\rho_{14} + ig_1(\rho_{11} - \rho_{33}) - (\gamma_{12} - i\Omega_{12})\rho_{12} \\
\dot{\rho}_{14} &= -2\gamma\rho_{14} - ig_1\rho_{34} + ig_1\rho_{12} - ig_2\rho_{24} + ig_2\rho_{13} \\
\dot{\rho}_{23} &= -\gamma\rho_{23} + 2\gamma_{12}\rho_{11} + ig_1\rho_{21} - ig_2^*\rho_{13} + ig_2^{ast}\rho_{24} - ig_1\rho_{43} \\
&\quad -(\gamma_{12} + i\Omega_{12})\rho_{33} - (\gamma_{12} - i\Omega_{12})\rho_{22} \\
\dot{\rho}_{24} &= -\gamma\rho_{24} + 2\gamma\rho_{13} + 2\gamma_{12}\rho_{12} + ig_2\rho_{23} - ig_2^*\rho_{14} + ig_1(2\rho_{22} + \rho_{11} + \rho_{33}) \\
&\quad -(\gamma_{12} + i\Omega_{12})\rho_{34} + ig_1^* \\
\dot{\rho}_{34} &= -\gamma\rho_{34} + 2\gamma\rho_{21} + 2\gamma_{12}\rho_{31} + ig_1\rho_{32} - ig_1^*\rho_{14} + ig_2(2\rho_{33} + \rho_{11} + \rho_{22}) \\
&\quad -(\gamma_{12} - i\Omega_{12})\rho_{24} - ig_2 \\
\mathsf{Tr}\rho &= 1, \quad \rho_{ij}^* = \rho_{ji}
\end{aligned}
\tag{A.1}
$$

where we have $g_1 = Ge^{i\vec{k}\cdot\vec{r}_1}$ and $g_2 = Ge^{i\vec{k}\cdot\vec{r}_2}$ In a compact matrix form these equations can be written as

$$\dot{\Psi}(t) = \mathcal{M}\Psi + \mathcal{I} \tag{A.2}$$

where Ψ and $\mathcal{I}$ are a 15×1 column vector and $\mathcal{M}$ is a 15×15 square matrix. Taking the laplace transform of equation (A.2) one then gets,

$$\Psi(z) = (z-\mathcal{M})^{-1}\Psi(0) + z^{-1}(z-\mathcal{M})^{-1})\mathcal{I} \tag{A.3}$$

Using equation (A.3) and the quantum regression theorem one can then calculate the incoherent emission spectrum. As an example let me show how one can calculate say the term $\int_0^\infty d\tau e^{-z\tau}\langle S_1^+(t+\tau)S_2^-(t)\rangle$. To do this first we will evaluate $\langle S_1^+(z)\rangle$.

$$\begin{aligned}
\langle S_1^+(z)\rangle &= \int_0^\infty dt e^{-zt}\langle S_1^+(t)\rangle \\
&= \int_0^\infty dt e^{-zt}\mathsf{Tr}(\rho S_1^+) \\
&= \int_0^\infty dt e^{-zt}[\rho_{31}(t)+\rho_{42}(t)] \\
&= \int_0^\infty dt e^{-zt}[\Psi_7(t)+\Psi_{13}(t)] \\
&= \Psi_7(z)+\Psi_{13}(z)
\end{aligned} \tag{A.4}$$

Then on using equation (A.3) in (A.4)we get,

$$\begin{aligned}
\langle S_1^+(z)\rangle &= \sum_{j=1}^{15}[(z-\mathcal{M})_7^{-1} + (z-\mathcal{M})_{13}^{-1}]_j\Psi_j(0) \\
&\quad + z^{-1}\sum_{j=1}^{15}[(z-\mathcal{M})_7^{-1} + (z-\mathcal{M})_{13}^{-1}]_j\mathcal{I}_j
\end{aligned} \tag{A.5}$$

Then using equation (A.5) and the quantum regression theorem we have

$$\begin{aligned}
\int_0^\infty d\tau e^{-z\tau}\langle S_1^+(t+\tau)S_2^-(t)\rangle &= \langle S_1^+(z)S_2^-(0)\rangle \\
&= \sum_{j=1}^{15}[(z-\mathcal{M})_7^{-1} + (z-\mathcal{M})_{13}^{-1}]_j\langle\Psi_j(0)S_2^-(0)\rangle \\
&+ z^{-1}\sum_{j=1}^{15}[(z-\mathcal{M})_7^{-1} + (z-\mathcal{M})_{13}^{-1}]_j\langle S_2^-(0)\rangle
\end{aligned} \tag{A.6}$$

Now one can calculate the quantities $\langle\Psi_j(0)S_2^-(0)\rangle$ and $\langle S_2^-(0)\rangle$ using the definition $\langle A\rangle = \mathsf{Tr}(\rho A)$ and the steady state solution of equation (A.3) which is given by $\Psi(\infty) = \lim_{z\to\infty} z\Psi(z) = -\mathcal{M}^{-1}\mathcal{I}$.

The density matrix equations in the Dicke symmetric and anti-symmetric state basis :

$$\begin{aligned}
\dot{\rho}_{ss} &= -2[\gamma + \gamma_{12}\cos(\phi)]\rho_{ss} - i\sin(\phi)[\gamma_{12} + i\Omega_{12}]\rho_{as} + i\sin(\phi)[\gamma_{12} - i\Omega_{12}]\rho_{sa} \\
\dot{\rho}_{aa} &= -2[\gamma - \gamma_{12}\cos(\phi)]\rho_{aa} - i\sin(\phi)[\gamma_{12} - i\Omega_{12}]\rho_{as} + i\sin(\phi)[\gamma_{12} + i\Omega_{12}]\rho_{sa} \\
\dot{\rho}_{gg} &= 2[\gamma + \gamma_{12}\cos(\phi)]\rho_{ss} + 2[\gamma - \gamma_{12}\cos(\phi)]\rho_{aa} + 2i\gamma_{12}\sin(\phi)[\rho_{as} - \rho_{sa}] \\
\dot{\rho}_{as} &= -2[\gamma - i\Omega_{12}\cos(\phi)]\rho_{as} + i\gamma_{12}\sin(\phi)[\rho_{ss} + \rho_{aa}] - \sin(\phi)\Omega_{12}[\rho_{ss} - \rho_{aa}] \\
\dot{\rho}_{sg} &= -[\gamma + \gamma_{12}\cos(\phi) + i\Omega_{12}\cos(\phi)]\rho_{sg} - i\sin(\phi)[\gamma_{12} + i\Omega_{12}]\rho_{ag} \\
\dot{\rho}_{ag} &= -[\gamma - \gamma_{12}\cos(\phi) - i\Omega_{12}\cos(\phi)]\rho_{ag} + i\sin(\phi)[\gamma_{12} + i\Omega_{12}]\rho_{sg}
\end{aligned} \tag{A.7}$$

and the remaining equations can be written using $\rho^*_{ij} = \rho_{ji}$

APPENDIX B

CALCULATION OF TRANSITION AMPLITUDE BETWEEN THE SYMMETRIC AND ANTI-SYMMETRIC STATE

This appendix gives the explicit derivation of the transition amplitude between the symmetric and antisymmetric Dicke states as discussed in chapter 3 equation (3.11)

If the initial state is $|s\rangle$; what is the probability that final state is $|a\rangle$?

$$H_I = -\vec{d}\cdot\vec{E} = -\vec{d}(S_1^{\dagger}e^{i\omega t} + S_1^{-}e^{-i\omega t})\cdot\vec{E}(\vec{r}_1,t) - \vec{d}(S_2^{\dagger}e^{i\omega t} + S_2^{-}e^{-i\omega t})\cdot\vec{E}(\vec{r}_2,t) \quad \text{(B.1)}$$

$$E(\vec{r},t) = i\sum(\frac{2\pi ck}{L^3})^{1/2}a_{\vec{k}s}\varepsilon_{\vec{k}s}e^{i\vec{k}\cdot\vec{r}-i\omega_{ks}t} - i\sum(\frac{2\pi ck}{L^3})^{1/2}a_{\vec{k}s}^{\dagger}\varepsilon_{\vec{k}s}^{*}e^{-i\vec{k}\cdot\vec{r}+i\omega_{ks}t} \quad \text{(B.2)}$$

Schrodinger equation

$$\dot{\psi} = -\frac{i}{\hbar}H_I(t)\psi \quad \text{(B.3)}$$

$$\psi(t) = \psi(0) - \frac{i}{\hbar}\int_0^t H_I(t)\psi(0)dt_1 - \frac{1}{\hbar^2}\int_0^t H_I(t_1)\int_0^{t_1} H_I(t_2)\psi(0)dt_2dt_1 \quad \text{(B.4)}$$

$$\begin{aligned} H_I(t) = {} & g_{ks}^{(1)}(S_1^{\dagger}e^{i\omega t} + S_1^{-}e^{-i\omega t})a_{ks}e^{-i\omega_{ks}t} + g_{ks}^{*(1)}(S_1^{\dagger}e^{i\omega t} + S_1^{-}e^{-i\omega t})a_{ks}^{\dagger}e^{i\omega_{ks}t} \\ & + g_{ks}^{(2)}(S_2^{\dagger}e^{i\omega t} + S_2^{-}e^{-i\omega t})a_{ks}e^{-i\omega_{ks}t} + g_{ks}^{*(2)}(S_2^{\dagger}e^{i\omega t} + S_2^{-}e^{-i\omega t})a_{ks}^{\dagger}e^{i\omega_{ks}t} \end{aligned} \quad \text{(B.5)}$$

$$g_{ks}^{(i)} = -i(\frac{2\pi ck}{L^3})^{1/2}(-\vec{d}\cdot\vec{\varepsilon}_{\vec{k}s})e^{i\vec{k}\cdot\vec{r}_i} \quad \text{(B.6)}$$

On short

$$H_I = g_{\vec{k}s}^{(i)}[a_{\vec{k}s}(S_i^{\dagger}e^{i\omega t} + S_i^{-}e^{-i\omega t})] + H.C. \quad \text{(B.7)}$$

$$|s\rangle = e^{i\vec{k}_l\cdot\vec{r}_1}|e_1g_2\rangle + e^{i\vec{k}_l\cdot\vec{r}_2}|g_1e_2\rangle \quad \text{(B.8)}$$

$$|a\rangle = e^{i\vec{k}_l\cdot\vec{r}_1}|e_1g_2\rangle - e^{i\vec{k}_l\cdot\vec{r}_2}|g_1e_2\rangle \quad \text{(B.9)}$$

$$\begin{aligned}\langle\{0\},a|H_I|s,\{0\}\rangle &= \langle\{0\},a|g^{(i)}_{\vec{k}s}[a_{\vec{k}s}(S_i^\dagger e^{i\omega t}+S_i^- e^{-i\omega t})]e^{-i\omega_{ks}t}\\ &+g^{*(i)}_{\vec{k}s}[(S_i^\dagger e^{i\omega t}+S_i^- e^{-i\omega t})]a^\dagger_{\vec{k}s}e^{i\omega_{ks}t}|s,\{0\}\rangle\\ &= \langle\{0\},a|g^{(i)}_{\vec{k}s}[a_{\vec{k}s}(S_i^\dagger e^{i\omega t}+S_i^- e^{-i\omega t})]e^{-i\omega_{ks}t}|s,\{0\}\rangle\\ &+\langle\{0\},a|g^{*(i)}_{\vec{k}s}[(S_i^\dagger e^{i\omega t}+S_i^- e^{-i\omega t})]a^\dagger_{\vec{k}s}e^{i\omega_{ks}t}|s,\{0\}\rangle\end{aligned} \tag{B.10}$$

$$\langle\{0\},a|H_I|s,\{0\}\rangle = 0 \tag{B.11}$$

$$\psi_0 = \langle a|s\rangle_0 = 0 \tag{B.12}$$

Hence we are left with the second order perturbation term.

$$\begin{aligned}\langle a|s\rangle_t &= -\frac{1}{\hbar^2}\int_0^t\int_0^{t_1}\langle a|H_I(t_1)H_I(t_2)|s\rangle dt_2dt_1\\ &= -\frac{1}{\hbar^2}\int_0^t\int_0^{t_1}\langle\{0\},a|H_I(t_1)H_I(t_2)|s,\{0\}\rangle dt_2dt_1\end{aligned} \tag{B.13}$$

$$H_I(t_1) = \sum_{jks} g_{jks}a_{ks}(S_j^\dagger e^{i\omega t_1}+S_j^- e^{-i\omega t_1})e^{-i\omega_{ks}t_1}+H.C. \tag{B.14}$$

$$H_I(t_2) = \sum_{lks} g_{lks}a_{ks}(S_l^\dagger e^{i\omega t_2}+S_l^- e^{-i\omega t_2})e^{-i\omega_{ks}t_2}+H.C. \tag{B.15}$$

$$\begin{aligned}H_I(t_1)H_I(t_2) = \sum_{ljks}[&g_{jks}a_{ks}(S_j^\dagger e^{i\omega t_1}+S_j^- e^{-i\omega t_1})e^{-i\omega_{ks}t_1}\\ &+g^*_{jks}(S_j^\dagger e^{i\omega t_1}+S_j^- e^{-i\omega t_1})a^\dagger_{ks}e^{i\omega_{ks}t_1}]\\ &\times[g_{lks}a_{ks}(S_l^\dagger e^{i\omega t_2}+S_l^- e^{-i\omega t_2})e^{-i\omega_{ks}t_2}\\ &+g^*_{lks}(S_l^\dagger e^{i\omega t_2}+S_l^- e^{-i\omega t_2})a^\dagger_{ks}e^{i\omega_{ks}t_2}]\end{aligned} \tag{B.16}$$

Using RWA

$$\begin{aligned}\langle\{0\},a|H_I(t_1)H_I(t_2)|s,\{0\}\rangle &= \sum_{ljks} g_{jks}g^*_{lks}e^{-i\omega_{ks}(t_1-t_2)}\\ &\times\langle a|(S_j^\dagger e^{i\omega t_1}+S_j^- e^{-i\omega t_1})(S_l^\dagger e^{i\omega t_2}+S_l^- e^{-i\omega t_2})|s\rangle\\ &= \sum_{ljks} g_{jks}g^*_{lks}e^{-i\omega_{ks}(t_1-t_2)}\\ &\times[\langle a|S_j^\dagger S_l^-|s\rangle e^{i\omega(t_1-t_2)}+\langle a|S_j^- S_l^\dagger|s\rangle e^{-i\omega(t_1-t_2)}]\end{aligned} \tag{B.17}$$

$$\int_0^t dt_1 \int_0^{t_1} dt_2 \langle\{0\}, a|H_I(t_1)H_I(t_2)|s, \{0\}\rangle$$

$$= \int_0^t dt_1 \int_0^{t_1} dt_2 \sum_{ljks} g_{jks} g^*_{lks} [\langle a|S_j^\dagger S_l^-|s\rangle e^{-i(\omega_{ks}-\omega)(t_1-t_2)}\rangle \tag{B.18}$$

$$+\langle a|S_j^- S_l^\dagger|s\rangle e^{-i(\omega_{ks}+\omega)(t_1-t_2)}]$$

As $t_1 \to t$; $t_2 \to t-\tau$,

$$\frac{d}{dt}\langle a|s(t)\rangle = -\frac{1}{\hbar^2}\sum_{ljks} g_{jks} g^*_{lks} \int_0^t d\tau e^{-i(\omega_{ks}-\omega)\tau}\langle a|S_j^\dagger S_l^-|s\rangle$$

$$-\frac{1}{\hbar^2}\sum_{ljks} g_{jks} g^*_{lks} \int_0^t d\tau e^{-i(\omega_{ks}+\omega)\tau}\langle a|S_l^\dagger S_j^-|s\rangle$$

$$= -\frac{1}{\hbar^2}\{\sum_{ljks} g_{jks} g^*_{lks} \lim_{t\to\infty}\int_0^t d\tau e^{-i(\omega_{ks}-\omega)\tau}\langle a|S_j^\dagger S_l^-|s\rangle$$

$$+\sum_{ljks} g_{jks} g^*_{lks} \lim_{t\to\infty}\int_0^t d\tau e^{-i(\omega_{ks}+\omega)\tau}\langle a|S_l^\dagger S_j^-|s\rangle\}$$

$$= -\frac{1}{\hbar^2}\sum_{ljks} g_{jks} g^*_{lks} \lim_{t\to\infty}\{\int_0^\infty d\tau e^{-\epsilon\tau} e^{-i(\omega_{ks}-\omega)\tau}\langle a|S_j^\dagger S_l^-|s\rangle \tag{B.19}$$

$$+\int_0^\infty d\tau e^{-\epsilon\tau} e^{-i(\omega_{ks}+\omega)\tau}\langle a|S_l^\dagger S_j^-|s\rangle\}$$

$$= -\frac{1}{\hbar^2}\sum_{ljks} g_{jks} g^*_{lks}\{\lim_{\epsilon\to 0}\frac{1}{\epsilon + i(\omega_{ks}-\omega)}\langle a|S_j^\dagger S_l^-|s\rangle$$

$$+\lim_{\epsilon\to 0}\frac{1}{\epsilon + i(\omega_{ks}+\omega)}\langle a|S_l^\dagger S_j^-|s\rangle\}$$

$$= -\frac{1}{\hbar^2}\sum_{ljks} g_{jks} g^*_{lks}\{\lim_{\epsilon\to 0}\frac{\epsilon - i(\omega_{ks}-\omega)}{\epsilon^2 + (\omega_{ks}-\omega)^2}\langle a|S_j^\dagger S_l^-|s\rangle$$

$$+\lim_{\epsilon\to 0}\frac{\epsilon - i(\omega_{ks}+\omega)}{\epsilon^2 + (\omega_{ks}+\omega)^2}\langle a|S_l^\dagger S_j^-|s\rangle\}$$

a,s; l,j are dummy indices, we can write

$$
\begin{aligned}
&= -\frac{1}{\hbar^2}\sum_{ij} g_{ks}g_{ks}^{*}\{\lim_{\epsilon\to 0}(\frac{\epsilon}{\epsilon^2+(\omega_{ks}-\omega)^2}+\frac{\epsilon}{\epsilon^2+(\omega_{ks}+\omega)^2}) \\
&\quad +\lim_{\epsilon\to 0}(\frac{i(\omega-\omega_{ks})}{\epsilon^2+(\omega_{ks}-\omega)^2}-\frac{i(\omega+\omega_{ks})}{\epsilon^2+(\omega_{ks}+\omega)^2})\}\langle a|S_i^{\dagger}S_j^{-}|s\rangle \\
&= -\frac{1}{\hbar^2}\sum_{i\neq j}(\gamma_{ij}+i\Omega_{ij})\langle a|S_i^{\dagger}S_j^{-}|s\rangle \\
&= -\frac{1}{\hbar^2}\{(\gamma_{12}+i\Omega_{12})\langle a|S_1^{\dagger}S_2^{-}|s\rangle+(\gamma_{12}+i\Omega_{12})\langle a|S_2^{\dagger}S_1^{-}|s\rangle\}
\end{aligned}
\tag{B.20}
$$

$$
\begin{aligned}
\frac{d}{dt}\langle a|s(t)\rangle &= -\frac{1}{\hbar^2}(\gamma_{12}+i\Omega_{12})(\langle a|S_1^{\dagger}S_2^{-}|s\rangle+\langle a|S_2^{\dagger}S_1^{-}|s\rangle) \\
&= -\frac{1}{\hbar^2}(\gamma_{12}+i\Omega_{12})(\frac{e^{-i\vec{k}_l\cdot(\vec{r}_1-\vec{r}_2)}-e^{i\vec{k}_l\cdot(\vec{r}_1-\vec{r}_2)}}{2}) \\
&= \frac{i}{\hbar^2}\sin(2\phi)(\gamma_{12}+i\Omega_{12})
\end{aligned}
\tag{B.21}
$$

APPENDIX C

DYNAMICAL EVOLUTION OF TWO INTERACTING QUBITS IN DISSIPATIVE ENVIRONMENT

The solutions correspond to the initial matrix ρ defined in equation (5.9)

$$
\begin{aligned}
\rho_{11}(t) &= \rho_{11}(0)e^{-2\gamma t}, \\
\rho_{22}(t) &= \frac{1}{2}\rho_{22}(0)e^{-\gamma t}(1+\cos(2vt)) + \frac{1}{2}\rho_{33}(0)e^{-\gamma t}(1-\cos(2vt)) \\
&+ \rho_{11}(0)e^{-2\gamma t}(e^{\gamma t}-1) - \frac{i}{2}(\rho_{32}(0)-\rho_{23}(0))e^{-\gamma t}\sin(2vt) \\
\rho_{33}(t) &= \frac{1}{2}\rho_{22}(0)e^{-\gamma t}(1-\cos(2vt)) + \frac{1}{2}\rho_{33}(0)e^{-\gamma t}(1+\cos(2vt)) \\
&+ \rho_{11}(0)e^{-2\gamma t}(e^{\gamma t}-1) + \frac{i}{2}(\rho_{32}(0)-\rho_{23}(0))e^{-\gamma t}\sin(2vt) \\
\rho_{12}(t) &= \rho_{12}(0)e^{-3\gamma t/2}\cos(vt) + i\rho_{13}(0)e^{-3\gamma t/2}\sin(vt) \\
\rho_{13}(t) &= \rho_{13}(0)e^{-3\gamma t/2}\cos(vt) + i\rho_{12}(0)e^{-3\gamma t/2}\sin(vt) \\
\rho_{14}(t) &= \rho_{14}(0)e^{-\gamma t} \\
\rho_{23}(t) &= \frac{i}{2}(\rho_{22}(0)-\rho_{33}(0))\sin(2vt)e^{-\gamma t} + \frac{1}{2}\rho_{23}(0)e^{-\gamma t}(1+\cos(2vt)) \\
&+ \frac{1}{2}\rho_{32}(0)e^{-\gamma t}(1-\cos(2vt))
\end{aligned}
$$

$$
\begin{aligned}
\rho_{24}(t) &= \rho_{24}(0)e^{-\gamma t/2}\cos(vt) - i\rho_{34}(0)e^{-\gamma t/2}\sin(vt) - \rho_{12}(0)\left(\frac{1}{v^2+(9/4)\gamma^2}\right)[2ive^{-2\gamma t} \\
&+ e^{-\gamma t/2}\{2v\cos(vt) - 3i\gamma\sin(vt)\}] - \rho_{13}(0)\left(\frac{1}{v^2+(9/4)\gamma^2}\right)[3\gamma e^{-2\gamma t} \\
&- e^{-\gamma t/2}\{2v\sin(vt) + 3\gamma\cos(vt)\}]
\end{aligned}
$$

$$
\begin{aligned}
\rho_{34}(t) &= \rho_{34}(0)e^{-\gamma t/2}\cos(vt) - i\rho_{24}(0)e^{-\gamma t/2}\sin(vt) \\
&- \rho_{12}(0)\left(\frac{1}{v^2+(9/4)\gamma^2}\right)[3\gamma e^{-2\gamma t} - e^{-\gamma t/2}\{2v\sin(vt) + 3\gamma\cos(vt)\}]
\end{aligned}
$$

$$- \quad \rho_{13}(0)\left(\frac{1}{v^2+(9/4)\gamma^2}\right)[2ive^{-2\gamma t}+e^{-\gamma t/2}\{2v\cos(vt)-3i\gamma\sin(vt)\}] \tag{C.1}$$

and $\rho_{32}(t)=\rho_{23}^*(t), \rho_{21}(t)=\rho_{12}^*(t), \rho_{31}(t)=\rho_{13}^*(t), \rho_{41}(t)=\rho_{14}^*(t), \rho_{42}(t)=\rho_{24}^*(t), \rho_{43}(t)=\rho_{34}^*(t),\ \rho_{44}(t)\ =\ 1-\rho_{11}(t)-\rho_{22}(t)-\rho_{33}(t)$. Note that here we have considered $\gamma_A=\gamma_B=\gamma$.

APPENDIX D

DYNAMICAL EVOLUTION OF TWO INTERACTING QUBITS IN DEPHASING ENVIRONMENT

The solutions correspond to the initial matrix ρ defined in equation (5.9)

$$\rho_{11}(t) = \rho_{11}(0) \quad , \tag{D.1}$$

$$\begin{aligned}\rho_{22}(t) &= \frac{1}{2}\rho_{22}(0)\left[1+e^{-(\Gamma_A+\Gamma_B)t/2}\left\{\cos(2\Omega t)+\frac{(\Gamma_A+\Gamma_B)}{4\Omega}\sin(2\Omega t)\right\}\right] \\ &+ \frac{1}{2}\rho_{33}(0)\left[1-e^{-(\Gamma_A+\Gamma_B)t/2}\left\{\cos(2\Omega t)+\frac{(\Gamma_A+\Gamma_B)}{4\Omega}\sin(2\Omega t)\right\}\right] \\ &+ \frac{i[\rho_{23}(0)-\rho_{32}(0)]ve^{-(\Gamma_A+\Gamma_B)t/2}}{2\Omega}\sin(2\Omega t)\,,\end{aligned} \tag{D.2}$$

$$\begin{aligned}\rho_{33}(t) &= \frac{1}{2}\rho_{22}(0)\left[1-e^{-(\Gamma_A+\Gamma_B)t/2}\left\{\cos(2\Omega t)+\frac{(\Gamma_A+\Gamma_B)}{4\Omega}\sin(2\Omega t)\right\}\right] \\ &+ \frac{1}{2}\rho_{33}(0)\left[1+e^{-(\Gamma_A+\Gamma_B)t/2}\left\{\cos(2\Omega t)+\frac{(\Gamma_A+\Gamma_B)}{4\Omega}\sin(2\Omega t)\right\}\right] \\ &- \frac{i[\rho_{23}(0)-\rho_{32}(0)]ve^{-(\Gamma_A+\Gamma_B)t/2}}{2\Omega}\sin(2\Omega t)\,,\end{aligned} \tag{D.3}$$

$$\begin{aligned}\rho_{23}(t) &= \frac{1}{2}e^{-(\Gamma_A+\Gamma_B)t/2}[\rho_{23}(0)\{e^{-(\Gamma_A+\Gamma_B)t/2}+\cos(2\Omega t)+\frac{(\Gamma_A+\Gamma_B)}{4\Omega}\sin(2\Omega t)\} \\ &+ \rho_{32}(0)\{e^{-(\Gamma_A+\Gamma_B)t/2}-\cos(2\Omega t)-\frac{(\Gamma_A+\Gamma_B)}{4\Omega}\sin(2\Omega t)\}] \\ &+ \frac{ive^{-(\Gamma_A+\Gamma_B)t/2}}{2\Omega}\sin(2\Omega t)\,[\rho_{22}(0)-\rho_{33}(0)],\end{aligned} \tag{D.4}$$

$$\Omega = \sqrt{v^2-\left(\frac{\Gamma_A+\Gamma_B}{4}\right)^2}. \tag{D.5}$$

$$\rho_{32}(t)=\rho_{23}^*(t), \quad \rho_{44}(t)=1-\rho_{11}(t)-\rho_{22}(t)-\rho_{33}(t). \tag{D.6}$$

All other elements of the density matrix ρ defined in the two qubit product basis (5.2) remains zero for all time t.

APPENDIX E

DYNAMICAL EVOLUTION OF TWO NON-INTERACTING QUBITS IN CORRELATED DISSIPATIVE ENVIRONMENT

The solutions correspond to the initial matrix ρ defined in equation (5.9)

$$\rho_{11}(t) = \rho_{11}(0)e^{-2\gamma t} \quad ; \tag{E.1}$$

$$\begin{aligned}\rho_{22}(t) &= \frac{1}{2}\rho_{22}(0)e^{-\gamma t}(1+\cosh(\Gamma_{12}t)) - \frac{1}{2}\rho_{33}(0)e^{-\gamma t}(1-\cosh(\Gamma_{12}t)) \\ &- \rho_{11}(0)e^{-2\gamma t}\left(\frac{\gamma^2+\Gamma_{12}^2}{\gamma^2-\Gamma_{12}^2}\right) - \frac{1}{2}[\rho_{23}(0)+\rho_{32}(0)]e^{-\gamma t}\sinh(\Gamma_{12}t) \\ &+ \frac{1}{2}\rho_{11}(0)e^{-\gamma t}\left[\left(\frac{\gamma+\Gamma_{12}}{\gamma-\Gamma_{12}}\right)e^{\Gamma_{12}t} + \left(\frac{\gamma-\Gamma_{12}}{\gamma+\Gamma_{12}}\right)e^{-\Gamma_{12}t}\right];\end{aligned} \tag{E.2}$$

$$\begin{aligned}\rho_{33}(t) &= \frac{1}{2}\rho_{33}(0)e^{-\gamma t}(1+\cosh(\Gamma_{12}t)) - \frac{1}{2}\rho_{22}(0)e^{-\gamma t}(1-\cosh(\Gamma_{12}t)) \\ &- \rho_{11}(0)e^{-2\gamma t}\left(\frac{\gamma^2+\Gamma_{12}^2}{\gamma^2-\Gamma_{12}^2}\right) - \frac{1}{2}[\rho_{23}(0)+\rho_{32}(0)]e^{-\gamma t}\sinh(\Gamma_{12}t) \\ &+ \frac{1}{2}\rho_{11}(0)e^{-\gamma t}\left[\left(\frac{\gamma+\Gamma_{12}}{\gamma-\Gamma_{12}}\right)e^{\Gamma_{12}t} + \left(\frac{\gamma-\Gamma_{12}}{\gamma+\Gamma_{12}}\right)e^{-\Gamma_{12}t}\right];\end{aligned} \tag{E.3}$$

$$\begin{aligned}\rho_{23}(t) &= \frac{1}{2}\rho_{23}(0)e^{-\gamma t}(1+\cosh(\Gamma_{12}t)) - \frac{1}{2}\rho_{32}(0)e^{-\gamma t}(1-\cosh(\Gamma_{12}t)) \\ &- \frac{1}{2}[\rho_{22}(0)+\rho_{33}(0)]e^{-\gamma t}\sinh(\Gamma_{12}t) - \rho_{11}(0)e^{-2\gamma t}\left(\frac{2\gamma\Gamma_{12}}{\gamma^2-\Gamma_{12}^2}\right) \\ &+ \frac{1}{2}\rho_{11}(0)e^{-\gamma t}\left[\left(\frac{\gamma+\Gamma_{12}}{\gamma-\Gamma_{12}}\right)e^{\Gamma_{12}t} + \left(\frac{\gamma-\Gamma_{12}}{\gamma+\Gamma_{12}}\right)e^{-\Gamma_{12}t}\right];\end{aligned} \tag{E.4}$$

$$\rho_{32}(t) = \rho_{23}^*(t), \quad \rho_{44}(t) = 1-\rho_{11}(t)-\rho_{22}(t)-\rho_{33}(t). \tag{E.5}$$

All other elements of the density matrix ρ defined in the two qubit product basis (5.2) remains zero for all time t.

APPENDIX F

DYNAMICAL EVOLUTION OF TWO INTERACTING QUBITS IN CORRELATED DISSIPATIVE ENVIRONMENT

The solutions correspond to the initial matrix ρ defined in equation (5.9)

$$\rho_{11}(t) = \rho_{11}(0)e^{-2\gamma t} \quad ; \tag{F.1}$$

$$\begin{aligned}\rho_{22}(t) &= \frac{1}{2}\rho_{22}(0)e^{-\gamma t}(\cos(2vt)+\cosh(\Gamma_{12}t)) - \frac{1}{2}\rho_{33}(0)e^{-\gamma t}(\cos(2vt)-\cosh(\Gamma_{12}t)) \\ &- \rho_{11}(0)e^{-2\gamma t}\left(\frac{\gamma^2+\Gamma_{12}^2}{\gamma^2-\Gamma_{12}^2}\right) + \frac{1}{2}\rho_{11}(0)e^{-\gamma t}\left[\left(\frac{\gamma+\Gamma_{12}}{\gamma-\Gamma_{12}}\right)e^{\Gamma_{12}t} + \left(\frac{\gamma-\Gamma_{12}}{\gamma+\Gamma_{12}}\right)e^{-\Gamma_{12}t}\right] \\ &- \frac{1}{2}[\rho_{23}(0)+\rho_{32}(0)]e^{-\gamma t}\sinh(\Gamma_{12}t) + \frac{1}{2}[\rho_{23}(0)-\rho_{32}(0)]e^{-\gamma t}\sin(2vt);\end{aligned} \tag{F.2}$$

$$\begin{aligned}\rho_{33}(t) &= \frac{1}{2}\rho_{33}(0)e^{-\gamma t}(\cos(2vt)+\cosh(\Gamma_{12}t)) - \frac{1}{2}\rho_{22}(0)e^{\gamma t}(\cos(2vt)-\cosh(\Gamma_{12}t)) \\ &- \rho_{11}(0)e^{-2\gamma t}\left(\frac{\gamma^2+\Gamma_{12}^2}{\gamma^2-\Gamma_{12}^2}\right) + \frac{1}{2}\rho_{11}(0)e^{-\gamma t}\left[\left(\frac{\gamma+\Gamma_{12}}{\gamma-\Gamma_{12}}\right)e^{\Gamma_{12}t} + \left(\frac{\gamma-\Gamma_{12}}{\gamma+\Gamma_{12}}\right)e^{-\Gamma_{12}t}\right] \\ &- \frac{1}{2}[\rho_{23}(0)+\rho_{32}(0)]e^{-\gamma t}\sinh(\Gamma_{12}t) - \frac{1}{2}[\rho_{23}(0)-\rho_{32}(0)]e^{-\gamma t}\sin(2vt);\end{aligned} \tag{F.3}$$

$$\begin{aligned}\rho_{23}(t) &= \frac{1}{2}\rho_{23}(0)e^{-\gamma t}(\cos(2vt)+\cosh(\Gamma_{12}t)) - \frac{1}{2}\rho_{32}(0)e^{-\gamma t}(\cos(2vt)-\cosh(\Gamma_{12}t)) \\ &- \rho_{11}(0)e^{-2\gamma t}\left(\frac{2\gamma\Gamma_{12}}{\gamma^2-\Gamma_{12}^2}\right) + \frac{1}{2}\rho_{11}(0)e^{-\gamma t}\left[\left(\frac{\gamma+\Gamma_{12}}{\gamma-\Gamma_{12}}\right)e^{\Gamma_{12}t} + \left(\frac{\gamma-\Gamma_{12}}{\gamma+\Gamma_{12}}\right)e^{-\Gamma_{12}t}\right] \\ &- \frac{1}{6}[\rho_{22}(0)+\rho_{33}(0)]e^{-\gamma t}\sinh(\Gamma_{12}t) + \frac{1}{2}e^{-\gamma t}[\rho_{22}(0)-\rho_{33}(0)]i\sin(2vt);\end{aligned} \tag{F.4}$$

$$\rho_{32}(t) = \rho_{23}^*(t), \quad \rho_{44}(t) = 1-\rho_{11}(t)-\rho_{22}(t)-\rho_{33}(t). \tag{F.5}$$

All other elements of the density matrix ρ defined in the two qubit product basis (5.2) remains zero for all time t.

APPENDIX G

DYNAMICAL EVOLUTION OF TWO INTERACTING QUBITS IN CORRELATED DEPHASING ENVIRONMENT

The solutions correspond to the initial matrix ρ defined in equation (5.9)

$$\rho_{11}(t) = \rho_{11}(0) \quad , \tag{G.1}$$

$$\begin{aligned}\rho_{22}(t) &= \frac{1}{2}\rho_{22}(0)\left[1+e^{-(\Gamma_A+\Gamma_B-2\Gamma_0)t/2}\cos(2\Omega' t)+\frac{(\Gamma_A+\Gamma_B-2\Gamma_0)}{4\Omega'}\sin(2\Omega' t)\right] \\ &+ \frac{1}{2}\rho_{33}(0)\left[1-e^{-(\Gamma_A+\Gamma_B-2\Gamma_0)t/2}\cos(2\Omega' t)+\frac{(\Gamma_A+\Gamma_B-2\Gamma_0)}{4\Omega'}\sin(2\Omega' t)\right] \\ &+ \frac{i[\rho_{23}(0)-\rho_{32}(0)]ve^{-(\Gamma_A+\Gamma_B-2\Gamma_0)t/2}}{2\Omega'}\sin(2\Omega' t) \quad ,\end{aligned} \tag{G.2}$$

$$\begin{aligned}\rho_{33}(t) &= \frac{1}{2}\rho_{22}(0)\left[1-e^{-(\Gamma_A+\Gamma_B-2\Gamma_0)t/2}\cos(2\Omega' t)+\frac{(\Gamma_A+\Gamma_B-2\Gamma_0)}{4\Omega'}\sin(2\Omega' t)\right] \\ &+ \frac{1}{2}\rho_{33}(0)\left[1+e^{-(\Gamma_A+\Gamma_B-2\Gamma_0)t/2}\cos(2\Omega' t)+\frac{(\Gamma_A+\Gamma_B-2\Gamma_0)}{4\Omega'}\sin(2\Omega' t)\right] \\ &- \frac{i[\rho_{23}(0)-\rho_{32}(0)]ve^{-(\Gamma_A+\Gamma_B-2\Gamma_0)t/2}}{2\Omega'}\sin(2\Omega' t) \quad ,\end{aligned} \tag{G.3}$$

$$\begin{aligned}\rho_{23}(t) &= \frac{1}{2}e^{-(\Gamma_A+\Gamma_B-2\Gamma_0)t/2}[\rho_{23}(0)\{e^{-(\Gamma_A+\Gamma_B-2\Gamma_0)t/2} \\ &+ \cos(2\Omega' t)+\frac{(\Gamma_A+\Gamma_B-2\Gamma_0)}{4\Omega'}\sin(2\Omega' t)\} \\ &+ \rho_{32}(0)\{e^{-(\Gamma_A+\Gamma_B-2\Gamma_0)t/2}-\cos(2\Omega' t)-\frac{(\Gamma_A+\Gamma_B-2\Gamma_0)}{4\Omega'}\sin(2\Omega' t)\}] \\ &+ \frac{ive^{-(\Gamma_A+\Gamma_B-2\Gamma_0)t/2}}{2\Omega'}\sin(2\Omega' t)\left[\rho_{22}(0)-\rho_{33}(0)\right] \quad ,\end{aligned} \tag{G.4}$$

$$\Omega' = \sqrt{v^2-\left(\frac{\Gamma_A+\Gamma_B-2\Gamma_0}{4}\right)^2} \tag{G.5}$$

$$\rho_{32}(t)=\rho_{23}^*(t), \quad \rho_{44}(t)=1-\rho_{11}(t)-\rho_{22}(t)-\rho_{33}(t). \tag{G.6}$$

All other elements of the density matrix ρ defined in the two qubit product basis (5.2) remains zero for all time t.

VITA

Sumanta Das

Candidate for the Degree of

Doctor of Philosophy

Dissertation: QUANTUM INTERFERENCE AND DECOHERENCE EFFECTS IN NOVEL SYSTEMS

Major Field: Physics

Biographical:

Personal Data:

Born in Kolkata, India, on February 13, 1980
Son of Mr. Rabindra Nath Das and Mrs. Suniti Das.

Education:

Received Bachelor of Science degree from Presidency College, Calcutta university, Kolkata, West Bengal, India in June 2001
Received Master of Science degree in Physics from Pune University, Pune, Maharastra, India in July 2003
Completed the requirements for the Doctor of Philosophy degree with a major in Physics at Oklahoma State University in December 2009.

Experience:

Taught several undergraduate level physics courses for more than 2 years
Extensive theoretical knowledge in quantum statistical properties of radiation, master equation approach for atom-field interactions, quantum interference effects, vacuum induced coherence, quantum correlations in atomic and mesoscopic systems, quantum optical study of waveguides, study of decoherence and application to quantum information
Extensive experience in Fortran and C for scientific simulations
Reviewed undergraduate level books from Thomson and John Wiley.

Professional membership :

American Physical Society
Optical Society of America.

Name: Sumanta Das Date of Degree: December, 2009

Institution: Oklahoma State University Location: Stillwater, Oklahoma

Title of Study: QUANTUM INTERFERENCE AND DECOHERENCE EFFECTS IN NOVEL SYSTEMS

Pages in Study: 187 Candidate for the Degree of Doctor of Philosophy

Major Field: Physics

In this thesis we studied quantum interference and decoherence effects in systems like atoms, ions, quantum dots and photonic waveguides. These systems are presently widely studied in different areas of quantum optics and quantum information sciences. Our investigations showed that trapped ions with $j = 1/2$ to $j = 1/2$ can be efficient systems where quantum interference effects like the vacuum induced coherences can be studied. We discovered new quantum interference effects induced by spatial variation of laser phase in the Dicke superradiance from atomic or atom like systems. Our investigations also showed the presence of vacuum mediated superexchange and strong quantum correlations in this systems. Further we studied quantum correlations of photons emitted from cascade emission in quantum dots. We showed how the excitonic level splitting and decoherence in the quantum dot can effect such quantum correlations. Moreover we did a detailed analysis of the dynamics of entanglement and environmental decoherence effects for two interacting qubits coupled to several different models of environment. We discovered the phenomenon of bright and dark period in the entanglement dynamics as a result of competing effect of qubit-qubit interactions and environmental decoherence. We also studied entanglement and losses in photonic waveguide for single mode and two mode squeezed states as input. Our investigations showed that waveguides can be potentially useful in generating entanglement and preserving them over time due to their robustness against decoherence. Our investigations hence shows the potential viability's of this novel systems for application in quantum information sciences and opens up important directions in the study of decoherence in such systems.

ADVISOR'S APPROVAL: _____